The Dissertation Committee for Amber Nichole Heard-Booth Certifies that this is the approved version of the following dissertation:

Morphological and Functional Correlates of Variation in the Human Longitudinal Arch

Committee:

Liza J. Shapiro, Supervisor

John W. Kappelman, Jr.

Edward Christopher Kirk

Roshna Wunderlich

Morphological and Functional Correlates of Variation in the Human Longitudinal Arch

by

Amber Nichole Heard-Booth, B.A.; M.S.

Dissertation

Presented to the Faculty of the Graduate School of

The University of Texas at Austin

in Partial Fulfillment

of the Requirements

for the Degree of

Doctor of Philosophy

The University of Texas at Austin

May 2017

Dedication

For Mom, who gave me everything I needed to begin this journey. And for Ryan, who gave me the support to finish it.

Acknowledgements

Thanks to the National Science Foundation and The Leakey Foundation for providing funding to support the research included in this dissertation. Thanks are also due to the following people and organizations that made this project possible: Dr. Craig Thomajan, DPM, and the staff at Austin Foot and Ankle Specialists for access to lateral foot and ankle X-rays; Dr. Todd Fenton, Department of Anthropology, Michigan State University, for access to the Mis Island Ancient Nubian human skeletal collection housed at Michigan State University; Dr. George Milner, Department of Anthropology, Penn State Univeristy, and Dr. Terrance Martin, Curator and Chair of Anthropology, Illinois State Museum, for access to the Norris Farms Oneota human skeletal collection housed at Penn State University; Dr. Jeremy DeSilva, Department of Anthropology, Dartmouth College, for access to Magnetic Resonance Images; and Dr. Roshna Wunderlich, Department of Biology, James Madison University, for access to her pedobarograph.

Special thanks to my dissertation committee members for their mentorship and expertise that helped to improve both this project and my personal development as an academic. To my committee chair and supervisor, Liza, I could not be more in debt. Liza, thank you for being a thoughtful and critical advisor, with a keen methodological eye who always asks the "so what?" questions. Moreover, you are empathetic and kind, and I am so grateful to have had you guide me over the past nine years. To Chris, thank you for always treating me like a colleague and asking my opinion, no matter how novice. You taught me to write clearly, to go for the "low hanging fruit", and inspired me to take an interest in anatomy *above* the neck. To John, thank you for making me feel welcome in your lab, and for reminding me to go back to the basics and never assume that we already know the

answer. To Roshna, thank you for generously allowing me to use your equipment and for teaching me about plantar pressure analysis. I have learned so much, and yet still feel like I know so little. I look forward to continuing our work together!

Thanks are also due to individuals who helped with the data collection and processing components of this dissertation. I owe thanks to a number of undergraduate students who helped collect data for this project, notably Truc Nguyen. Many thanks to Addison Kemp for her expertise writing R code, and who wrote the code to compute metatarsal torsion for Chapter 4 of this dissertation. Finally, thanks to all of the participants who walked and ran across the pressure mat!

Graduate school is a time of intellectual, emotional, and professional growth, and I was very fortunate to share this journey with a number of outstanding fellow graduate students. Special thanks to Carrie Veilleux, Angel Zeininger, Andrew Barr, Gabrielle Russo, Brett Nachman, Kelsey Ellis, Katherine Bannar-Martin, Kim Valenta, Jaime Mata-Miguez, Lina Maria Valencia, Rick Smith, Addison Kemp, Laura Abondano, and Maria Darr, all of whom shared a significant part of this experience with me and who were a constant source of encouragement.

My interest in anthropology began at an early age and was nurtured by a number of role models throughout my high school and undergraduate years. I thank Mrs. Denise Gimpel, who taught cultural and physical anthropology at Plymouth Salem High School, for introducing me to the field that would ultimately become my passion. She called me her “anthro geek gal”, involved me in my first archaeological excavation, and lit a flame in me that continues to burn. I thank Dr. Laura MacLatchy of the University of Michigan, for introducing me to the study of functional morphology, and for being such a positive female role model and mentor. And I owe the greatest thanks to Dr. William Sanders (Bill) of the University of Michigan Museum of Paleontology, for welcoming me into his lab and

teaching me how to *do* science. The lessons I learned in Bill's lab are innumerable and the experience was incomparable. I must also thank Bill for recommending that I attend The University of Texas under the tutelage of Liza Shapiro for my doctoral work. Bill said that Liza was the best, and—as usual—he was right.

And finally, heartfelt thanks is given to my family, whose support has been unconditional and unwavering. I thank my mom, Debbie, for working a lifetime of long hours so that I could attend college, and for allowing me to study the topics that interested and inspired me, no matter how impractical. I thank my sister, Ashley, for her constant encouragement, and whose voice always makes me feel "home", regardless of the distance between us. Thanks to my grandmother, Gwen (who earned her PhD in her early 70s!), for being my sounding board for all things related to graduate school, and who stands as a constant reminder that you are never too old to learn, to grow, and to achieve. I thank my dad, Mike, and my Aunt Honor for their love and support that has helped to shape me. And finally, I thank Ryan and our two smart and curious boys, Liam and Patrick. Ryan, thank you for saying, "Okay. Texas it is!", and for never looking back.

Morphological and Functional Correlates of Variation in the Human Longitudinal Arch

Amber Nichole Heard-Booth, PhD

The University of Texas at Austin, 2017

Supervisor: Liza J. Shapiro

The human longitudinal arch has long been considered to be an important adaptation for proper foot function and efficient locomotion. The anatomy and evolution of the arch has been a topic of discussion in biological anthropology for nearly a century, as its appearance presumably marked an important shift in human evolution towards use of a gait that was biomechanically-similar to that of modern humans. However, recent studies have challenged the paradigm that has historically characterized human feet as stiff and having an arch, in contrast to the highly-mobile feet of non-human primates, which lack an arch. Increasingly, studies report that humans exhibit variation in arch height, including flat-footedness, as well as variation in midfoot mobility. These findings have important implications for how paleoanthropologists interpret fossil foot bones that exhibit "human-like" morphology. This dissertation uses a novel, yet straightforward approach to look for direct links among foot bone morphology, arch height, and pedal loading mechanics. Rather than comparing human foot bone morphology to that of apes (like previous studies), this dissertation examines how foot bone shape varies *within humans*, and seeks to determine whether that variation is directly related to differences in arch height between individuals. This dissertation also investigates how variation in foot shape is

related to variation in midfoot loading. Using data collected from X-rays, magnetic resonance imagery, and human osteological remains, the chapters of this dissertation discuss whether variation in the morphology of the distal tibia, calcaneus, and metatarsals is related to variation in arch height. Here, it is argued that features of the distal tibia and metatarsals previously used to infer arch presence in fossil hominins cannot be used to draw such conclusions. A feature of the calcaneus does correlate with variation in arch height, however, and may be useful for reconstructing arch height. Finally, humans who have a low longitudinal arch and a relatively wide foot were found to experience greater loading of the midfoot, irrespective of age. Given that early hominins are estimated to have had relatively broad feet, these results suggest that early hominins may have experienced greater midfoot loading than modern humans.

Table of Contents

List of Tables

List of Figures

Chapter 1: Introduction

The human foot exhibits a series of unique adaptations that are functionally linked to our distinct form of bipedal locomotion. One of these adaptations is the plantar longitudinal arch. The longitudinal arch has long been considered to be a crucial structural adaptation of the foot that transforms it into a rigid lever to facilitate and optimize bipedal walking mechanics (Morton, 1924). The anatomy and evolution of the longitudinal arch has been a focus of discussion in biological anthropology for nearly a century, as the appearance of this structure presumably marked an important shift in human evolution towards use of a bipedal gait that was biomechanically similar to that of modern humans (Morton, 1922; Weidenreich, 1923; Morton, 1924; Keith, 1929). However, questions about the development, anatomical variation, functional morphology, and evolutionary history of the longitudinal arch remain unresolved. To understand the biological, behavioral, and/or environmental context that shaped the emergence of this unique human adaptation, biological anthropologists must first be able to confidently reconstruct the height of the longitudinal arch from fossilized pedal remains.

The goal of this dissertation research is to improve methods for assessing whether a longitudinal arch was present (and/or estimating arch height) from isolated fossil foot bones by strengthening our understanding of how variation in foot bone shape is related to variation in arch height among modern humans. In past studies, the morphology of the distal tibia (DeSilva & Throckmorton, 2010), talus (Day & Wood, 1968), calcaneus (Berillon, 2003; Lamy, 1986; Prang, 2015), and fourth metatarsal (Berillon, 2003; Ward *et al*., 2011)—or some combination thereof—have been examined to determine whether a longitudinal arch was present in a fossil hominin individual. In these studies, the longitudinal arch is treated as a categorical variable that is either present or absent. This

approach is problematic, however, given that ethnographic and clinical studies have shown that humans exhibit a wide range of variation in longitudinal arch height, including flat-footedness (*e.g.*, Hoffmann, 1905; Staheli *et al*., 1987; Cavanagh *et al*., 1997; Morag & Cavanagh, 1999; Wunderlich & Cavanagh, 2001; D'Août *et al*., 2009). Therefore, it cannot be assumed that the presence of so-called "human-like" morphology indicates that a longitudinal arch was present. Moreover, by treating the longitudinal arch as a categorical variable, as opposed to a continuous one that varies in height, previous studies have likely overlooked more nuanced relationships between foot bone shape and arch height that could inform reconstructions of hominin foot anatomy and locomotor biomechanics.

The study presented here abandons the longitudinal arch presence-versus-absence framework, and instead uses a novel, yet straightforward approach to look for direct links among foot bone morphology, longitudinal arch height, and pedal loading mechanics. Rather than comparing human foot bone morphology to that of apes (as previous studies have done), this study examines how foot bone shape varies *within humans*, and seeks to determine whether that variation is related to differences in arch height between individuals. In addition to exploring this trend among adults who vary in arch height, this study includes an ontogenetic component to examine how select foot bones change shape in early childhood during the period of longitudinal arch development. Finally, this study tests how variation in longitudinal arch height and foot shape is related to variation in midfoot loading patterns. Where applicable, the results of these analyses are applied to the fossil record to discuss the probable height of the longitudinal arch and bipedal walking mechanics of our hominin ancestors.

ANATOMY, FUNCTION AND HUMAN VARIATION OF THE LONGITUDINAL ARCH

The Arch as a Mechanical Structure

In architectural terms, an arch is a curved structure that spans a space and it may, or may not, support weight above it. The function of an arch is to mitigate bending stress experienced by the material that spans the space. Bending stress occurs when a material experiences a load perpendicular to its longitudinal axis, which could be the weight of the material itself and/or an external load that the material is supporting. Bending stress is comprised of both compressive stress (compression), experienced above or on the unsupported side of the material, and tensile stress (tension), experienced below or on the supported side of the material. An arch acts to resolve forces experienced by the material into compressive stresses, thereby eliminating tension (**Figure 1.1**). Many materials used in building construction are better able to resist compression than tension, deeming the arch to be a useful architectural solution for spanning gaps (*e.g.*, bridges) and/or supporting weight from above (Reid, 1984; Tripeny & Ambrose, 2012). Forces are transferred down the supports of the arch to its base and are directed outward as a force known as thrust. Thrust must be restrained by internal ties and/or external bracing to maintain the integrity of the arch and prevent it from collapsing (Tripeny & Ambrose, 2012).

The Longitudinal Arch of the Human Foot

Bones of the Longitudinal Arch

The longitudinal arch of the human foot is a structural adaptation that acts to distribute the body's weight across the foot while simultaneously minimizing stress experienced by the bony elements that form it (Morton, 1924). Like many structural materials, bone is stronger in its ability to resist compressive stress than tensile stress

(Reilly & Burstein, 1975). Therefore, the presence of a bony arch is an architectural solution to the functional challenge of supporting a large mass over a relatively small base of support, such as the human foot. The bones that form the longitudinal arch include the talus, calcaneus, navicular, cuboid, three cuneiform bones, and five metatarsals. The talus is positioned at the apex of the arch, and is the bony element that receives the body's weight from above and transfers it down the arch's pillars. The calcaneus is positioned as the posterior pillar of the arch, and is the bone primarily responsible for transferring the body's weight to the ground during standing (Morton, 1924). The anterior pillar of the arch is commonly divided into medial and lateral columns. The medial column is formed by the navicular, three cuneiform bones, and medial three metatarsals, while the lateral column is formed by the cuboid and lateral two metatarsals (**Figure 1.2**). The medial aspect of the longitudinal arch is elevated higher than the lateral aspect of the arch.

Passive and Dynamic Support of the Longitudinal Arch

The architectural integrity of the bony longitudinal arch is supported passively by ligaments on the plantar surface of the foot, including the long and short plantar ligaments, the calcaneonavicular ("spring") ligament, and the plantar aponeurosis (Donatelli, 1985; Franco, 1987). These ligaments act as the internal ties that maintain the integrity of the bony arch by resisting the thrust forces directed at the calcaneal base and metatarsal heads when the arch deforms in response to loading. As the arch deforms during stance, these ligaments become stretched and store elastic strain energy that is returned to the foot as it enters swing phase and the ligaments recoil, reducing locomotor cost (Alexander *et al*., 1987; Stearne *et al*., 2016). The energy cost-saving mechanism of the arch is negligible in walking, but increases with speed during running (Stearne *et al*., 2016).

The integrity of the longitudinal arch receives dynamic muscular support from the intrinsic muscles of the foot and muscles of the posterior leg that have a distal tendinous attachment on the plantar aspect of foot bones. Like the ligaments that support the arch, the abductor hallucis, flexor digitorum brevis, and quadratus plantae stretch in response to arch deformation during stance and then actively contract, offering additional support beneath the arch (Basmajian and Bentzon, 1954; Fiolkowski *et al*., 2003; Pataky *et al*., 2008; Bates *et al*., 2013; Caravaggi *et al*., 2010; Kelly *et al*., 2014). During the push-off, propulsive phase of the gait cycle, contraction of the tibialis posterior muscle, which has distal attachments on the navicular tuberosity, medial cuneiform, and proximal metatarsals, acts to maintain the height of the arch (Edwards *et al*., 2008; Hankey, 2009). Dysfunction of tibialis posterior has been associated with adult acquired flatfoot disorder, highlighting the importance of its role in arch maintenance (Edwards *et al*., 2008; Hankey, 2009). Other leg muscles whose action contributes to arch maintenance during walking include tibialis anterior and flexor digitorum longus (Reeser *et al*., 1983; Donatelli, 1985).

The "Windlass Mechanism"

During the propulsive phase of the locomotor cycle, the compliant arch is transformed into a rigid lever to propel the body's mass over the forefoot. Hicks (1954) modeled this transformation as a "windlass mechanism," in which a rope or cable is wound around a crank or pulley to move a heavy load attached to the opposite end. In the foot, the plantar aponeurosis acts as the rope or cable that is wound around the metatarsal heads during push-off in order to move the body's weight over the foot (Hicks, 1954). As the digital slips of the plantar aponeurosis are wound around the metatarsal heads during dorsiflexion of the metatarsophalangeal joints, tension builds in the plantar aponeurosis

and the longitudinal arch heightens as the calcaneus and metatarsal heads are drawn closer together, compressing the bones of the midfoot (Hicks, 1954; Franco, 1987; Griffin *et al*., 2015). As the bones of the midfoot are compressed, the foot is transformed into a rigid lever on which the body's weight is propelled over the metatarsophalangeal joints as the triceps surae muscles plantarflex the foot at the ankle joint.

Human Variation in Longitudinal Arch Height

The presence of a longitudinal arch has long been considered to be characteristic of the feet of modern humans (Morton, 1922; Morton, 1924; Elftman & Manter, 1935a;b), yet humans have been observed to exhibit a wide range of variation in arch height, including asymptomatic flat-footedness (Engle & Moron, 1931; Sim-Fook & Hodgson, 1958; Sachithanandam & Joseph, 1995; Wunderlich & Cavanagh, 2001; D'Août *et al*., 2009). Therefore, it is more appropriate to discuss the human longitudinal arch as existing on a height continuum, as opposed to characterizing it as a structure that is either present or absent. However, there is no consensus as to what the "normal" height of the longitudinal arch is. While clinicians often describe individuals as having "low," "normal"/"average," or "high" arches, there are no objective criteria upon which these designations are based. The following section summarizes how longitudinal arch height has been reported to vary among humans and the effects of foot loading.

Ontogenetic Variation in Longitudinal Arch Height

Human feet appear flat at birth and in young infants, making flat footedness the first stage of normal human foot development. The feet of infants and toddlers are flat along the plantar surface due in large part to the presence of a pediatric fat pad beneath the

child's midfoot (Staheli *et al*., 1987; García-Rodríguez *et al*., 1999; Bertsch *et al*., 2004; El *et al*., 2006; Pfeiffer *et al*., 2006; Harris, 2010). In some cases, an incipient longitudinal arch appears present when an infant or young child is in a non-weight-bearing position, and then the arch disappears when the child stands. These cases are described as "flexible flatfoot" and are considered normal (García-Rodríguez *et al*., 1999; El *et al*., 2006; Chang *et al*., 2010; Harris, 2010).

Studies of plantar pressure beneath the feet of young children show that the longitudinal arch begins to develop shortly after a child begins walking and continues until approximately age six (Bertsch *et al*., 2004; Onodera *et al*., 2008; Müller *et al*., 2012; but see Forriol and Pascual, 1990 and Waseda *et al.,* 2014 who contend that the arch continues to develop into the teenage years). The development (*i.e*., heightening) of the longitudinal arch is accelerated during the first two years following the onset of walking and then continues at a slower rate for approximately 2-3 additional years (Bertsch *et al*., 2004; Onodera *et al*., 2008; Müller *et al.,* 2012). The fact that arch development concludes around age 6 is noteworthy because this is the approximate age at which a child's gait matures to exhibit adult-like characteristics (Sutherland, 1997; Samson *et al*., 2011). This observation underscores the functional association between the presence of a well-developed longitudinal arch and human-like bipedal walking mechanics.

Longitudinal arch development appears to progress at a different rate in boys and girls, and is highly variable between individuals (Echarri and Forriol, 2003; Bertsch *et al*., 2004; Stavlas *et al*., 2005; Pfeiffer *et al.,* 2006; Mickle *et al*., 2008; Bosch *et al*., 2010; Chang *et al.,* 2010; but see El *et al*., 2006). In a large number of populations, boys are reported to exhibit a wider mid-foot region and a lower longitudinal arch than age-matched girls (Echarri and Forriol, 2003; Stavlas *et al.,* 2005; Pfeiffer *et al*., 2006; Mickle *et al*., 2008; Bosch *et al*., 2010; Chang *et al*., 2010; but see El *et al*., 2006). This finding is

consistent with reports of sex differences in arch height among adults, where women have been found to exhibit a higher longitudinal arch than men for a given foot length (Wunderlich & Cavanagh, 2001).

Much of what is known about the ossification schedule, growth, and maturation of foot bones is derived from radiographic atlases of the human foot or complete skeleton (O'Rahilly *et al*., 1960; Hoerr, 1962; Birkner, 1978) and has been summarized by Scheuer and Black (2004). At birth, the primary ossification centers of the talus, calcaneus, metatarsals, and phalanges are present, while the ossification centers of the bones of the midfoot region have not yet developed. Ossification centers appear for the cuboid and lateral cuneiform within the first six months of post-natal life, as do epiphyses for the pedal phalanges. Ossification centers for more medially-positioned midtarsal elements, such as the medial and intermediate cuneiforms, as well as the navicular, appear between the first and third year of life. It is notable that this is also the period during which the child begins to walk, the pediatric fat pad beneath the mid-foot recedes, and the longitudinal arch commences its development (Bertsch *et al*, 2004). It is also worth noting that the appearance of these ossification centers occurs approximately one year sooner in girls compared to boys, and this gender difference in ossification schedule increases as the foot develops (Scheuer & Black, 2004). For example, the ossification center of the medial cuneiform appears between 12 and 24 months of age in girls, and 24 and 36 months in boys, while the ossification center of the navicular appears between 3 and 5 years in girls, and 5 and 7 years in boys (Scheuer & Black, 2004). This gender difference in foot bone ossification likely underlies the observed gender differences in foot shape and function (Echarri and Forriol, 2003; Bertsch *et al.,* 2004; Stavlas *et al*., 2005; Pfeiffer *et al*., 2006; Mickle *et al*., 2008; Bosch *et al*., 2010; Chang *et al*., 2010; but see El *et al*., 2006). In other words, the pediatric fat pad may persist later in development in boys compared to girls due

to the delayed appearance in the ossification centers of the midfoot elements, leading boys to have a relatively wider midfoot region and lower longitudinal arch compared to age-matched girls.

While the schedule of foot bone development has been well documented, we know relatively little about how the individual bones change shape throughout ontogeny, and how these changes may be related to longitudinal arch development. The study of foot anatomy has been, and continues to be, limited by access to specimens and/or medical imagery, and these resources are especially limited for pediatric populations. Radiographs can be used to measure changes in foot bone orientation and in two-dimensional size and shape, but the risks associated with radiation exposure limits ethical use of these studies. Previous studies have successfully used magnetic resonance imaging (MRI) to measure aspects of adult foot bony and soft tissue anatomy (e.g., Tan & Teh, 2007; Miller *et al.*, 2014; DeSilva *et al*., 2015), though similar studies have not been performed on children. Although MRI has no risk of radiation exposure, it does require that subjects remain still while the machine scans the region of interest, which may be a difficult task for young children. Moreover, the cost of an MRI scan—or a computed tomography (CT) scan, which also produces a three-dimensional image, although with low radiation exposure—is prohibitive for studying internal anatomy on large samples of subjects. Together, these factors have restricted our ability to study ontogenetic changes in the internal anatomy of the human foot or any other region of the body.

Adult Gender Differences in Longitudinal Arch Height

Male and female human feet differ in size and shape (Wunderlich & Cavanagh, 2001; Fessler *et al*., 2005; Krauss *et al*., 2008). For most populations that have been studied,

females have shorter feet (relative to stature) than males (Fessler *et al*., 2005). This trend is evident across geographically-disparate populations, including those such as urban Japanese (Ashizawa *et al*., 1997), rural Javanese (Ashizawa *et al*., 1997), American soldiers (Giles & Vallandigham, 1991; Wunderlich & Cavanagh, 2001), and Londonites (Barker & Scheuer, 1998). Female feet also differ in shape from the feet of males, including having a higher longitudinal arch for a given foot length (Wunderlich and Cavanagh, 2001). As previously stated, this observation corresponds to gender differences in arch height throughout ontogeny, where girls are reported to have a higher arch than age-matched boys (Echarri and Forriol, 2003; Stavlas *et al.,* 2005; Pfeiffer *et al*., 2006; Mickle *et al*., 2008; Bosch *et al*., 2010; Chang *et al*., 2010; but see El *et al*., 2006). Therefore, it appears that a gender difference in arch height begins in early childhood and continues into adulthood. The reason for this difference is unclear, however.

Population Differences in Longitudinal Arch Height and the Effects of Footwear Use

Footwear is a relatively recent human invention and is commonly cited as a primary cause of the observed differences in foot size, shape, and longitudinal arch height between populations (Hoffmann, 1905; Barnicot & Hardy, 1955; Barnett, 1962; Funakoshi, 1988; Ashizawa *et al*., 1997). Since the early twentieth century, clinicians and anthropologists have sought to observe the feet of habitually unshod populations in an effort to understand the morphology of the foot in its most natural state, and to investigate the effects of footwear on foot form. Some of the earliest observations were made by Hoffmann, a clinician who studied the feet of 186 members of various tribes of the Philippine Islands (Hoffmann, 1905). Hoffmann reported that the length of the foot relative to body height, and the length of the phalanges relative to foot length, was similar among the unshod

Philippinos and shoe-wearing populations, but that the unshod individuals had relatively wider feet, especially in the forefoot region (Hoffmann, 1905). He explained that this increase in forefoot width occurred because the phalanges of each digit were aligned with their respective metatarsals, and there was a large space separating the hallux from the second digit. The feet of the unshod Philippinos exhibited a wide range of variation in longitudinal arch height, including flat-footedness. Interestingly, however, Hoffmann (1905) noted that occurrences of flatfoot were not associated with weakness or pain as is often the case in Western populations. He made a similar observation about the feet of members of various unshod South African tribes, including the Matabele, Zambesi, and Hottentots, many of whom (approximately 40%) exhibited low to flat longitudinal arches (Hoffmann, 1905).

The observations that Hoffmann (1905) made regarding the shape of the foot of unshod populations have been echoed by others studying foot morphology and function among barefoot peoples. A review of the literature reveals that the feet of unshod populations are generally longer relative to stature, and they have a wide forefoot region with a wide gap between the first and second digit (Barnicot & Hardy, 1957; Sim-Fook & Hodgson, 1958; Tuttle *et al*., 1990; Tuttle *et al*., 1991; Kusumoto *et al*., 1996; Ashizawa *et al*., 1997; Musiba *et al*., 1997; D'Août *et al*., 2009). In direct comparisons between unshod and shod populations, most studies report that the people of unshod populations have higher longitudinal arches than those from shod populations (Sim-Fook & Hodgson, 1958; Rao & Joseph, 1992; Sachithanandam & Joseph, 1992; Echarri & Forriol, 2003). Others, however, have reported that individuals from unshod populations seem to have lower longitudinal arches than those from shod populations (*e.g*., D'Août *et al*., 2009) or that there is no difference in arch height between those who use footwear and those who are habitually barefoot (Engle & Morton, 1931).

From a functional perspective, it makes sense that use of constrictive footwear in shod populations would be associated with a lower longitudinal arch. Footwear acts as a cast for the foot that offers protection and support, but at the expense of restricting arch deformation during locomotion. If the longitudinal arch does not deform during stance, the ligaments and muscles on the plantar aspect of the foot fail to stretch, and therefore the muscles do not contract in response. Over time, muscle inactivity would lead to atrophy of the intrinsic musculature of the foot, minimizing its ability to support the arch, and ultimately leading to a reduction in arch height (or failure of the arch to develop, if constrictive footwear is habitually worn during childhood). Experimental studies support this logic, as it has been reported that performing activities barefoot or while wearing so-called "minimalist" footwear (*i.e.*, flexible sole with no arch support) leads to an increase in the muscle volume and/or strength of select intrinsic foot muscles and an overall heightening or stiffening of the longitudinal arch (Robbins & Hanna, 1987; Goldmann *et al*., 2013; Miller *et al*., 2014). Therefore, if footwear use does indeed lead to weakness in pedal musculature that supports the arch, it appears that the effect is reversible.

Pathological Variation in Longitudinal Arch Height

As stated previously, there is no consensus regarding what the "normal" height of the longitudinal arch is. Arch height varies continuously in populations, and individuals at the tails of the distribution are described as having either low or high arches. In a 1985 study, Subotnick characterized 60% of the population as having "normal" arches, 20% as having "low" arches, and 20% as having "high" arches (Subotnick, 1985). In many, but not all, cases, individuals with feet at both tails of the arch continuum are at a greater risk

for foot and lower limb pathology and/or injury, especially if they engage in running (Williams *et al.*, 2001).

Feet that are characterized as having a pathologically-low or absent arch (under weight-bearing conditions) are commonly referred to as "flatfeet" or "flatfoot", and pathological conditions are referred to as *pes planus*. A nation-wide survey of foot health that included 74,721 respondents from all 50 United States and the District of Columbia found that flatfoot was equally-likely to occur in men and women, regardless of age, and is more common among those with a higher BMI and lower health status (Shibuya *et al*., 2010). In a study of Saudi Arabian army recruits, flatfoot was higher among those who were of a higher BMI, had worn constrictive footwear during childhood, and who also had a family history of flatfoot, suggesting that there may be a genetic component to its etiology (Abdel-Fattah *et al*., 2006).

In flat-footed individuals, the head of the talus is often deviated both medially and plantarly, which stretches the calcaneonavicular ("spring") ligament and disrupts its ability to support the arch (Franco, 1987). Dysfunction of the tibialis posterior muscle is also associated with flatfoot, especially in adult acquired cases *(*Edwards *et al*., 2008; Shibuya *et al*., 2008; Hankey, 2009). Individuals with flat feet or low arches walk with a gait that is characterized by exaggerated pronation, placing additional stress on the medial structures of the foot (Franco, 1987; Williams *et al*., 2001). Over time, individuals with flat feet may develop pain in their knees, hips, and lower back (Franco, 1987). Runners with low or absent arches are especially at a greater risk of injury, as the force experienced by the foot during the support phase of running is 2.5 times body weight (Robbins and Hanna, 1987). Given that the foot's ability to mitigate high forces is compromised due to ligament laxity, individuals with flat feet or low arches experience higher rates of plantar fasciitis, patellar

tendinitis, and general knee pain than do runners with "normally-arched" feet (Williams *et al*., 2001).

Individuals with high longitudinal arches are described as "high arched," and pathological conditions are known as *pes cavus* (Franco, 1987). *Pes cavus* can be classified as "flexible" or "rigid," depending on whether the arch depresses under weight-bearing conditions (Franco, 1987). If the arch is high during non-weight bearing, but depresses when the individual stands, the condition is flexible *pes cavus*. If the arch is high during non-weight bearing and does not depress under the individual's body weight, the condition is rigid *pes cavus*. Unlike flatfoot, which is caused by a structural abnormality of the foot, high-arched feet most often result from a neuromuscular abnormality and/or tight plantar fascia, especially in children (Mosca, 2001).

The feet of individuals with high arches often have a tripod structure where weight is primarily supported by the calcaneus, first and second metatarsal heads, and the fifth metatarsal head (Franco, 1987). As a result, high arched individuals often develop large calluses beneath the first, second, and fifth metatarsal heads in response to the high forces experienced at these locations (Franco, 1987). Given that a smaller area of the foot contacts the ground in high arched individuals, the total pressure experienced by the foot is higher, and may lead to heel pain and stress fractures, particularly of the lateral metatarsals (Williams *et al*., 2001). Moreover, because the foot is unable to effectively absorb shock during the gait cycle, runners with high arches experience greater vertical loading than runners with low or normal arches (Williams *et al*., 2001). These high forces are then transferred up the kinetic chain of the lower limb, leading to increased stress on the knees and hips, which may result in overuse injuries and/or stress fractures of the lower extremities (Kaufman *et al*., 1999; Williams *et al*., 2001; Korpelainen *et al*., 2011).

Human Variation in Foot Mobility

Human feet are not only variable with respect to longitudinal arch height, they are also variable with respect to mobility and loading pattern (Cavanagh *et al.* 1997; Morag & Cavanagh, 1999; D'Août *et al*., 2009; Crompton et al., 2012; Bates *et al*., 2013; DeSilva & Gill, 2013; DeSilva *et al*., 2015). Historically, humans have been characterized as having stiff feet for propulsion as a result of the presence of the longitudinal arch (Elftman & Manter, 1935a). However, more recent studies have demonstrated that human feet are more mobile than previously thought, particularly in the midfoot region (Greiner & Ball, 2014; Holowka *et al*., 2017). Therefore, it is not appropriate to characterize human feet as stiff, particularly in contrast to non-human primate feet. In fact, midfoot mobility may have more interspecific overlap among primates than what has previously been recognized.

The underlying basis for variation in human midfoot mobility is not well understood. While there are studies of motion in cadaveric feet and those of living humans (*e.g.*, Greiner & Ball, 2014; Holowka *et al*., 2017), these studies do not link human variation in motion to differences in joint shape and/or soft tissue properties. Instead, these studies characterize inter-specific variation in foot mobility, while the topic of intra-specific variation in mobility remains largely unexplored. A recent study by DeSilva and colleagues (2015) is arguably the first to link variation in foot bone shape, foot mobility, and foot loading for a sample of humans. DeSilva and colleagues found that humans who exhibit a concave proximal base of the fourth metatarsal exhibit greater dorsiflexion along the lateral midfoot (presumably at the cubometatarsal joint) and also higher peak pressure beneath this region. Higher peak pressure of the lateral midfoot was also found to be associated with large body mass and a low longitudinal arch, a finding that was consistent with previous studies of foot loading in humans (Morag & Cavanagh, 1999; DeSilva *et al*., 2015). Therefore, it seems that there could be a relationship between foot bone shape,

longitudinal arch height, midfoot mobility, and foot loading. Untangling this relationship is complicated, however, given that it requires information about foot bone shape, gross foot shape, foot kinematics, and foot loading for a given individual.

EVOLUTION OF THE LONGITUDINAL ARCH

Morton's Model of Longitudinal Arch Evolution

In the early 20th century, Morton (1924) proposed that the longitudinal arch of the human foot evolved in response to forces experienced by the foot during terrestrial bipedal standing and walking. According to Morton, adoption of a bipedal stance, in and of itself, would have led to changes in foot bone morphology as the location of the center of mass over the foot shifted proximally from its distal position over the grasping phalanges that is characteristic of quadrupedal primates. The proximal shift in the location of the body's center of mass over the foot would have led to an enlargement of the calcaneal body, a trait shared between humans and other terrestrial primates, such as gorillas (Morton, 1924). Following the adoption of a bipedal stance, Morton (1924) proposed that a pattern of heel-to-toe bipedal walking would have inevitably emerged as forces followed the line of leverage through the foot from the heel to a space between the first and second digits. Given this trajectory of force, Morton (1924) argued that selection would have favored changes in forefoot anatomy to stabilize the foot, including adduction and enlargement of the first pedal ray. As a stable anterior-posterior base became established between the enlarged calcaneus ("posterior pillar") and first pedal ray (part of the "anterior pillar"), Morton proposed that the longitudinal arch evolved in response to the leverage action of the foot against the substrate.

Morton proposed that the longitudinal arch evolved as an "economically and efficiently built lever" (1924:75) to withstand stresses experienced by the foot during bipedal locomotion. He modeled the foot as a block being lifted against the ground as a second-class lever. As the block is lifted at one end, with its fulcrum (axis) located at the other, the block experiences stress aligned in a series of arcs across its volume. In non-human primates, the foot can be divided into proximal and distal segments (*i.e.*, two consecutive blocks) with fulcrums (axes) located at the midtarsal region[1] and metatarsal heads. This two-block arrangement would lead to a double-arc of stress passing through the foot—first, as the heel is elevated and force is transferred to the midfoot at the medial cuneiform, and a second as the midfoot elevates and force is transferred to the forefoot. This pattern of force transfer is altered by the presence of the longitudinal arch in humans, where the leverage is reduced to a single arc. By elevating the midfoot region, the proximal fulcrum (axis) of the non-human primate foot was eliminated, and a single axis remained at the metatarsal heads. This change effectively lengthened the force arm of the foot as a lever by increasing the distance between the line of force (triceps surae muscles) and the axis of rotation. Such a change in the mechanics of the foot increased the mechanical advantage of the muscles acting to plantar-flex the foot, improving the foot's ability to support and propel the body's mass forward during locomotion.

Morton's model of longitudinal arch evolution emphasizes the role of the arch in transforming the foot into a rigid lever for propulsion. While he discussed the ability of the arch to deform as a compliant structure during loading, Morton believed that the arch served primarily as an adaptation to withstand forces experienced by the foot and efficiently transfer them through the foot during walking. Therefore, Morton's hypothesis

[1] Morton (1924) identified the proximal axis ("primary fulcrum") as being located at the medial cuneiform. More recent studies demonstrate that the so-called "midtarsal break" (Elftman & Manter, 1935a) observed in non-human primates primarily occurs at the lateral tarsometatarsal joint (DeSilva, 2010).

suggests that we would expect to see evidence for the presence of a longitudinal arch shortly following the evolution of other aspects of pedal anatomy associated with bipedalism, such as the enlargement of the calcaneus, and adduction and an increase in size of the first pedal ray. These features should be present in early hominin species that show evidence of bipedal locomotion.

The Role of Endurance Running in the Evolution of the Longitudinal Arch

Over the past decade, there has been increasing discussion about the role that endurance running might have played in human evolution. The "Endurance Running Hypothesis" was first presented by Carrier (1984), who proposed that a series of morphological and physiological aspects of humans, such as directly innervated sweat glands, relative lack of body hair, and an ability to regulate one's breathing pattern independent of the locomotor cycle, emerged as adaptations for effective thermoregulation and locomotor flexibility associated with endurance running. According to Carrier, these adaptations most likely evolved in the earliest members of genus *Homo*, and are associated with the movement of hominins into a diurnal predatory niche that included persistence hunting. Bramble and Lieberman (2004) have since argued that endurance running is responsible for shaping many aspects of modern human anatomy and physiology, including the evolution of the plantar longitudinal arch. During running, the ligaments that support the longitudinal arch are stretched under the impact of the runner's mass when the foot is in support phase and the arch deforms (Alexander *et al*., 1987; Stearne *et al*., 2016). A portion of the body's kinetic energy becomes stored as potential elastic strain energy in the ligamentous structures supporting the arch, and this energy is returned to the body as kinetic energy when the ligaments recoil during the push-off phase of the gait cycle,

reducing the mechanical cost of locomotion (Alexander *et al*., 1987; Stearne *et al*., 2016). Given that arch deformation and stretching of the ligamentous structures is greater in running than walking, Bramble and Lieberman (2004) argue that the longitudinal arch evolved to mitigate impact forces experienced by the foot during running, specifically.

If endurance running was the primary selective pressure that drove the evolution of the longitudinal arch, we should expect to see fossil evidence for arch presence emerge in concert with other changes in anatomy that enhance running performance, such as gracilization of the distal limb segments and lengthening of the bones of the hind limb (Bramble & Lieberman, 2004). These changes are associated with the emergence of genus *Homo*, and are not present in earlier hominins belonging to genus *Australopithecus* or *Paranthropus* (Bramble & Lieberman, 2004).

Fossil Evidence of the Longitudinal Arch

Biological anthropologists have looked for bony evidence of a longitudinal arch in the distal tibia, talus, calcaneus, navicular, calcaneus, cuboid, and metatarsal bones of fossil hominins. **Table 1.1** summarizes the fossils that have been assessed to draw conclusions about arch morphology, and denotes whether the morphology of that fossil was interpreted to suggest that a longitudinal arch was present (P) or absent (A). Here, it is clear that, 1) different bony elements have resulted in conflicting conclusions about whether a longitudinal arch was present; and 2) in some cases, the morphology of a single fossil element has been interpreted to indicate both that an arch was present and that it was absent (*e.g*., calcaneus of OH-8). The following section offers a summary of the debates surrounding fossils attributed to *Au. afarensis* and early *Homo*, as evidenced by the OH-8 pedal fossil. This discussion is not intended to be exhaustive, but rather highlights a few of

the ongoing disagreements surrounding the interpretation of longitudinal arch-related foot bone morphologies.

Australopithecus afarensis (3.8 - 2.9 Ma)

Current interpretations of fossil foot bone morphology suggest that a longitudinal arch first evolved in the Pliocene in *Australopithecus afarensis.* Lamy (1986) argued that the specimen A.L. 333-75, a talus from Hadar, exhibits an area of eburnation on the talar head that corresponds to the location where this structure would have been supported by a calcaneonavicular ("spring") ligament. The calcaneonavicular ligament plays an important role in maintaining the height of the medial longitudinal arch in its support of the talar head. Therefore, Lamy contended that fossil tali which exhibit a "ligamentar field" were likely to have been supported by a human-like calcaneonavicular ligament, and therefore the hominin was likely to have had a longitudinal arch. Lamy noted that the ligamentar field of the A.L. 333-75 specimen was more developed than that of A.L. 288-1 ("Lucy"), and suggested that there was variation in the expression of this feature within *Au. afarensis.* The A.L. 333-75 specimen also exhibits greater torsion of the talar head than A.L. 288-1, offering further evidence that the former is more human-like in its morphology. The notion that the longitudinal arch could be variably present within *Au. afarensis* was echoed and most recently advanced by DeSilva and Throckmorton (2010). These authors studied the relationship between the sagittal angle of the distal tibia and longitudinal arch height, and argued that the sagittal angle of the distal tibia is positively associated with arch height. The A.L. 333-6 and A.L. 333-7 fossil tibiae attributed to *Au. afarensis* exhibit an anteriorly inclined distal surface, and this morphology was interpreted to suggest that these hominins had a human-like longitudinal arch (DeSilva & Throckmorton, 2010). A.L. 288-1 has a

posteriorly-inclined distal tibia, however, similar to what has been observed in extant apes. Therefore, A.L. 288-1 was been interpreted to have had flat feet (DeSilva & Throckmorton, 2010). In sum, the studies by Lamy (1986) and DeSilva and Throckmorton (2010) independently characterize the A.L. 333 hominins as being more human-like in their foot and ankle morphology than A.L. 288-1, and argue for the presence of a longitudinal arch in the former and either its absence or only weak development in the latter.

Further evidence for the presence of a longitudinal arch in the A.L. 333 hominins derives from an analysis of the morphology of the A.L. 333-160 specimen, a complete fourth metatarsal from Hadar, Ethiopia (Ward *et al*., 2011). Ward and colleagues (2011) argue that the angle formed between the proximal metatarsal base and its diaphysis (base-diaphysis angle) is consistent with the presence of a longitudinal arch. They also note that the degree of torsion present in this specimen is similar to that exhibited by modern humans, indicating that the transverse arch would have also been human-like. In considering this evidence, Ward and colleagues argued that *Au. afarensis* was a committed biped with feet that included all the functionally-significant anatomical structures for modern human-like locomotion. However, a study by Mitchell and colleagues (2012) has questioned the findings of Ward and colleagues (2011). In a large comparative study, Mitchell and colleagues (2012) showed that the base-diaphysis angle of A.L. 333-160 falls well within the measured range of variation of both modern humans and *Gorilla gorilla beringei* males. Given that a longitudinal arch is not present in *G. g. beringei*, the results of Mitchell and colleagues' (2012) study weaken the association between the base-diaphysis angle and longitudinal arch presence outlined by Ward and colleagues (2011).

Most recently, Prang (2015) argued that a longitudinal arch was present in both the A.L. 333 hominins and A.L. 288-1 based on the angular morphology of their talar and calcaneal articular surfaces. The A.L. 288-1 and A.L. 333-147 talar specimens have a head

with a plantar declination similar to modern humans, and the A.L. 333-8 calcaneus has a human-like triceps surae attachment (Prang, 2015). Therefore, the results of Prang's study are somewhat inconsistent with previous studies which have characterized A.L. 288-1 as flatfooted (*e.g.*, Lamy, 1986; DeSilva and Throckmorton, 2010).

Studies of the navicular morphology of *Au. afarensis* have argued that a longitudinal arch was not present in this taxon. Harcourt-Smith (2002) and Sarmiento and Marcus (2000) have noted that the navicular tuberosity of *Au. afarensis* (A.L. 333-36 and A.L. 333-47) is large compared to that of modern humans, and may indicate that loads were carried on the medial side of the foot, thus negating the presence of a medial longitudinal arch (Elftman & Manter, 1935a; Harcourt-Smith, 2002; Harcourt-Smith & Aiello, 2004). Berillon (2003) concurs that the morphology of the navicular suggests that the medial column of the *Au. afarensis* foot lacked a longitudinal arch. The A.L. 333-36 and A.L. 333-47 navicular bones exhibit distal articular surfaces that are inclined dorsally, similar to values reported for *Pan*, as opposed to the more neutral or slightly-plantar inclination observed in modern humans (Berillon, 2003).

Early *Homo* (OH-8)

The OH-8 pedal fossil (*ca*. 1.84 Ma; Blumenschine *et al*., 2012) is arguably the most studied hominin pedal fossil specimen, yet there continues to be disagreement regarding whether this hominin had a longitudinal arch. The OH-8 fossil preserves the partial left foot of a small-bodied hominin attributed to *Homo habilis*, and includes the talus, distal calcaneus, navicular, cuneiform bones, cuboid, and the proximal end and majority of the shaft of all five metatarsals (Day & Napier, 1964). The initial description by Day and Napier (1964) suggested that an arch was present in the OH-8 hominin, and a

multivariate analysis by Day and Wood (1968) supported this conclusion by demonstrating that the talar head was more human-like than ape-like because it has a plantarly-directed angle relative to the ankle joint. Others, however, have argued that the OH-8 talus (as well as other hindfoot elements) is intermediate between humans and apes with regards to many aspects of its morphology (Oxnard, 1972; Lisowski *et al*., 1974, 1976; Oxnard & Lisowski, 1980; Kidd *et al*., 1996). Berillon (2003) studied the relationships between the angles of the articular surfaces of the OH-8 specimen and concluded that a longitudinal arch was most likely present. However, the recent study by Prang (2015) came to a different conclusion, arguing instead that a longitudinal arch was absent in OH-8 because the specimen exhibits a talonavicular joint angle that is similar to apes and well outside of the human range. However, Prang (2015) reported that the calcaneocuboid joint angle of OH-8 — which is argued to be an architectural marker of longitudinal arch presence (Berillon, 2003) — *is* within the human range, and is greater than what is observed in apes, yet still concluded that an arch was not present in OH-8.

These disagreements about whether a longitudinal arch was present in *Au. afarensis* and the OH-8 hominin stem from an incomplete understanding of how variation in foot bone morphology is related to variation in arch height. By studying these relationships *within* humans, this study tests whether select aspects of foot bone morphology are directly related to longitudinal arch height and seeks to refine our ability to assess arch presence from isolated hominin foot fossils.

STRUCTURE OF THE DISSERTATION

This dissertation is divided into six chapters. This introductory chapter has provided an introduction to the topics that will be discussed in the subsequent chapters.

Chapter 2 builds on previous work by DeSilva and Throckmorton (2010) that suggested the sagittal angle of the distal tibia could be used to assess whether a longitudinal arch was present from fossilized tibiae. Using a new sample of lateral foot and ankle radiographs, this study independently investigates whether variation in the distal tibia sagittal angle is correlated with longitudinal arch height following the methods of DeSilva and Throckmorton (2010). In addition, this study uses an ontogenetic series of human tibiae from two archaeological populations to test a hypothesis put forth by DeSilva and Throckmorton (2010), which proposed that the sagittal angle of the distal tibia develops in response to asymmetric loading of the ankle joint during the period of longitudinal arch development.

Chapter 3 investigates whether variation in aspects of human calcaneal morphology is directly linked to variation in longitudinal arch height using a sample of humans known to exhibit variation in arch height. Using data from lateral foot and ankle radiographs and magnetic resonance images (MRIs), the study presented in Chapter 3 tests whether variation in two purported markers of longitudinal arch presence are related to arch height, including the cuboid facet angle and sustentaculum tali angle of the calcaneus. The chapter then takes a further look at ontogenetic changes and adult human variation in the cuboid facet angle in two archaeological samples of skeletonized human remains. The chapter then discusses the implications of the results for estimating arch height from fossil hominin calcanei.

Chapter 4 is similar in outline to Chapter 3, but focuses on variation in metatarsal morphology and its relation to longitudinal arch height. Using data from magnetic resonance images (MRIs), the study presented in Chapter 4 tests whether variation in two purported markers of longitudinal arch presence are related to arch height, including the base-diaphysis angle and torsion of the metatarsals. The chapter then investigates

ontogenetic changes and adult human variation in metatarsal torsion in two archaeological samples of skeletonized human remains.

Chapter 5 builds on recent studies of plantar pressure variation in humans that have challenged the long-standing paradigm characterizing the human foot as a rigid structure (*e.g*., Bates *et al*., 2013; DeSilva *et al*., 2015), and investigates the effects of variation in body size, longitudinal arch height, foot shape, and speed on midfoot and total loading. While previous studies have investigated the relationship between a selection of these variables in adults, less is known about how variation in body size, arch height, and foot shape is related to midfoot loading in children. Because early hominins were of a small body size, understanding whether these variables are related among children will inform out ability to interpret foot function from fossilized pedal remains.

Chapter 6 includes a closing summary of the dissertation and discusses unresolved questions and directions for future work.

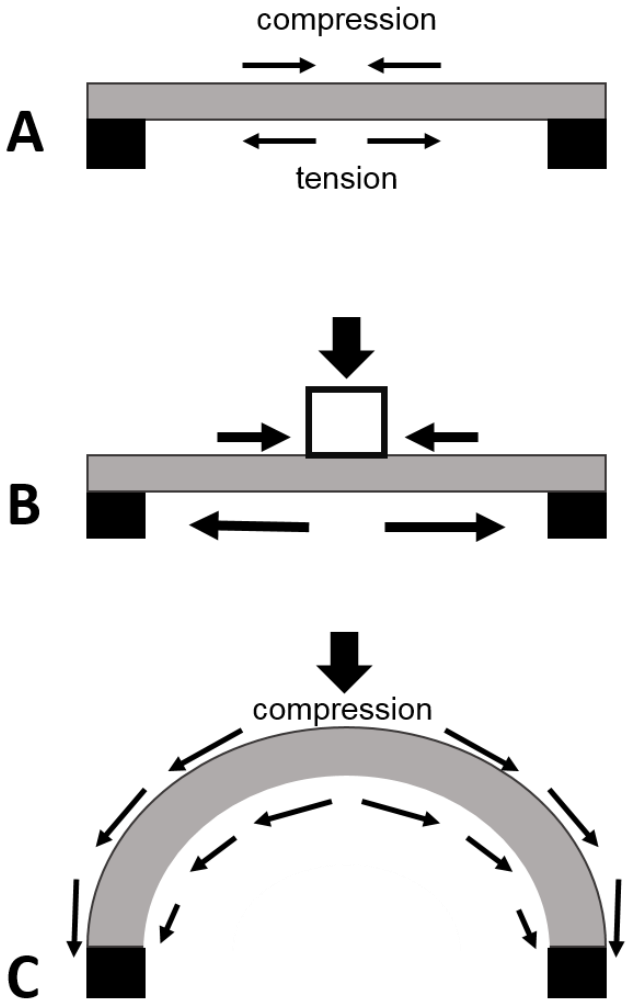

Figure 1.1: An arch resolves tension stress experienced by a material under bending into compressive stress. A) A beam that spans a space and is supported at each end will experience bending stress in response to its own weight. This bending stress is comprised of compression experienced along the beam's superior, unsupported surface, and tension along its inferior, supported surface. B) Bending stress will increase within the beam (depicted by thicker arrows) if it must also support weight from above (white square). C) An arch is a structural solution to resolve stress experienced by the beam into compression, thereby eliminating tension on the inferior surface. An arched beam can support a greater load from above without risk of fracture.

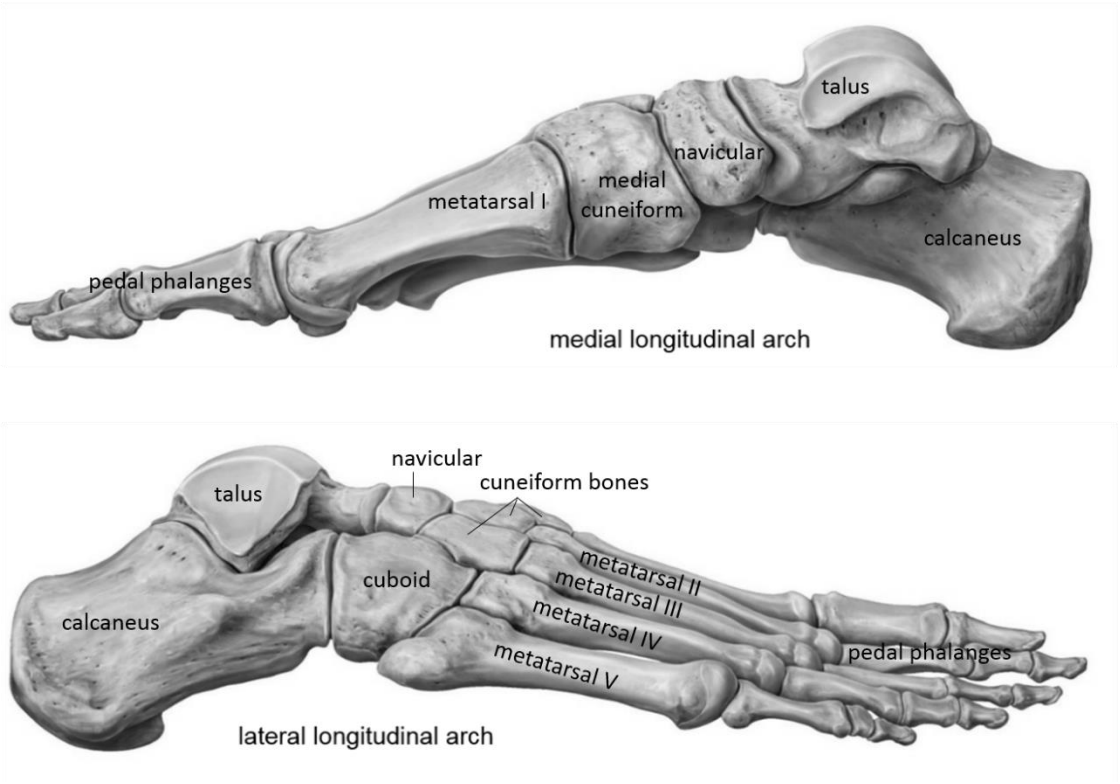

Figure 1.2: Bones of a right human foot showing the medial and lateral longitudinal arches. Image modified from Schuenke *et al*., 2017.

Specimen	Age (Ma)	Tibia	Talus	Navicular	Calcaneus	Cuboid	Metatarsals
Au. anamensis							
KNM-KP 29285	4.12	A[1]					
Au. afarensis							
A.L. 333-6	3.2	P[1]					
A.L. 333-7	3.2	P[1]					
A.L. 333-8					P[3]		
A.L. 333-36				A[6,8], P[7]			
A.L. 333-47				A[6,8], P[7]			
A.L. 333-75			P[7]				
A.L. 333-147							
A.L. 333-160	3.2		P[3]				P[4], A[5]
A.L. 288-1	3.18	A[1]	P[3,7]				
Au. africanus							
StW 88			A[3]				
StW 358	2.0-2.6	P[1]					
StW 363			A[3]				
StW 389	2.0-2.6	P[1]					
Au. sediba							
UW 88-21	2.0	P[2]					
UW 88-97	2.0	P[2]					
UW 88-98	2.0		A[3], P[10]				
UW 88-99					A[3], P[10]		
early *Homo*							
KNM-ER 813			A[3], P[7]				
KNM-ER 1464			A[3], P[7]				
KNM-ER 1476			P[7]				
KNM-ER 1481	1.9	A[1]					
KNM-ER 1500*	1.9	P[1]					
KNM-ER 2596	1.9	P[1]					
KNM-ER 5428			A[3]				
OH-8	1.84		A[3], P[6,7,11]	P[6], P[8]	A[3], P[6,7]	P[6]	P[6]
OH-35	1.85	P[1]					
Omo 33-74-896					A[3], P[9]		
Omo 323-76-898			A[3]				
StW567	1.4-1.7	A[1]					
Homo erectus							
KNM-WT 15000	1.5	P[1]					
Homo naledi			A[12]		A[12]		P[12]

[1]DeSilva & Throckmorton, 2010; [2]DeSilva, personal communication; [3]Prang, 2015; [4]Ward *et al*., 2011; [5]Mitchell *et al*., 2012; [6]Berillon, 2003; [7]Lamy, 1986; [8]Sarmiento & Marcus, 2000; [9]Deloison, 1986; [10]Zipfel *et al*., 2011; [11]Day & Wood, 1968; [12]Harcourt-Smith *et al*., 2015; *possibly *Paranthropus boisei.*

Table 1.1: Summary of literature discussing the presence or absence of a longitudinal arch in hominins. A = absent, P = present, and superscript indicates the source, listed below the table.

Chapter 2: A Second Look at the "Tibial Arch Angle" and its Relation to Longitudinal Arch Height

INTRODUCTION

Paleoanthropologists have long used fossilized foot bones and footprints to reconstruct whether a hominin had human-like, longitudinally-arched feet (*e.g.*, Stern and Susman, 1983; Lamy, 1986; Tuttle *et al*., 1990; Kidd *et al*., 1996; Berillon, 2003; Bennett *et al*., 2009; Ward *et al*., 2011; Prang, 2015). Within recent years, however, DeSilva and Throckmorton (2010) have proposed that the morphology of the distal tibia (*i.e*., ankle joint) may also indicate whether a hominin had flat or longitudinally-arched feet. Given the dearth of hominin foot bone and footprint fossils that are suitable for reconstructing gross foot form, the notion that the distal tibia could either augment or substitute for these elements has been welcomed by paleoanthropologists eager to speculate about the human-like nature of a hominin's foot and bipedal gait (*e.g*., Ward *et al*., 2011; Zipfel *et al*., 2011; Ryan and Sukhdeo, 2016). The usefulness and reliability of distal tibial morphology for reconstructing longitudinal arch height is currently unclear, however. Although DeSilva and Throckmorton (2010) discovered a statistically significant relationship between the "tibial arch angle" and two measures of medial longitudinal arch height, the relationship between these morphometric variables was weak (*i.e.*, low r^2 value) and has not been independently replicated. Moreover, the underlying basis for the proposed relationship between the morphology of the distal tibia and longitudinal arch height remains elusive and deserves further study.

DeSilva and Throckmorton (2010) proposed that the anterior inclination of the human distal tibia (in the sagittal plane) is related to the presence of the medial longitudinal

arch. In humans, the posterior margin of the distal tibial articular surface projects more inferiorly than the anterior margin, creating an anterior tilt to the distal tibia when viewed laterally. This morphology is opposite to that observed in great apes, where the anterior margin has a greater inferior projection than the posterior margin, creating a posterior tilt to the distal tibia (**Figure 2.1**; Stern and Susman, 1983). Using a large sample of human lateral foot and ankle X-rays, DeSilva and Throckmorton (2010) found a statistically significant positive relationship between the degree of anterior tilt of the human distal tibia and two measures of longitudinal arch height commonly used to assess arch height from X-rays. In addition, the authors found that individuals who had a posteriorly-inclined (*i.e.*, great ape-like) set to their distal tibia had a significantly lower longitudinal arch than those with an anteriorly-inclined distal tibia (DeSilva and Throckmorton, 2010). Given the observed relationship between the sagittal angle of the distal tibia and longitudinal arch height, the former trait was named the "tibial arch angle."

The underlying basis for the positive relationship between the anterior tilt of the human distal tibia and medial longitudinal arch height is unclear. DeSilva and Throckmorton (2010) proposed that the distal tibia may acquire an anterior tilt during early childhood as the longitudinal arch develops based on a principle known as Heuter-Volkmann law. Heuter-Volkmann law is a principle used to explain mechanical modulation of bone growth (Villemure and Stokes, 2009). As long bones grow in length, an increase in compressive loading is argued to lead to bone growth suppression, whereas a decrease in loading may lead to an acceleration in bone growth (Villemure and Stokes, 2009). With respect to the distal tibia, DeSilva and Throckmorton (2010) proposed that the developing (*i.e.*, heightening) longitudinal arch could direct asymmetric compressive loads at the distal tibia physis, which would result in an asymmetric distal tibia surface in adulthood. Specifically, they hypothesized that larger compressive loads would be directed

at the anterior margin of the distal tibia due to its proximity to the developing medial longitudinal arch, while the posterior margin would experience weaker loading. The large compressive loads experienced by the anterior margin would inhibit the proliferation of chondrocytes in this area, while chondrocyte proliferation would be either less, or unaltered, along the posterior margin. This asymmetry in chondrocyte proliferation would result in asymmetric bone growth, and ultimately the anterior inclination observed in the adult human distal tibia.

Experimental study of bone development has demonstrated that an increase in compressive mechanical loading can slow long bone growth (Villemure and Stokes, 2009), but the effects of asymmetric loading of a given long bone physis have not been investigated. Studies have, however, investigated the effects of asymmetric loading on vertebral physes in an effort to understand how mechanical loading results in vertebral wedging, as well as to develop therapies for correction of scoliosis (*e.g.*, Mente *et al*., 1997; Mente *et al*., 1999). These studies demonstrate that application of an asymmetric load to the spine can lead to vertebral wedging, and this wedging can be subsequently corrected if a reverse asymmetric load is applied (Mente *et al*, 1999). Therefore, it seems reasonable to hypothesize that long bone physes would behave similarly if subjected to asymmetric compressive loads during development.

While experimental study of distal tibia growth modulation in response to asymmetric loading is outside the scope of this chapter, the mechanism proposed by DeSilva and Throckmorton (2010) does outline a hypothesis than can be tested using data from human distal tibiae. If the anterior tilt of the human distal tibia is a developmental by-product of asymmetric loading of the distal tibial physis resulting from medial longitudinal arch development, then the sagittal angle of the distal tibia should undergo age-related changes that correspond to the timing of arch development. Specifically, the distal tibia

should become more anteriorly inclined during early childhood, especially the period from approximately 3 to 8 years of age when longitudinal arch development is most active (Bertsch *et al*., 2004).

The goals of this study are two-fold. First, this study uses a new sample of lateral foot and ankle X-rays to independently test the relationship between the sagittal angle of the distal tibia ("tibial arch angle") and medial longitudinal arch height in an attempt to replicate the findings of DeSilva and Throckmorton (2010). Second, this study investigates age-related changes in the sagittal angle of the distal tibia in an ontogenetic sample of human skeletal remains to test the hypothesis that the distal tibia becomes anteriorly-inclined during the period of longitudinal arch development.

MATERIALS AND METHODS

Sample

X-rays

Acquisition of X-rays was approved by The University of Texas at Austin IRB, study #00002030. The X-ray sample includes 123 digital planar X-ray files of the adult foot and ankle in lateral view taken from a standing, weight-bearing position. These files were collected by the staff of Austin Foot and Ankle Specialists (5000 Bee Caves Road, Austin, Texas 78746) during routine initial (*i.e*., not post-operative) podiatric exams. Each X-ray is anonymous, but is associated with the following biographical and anthropometric information: sex, age, body mass, and body mass index. The podiatrist's description and categorical classification of the patient's longitudinal arch was also available. Here, the patient's arch was classified as either "low", "low to average", "average", "average to high", or "high." This classification was based on the podiatrist's observation of the

external foot (as opposed to an X-ray), and is therefore a subjective description of the individual's longitudinal arch height[2]. **Table 2.1** summarizes the descriptive statistics for the X-ray sample.

Using a sample of clinical X-rays has inherent limitations due to the fact that the population is essentially "pathological." A strong effort was made to ensure that the X-rays included in this study represented individuals whose feet represent normal human variation. To this end, the X-rays were selected from cases where individuals presented to the clinic with a recent onset of pain or edema, but otherwise did not have a history of foot pathology. Individuals who had been long-term patients and/or suffered from long-term foot pathology were excluded from the sample. Additionally, individuals who presented to the clinic with a bony fracture were also excluded, because it is unlikely that they would have been able to stand in a full weight-bearing position during obtainment of the X-ray. And finally (although instances were rare), X-rays of the asymptomatic foot were included in cases where bilateral X-rays had been taken to serve as a comparison between the symptomatic and asymptomatic feet.

Human Osteological Remains

The human osteological sample includes the tibiae of skeletonized individuals from two archaeological populations. The first sample includes the tibiae of 179 individuals from the Mis Island Ancient Nubian skeletal collection (on loan to Michigan State University from the British Museum). The Mis Island collection includes the remains of individuals who belonged to a small medieval (*ca.* 500-1400AD) farming community located along the 4th cataract of the Nile in present-day North Sudan (Soler, 2012; Hurst, 2013). The

[2] The criteria used to classify each individual's arch height, as well as the repeatability of these classifications, is unknown.

second sample includes the tibiae of 96 individuals from the Norris Farms 36 Cemetery skeletal collection (on loan to Penn State University from the Illinois State Museum). The Norris Farms 36 Cemetery skeletal collection includes the remains of individuals of upper western Oneota tradition who occupied the central Illinois river valley of North America *ca.* 1300AD (Milner & Smith, 1990). **Table 2.2** summarizes the number of tibiae included in the study grouped according to the estimated age of the individual. Skeletal age and sex were estimated for individuals in the osteological samples using standard skeletal aging and sex-estimation techniques (Mis Island sample: Soler, 2012; Hurst, 2013; Norris Farms sample: Milner and Smith, 1990).

Fossil Hominins

Distal tibia sagittal angle values for fossil hominins were collected from the published literature and are summarized in **Table 2.3**.

Data Collection

X-rays

The distal tibia sagittal angle was measureable on 114 of the lateral foot and ankle X-rays, and was measured using ImageJ NIH software and following the methods of DeSilva and Throckmorton (2010) (**Figure 2.2**). The distal tibia sagittal angle was defined as the anterior angle of the distal tibia relative to the long axis of the tibial shaft in the sagittal plane (DTSA = distal tibia sagittal angle[3]). The line and angle measure tools were

[3] The "distal tibia sagittal angle" (DTSA) is equivalent to the "tibial arch angle" described by DeSilva and Throckmorton (2010). I have elected to use a different descriptor for this trait because "tibial arch angle" assumes that the sagittal angle of the distal tibia is linked with the morphology of the longitudinal arch. Given that this relationship is tenuous and is currently being tested, I feel it is more appropriate to use a descriptor for the trait that is directly related to its anatomy.

used to quantify the DTSA as the angle enclosed between a line connecting the anterior and posterior distal-most margins of the tibia (in lateral view) and a line bisecting the tibial diaphysis. First, the line tool was used to determine the mid-point of the tibial diaphysis in cross-section. By default, ImageJ places a tick mark at the midpoint of a line. The mid-point of the diaphysis was marked at multiple locations along its length by drawing lines across the anterior-posterior axis of the tibia perpendicular to the diaphysis. A line was then applied to connect the mid-points of these lines and mark the middle of the tibial diaphysis. Second, the line tool was used to draw a line connecting the distal-most projections of the anterior and posterior margins of the tibia. Finally, the angle measure tool was used to trace over these lines and measure the anterior angle formed between the line bisecting the tibial diaphysis and the line connecting the distal margins. The value of this angle was subtracted from 90° to calculate the deviation of the distal margins from a horizontal line perpendicular to the tibial diaphysis. Positive values of the DTSA indicate an anteriorly-inclined distal tibia, while negative values indicate a posteriorly-inclined distal tibia.

Longitudinal arch height was measured using four different metrics for each X-ray (when possible). First, Image J NIH software was used to collect two angular measurements from each digital X-ray that are commonly used among podiatrists and other health care professionals to assess longitudinal arch height (Cavanagh *et al*., 1997), and both of which were included in the DeSilva and Throckmorton (2010) study. These metrics include: α) calcaneal inclination angle (CIA) = angle between the inferior surface of the calcaneus and the substrate; and the θ) talar declination angle (TDA) = angle between a line that bisects the neck and head of the talus and the substrate (**Figure 2.2**)[4]. Next, the

[4] DeSilva and Throckmorton (2010) included a third measure of longitudinal arch height, the talocalcaneal angle, which is the sum of the calcaneal inclination angle (CIA) and the talar declination angle (TDA). I find it circular to test for a relationship between the distal tibia sagittal angle (DTSA) and the talocalcaneal angle, given that the talocalcaneal angle is the sum of the CIA and TDA. Therefore, I have chosen to omit

line measure tool was used to collect linear measurements of navicular height, talar height, and bony foot length that were then used to calculate two additional measures of longitudinal arch height, including a navicular height index (navicular height divided by bony foot length) and a talar height index (talar head height divided by bony foot length) following the methods of Cavanagh and colleagues (1997) and Salzman and colleagues (1995) (**Figure 2.3**).

Human Osteological Remains

Digital photographs were taken of the lateral distal tibia aligned parallel to the camera lens in order to mimic the orientation of the tibia in the planar X-rays. ImageJ NIH software was used to measure the DTSA following the same protocol as used to measure the DTSA on the digital planar X-rays (**Figure 2.4**). The measurement protocol was tested for both intra- and inter-rater repeatability. A subset (N = 62) of the tibiae from the Mis Island sample were photographed and measured for a pilot version of this study (Heard-Booth, 2013), and photographed and measured again 18 months later when data for the full study was collected. The correlation between measures of the DTSA taken from these separate events was $r = 0.891$ ($p < 0.001$) (**Figure 2.5**). Inter-rater repeatability was tested by having a second observer (a University of Texas undergraduate student) measure the DTSA on a subset of photographs of 47 tibiae from the Mis Island sample. The correlation between the measures taken by the author and the undergraduate student was $r = 0.987$ ($p < 0.001$), indicating that there is a strong inter-observer repeatability in the measurements of the DTSA from the photographs of the human skeletal remains (**Figure 2.6**).

---

the talocalcaneal angle and instead only test the relationship between the DTSA and the two components of the talocalcaneal angle, the CIA and TDA.

Adjustments to the described protocol were made when photographing juvenile tibiae to account for the lack of tibial torsion in infant and child remains. The tibial shaft undergoes lateral torsion (external rotation) of approximately 14º - 25º throughout childhood (Staheli and Engel, 1972; Ritter *et al*., 1976). Adult-like torsion values are usually achieved between the ages of 5 and 7 years (Turner and Smillie, 1981). Therefore, the tibia of those estimated to be younger than 6 years of age was positioned for photographs so that the surface that would ultimately *become* the lateral aspect (*i.e*., the antero-lateral surface) was parallel to the camera lens.

An additional adjustment was made to account for the absence and/or separation of epiphyses in the juvenile sample. The distal epiphysis of the tibia begins to ossify during the first year of life and is recognizable between 3 and 4 years of age as an oval-shaped disc (Scheuer and Black, 2004). The margins of the distal epiphysis approximate those of the metaphysis between the ages of 5 and 6 years (Scheuer and Black, 2004), at which point the isolated epiphysis can be snugly attached to the tibial diaphysis. The epiphysis begins to fuse to the diaphysis around the age of 12-13 years in females and 14-15 years in males (Hoerr *et al*., 1962), with complete fusion occurring between the ages of 14-16 years in females and 15-18 years in males (Scheuer and Black, 2004). Tibiae for which the distal epiphysis was missing were photographed without the epiphysis and the DTSA was measured along the distal margin of the metaphysis. In cases where the epiphysis was present but not yet fused, a small piece of clay was used to secure the epiphysis to the shaft in correct anatomical position. For these cases, the DTSA was measured at both the metaphyseal margin and the epiphyseal margin (**Figure 2.7**). The DTSA was measureable at both the epiphyseal and metaphyseal margins on 42 individuals, and results of a Pearson correlation analysis show that the DTSA measured at the epiphyseal margin is significantly positively correlated with the DTSA measured at the metaphyseal margin ($r = 0.59$, $p <$

0.01) (**Figure 2.8**). This result indicates that there is a statistically significant, yet only moderately strong, relationship between the sagittal angle of the metaphyseal margin and that of the epiphyseal margin. Therefore, the DTSA measured at the metaphyseal margin on young individuals whose tibiae lack an epiphysis approximates the DTSA value at their epiphyseal margin, but error remains in this estimate. Given the small sample sizes for juvenile individuals in the archaeological populations, however, tibiae that lacked an epiphysis were included in the analysis, and their results were interpreted with caution.

Data Analysis

Relationship between the Distal Tibia Sagittal Angle and Longitudinal Arch Height

The first goal of this study was to use a new sample of lateral foot and ankle X-rays to independently test the relationship between the DTSA and longitudinal arch height. First, each radiographic measure of longitudinal arch height was compared across the four podiatrist-designated arch height categories using a one-way analysis of variance (ANOVA). The purpose of this step was to assess the strength of the association between the radiological measures of longitudinal arch height and assessments of arch height made from the external foot surface. In other words, individuals described as having "low" arches were predicted to exhibit a mean calcaneal inclination value that was lower than individuals described as having "low to average", "average", and "average to high" arches, for example, and so on. The mean DTSA was also compared across the arch height categories, and DTSA was predicted to increase with arch height.

The analysis for the remaining portion of the study followed the methods of DeSilva and Throckmorton (2010). A non-parametric Kruskal-Wallis Test was performed to investigate whether longitudinal arch height was significantly different between

individuals with a posteriorly-inclined DTSA and those with an anteriorly-inclined DTSA. It was appropriate to use a non-parametric test for this analysis because although DTSA values were normally distributed for the entire sample, they were not normally distributed within each group (*i.e.*, Posteriorly-inclined vs. Anteriorly-inclined). If the DTSA is related to the presence of the longitudinal arch, then a significant difference in each of the four measures of arch height between individuals who have an anteriorly-inclined DTSA and those with a posteriorly-inclined DTSA should be observed. Next, a Pearson's product moment correlation test was used to investigate the relationship between the DTSA and each of the four radiographic measures of longitudinal arch height. The DTSA was predicted to exhibit a positive correlation with the four measures of longitudinal arch height.

Finally, the DTSA values for hominin fossils were plotted alongside those from the radiographic sample in order to discuss what can be gleaned about longitudinal arch height from hominin distal tibial morphology.

Ontogenetic Changes in the Distal Tibia Sagittal Angle

The second goal of this study was to investigate whether the sagittal angle of the distal tibia becomes more anteriorly inclined throughout ontogeny, particularly during the period of medial longitudinal arch development. For statistical analyses, individuals were placed into the following age categories: 1-2 years (early bipedal walkers that lack a longitudinal arch); 2-4 years (bipedal walkers beginning to develop a longitudinal arch); 4-6 years (bipedal walkers with a developing longitudinal arch); 6-12 years (bipedal walkers with a developed longitudinal arch and a growing foot); 12-20 years (bipedal walkers with a developed longitudinal arch and adult-sized foot, but who continue to grow in stature);

and 20+ (bipedal walkers with an adult foot size and stature). These developmental milestones were identified from studies of foot and body growth in contemporary populations (Bertsch *et al*., 2004; Scheuer & Black, 2004), and it is unknown whether this schedule of development has changed through time. Mean DTSA values were compared between age categories using a one-way ANOVA. The mean DTSA was predicted to be smallest in the youngest age category, and then increase with age. Mean DTSA was predicted not to differ between those aged 6-12, 12-20, and 20+ years, given that the arch reaches maturity around age 6 (Bertsch *et al*., 2004).

All statistical analyses were performed in SPSS version 23.0 (IBM).

RESULTS

Relationship between the Distal Tibia Sagittal Angle and Longitudinal Arch Height

Descriptive statistics for the four radiographic measures of longitudinal arch height are presented in **Table 2.4**. The longitudinal arch height was categorized by the podiatrist for 102 individuals, where 6 (5.9%) were described as having a "low" arch, 75 (73.5%) were described as having a "low to average" arch, 19 (18.6%) were described as having an "average" arch, and 2 (2.0%) were described as having an "average to high" arch.

A one-way ANOVA was performed to determine whether each of the four, continuous radiographic measures of longitudinal arch height was significantly different between individuals in the four arch height categories. **Figures 2.9 A-D** show box-plots of the median and interquartile range of each radiographic measure of longitudinal arch height across the four arch height categories. Arch height category had a significant effect on calcaneal inclination angle (CIA) [$F(3, 102) = 4.82$, $p = 0.004$], and post-hoc comparisons using the Tukey HSD test indicate that the mean CIA of individuals categorized as having

"low" arches (Mean = 14.00, SD = 6.07) is significantly lower than the mean CIA of those categorized as having "average" (Mean = 21.37, SD = 3.52) and "average to high" arches (Mean = 25.64, SD = 3.76) (**Figure 2.9A**). Arch height category also had a significant effect on talar height index (THI) [$F(3, 96) = 3.4$, $p = 0.021$], and post-hoc comparisons indicate that the mean THI of those categorized as having "low" arches (Mean = 0.21, SD = 0.04) is significantly lower than those described as having "average to high" arches (Mean = 0.28, SD = 0.01) (**Figure 2.9D**). The talar declination angle was not statistically different between arch height categories [$F(3, 101) = 1.898$, $p = 0.135$] (**Figure 2.9B**), nor was the navicular height index [$F(3, 86) = 2.525$, $p = 0.063$] (**Figure 2.9C**). However, **Figure 2.9C** shows that the median navicular height index increases with arch height category, and this trend is consistent with predictions.

The DTSA was measured on 114 X-rays. Of these, 105 individuals (92%) had an anterior tilt at the distal tibia (DTSA > 0°), and 9 (8%) had a posterior tilt (DTSA < 0°). The DTSA was not correlated with body weight ($r = -0.092$, $p = 0.357$), body mass index ($r = -0.181$, $p = 0.069$), or age ($r = -0.002$, $p = 0.981$), and did not differ between males and females [$t(112) = 1.119$, $p = 0.233$]. **Table 2.5** summarizes the descriptive statistics for the DTSA across the entire sample, and also for the individuals within each of the arch height categories. A one-way ANOVA found no statistical difference in DTSA between the qualitative arch height groups [$F(3, 98) = 1.459$, $p = 0.230$] (**Figure 2.10**). In fact, the mean DTSA was lowest for the group of individuals whose arch was described as "average to high" in height, a result that is the direct opposite of what was predicted (**Table 2.5**).

The relationship between longitudinal arch height and the DTSA was tested using both a non-parametric Kruskal-Wallis Test and a Pearson's product-moment correlation following the methods of DeSilva and Throckmorton (2010). The Kruskal-Wallis Test found no statistical difference in any of the four radiographic measures of longitudinal arch

height between those individuals whose distal tibia has a posterior tilt and those with an anterior tilt (**Table 2.6**). In other words, individuals with an anteriorly-inclined distal tibia had a similar longitudinal arch height as those with a posteriorly-inclined distal tibia, irrespective of the radiographic method used to measure longitudinal arch height.

A Pearson's product-moment correlation test was performed to investigate the relationship between the DTSA and each of the four radiographic measures of longitudinal arch height. No statistically significant relationship was detected between the DTSA and any of the measures of longitudinal arch height (**Table 2.7**; **Figures 2.11 A-D**).

Ontogenetic Changes in the Distal Tibia Sagittal Angle

The DTSA was measured on 275 tibiae belonging to two archaeological samples (Mis Island, N=179; Norris Farms, N=96). **Table 2.8** summarizes the descriptive statistics for the DTSA for the six age categories across both samples and for the sample as a whole. These statistics were calculated using the DTSA value measured at the metaphyseal margin for young individuals for whom an epiphysis was absent, and at the epiphyseal margin in cases where a) an epiphysis was not yet fused but could be accurately placed and adhered to the metaphysis, and b) the epiphysis was fused. An independent samples t-test found no significant difference in the DTSA between the Mis Island and Norris Farms samples [$t(271) = 0.264$, $p = 0.792$], so the samples were combined for further analyses (**Figure 2.12**).

A total of 257 (94.1%) tibiae had an anteriorly-inclined distal tibia sagittal angle (DTSA > 0º), while 16 (5.9%) had a posteriorly-inclined distal tibia (DTSA < 0º) when the entire sample is considered. Of those individuals who exhibited a posteriorly-inclined DTSA, seven were juveniles aged 1-2 years, one was a juvenile aged 2-4 years, one was a

juvenile aged 4-6 years, and two were juveniles aged 6-12 years. Of these eleven juveniles, the distal epiphysis was not present for ten of them, which suggests that the epiphysis may contribute to the anterior inclination of the human distal tibia. Five of the sixteen individuals with a posteriorly-inclined DTSA were adults over the age of 20.

A one-way ANOVA test found that estimated age had a significant effect on DTSA for the combined archaeological samples [$F(5, 267) = 4.57$, $p < 0.01$] (**Figure 2.13**). Post-hoc comparisons using the Tukey HSD test indicated that the mean DTSA at ages 1-2 years (Mean = 3.47, SD = 4.62) is significantly different from the mean DTSA at ages 12-20 years (Mean = 7.61, SD = 3.20) and >20 years (Mean = 6.03, SD = 3.28); and mean DTSA at ages 2-4 years (Mean = 4.55, SD = 3.21) is significantly different from the mean DTSA at ages 12-20 years (Mean = 7.61, SD = 3.20). In other words, individuals aged 1-2 years and 2-4 years had a significantly smaller (*i.e.*, less anteriorly-inclined) DTSA than individuals aged 12-20 years, and those aged 1-2 years also had a significantly smaller DTSA than adult individuals >20 years of age. The smaller DTSA value observed in individuals aged 1-2 and 2-4 years is likely due to the absence of the distal epiphysis.

Fossil Hominin Distal Tibiae and Longitudinal Arch Height

This study was not able to independently replicate the findings of DeSilva and Throckmorton (2010), who found a statistically significant relationship between the DTSA and two radiographic measures of longitudinal arch height. Therefore, the DTSA may not be an appropriate marker of longitudinal arch height in fossil hominins. **Figure 2.14A** shows the distribution of DTSA values reported in the literature for fossil hominins alongside those measured in this study for individuals with "low", "low to average", "average", and "average to high" arches. **Figure 2.14B** shows the same data with each

fossil hominin represented as a single specimen (see **Table 2.3** for the fossil hominin DTSA values). These figures demonstrate that the DTSA values reported for fossil hominins overlap with those of modern humans of all arch heights, and it is therefore not possible to describe the arch of a given specimen based on the sagittal angle of their distal tibia. For example, the DTSA value of 4.2° for StW 358 falls within the interquartile range of DTSA values for individuals whose medial longitudinal arch has been described as "low", "low to average", and "average". Therefore, based on the results of the present study, the distal tibia sagittal angle of fossil hominins should not be used to inform the reconstruction of their longitudinal arch height.

DISCUSSION

Human Variation in the Distal Tibia Sagittal Angle

The results of this study are consistent with previous studies reporting that the majority of modern humans have an anteriorly-inclined distal tibia articular surface (Davis, 1964; Stern & Susman, 1983; DeSilva & Throckmorton, 2010). In the current study, 92% of the contemporary X-ray sample, and 96.1% and 89.6% of the Mis Island and Norris Farms samples, respectively, exhibited an anteriorly-inclined distal tibia. These percentages are within the range of percentages reported by DeSilva and Throckmorton (2010) for the contemporary and archaeological samples included in their study (**Table 2.9**). Therefore, the available data support the conclusion that an anteriorly-inclined distal tibia is characteristic of modern humans, although a small percentage of humans exhibit an ape-like, posteriorly-inclined distal tibia articular surface.

While it is clear that the majority of humans exhibit an anteriorly-inclined distal tibia, there remains a wide range of variation in the distal tibia sagittal angle (DTSA) among

individuals. **Table 2.9** presents descriptive statistics describing the range of variation for the samples included in the present study and those included in the DeSilva and Throckmorton (2010) study. If all individuals in the archaeological samples from the present study are considered, the DTSA had a total range of 26.09°, and this range drops to 18.5° if only adults are considered. This decrease occurs because younger individuals, especially those younger than 4 years of age, tend to have a smaller DTSA than adults, so their inclusion expands the overall size of the range. Therefore, including subadult remains in the sample increases the total range. The X-ray sample was limited to adult individuals and the total range of DTSA values was smaller (15.64°) than what was observed in the archaeological samples. The X-ray sample from the DeSilva and Throckmorton (2010) study had the highest range (23.0°) of all samples, though this could be the result of also having the largest sample size.

The cross-sectional ontogenetic data presented here suggest that the DTSA becomes more anteriorly inclined with age, with the greatest distinction in incline between the youngest and oldest individuals in the sample. According to the hypothesis put forth by DeSilva and Throckmorton (2010), the anterior inclination of the DTSA was predicted to increase in early childhood during the period of longitudinal arch development. This prediction would have corresponded to an increase in the DTSA between ages 1-2, 2-4 and 4-6, given that arch development is most active during this age range (Bertsch *et al*., 2004). Instead, individuals in the sample aged 1-2 years and 2-4 years had a significantly lower DTSA than those aged 12-20 years, and those aged 1-2 years were also distinct from the adults in the sample. There was not a significant increase in the DTSA between the ages of 1-2, 2-4, and 4-6, however. These results indicate that very young children for whom the longitudinal arch is just beginning to develop have a lower (*i.e*., less anteriorly-inclined) DTSA than those individuals whose feet have achieved their adult size (though the 12-20

year olds still experience variable growth in stature). The tibiae of these young individuals (aged 1-2 and 2-4 years) lack a distal epiphysis, however, which may explain the lower DTSA value for these groups.

The ontogenetic data used in this study have a number of limitations, and age-related changes in the DTSA detected here should be interpreted with caution. First, the ages used in this study were estimated from dental and osteological remains, and many standard skeletal aging techniques have a wide margin of error. The effect of over or under estimating the age of the individual is potentially large given that this study attempted to track changes in the DTSA over a relatively narrow age range. The analysis would be improved by using a sample of osteological remains or contemporary X-rays where the exact chronological age of the individual is known. Second, the data are cross-sectional in nature, and do not actually measure how the DTSA may have changed throughout a given individual's lifetime. Being able to track age-related changes in the DTSA within individuals would refine our understanding of whether the DTSA becomes more anteriorly-inclined with age and, if so, during what developmental period(s).

The Distal Tibia Sagittal Angle and Longitudinal Arch Height

Using an independent sample of radiographs, this study was not able to replicate the results of DeSilva and Throckmorton (2010), and did not find a positive relationship between the sagittal angle of the distal tibia and longitudinal arch height. This result was not unexpected, however, given that the correlation previously detected between the DTSA and radiographic measures of longitudinal arch height was weak, albeit statistically significant. DeSilva and Throckmorton (2010) found that the DTSA was positively correlated with the talar declination angle ($r = 0.21$, $p = 0.001$) and talocalcaneal angle (r

= 0.16, p = 0.009), but not the calcaneal inclination angle (r = 0.03, p = 0.61). The coefficients for these relationships are low, and show that the talar declination angle and talocalcaneal angle explain only a very small proportion of the variance in longitudinal arch height (4.4% and 2.6%, respectively). The weakness of this correlation questions whether the statistical significance detected by DeSilva and Throckmorton (2010) between the DTSA and longitudinal arch height has any real biological significance. The fact that the present study failed to find a statistically significant relationship between the DTSA and longitudinal arch height underscores the weakness of the association detected in the original DeSilva and Throckmorton (2010) paper, and suggests that the DTSA should not be used to estimate longitudinal arch height from fossilized hominin tibiae.

.

Implications for Fossil Hominins

The results presented here argue that conclusions about whether a hominin's foot had a longitudinal arch should not be drawn from the morphology of their distal tibia. In the original DeSilva and Throckmorton (2010) study, the DTSA was used to assess whether a longitudinal arch was present for 12 hominin individuals representing the species *Australopithecus anamensis, Au. afarensis, Au. africanus,* and genus *Homo* (**Table 2.3**). In subsequent years, the DTSA has been used by Zipfel and colleagues (2011) to comment on the nature of the longitudinal arch of *Au. sediba*, and has also been cited by Ward and colleagues (2011) to bolster the claim that *Au. afarensis* had a longitudinally-arched foot. Most recently, Ryan and Sukhdeo (2016) have used the DTSA to suggest that the KSD-VP-1/1 hominin (*Au. afarensis*) had a longitudinally-arched foot.

For a number of hominin fossil individuals featured in the DeSilva and Throckmorton (2010) study, the finding that the DTSA is uninformative with respect to

whether their foot had a longitudinal arch will alter current reconstructions of foot morphology and/or locomotor biomechanics because the distal tibia was the only evidence used to discuss the longitudinal arch. For example, there are no pedal fossils attributed to *Au. anamensis*, a species for whom most available fossil specimens are cranio-dental (Leakey *et al*., 1998; Ward *et al*., 2001). The fossil specimen KNM-KP 29285B is a distal tibia from Kanapoi, Kenya (4.07-4.17 ± 0.03 Ma; Leakey *et al*., 1998; Ward *et al*., 2001) that has a posteriorly-inclined distal tibia with a DTSA of -1.8º (DeSilva and Throckmorton, 2010). The negative DTSA led DeSilva and Throckmorton (2010) to conclude that *Au. anamensis* was flat footed. However, data from the current study shows that individuals from the contemporary X-ray sample who had a similar DTSA value had feet that were described by a podiatrist as having a "low to average" longitudinal arch height, while an individual who had an even lower DTSA value was described as having an "average" arch height (**Figure 2.14B**). Therefore, it is not possible to conclude whether the KP 29285 *Au. anamensis* individual was flat footed, or that its feet had a longitudinal arch, based on their DTSA value of -1.8º. The distal tibia of *Au. anamensis* is human-like in other aspects of its morphology, such as having a relatively narrow width of the anterior margin of the distal tibia articular surface, and a shaft positioned roughly perpendicular to the ankle joint (DeSilva, 2009). These morphologies suggest that the foot of *Au. anamensis* was not habitually loaded in a dorsiflexed position (as occurs during vertical climbing bouts in apes), and that it contacted the ground on its plantar surface (*i.e*., was not inverted) (Ward *et al*., 2001; DeSilva, 2009). Whether the foot of *Au. anamensis* was also human-like with respect to arch morphology is unknown, however, and determination will have to wait until pedal fossils are discovered.

For other hominin fossil individuals, finding that the DTSA is uninformative with respect to whether their foot had a longitudinal arch does not alter current reconstructions

of foot morphology because other—and arguably, more informative—fossil evidence has been used to reconstruct arch morphology. In the case of *Au. sediba*, there was disagreement about whether a longitudinal arch was present based on the morphology of the distal tibia and the pedal fossils (Zipfel *et al*., 2011; Prang, 2015). Zipfel and colleagues (2011) described two distal tibiae recovered from Malapa, including U.W. 88-97 and U.W. 88-21, both of which exhibit a human-like, anteriorly-inclined DTSA, valued at 6.7° and 4.9º, respectively (DeSilva, personal communication). The presence of an anterior tilt at the distal tibia was initially interpreted by Zipfel and colleagues (2011) to suggest that a longitudinal arch was present in *Au. sediba*, in spite of the fact that the overall ankle and foot morphology of the Malapa hominins exhibits a unique mosaic of primitive and derived traits. While the ankle of *Au. sediba* was human-like in having an anteriorly-inclined DTSA and a tibial shaft positioned perpendicular to the distal tibia articular surface, other aspects of the *Au. sediba* ankle, such as the presence of a robust medial malleolus, are ape-like (Zipfel *et al*., 2011). Similarly, the foot exhibits an ape-like large talar head and absence of a lateral plantar process on the calcaneus, combined with evidence for a human-like retrocalcaneal bursa and Achilles tendon (Zipfel *et al*., 2011). In a recent study, Prang (2015) argued that the angulation of the joint surfaces of the talus and calcaneus of *Au. sediba* indicated that it did not have a longitudinally-arched foot. One of the angles included in the Prang (2015) study—the cuboid facet angle of the calcaneus—will be discussed in the following chapter as having a statistically significant positive relationship with longitudinal arch height. The low value of this angle in *Au. sediba* is one line of evidence used by Prang (2015) to suggest that an arch was absent, and the results of Chapter 3 in this dissertation are in support of this conclusion. Therefore, given that the anteriorly-inclined DTSA was the only morphology cited to suggest that the feet of *Au. sediba* had a longitudinal arch, the results of this study lend support to the findings of Prang (2015) that

an arch was absent in the Malapa hominins. The reconstruction of *Au. sediba* as having flat feet is consistent with the presence of numerous ape-like morphologies of the medial foot and ankle which suggest that *Au. sediba* had a more mobile subtalar joint with a primitive mechanism of force transmission through hind-foot and ankle (Zipfel *et al*., 2011).

The fossil hominin that featured most prominently in the DeSilva and Throckmorton (2010) study was A.L. 288-1 ("Lucy"), the only *Au. afarensis* specimen sampled to exhibit a posteriorly-inclined distal tibia. A.L. 288-1 has a DTSA value of -5.0º, which is the most posteriorly-inclined distal tibia of all fossil hominins and near the median reported for chimpanzees and gorillas (DeSilva and Throckmorton, 2010). DeSilva and Throckmorton (2010) interpreted this morphology to suggest that Lucy was asymptomatically flat footed, given that other aspects of Lucy's ankle morphology are human-like (DeSilva, 2009). No human in the current study exhibited a DTSA as low as Lucy's, though DeSilva and Throckmorton (2010) reported a minimum DTSA of -5.0º for their X-ray sample. Therefore, Lucy's DTSA is at the bottom of the observed range for modern humans, but fits at the center of the observed range for chimpanzees and gorillas (DeSilva & Throckmorton, 2010). Given the results of the current study, Lucy's low DTSA value does not necessarily mean that she was flat footed, although she may have been. An alternative interpretation is that the posterior tilt of Lucy's distal tibia is simply another example of a primitive morphology present in the A.L. 288-1 skeleton (Stern and Susman, 1983). Stern and Susman (1983) noted that this "plantarflexion set" to Lucy's distal tibia was consistent with the morphology of her distal fibula, which articulates with her talus in a very ape-like manner, permitting a large range of plantarflexion. Overall, the morphology of Lucy's ankle joint is distinct from that of the large-bodied Hadar hominins in a number of ways, observations that initially led Stern and Susman (1983) to suggest that there were biomechanical differences in the bipedal locomotion of the small- and large-bodied

hominins at Hadar. The recently discovered KSD-VP-1/1 partial skeleton from Woranso-Mille represents a large-bodied *Au. afarensis* individual that pre-dates Lucy (Saylor *et al*., 2015). KSD-VP-1/1 preserves a distal tibia with a DTSA of 3.0º, a value more similar to other large-bodied *Au. afarensis* hominins from Hadar (*e.g*., A.L. 333-6 = 2.9º; A.L. 333-7 = 5.5º; DeSilva and Throckmorton, 2010; Ryan and Sukhdeo, 2016; **Table 2.3**). While Ryan and Sukhdeo (2016) interpreted the anterior inclination of the KSD-VP-1/1 hominin as suggestive of the presence of a longitudinal arch, the more parsimonious explanation may be the one initially offered by Stern and Susman (1983), that there were differences in the locomotor repertoire between small and large-bodied members of *Au. afarensis*, and that large-bodied members of *Au. afarensis* had an ankle morphology that was more similar to modern humans.

Functional Explanations for Variation in the Distal Tibia Sagittal Angle

If the DTSA is not related to medial longitudinal arch height, then the question remains as to what functional explanation can be offered to explain the difference in its expression between humans and apes. Early functional explanations focused on inter-specific differences in the range of motion allowed at the ankle joint. Davis (1964) was the first to comment on the morphology of the DTSA, and proposed that the anterior inclination of the human distal tibia was an adaptation to accommodate the large dorsiflexion angles produced just prior to the push-off phase of the bipedal gait cycle. Similarly, Stern and Susman (1983) argued that a posteriorly inclined distal tibia allowed apes to achieve large plantarflexion angles during hanging postures. These explanations are improbable, however, given logic previously discussed by DeSilva and Throckmorton (2010). First, humans are not unique in using large dorsiflexion angles. In fact, chimpanzees habitually

utilize greater dorsiflexion angles during vertical climbing (DeSilva, 2009), and they do so with a distal tibia presumably adapted to promote plantarflexion, not dorsiflexion. Second, humans are able to achieve large plantarflexion angles in spite of having a distal tibia presumably adapted to promote dorsiflexion, a feat particularly evident in professional ballet dancers (Hamilton *et al*., 1992). And while it has been shown that humans who habitually engage in climbing are capable of achieving chimpanzee-like degrees of dorsiflexion (Venkataraman *et al*., 2013), it is unclear how human plantarflexion compares to that observed in chimpanzees or other apes.

Adult joint shape results, in part, from mechanical loads applied during growth (Frost, 1999). DeSilva and Throckmorton (2010) cited Heuter-Volkmann's law as a possible explanation for why humans have an anteriorly-inclined distal tibia. They proposed that asymmetric compressive forces directed at the distal tibia would slow bone development along the anterior margin (where compression was highest), and leave bone development along the posterior margin uninterrupted. By this same logic, apes must then experience higher compressive loads and reduced bone development along the posterior margin of their distal tibia, and bone development should be uninterrupted along the anterior margin. Currently, there is little information about how the ankle joint is loaded during the early stages of locomotor independence that could be used to assess whether humans and apes experience greater loading of the anterior and posterior margins of their ankle joint, respectively. Recent work by Zeininger (2014) has shown that the direction of ground reaction forces changes with age and foot posture in human toddlers learning to walk, shifting from anterior to posterior as the toddler's gait matures. Therefore, it is conceivable that chondrocyte proliferation and subsequent bone growth could be slowed along the anterior margin of the distal tibia in response to the anteriorly-located ground reaction forces in young toddlers, as opposed to the heightening of the longitudinal arch as

proposed by DeSilva and Throckmorton (2010). Whether chimpanzees and/or other apes experience more posteriorly-directed ground reaction forces during the early stages of locomotor development is unknown. Infant chimpanzees and gorillas are highly suspensory compared to adults, yet these early suspensory behaviors are primarily forelimb dominated (Doran, 1992; Doran, 1997). Data on the relative frequency of hind limb suspension is lacking for young apes, as is kinematic data for how behaviors such as vertical climbing and plantar-flexed hanging affect ankle joint loading.

Finally, it is worth noting that the mechanism of bone growth modulation proposed under Heuter-Volkmann Law is not the only way in which external, mechanical forces can affect bone growth. An alternative explanation follows the work of Frost (1997, 1999), who argued that, below a given threshold (which may be growth plate-specific), compressive loading will actually promote bone growth, rather than impede it. According to Frost (1997, 1999), it is only when compressive loads exceed a given threshold that bone growth will actually slow or cease all together. This understanding of skeletal physiology is directly opposite to that proposed under Heuter-Volkmann law, and therefore sets up the opposite set of predictions for the relationship between the location of compressive joint loading and subsequent bone growth for humans and apes. In other words, it is possible that humans have an anteriorly-inclined distal tibia with more bone present posteriorly because humans experience greater loading of the posterior margin of the tibia, and bone has developed in response to increased loading in that region. For apes, this scenario would dictate that they experience greater loading of the anterior margin of the distal tibia, and bone has developed in response to increased loading in that region. In this model, bone deposition occurs in areas that experience greater loading as a means of improving the bone's ability to resist stress in that region. In the case of humans, therefore, it could be that the posteriorly-directed ground reaction forces experienced as the bipedal gait matures

actually promote bone growth along the posterior margin of the distal tibia as a means of mitigating loads across this region of the ankle joint (Zeininger, 2014). In the case of apes, perhaps behaviors such as climbing with a highly dorsiflexed foot increase stress across the anterior margin of the distal tibia, causing bone growth to increase in this region as a means of buttressing against the additional joint stress. Again, further information about human and ape ankle joint loading throughout ontogeny and during different behaviors is needed to adequately test these hypotheses.

CONCLUSIONS

- The majority of modern humans have an anteriorly-inclined distal tibia sagittal angle, though up to approximately 10% of the population may exhibit a posteriorly-inclined (*i.e.*, ape-like) distal tibia.
- The distal tibia sagittal angle is highly variable between individuals and populations.
- The distal tibia sagittal angle appears to undergo age-related changes, becoming more anteriorly-inclined once adult foot size is achieved. However, these age-related differences may be influenced by epiphyseal fusion.
- In the current study sample, the distal tibia sagittal angle had no relation to medial longitudinal arch height, a result that is inconsistent with a previously published report (DeSilva & Throckmoron, 2010).
- The results of the current study caution against using the distal tibia sagittal angle to estimate longitudinal arch height for fossil hominins.

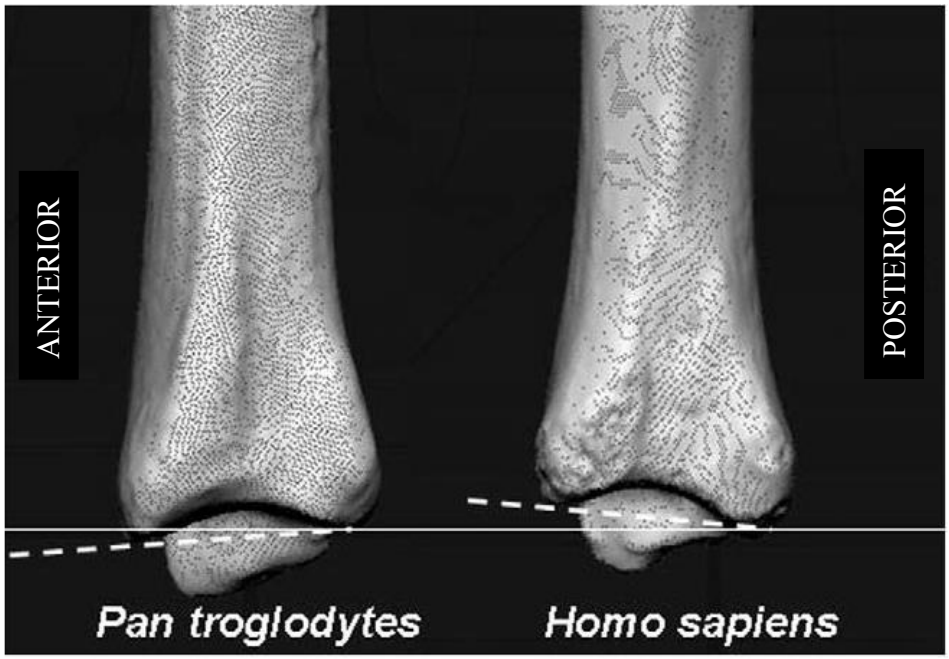

Figure 2.1: Comparison of the left distal tibia morphology of great apes and humans in lateral view. In great apes, as exhibited by *Pan troglodytes*, the anterior margin projects more inferiorly than the posterior margin, creating a posterior inclination of the joint surface. In *Homo sapiens*, the posterior margin projects more inferiorly than the anterior margin, creating an anterior inclination of the joint surface. Image modified from DeSilva and Throckmorton (2010).

	N	Mean	SD	Minimum	Maximum
Sex					
males	76	----	----	----	----
females	42	----	----	----	----
Age	----	34.66	15.97	7	79
Body Weight (lbs)	----	176.15	48.34	58.0	320.0
Body Mass Index	----	27.49	6.38	14.9	51.6
Arch					
low	6	----	----	----	----
low to average	75	----	----	----	----
average	19	----	----	----	----
average to high	2	----	----	----	----

Table 2.1 Descriptive statistics for the radiographic sample. Data were not available for all radiographs. The total number of radiographs used in the study was 123.

	Age Categories (years)						
	1-2	**2-4**	**4-6**	**6-12**	**12-20**	**>20**	**TOTAL**
Mis Island	7	10	9	16	9	128	179
Norris Farms	21	16	4	10	15	30	96
TOTAL	28	26	13	26	24	158	275

Table 2.2: Summary of the number of tibiae included in the study.

Specimen	Species	DTSA (°)	Source
KNM-KP 29285	*Au. anamensis*	-1.8	DeSilva & Throckmorton, 2010
KSD-VP-1/1e	*Au. afarensis*	3.0	Ryan & Sukhdeo, 2016
A.L. 333-6	*Au. afarensis*	2.9	DeSilva & Throckmorton, 2010
A.L. 333-7	*Au. afarensis*	5.5	DeSilva & Throckmorton, 2010
A.L. 288-1	*Au. afarensis*	-5.0	DeSilva & Throckmorton, 2010
StW 358	*Au. africanus*	4.2	DeSilva & Throckmorton, 2010
StW 389	*Au. africanus*	3.7	DeSilva & Throckmorton, 2010
U.W. 88-21	*Au. sediba*	4.0	DeSilva, personal communication
U.W. 88-97	*Au. sediba*	6.7	DeSilva, personal communication
KNM-ER 1481	early *Homo*	-2.1	DeSilva & Throckmorton, 2010
KNM-ER 1500	*P. boisei (?)*	3.7	DeSilva & Throckmorton, 2010
KNM-ER 2596	species unknown	0.8	DeSilva & Throckmorton, 2010
OH-35	early *Homo*	4.8	DeSilva & Throckmorton, 2010
StW576	early *Homo*	-3.0	DeSilva & Throckmorton, 2010
KNM-WT 15000	*Homo erectus*	1.8	DeSilva & Throckmorton, 2010

Table 2.3: Summary of distal tibia sagittal angle (DTSA) values reported for fossil hominin tibiae in the published literature.

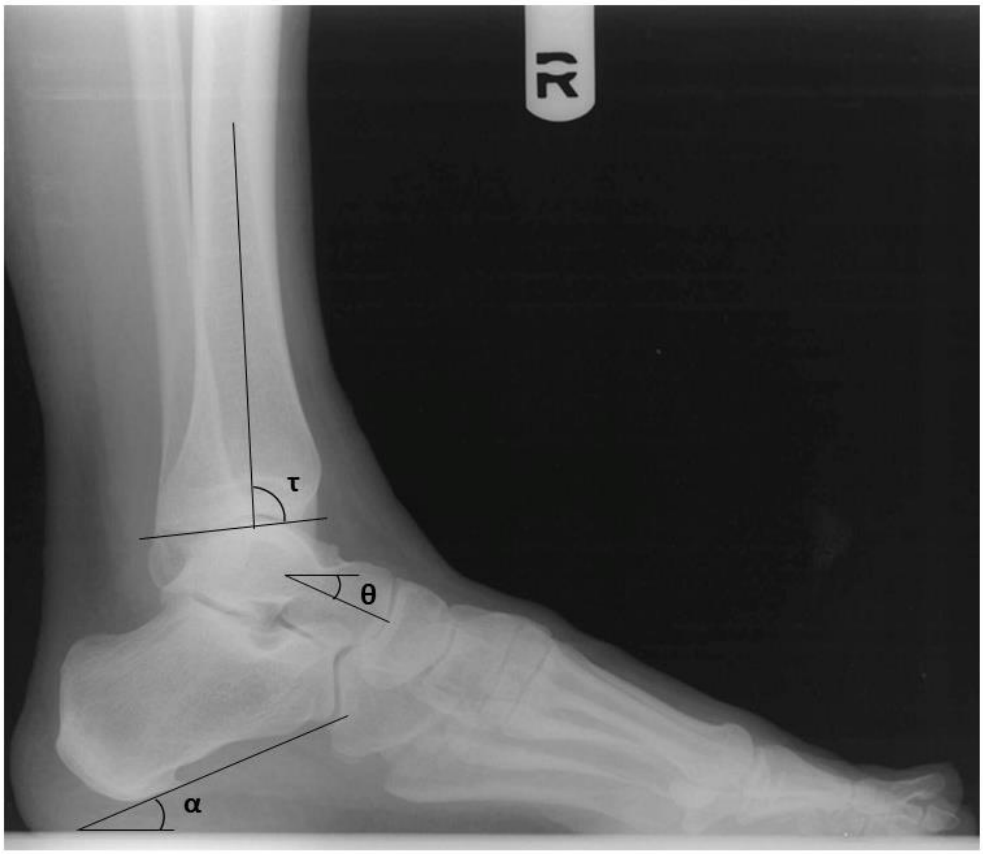

Figure 2.2: Measurement of the distal tibia sagittal angle (τ); talar declination angle (θ); and calcaneal inclination angle (α) on digital lateral foot and ankle radiographs. DTSA was calculated as 90º-τ. Positive values indicate an anteriorly-inclined DTSA; negative values indicate a posteriorly-inclined DTSA.

Figure 2.3: Linear measurements used to calculate the navicular height index and talar height index of longitudinal arch height. ε = talar head height; ω = navicular height; and λ = bony foot length. Navicular height index was calculated as ω/λ, and talar height index was calculated as ε/λ.

Figure 2.4: Measurement of the distal tibia sagittal angle (DTSA) of adult remains on digital photographs of a left tibia from the human osteological sample. DTSA was calculated as 90º-β. Positive values indicate an anteriorly-inclined DTSA; negative values indicate a posteriorly-inclined DTSA.

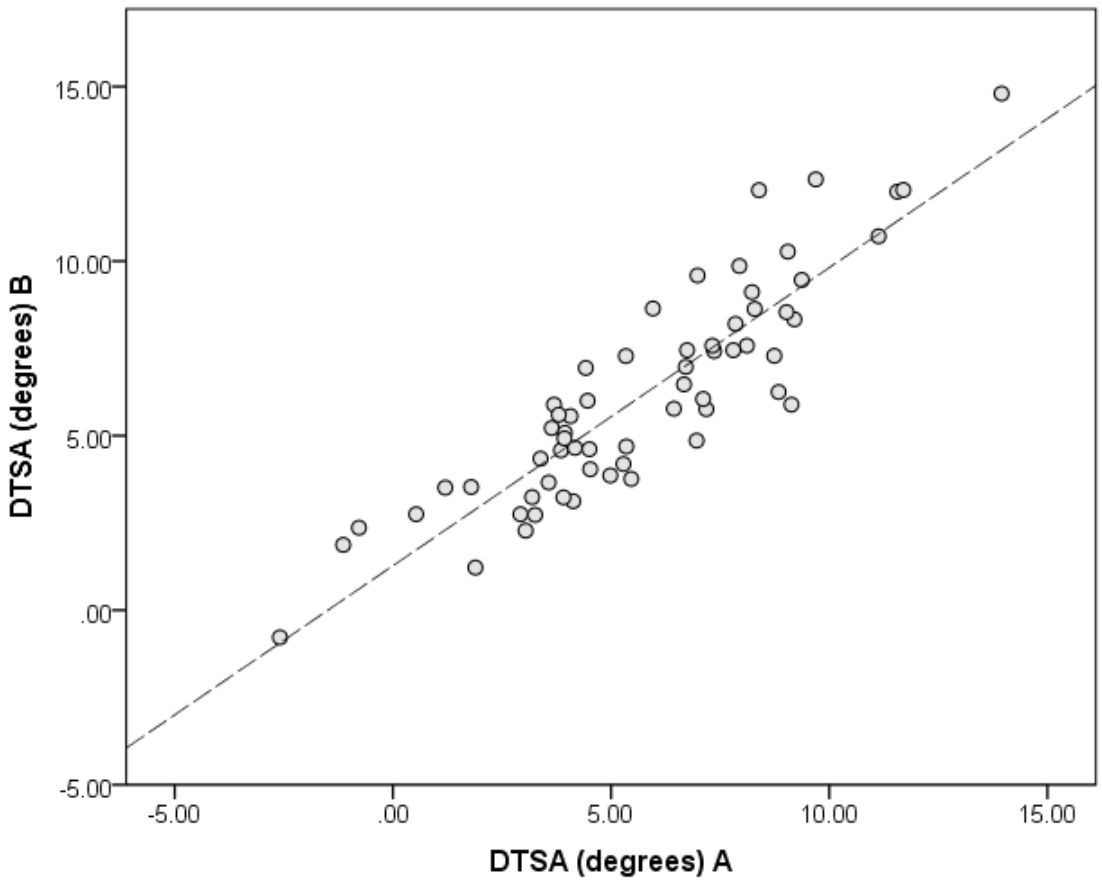

Figure 2.5: Scatter-plot of DTSA measurements taken by author during data collection for full study (A) and during data collection for a pilot study (B) on a subset of tibiae from the Mis Island sample (N = 62).

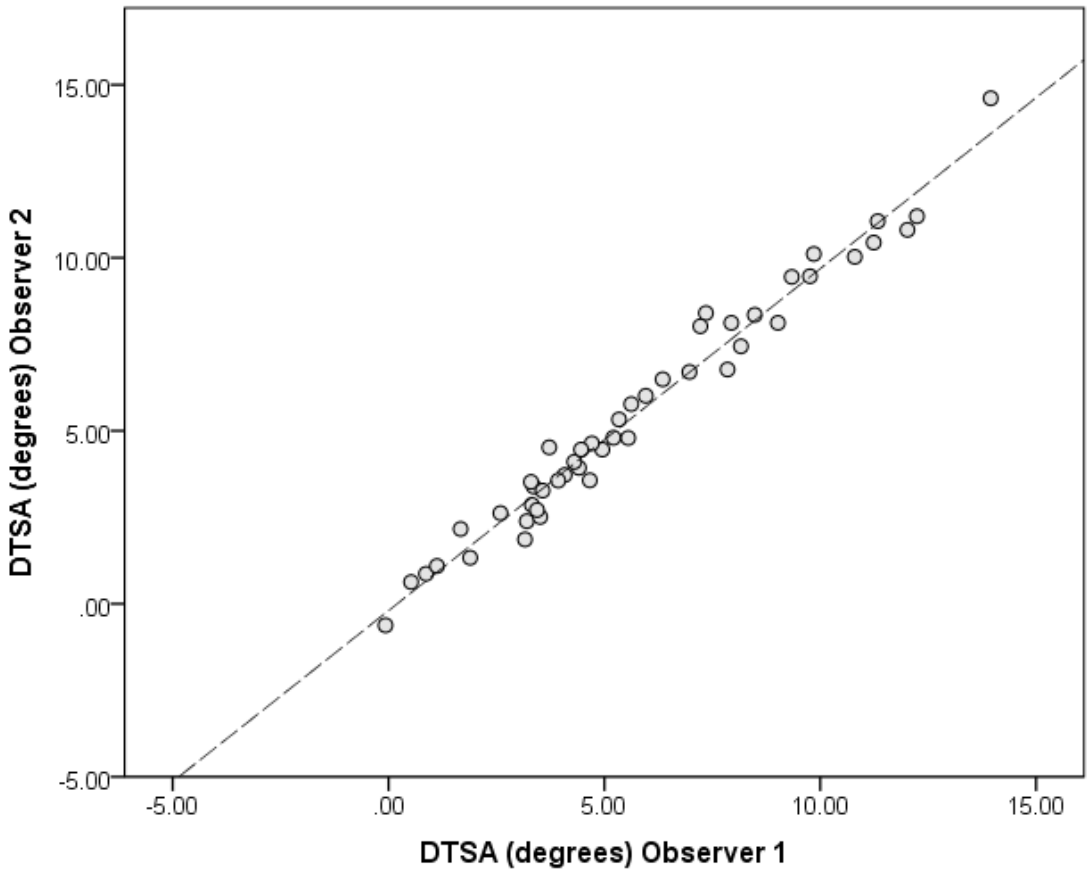

Figure 2.6: Scatter-plot of DTSA measurements taken by author (DTSA Observer 1) and measurements taken by second observer (DTSA Observer 2) on a subset of photographs of tibiae from the Mis Island sample (N = 47).

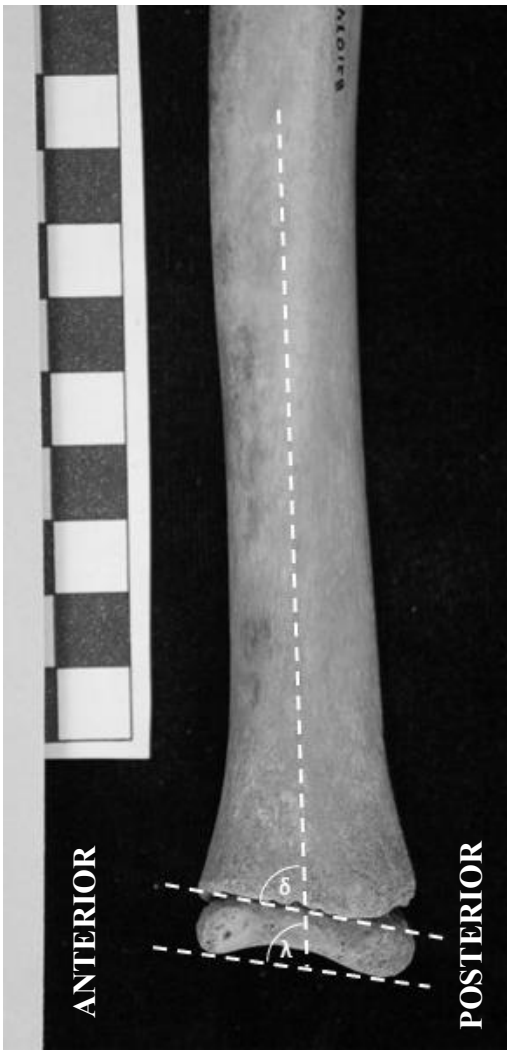

Figure 2.7: Measurement of the distal tibia sagittal angle of juvenile remains on digital photographs of a left tibia from the human osteological sample. DTSA was calculated as 90º-δ at the metaphyseal margin, and 90º-λ at the epiphyseal margin. Positive values indicate an anteriorly-inclined DTSA; negative values indicate a posteriorly-inclined DTSA.

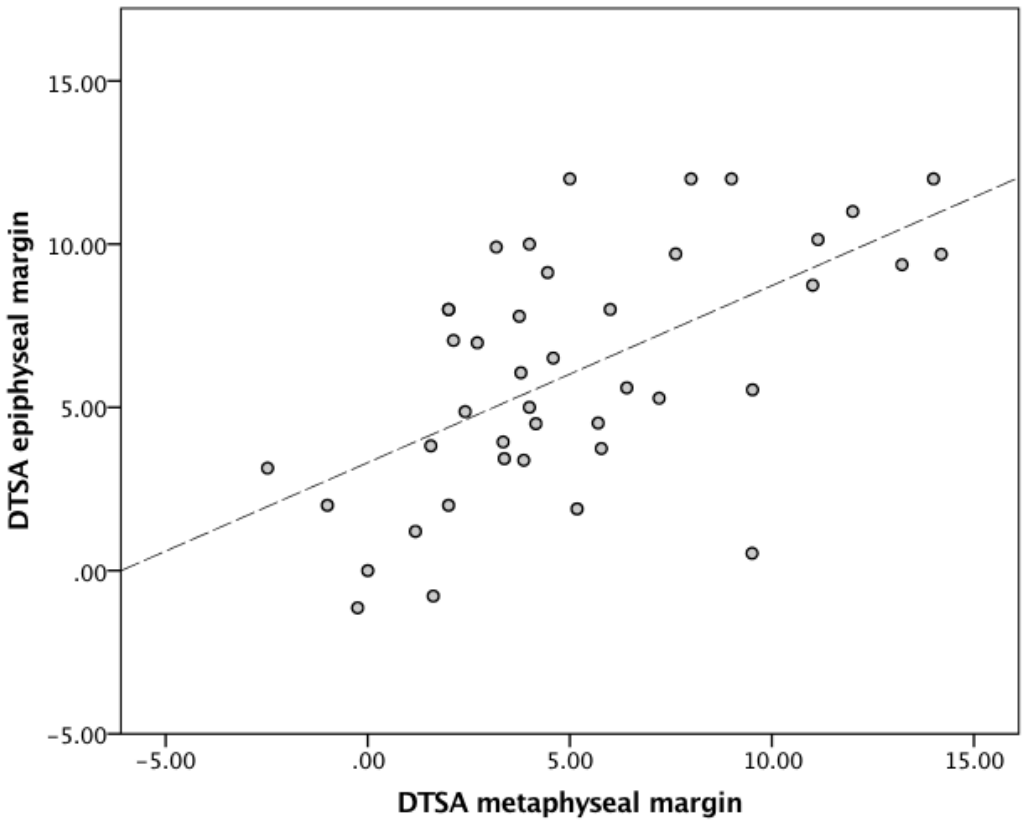

Figure 2.8: Scatter-plot showing the relationship between DTSA values measured at the epiphyseal and metaphyseal margins for 42 individuals ($r = 0.59$, $p < 0.01$).

Radiographic Measures of Arch Height	N	MEAN	STD	MIN	MAX
calcaneal inclination angle	119	19.68	5.17	4.58	37.07
talar declination angle	118	25.89	6.01	13.30	43.56
navicular height index	103	0.16	0.03	0.10	0.23
talar height index	113	0.24	0.03	0.17	0.34
Calcaneal Inclination Angle (CIA)					
"low"	6	14.00	6.07	4.58	20.87
"low to average"	79	19.20	4.94	8.34	29.08
"average"	19	21.37	3.52	14.7	26.57
"average to high"	2	25.64	3.76	22.98	28.30
Talar Declination Angle (TDA)					
"low"	6	26.42	10.88	13.30	43.56
"low to average"	78	26.62	5.66	14.04	37.75
"average"	19	23.63	5.79	13.90	32.77
"average to high"	2	20.09	5.62	16.11	24.06
Navicular Height Index (NHI)					
"low"	4	0.13	0.03	0.10	0.17
"low to average"	72	0.15	0.03	0.10	0.23
"average"	12	0.16	0.02	0.14	0.20
"average to high"	2	0.19	0.004	0.19	0.20
Talar Height Index (THI)					
"low"	5	0.21	0.04	0.17	0.26
"low to average"	76	0.24	0.03	0.18	0.34
"average"	17	0.25	0.02	0.23	0.28
"average to high"	2	0.28	0.01	0.27	0.29

Table 2.4: Descriptive statistics for the four radiographic measures of longitudinal arch height across the entire sample, and for each measure between those described as having "low", "low to average", "average", and "average to high" arches.

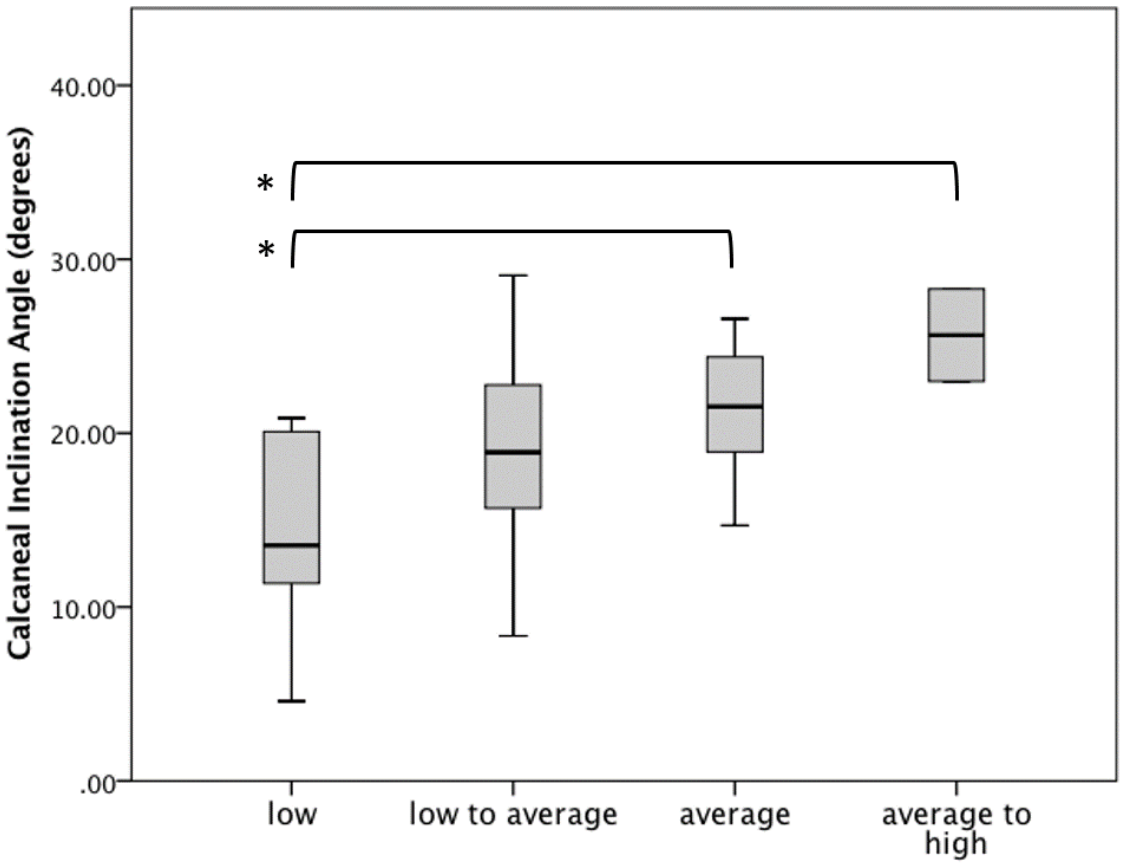

Figure 2.9A: Box-plot of the median and interquartile range of the calcaneal inclination angle for the radiographic sample across four arch height categories. Significant differences in the DTSA between categories are marked with an *.

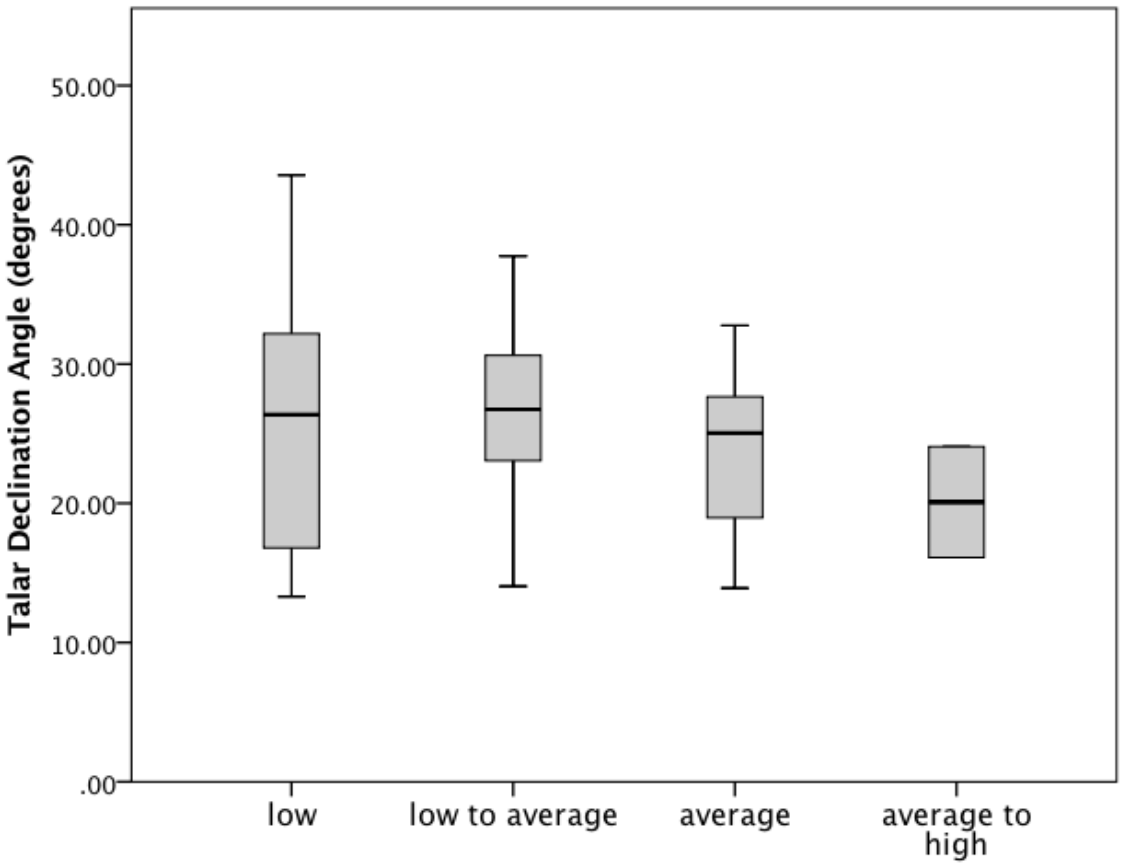

Figure 2.9B: Box-plot of the median and interquartile range of the talar declination angle for the radiographic sample across four arch height categories.

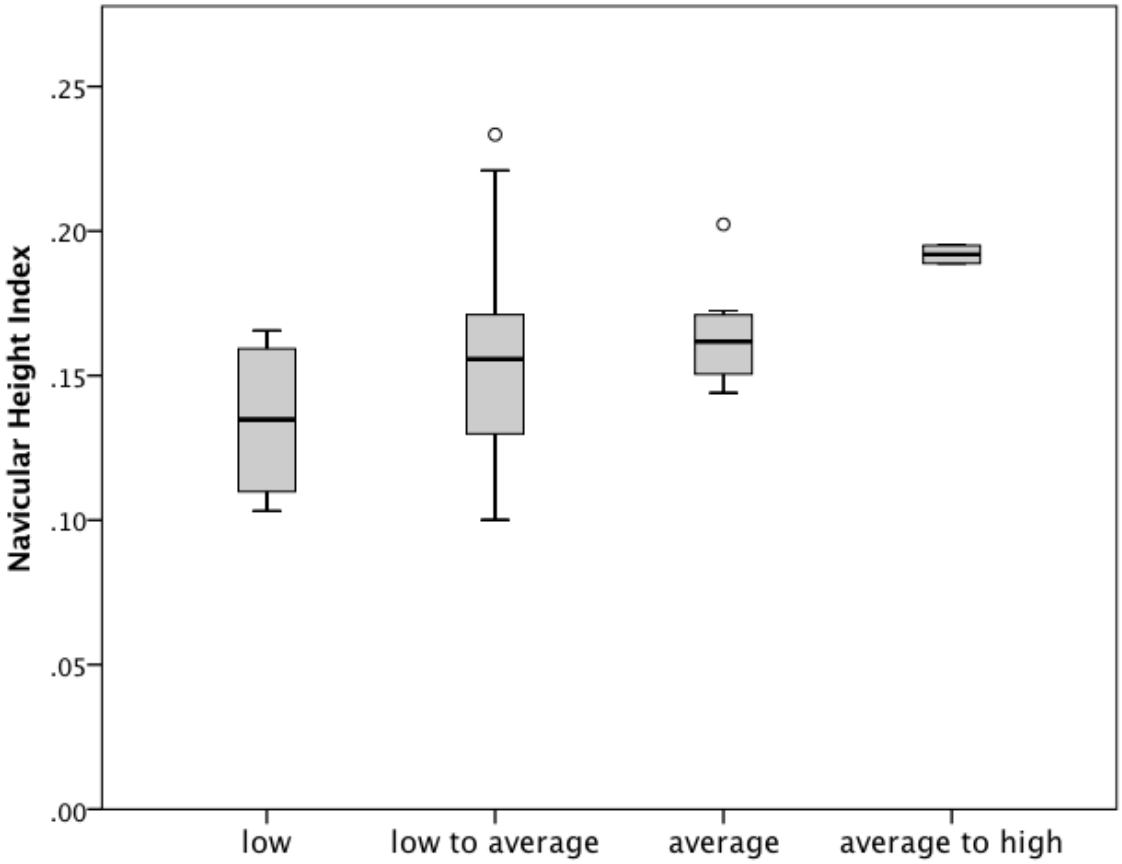

Figure 2.9C: Box-plot of the median and interquartile range of the navicular height index for the radiographic sample across four arch height categories.

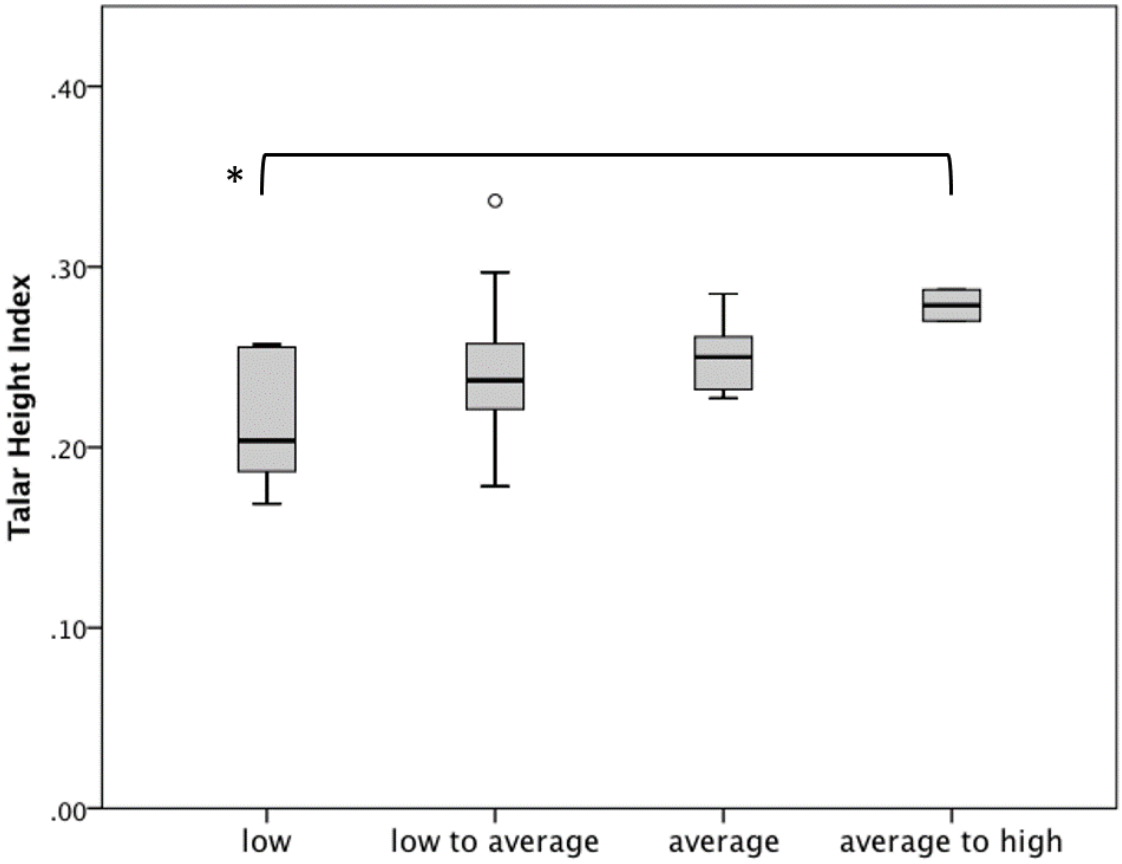

Figure 2.9D: Box-plot of the median and interquartile range of the talar height index for the radiographic sample across four arch height categories. Significant differences in the DTSA between categories are marked with an *.

Distal Tibia Sagittal Angle (DTSA)	N	Mean	SD	Min	Max
complete radiographic sample	114	4.37	3.17	-2.93	12.71
“low”	6	3.45	1.59	0.62	5.37
“low to average”	75	4.44	3.23	-2.93	12.71
“average”	19	2.96	4.03	-9.10	10.10
“average to high”	2	1.62	2.10	0.13	3.10

Table 2.5: Descriptive statistics for the distal tibia sagittal angle (DTSA) for the complete radiographic sample and within each of the four arch height categories.

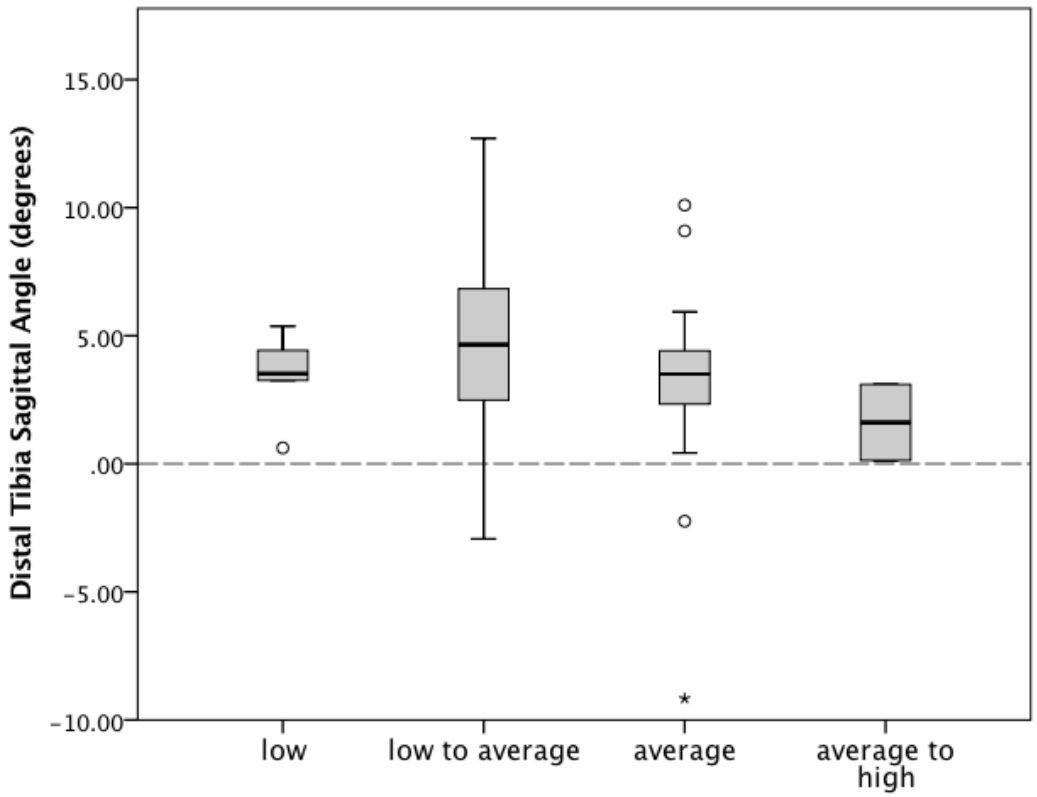

Figure 2.10: Box-plot of the median and interquartile range of the distal tibia sagittal angle (DTSA) of individuals in the radiographic sample grouped according to the podiatrist's description of their longitudinal arch as being of low, low to average, average, or average to high, in height. A DTSA of 0° = neutral; DTSA > 0° = anteriorly-inclined; DTSA < > 0° = posteriorly-inclined.

Radiographic Measure of Longitudinal Arch Height	N	Mean Rank	df	test statistic	p-value
calcaneal inclination angle			1	483.00	0.487
anteriorly inclined	105	57.33			
posteriorly inclined	10	65.00			
talar declination angle			1	2.554	0.110
anteriorly inclined	105	56.47			
posteriorly inclined	10	74.10			
navicular height index			1	0.514	0.474
anteriorly inclined	91	49.85			
posteriorly inclined	9	57.11			
talar height index			1	0.281	0.596
anteriorly inclined	100	54.99			
posteriorly inclined	10	60.60			

Table 2.6: Results of non-parametric Kruskal-Wallis Test for differences in longitudinal arch height between individuals with a posteriorly-inclined and anteriorly-inclined distal tibia sagittal angle.

Radiographic Measure of Arch Height	Pearson's r	p-value
calcaneal inclination angle	0.13	0.14
talar declination angle	-0.16	0.08
navicular height index	0.01	0.92
talar height index	0.07	0.45

Table 2.7: Correlation coefficients of distal tibia sagittal angle and radiographic measures of longitudinal arch height.

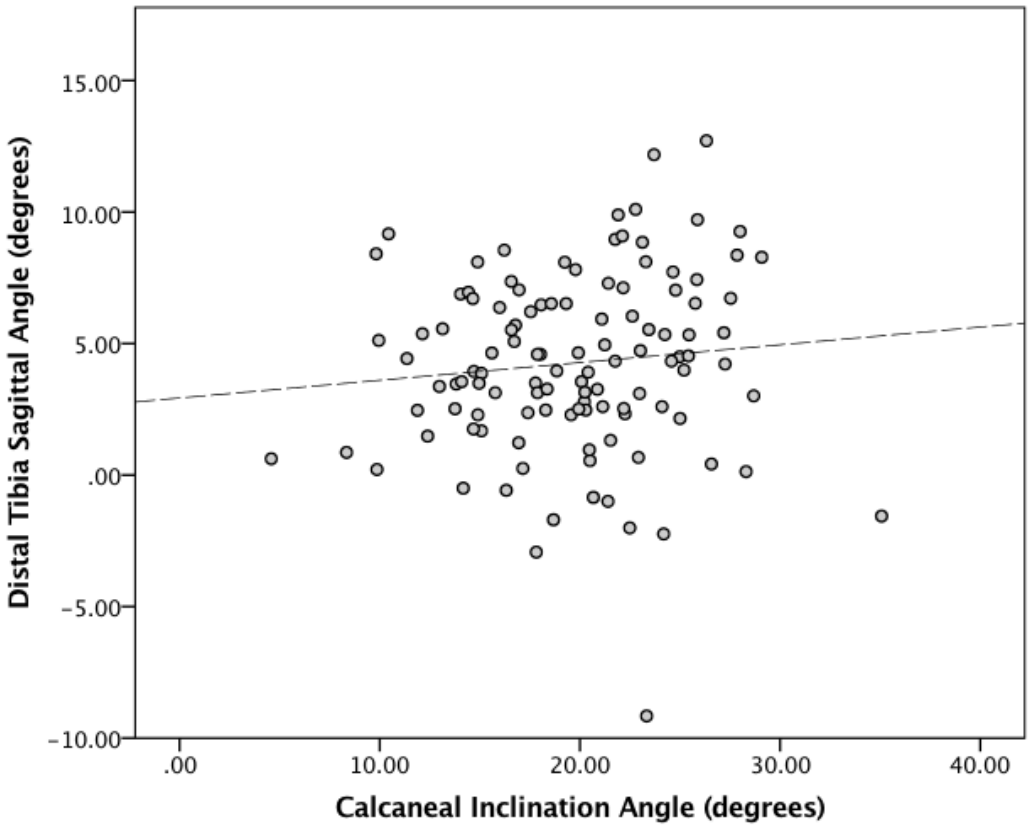

Figure 2.11A: Scatter-plot of the distal tibia sagittal angle (DTSA) and calcaneal inclination angle, a radiographic measure of longitudinal arch height ($r = 0.13$, $p = 0.14$).

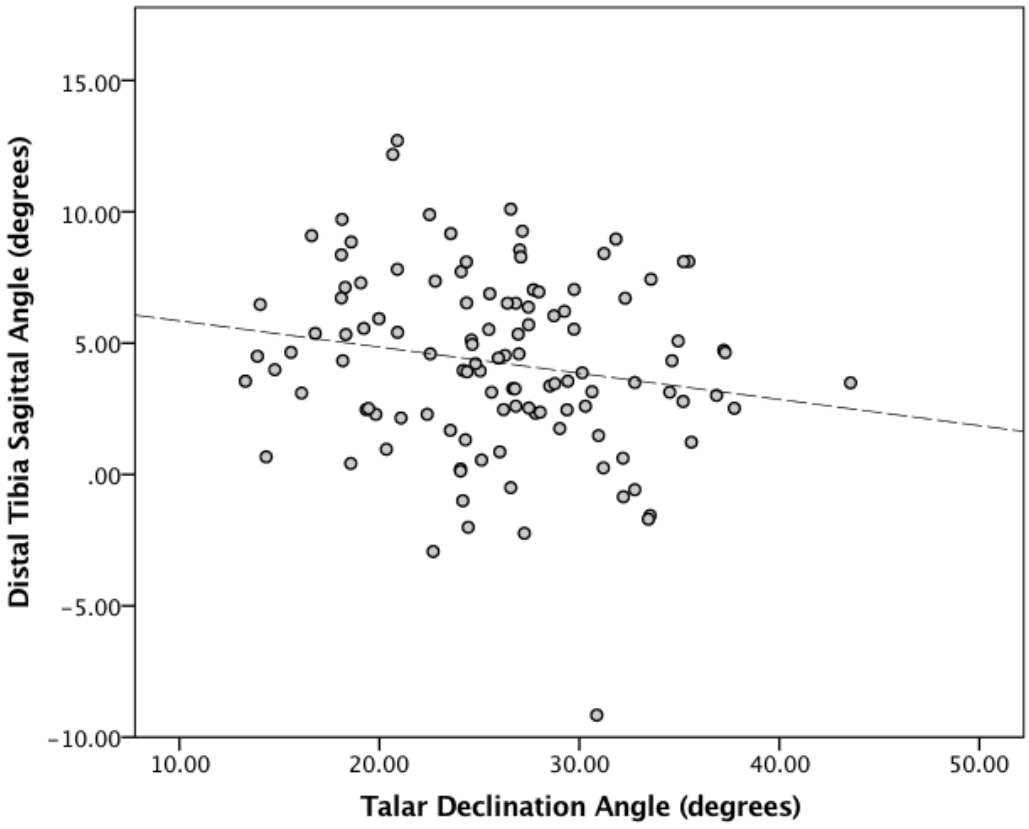

Figure 2.11B: Scatter-plot of the distal tibia sagittal angle (DTSA) and talar declination angle, a radiographic measure of longitudinal arch height ($r = -0.16$, $p = 0.08$).

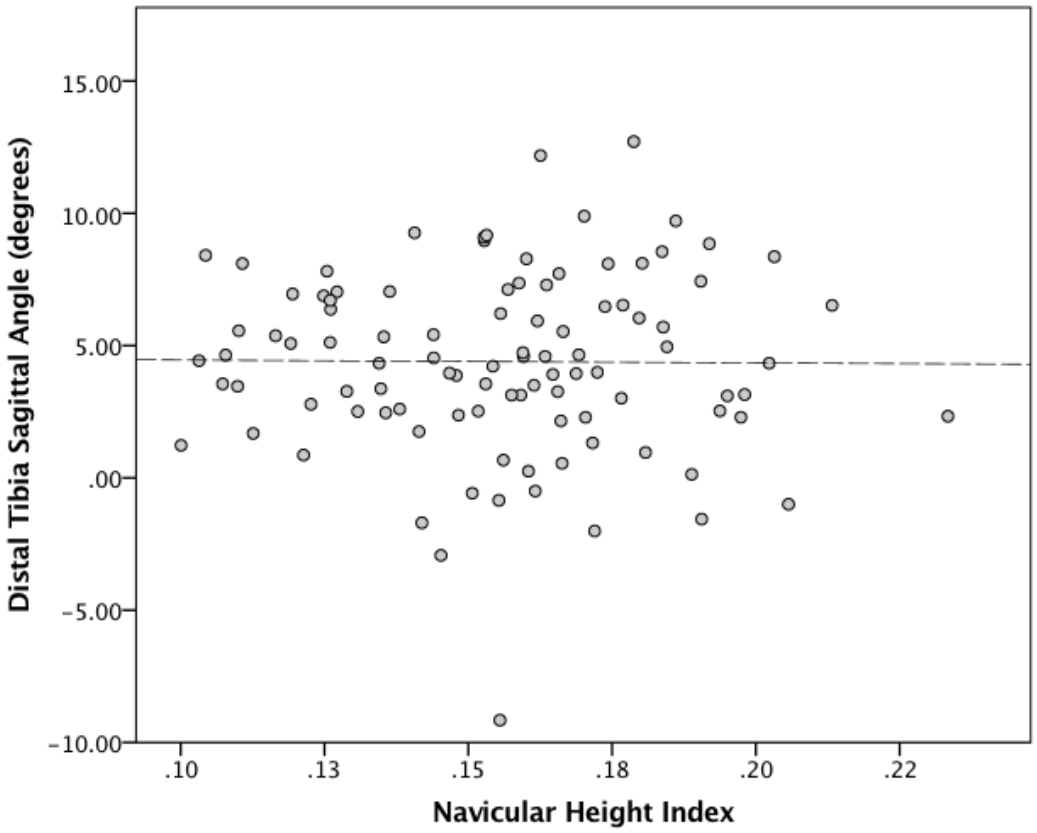

Figure 2.11C: Scatter-plot of the distal tibia sagittal angle (DTSA) and navicular height index, a radiographic measure of longitudinal arch height ($r = 0.01$, $p = 0.92$).

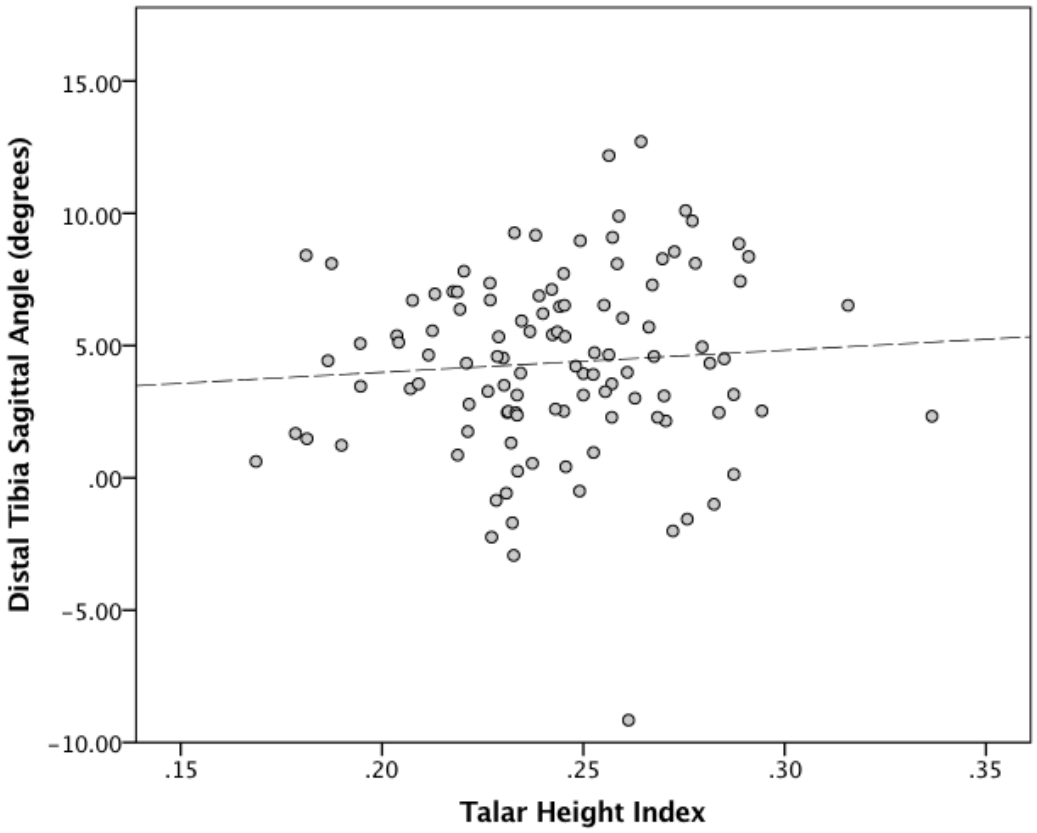

Figure 2.11D: Scatter-plot of the distal tibia sagittal angle (DTSA) and talar height index, a radiographic measure of longitudinal arch height ($r = 0.07$, $p = 0.45$).

AGE CATEGORY	SAMPLE	N	MEAN	SD	MIN	MAX
1-2	MI	7	7.44	2.35	4.54	10.84
	NF	21	2.14	4.44	-6.00	9.00
2-4	MI	10	5.22	2.53	1.64	9.70
	NF	16	4.63	3.52	-1.00	9.00
4-6	MI	9	5.55	3.42	-0.78	10.14
	NF	4	1.75	1.26	0.00	3.00
6-12	MI	16	3.83	4.98	-10.27	9.91
	NF	10	6.50	5.68	-4.00	12.00
12-20	MI	9	6.30	2.33	4.17	11.56
	NF	15	8.40	3.46	0.00	12.00
>20	MI	128	5.68	3.18	-2.59	15.85
	NF	28	7.61	3.31	-1.00	14.00
TOTAL PER SAMPLE	MI	179	5.59	3.32	-10.27	15.82
	NF	94	5.64	4.52	-6.00	14.00
TOTAL OVERALL	combined samples	275	5.63	3.75	-10.27	15.82

Table 2.8: Descriptive statistics of the distal tibia sagittal angle for the human osteological sample.

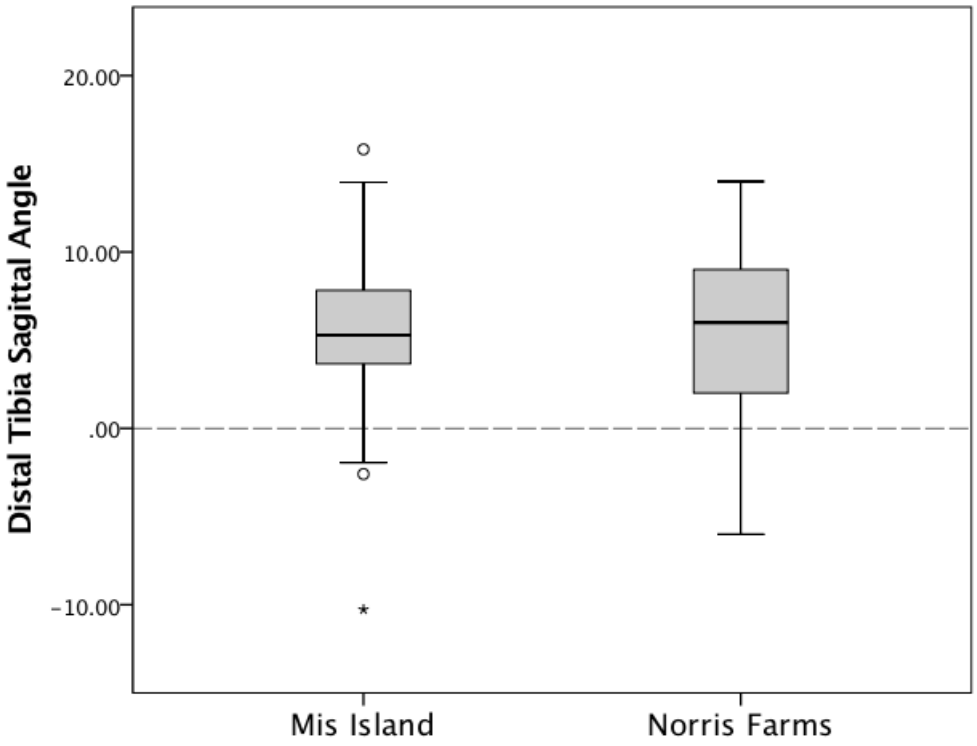

Figure 2.12: Box-plot of the distal tibia sagittal angle for the entire Mis Island and Norris Farms populations. A DTSA of 0° = neutral; DTSA > 0° = anteriorly-inclined; DTSA < > 0° = posteriorly-inclined.

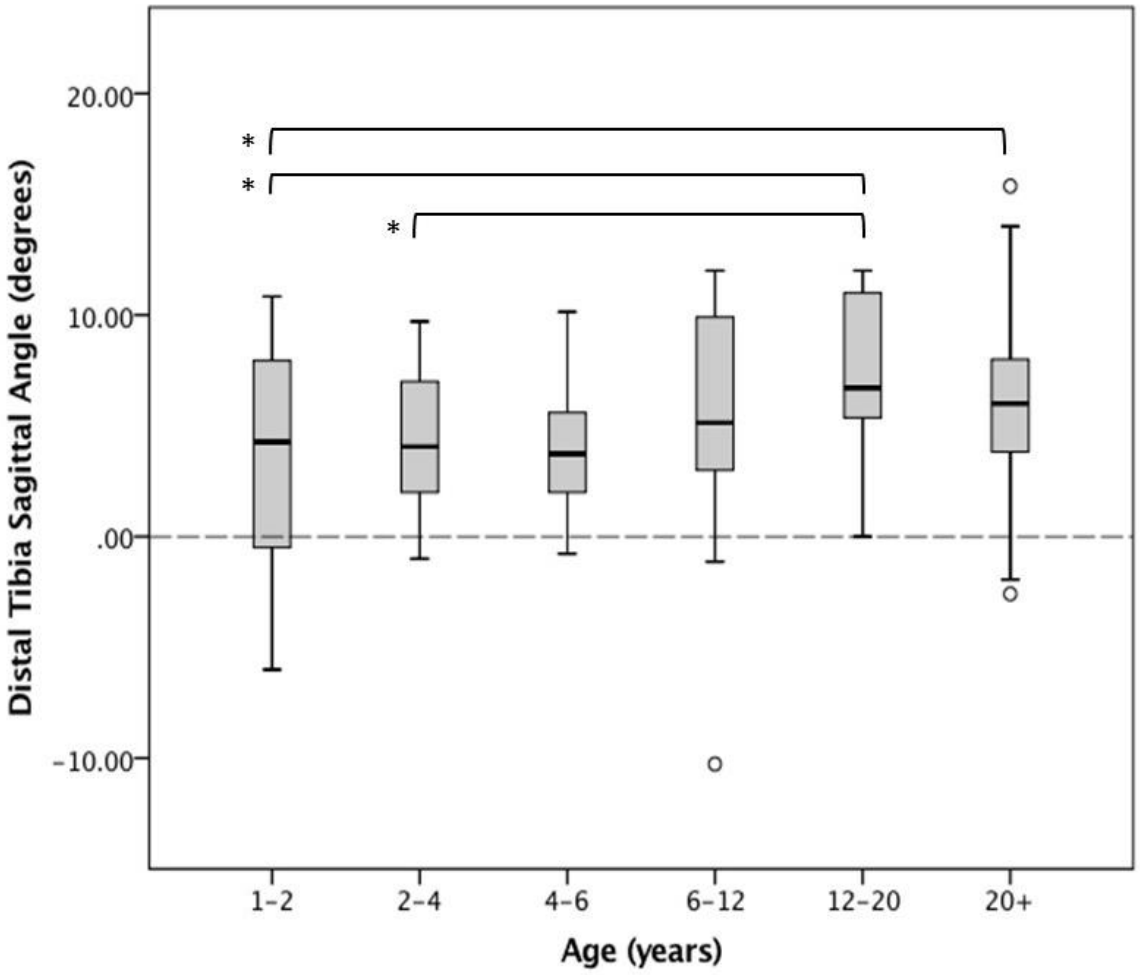

Figure 2.13: Box-plot of the median and interquartile range of the distal tibia sagittal angle (DTSA) for the combined Mis Island and Norris Farms populations across six age categories. Significant differences in the DTSA between age categories are marked with an *.

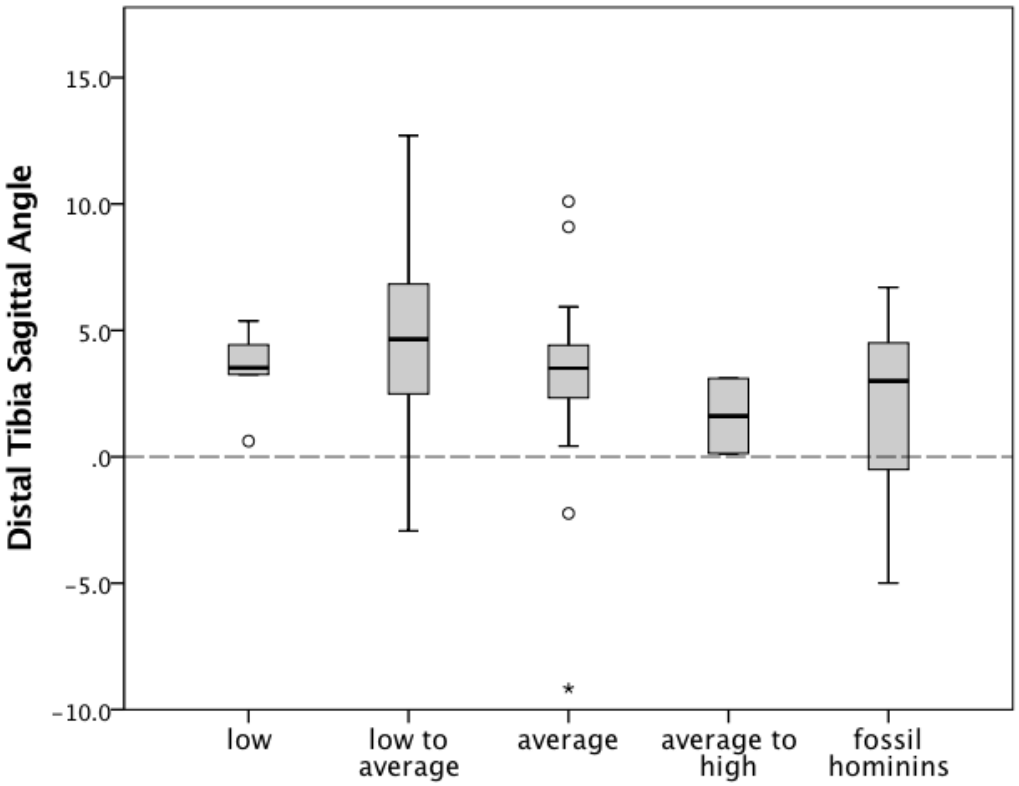

Figure 2.14A: Box-plot of the median and interquartile range of the distal tibia sagittal angle for individuals in the radiographic sample grouped according to the podiatrist's description of their longitudinal arch height. The DTSA of fossil hominins are included as a group.

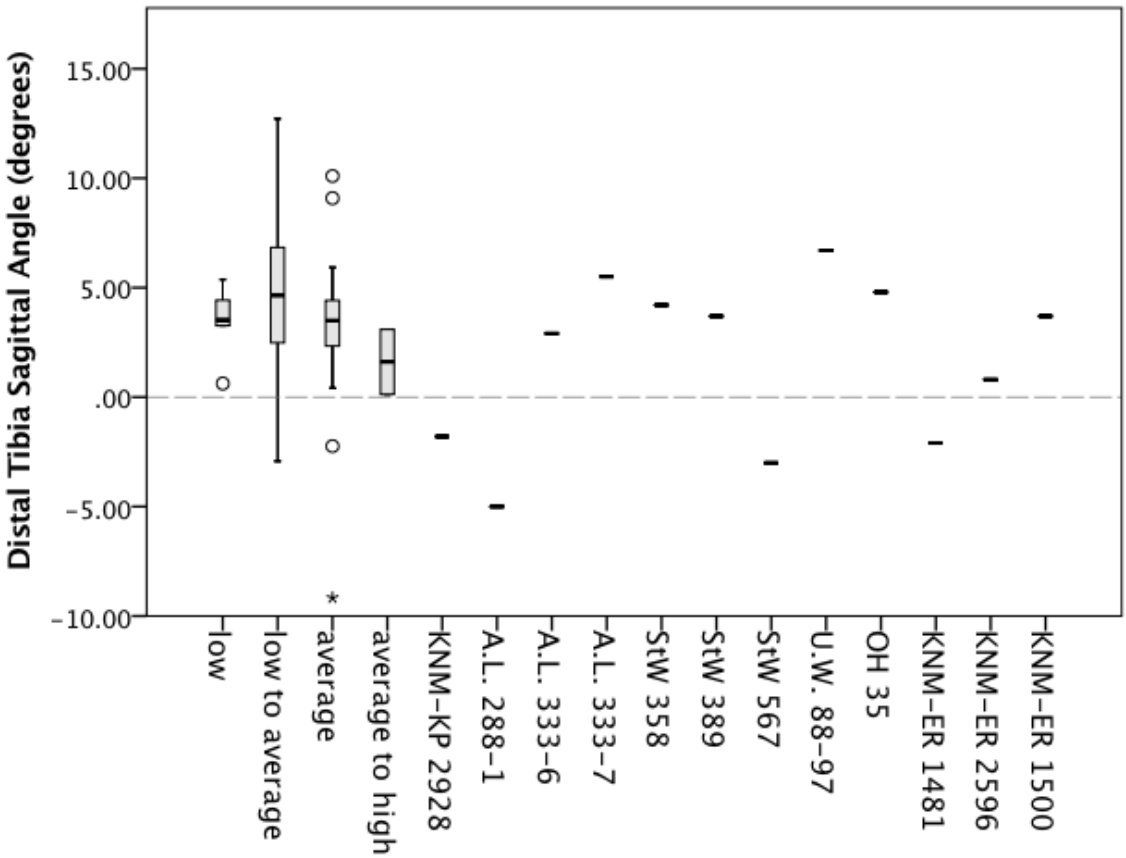

Figure 2.14B: Box-plot of the median and interquartile range of the distal tibia sagittal angle for individuals in the radiographic sample grouped according to the podiatrist's description of their longitudinal arch height. The DTSA of fossil hominins are included as individual specimens.

Sample (N)	Mean	SD	Min	Max	Range
Present Study					
Mis Island (128)	5.68	3.2	-2.59	15.9	18.5
Norris Farms (28)	7.61	3.3	-1.00	14.0	15.0
radiographs (114)	4.37	3.2	-2.93	12.7	15.6
DeSilva & Throckmorton, 2010					
radiographs (261)	4.0	3.6	-5.0	18.0	23.0
Hamann-Todd (24)	3.0	2.7	-3.0	8.0	11.0
Libben (45)	5.9	3.1	-1.0	13.0	14.0
Unprovenienced – Univ. of Michigan (66)	2.8	2.3	-4.0	8.0	12.0

Table 2.9: Descriptive statistics of variation in the DTSA for adult samples included in the present study and the DeSilva and Throckmorton (2010) study.

Chapter 3: An Osteological Correlate of Longitudinal Arch Height in the Human Calcaneus

INTRODUCTION

The calcaneus is the weight-bearing bony structure of the hind foot that acts as the "posterior pillar" of the human longitudinal arch (Morton, 1924). Comparative studies of human and ape foot bone shape have shown that their calcaneal morphologies differ in numerous ways (Weidenreich, 1923; Elftman & Manter, 1935b; Harcourt-Smith, 2002; DeSilva, 2009), and some morphological distinctions may be related to the presence of the longitudinal arch in humans (Berillon, 2003; Prang, 2015). Humans are known to exhibit variation in longitudinal arch height, however, and many humans are flat-footed (Hoffmann, 1905; Staheli *et al.*, 1987; Cavanagh *et al*., 1997; Morag & Cavanagh, 1999; Wunderlich & Cavanagh, 2001; D'Août *et al*., 2009). Whether human variation in longitudinal arch height could be driven, in part, by variation in calcaneal morphology is unknown.

While human and ape calcanei differ in many aspects of their morphology, the primary feature that has been argued to reflect a difference in arch presence versus arch absence is the angle of the cuboid facet of the distal calcaneus (Berillon, 2003). In humans, the distal end of the calcaneus is elevated from a horizontal position to articulate with the cuboid at the keystone position of the lateral column of the longitudinal arch. Apes, however, have a calcaneus that is positioned horizontally within the foot. Berillon (2003) described the cuboid facet of the distal calcaneus as having a plantar-inclination in humans, and a neutral angle in apes, reflecting this difference in calcaneal position. In other words, humans have a cuboid facet that is angled plantarly, away from the calcaneal body to a

degree greater than 90° (when viewed laterally), while the cuboid facet of the ape calcaneus is near, or slightly less than, a 90° angle relative to the calcaneal body (Berillon, 2003; **Figure 3.1**). Given this distinction, Berillon (2003) proposed that the obliquity of the cuboid facet of the calcaneus could serve as an architectural marker of the longitudinal structure of the lateral column of the foot. More specifically, hominin calcanei with a cuboid facet near 90° should be considered to have lacked a longitudinal arch, while those who exhibit a cuboid facet angle greater than 90° likely had an arch. This feature was recently included in a study by Prang (2015) who examined the cuboid facet angle and other features of talar and calcaneal joint morphology to assess whether a longitudinal arch was present in *Australopithecus sediba* and other fossil hominins. However, the relationship between the cuboid facet angle and longitudinal arch height has not been directly tested in a sample of humans known to exhibit variation in arch height. If a plantarly-inclined cuboid facet is a characteristic of the human calcaneus, then flat-footed humans may *also* have a plantarly-inclined cuboid facet. If this were so, then it would be possible to have a "human-like" cuboid facet angle yet also have a flat foot. Alternatively, it may be that flat-footed humans exhibit a cuboid facet that is more neutrally-aligned, or "ape-like", in which case a calcaneus could exhibit an ape-like cuboid facet angle, yet still have belonged to a biped, albeit a flat-footed one.

To date, no study has reported the degree to which humans exhibit variation in the cuboid facet angle of the calcaneus, nor has the relationship between this angle and longitudinal arch height been tested. Clinical studies have shown, however, that variation in human longitudinal arch height is driven, in part, by variation in the elevation of the distal calcaneus within the foot (*e.g.*, Simkin *et al*., 1989; Saltzman *et al*., 1995; Cavanagh & Morag, 1997; Morag & Cavanagh, 1999). Basic geometric principles dictate that the obliquity of the cuboid facet should be directly correlated to the elevation of the calcaneus,

and therefore, the height of the longitudinal arch, as long as the cuboid facet is aligned in a consistent position within the foot between individuals (**Figures 3.2 A-B**). If the cuboid facet (*i.e.*, calcaneocuboid joint) is aligned in the vertical coronal plane, for example, then any increase in the plantar inclination of the cuboid facet must be accommodated by a geometrically-similar increase in the elevation of the distal calcaneus in order to maintain congruency between the cuboid facet and the vertical plane (**Figures 3.2 A-B**). Given this relationship, there should be a direct positive correlation between the cuboid facet angle and calcaneal elevation (*i.e.*, longitudinal arch height).

A second osteological feature of the calcaneus that has been proposed to have a relationship with longitudinal arch height is the angle of the sustentaculum tali relative to the calcaneal body (Gould *et al*., 1989). The sustentaculum tali is a bony shelf on the medial aspect of the calcaneus that supports the head of the talus as part of the subtalar joint. According to a report by Gould and colleagues (1989), the development and position of the sustentaculum tali has a direct effect on the height of the medial longitudinal arch due to its role in supporting the talar head. A cranially-angled sustentaculum tali positions the talus directly above the calcaneus, contributing to the formation of a well-developed arch. In contrast, a neutral or caudally-angled sustentaculum tali is unable to effectively support the talar head, resulting in medial deviation of the talus and excessive pronation of the foot (Gould *et al*., 1989; **Figure 3.3**). To date, the sustentaculum tali angle has not been cited as a means of assessing whether a hominin had a longitudinally-arched foot. However, the angle of sustentaculum tali relative to the medial calcaneal body could be a useful feature for reconstructing hominin foot morphology if it can be shown to have a direct positive relationship with arch height.

The goals of this study are three-fold. First, this study directly tests the relationship between the cuboid facet angle, sustentaculum tali angle, and longitudinal arch height for

a sample of humans known to exhibit variation in arch height using a sample of lateral foot and ankle radiographs and magnetic resonance images. Second, this study further examines whether the cuboid facet angle changes throughout ontogeny over the period of longitudinal arch development using a sample of human osteological remains. And third, this study investigates the range of adult variation, gender differences, and population differences in the cuboid facet angle (as a proxy for longitudinal arch height) in the osteological sample.

MATERIALS AND METHODS

Sample

X-rays

The X-ray sample used in this study was previously described in Chapter 2. To summarize, the sample includes 123 digital X-ray files of the foot and ankle in lateral view taken from a standing, weight-bearing position. Each X-ray is anonymous, but is associated with the following biographical and anthropometric information: sex, age, weight, and body mass index. The podiatrist's description and categorical classification of the patient's longitudinal arch as either "low", "low to average", "average", "average to high", or "high" was also included. This classification was based on an observation of the external foot (as opposed to an X-ray).

Magnetic Resonance Images (MRI)

The second sample includes 19 Magnetic Resonance Images (MRIs) of the feet of healthy adults from the Boston University community. MRI collection protocol has been described elsewhere (see DeSilva *et al*., 2015). In brief, MRI scans were performed at the

Center for Biomedical Imagery at Boston University, where a Tesla Philips Acheiva scanner was used to collect proton-density weighted images at a resolution of 0.6 mm. These MRI scans are under the care of, and were provided by, Dr. Jeremy DeSilva, Department of Anthropology, Dartmouth College. Each MRI is anonymous, but is associated with the following biographical and anthropometric information: sex, age, height, leg length, weight, body mass index, and longitudinal arch height (measured as a Chippaux-Smirak Index). It should be noted, however, that the MRI scans were collected with the subject in a supine position and are non-weight bearing. Therefore, measurements of longitudinal arch height taken from these images are interpreted with caution.

Human Osteological Remains

The human osteological sample includes the calcanei of skeletonized individuals from two archaeological populations (Mis Island and Norris Farms) previously described in Chapter 2. **Table 3.1** summarizes the number of calcanei included in the study grouped according to the estimated age of the individual.

Fossil Hominins

Cuboid facet angle values for fossil hominins were collected from the published literature and are summarized in **Table 3.2.**

Data Collection

X-rays

Longitudinal Arch Height

Longitudinal arch height was quantified following the previously described protocol from Chapter 2. To summarize, Image J NIH software was used to measure the α) Calcaneal Inclination Angle = angle between the inferior surface of the calcaneus and the horizon; and θ) Talar Declination Angle = angle between a line that bisects the neck and head of the talus and the horizon (**Figure 3.4A**). Also, linear measurements of navicular height, talar height, and bony foot length were collected and used to calculate a navicular height index (navicular height divided by bony foot length) and a talar height index (talar head height divided by bony foot length) (**Figure 3.4B**).

Cuboid Facet Angle

The prediction that a larger cuboid facet angle (*i.e.*, more plantarly-inclined facet) is directly correlated with longitudinal arch height is based on the assumption that the cuboid facet is aligned along a vertical plane within the foot. Therefore, the position of the cuboid facet relative to the vertical plane was measured on each X-ray to test this assumption using ImageJ NIH software. The deviation of the cuboid facet from the vertical plane was measured using the angle measure tool as the angle enclosed between the flattest margin of the cuboid facet articular surface and the vertical plane. Deviations of the angle distal to the vertical plane are positive, while those angled proximal to the vertical plane are negative (**Figure 3.5**).

The cuboid facet angle was then measured on each X-ray using ImageJ NIH software. The angle measure tool was used to quantify the angle enclosed between the cuboid facet and the plantar surface of the calcaneus (in lateral view; modified from Berillon, 2003; **Figure 3.6**). The cuboid facet surface is variable in lateral appearance between individuals, with some exhibiting a flat lateral margin of the articular surface

along its entire length, and others exhibiting a small curved dorsal projection distally beyond the articular surface (see arrow in **Figure 3.6**). Here, the cuboid facet angle was measured along the flattest margin of the joint surface given that this is the primary articular surface of the joint.

Magnetic Resonance Images (MRI)

OsiriX DICOM image viewer software was used to collect linear and angular measurements of foot bone shape from the MRIs. The MRI of each subject was viewed using the 3D viewer, which allowed for simultaneous viewing of the foot from three orthogonal planes (**Figure 3.7**). Using the pan, rotate, and zoom tools, the calcaneus was positioned so that it was displayed in sagittal, coronal, and transverse cross-sections that bisected the element along the mid-sagittal, mid-coronal, and mid-transverse planes. Once the bone was in this position, the linear and angular measurement tools were used to measure the angles of interest (described below).

Longitudinal Arch Height

Longitudinal arch height was quantified on both the external surface and from the internal, bony anatomy, for each individual. The Chippaux-Smirak index (CSI) was used by DeSilva and colleagues to quantify longitudinal arch height (DeSilva *et al*., 2015). The CSI measures longitudinal arch height from footprints, and is the ratio between the minimum width of the mid-foot and the maximum width across the metatarsal heads. Because variation in soft tissue anatomy may affect measures of longitudinal arch height from external anatomy (Saltzman *et al*., 1995), however, longitudinal arch height was also

quantified from the bony anatomy present in the MRI scans. OsiriX DICOM image viewer software was used to collect linear measures of bony foot length (medial and lateral), navicular height, and cuboid height. These metrics were then used to calculate a navicular height index (navicular height / medial bony foot length) and a cuboid height index (cuboid height / lateral bony foot length) of longitudinal arch height (**Figure 3.8**). Recall, however, that the MRI scans were collected with the subject in a supine position and are non-weight bearing. Due to deformation of the midfoot region that result from weight-bearing, the foot length used to calculate these indices is likely an under-estimate of foot length, while the navicular and cuboid heights are likely an over-estimate. Nevertheless, these indices offer a way to quantify the bony arch height of each individual.

Cuboid Facet Angle

OsiriX DICOM image viewer software was used to quantify the cuboid facet angle on the MRI scans. First, the pan and rotation tools were used to position the foot in anatomical position with the dorsal aspect of the talar trochlea aligned in the horizontal plane. The image layers were then scrolled through in the sagittal plane viewer until the view box showed the lateral calcaneus. The angle tool was used to measure the cuboid facet angle according to the two protocols described above (**Figure 3.9**).

Sustentaculum Tali Angle

The sustentaculum tali angle was measured on the MRI sample using OsiriX DICOM image viewer software. First, the pan and rotation tools were used to position the foot in anatomical position with the dorsal aspect of the talar trochlea aligned in the horizontal plane. The image layers were then scrolled through in the coronal plane viewer

until the view box showed the distal calcaneus. The sustentaculum tali angle was measured using the angle tool as the angle enclosed between the medial wall of the calcaneal body and the plantar surface of the sustentaculum tali (**Figures 3.10 A-B**).

Human Osteological Remains

Cuboid Facet Angle

Digital photographs were taken with the lateral calcaneus aligned parallel to the camera lens in order to mimic the orientation of the calcaneus in the X-rays. ImageJ NIH software was used to measure the cuboid facet angle (CFA), defined as the angle enclosed between a line drawn along the flattest margin of the cuboid facet and a line along the plantar-most aspect of the calcaneus (**Figure 3.11A**).

On the youngest individuals in the sample, it was not always possible to measure the CFA because the cuboid facet of the calcaneus is convex distally, and there was not a flat margin on the joint surface. Therefore, an index of curvature of the distal calcaneus was calculated in order to test for age-related changes in curvature, and to determine at what age the cuboid facet becomes flattened. First, digital photographs were taken of the calcaneus in lateral view with the calcaneal body aligned parallel to the camera lens. Second, ImageJ NIH software was used to measure the dorso-plantar height of the cuboid facet articular surface at the dorsal and plantar points where the articular surface transitions to the calcaneal body (**Figure 3.11B**, line "B"). Third, the perpendicular distance between the mid-point of line B and the distal-most aspect of the calcaneus was measured (**Figure 3.11B**, line "A"). The cuboid facet curvature index was then calculated as the quotient of A/B. Where possible, both the CFA and the curvature index were measured, as represented in **Figure 3.11B**.

Intra-rater repeatability of measure for the cuboid facet angle was assessed for a subset of calcanei from the Mis Island sample. A subset of calcanei (N = 60) were photographed and measured as part of a pilot version of this study (Heard-Booth, 2013). These CFA values were compared to those measured on new photographs taken approximately 18 months later when data was collected for the full study. The correlation between these two measures was $r = 0.939$ ($p < 0.001$), indicating that the CFA has a high repeatability of measure (**Figure 3.12**).

Data Analysis

Relationship between Calcaneal Morphology and Longitudinal Arch Height

This study investigates whether two aspects of calcaneal morphology, the cuboid facet angle and the sustentaculum tali angle, are positively correlated with longitudinal arch height. First, descriptive statistics were calculated for the radiographically-obtained measurements of the deviation of the cuboid facet from the vertical plane in order to test the assumption that this joint surface is positioned vertically within the foot. Second, correlation statistics were used to examine the relationship between the cuboid facet angle and each of the four radiographic measures of longitudinal arch height. Also, the cuboid facet angle was compared between the four podiatrist designated arch height categories using a one-way ANOVA to determine whether there was an increase in the cuboid facet angle with arch height. Third, a correlation test was used to examine the relationship between the cuboid facet angle and the three measures of longitudinal arch height associated with each MRI, including two indices calculated from the MRI and the Chippaux-Smirak Index measured from the individual's footprint. The relationship

between the sustentaculum tali angle and these three measures of longitudinal arch height was also investigated.

Ontogenetic and Adult Variation in the Cuboid Facet Angle

Descriptive statistics were calculated for the cuboid facet angle in the archaeological samples. These statistics were calculated for the complete archaeological samples and for six age categories within each of the two archaeological samples. The six age categories are as follows: 1-2 years (early bipedal walkers that lack a longitudinal arch); 2-4 years (bipedal walkers beginning to develop a longitudinal arch); 4-6 years (bipedal walkers with a developing longitudinal arch); 6-12 years (bipedal walkers with a developed longitudinal arch and a growing foot); 12-20 years (bipedal walkers with a developed longitudinal arch and adult-sized foot, but continue to grow in stature); and 20+ (bipedal walkers with an adult foot size and stature). Age-related variation in the cuboid facet angle was investigated using either a nonparametric Kruskal-Wallis test or parametric one-way analysis of variance (ANOVA), where appropriate. Adult variation in the cuboid facet angle was investigated between sexes and between populations using an independent samples t-test.

All statistical analyses were carried out using SPSS version 23.0 (IMB).

RESULTS

Cuboid Facet Angle and Longitudinal Arch Height

The proposed positive relationship between the cuboid facet angle and the calcaneal inclination angle (*i.e.*, longitudinal arch height) is based on the assumption that the cuboid facet is aligned with a vertical plane within the foot. The deviation of the flattest margin of

the cuboid facet from a vertical plane was measured on 119 X-rays to test this assumption. The flattest margin of the cuboid facet has an average deviation of -0.10º from a vertical plane (**Table 3.3**). **Figure 3.13** shows a histogram of the distribution of vertical deviation values measured at the flattest margin of the cuboid facet surface. The deviation of the cuboid facet is normally distributed (skewness = 0.016) around a mean of -0.10º. The kurtosis of the curve is 0.679, indicating that the distribution has light tails with few outliers. These data indicate that the cuboid facet is often aligned at or near a vertical plane (0º) within the foot, though the position of this joint surface has a small degree of inter-individual variation.

The cuboid facet angle of the calcaneus was measured on 119 X-rays and 17 MRIs. All individuals exhibit a plantar inclination of the cuboid facet (CFA > 90°), consistent with the findings of Berillon (2003) and Prang (2015) (**Table 3.3**). The cuboid facet angle is variable between individuals, however, with a total range of 33.04º (Min = 94.8º, Max = 127.84º) for individuals in the X-ray sample and a range of 14.81º (Min = 96.12º, Max = 110.93º) for those in the MRI sample. The range of variation is smaller for the individuals in the MRI sample than the X-ray sample, and this difference is likely the result of a much smaller sample size in the former.

Table 3.4 summarizes the descriptive statistics for the cuboid facet angle across the four arch height categories based on the podiatrist's description of the external appearance of the individual's longitudinal arch. **Figure 3.14** shows a box-plot of the median and interquartile range of the CFA across the four arch height categories. Results of a one-way ANOVA found that the cuboid facet angle did not differ significantly between arch height categories [$F(3, 102) = 1.004$, $p = 0.394$].

Table 3.5 lists the correlation coefficients for the cuboid facet angle and measures of longitudinal arch height for the X-ray and MRI samples. For the X-ray sample, the

cuboid facet angle was significantly positively correlated with the calcaneal inclination angle ($r = 0.62$, $p < 0.001$) and the talar height index ($r = 0.238$, $p < 0.011$) (**Table 3.5**; **Figure 3.15 A-B**). The cuboid facet angle did not exhibit a significant correlation with the talar declination angle or the navicular height index, however. For the MRI sample, the cuboid facet angle was not significantly correlated with any of the three measures of longitudinal arch height (**Table 3.5**).

Sustentaculum Tali Angle and Longitudinal Arch Height

The sustentaculum tali angle was measured on 17 MRI scans, where all individuals were found to exhibit a sustentaculum tali angle that was cranially-directed (*i.e.*, > 90º) (**Table 3.3**). **Table 3.6** lists the correlation coefficients for the sustentaculum tali angle and the three measures of longitudinal arch height for the MRI sample. The angle of the sustentaculum tali relative to the medial border of the calcaneus was not significantly correlated with any measure of longitudinal arch height, indicating that a more cranially-directed sustentaculum tali was not associated with a higher arch in this sample.

Ontogenetic and Adult Variation in the Cuboid Facet Angle

This study further examined human variation in the cuboid facet angle in a large sample of skeletonized human remains. **Table 3.7** presents the descriptive statistics for the cuboid facet angle of the calcaneus for the two archaeological populations (N = 241). Results of an independent t-test found no statistical difference in mean cuboid facet angle between calcanei estimated to have belonged to males and those estimates to have belonged to females in the Mis Island [$t(155) = 0.050$, $p = 0.960$] or Norris Farms [$t(24) = 0.237$, $p = 0.815$] populations. Note that it was not possible to estimate sex for all individuals, so

the sample sizes used in this comparison are lower than adult sample sizes used for subsequent analyses. Given that a sex difference was not detected, males and females were combined for the adult sample.

An independent samples t-test found no difference in mean cuboid facet angle when the entire Mis Island and Norris Farms samples were compared [$t(239) = -0.816$, $p = 0.415$), when just adult individuals were compared [$t(187) = -1.452$, $p = 0.148$), or when just juvenile individuals were compared [$t(49) = -0.924$, $p = 0.360$). Therefore, data from the two samples were combined to test for age-related differences in cuboid facet angle.

The cuboid facet curvature index was measurable on 11 calcanei belonging to individuals aged 1 to 6 years (**Table 3.8**). The mean curvature index was similar in those aged 1-2 years (Mean = 0.245) and those aged 2-4 years (Mean = 0.235), and then decreased in those aged 4-6 years (Mean = 0.133) (**Figure 3.16**). A Kruskal-Wallis test found no difference in the distribution of the curvature index across age categories ($X^2 = 2.933$, $df = 2$, $p = 0.231$). However, it is possible that the lack of significance is due to the small sample sizes, as **Figure 3.16** shows that the cuboid facet becomes less round and more flattened by 6 years of age. Moreover, it was possible to measure the cuboid facet angle (*i.e.*, and not calculate the curvature index) on most of the calcanei estimated to have belonged to juveniles aged 4-6 years, offering additional evidence to support the claim that the facet becomes flattened around the age of 6 years.

A one-way ANOVA test was performed to investigate whether the mean cuboid facet angle differed significantly between age categories. Because the cuboid facet angle was measured on just one individual aged 1-2 years, this individual was included with the 2-4 years age range to create a new age range of 1-4 years. Estimated age had a significant effect on cuboid facet angle for the combined archaeological samples [$F(4, 235) = 3.737$, $p = 0.006$] (**Figure 3.17**) . However, a post-hoc Tukey HSD test did not identify any

significant pairwise comparisons between age categories, which may result from the conservative nature of the Tukey test. Of the pairwise comparisons performed, the greatest difference in the cuboid facet angle was detected between those aged 4-6 years and those greater than 20 years of age (Mean Difference = 6.44, $p = 0.092$), though this difference was not statistically significant. **Figure 3.17** shows that the median cuboid facet angle is lowest in the youngest individuals and is highest in those aged 12-20 and 20+ years. Rather than a gradual increase in the cuboid facet angle with age, there appears to be a difference in the median cuboid facet angle in those aged 1-12 years and those older than 12 years. This difference could be related to the fact that the proximal calcaneal epiphysis fuses after age 12 (15-16 years in females, 18-20 years in males; Scheuer & Black, 2004), indicating that there is a difference in the cuboid facet angle between those with an unossified proximal epiphysis and those with an ossified (and fused) epiphysis. As predicted, however, there appears to be little difference in the cuboid facet angle between the 12-20 and 20+ age ranges, consistent with reports that foot growth is complete in the early teenage years.

Following the observation that there is a difference in the median cuboid facet angle between those under and over the age of 12 years, an independent samples t-test was performed to determine if there was significant difference in the mean cuboid facet angle between these two groups. Results of the t-test show that there is a significant difference in the mean cuboid facet angle between those aged 1-12 years and those aged 12+ years [$t = -3.706$, $p < 0.001$]. **Figure 3.18** shows a box-plot of the median and interquartile range of the distribution of the cuboid facet angle between these two age categories. While a statistical difference in the mean was detected between these two groups, **Figure 3.18** shows that there is a considerable degree of overlap in their distributions.

Hominin Calcanei and Longitudinal Arch Height

Cuboid facet angle measurements were recently published by Prang (2015) for MH2 (U.W. 88-99, *Australopithecus sediba*), OH-8 (early *Homo*) and Omo 33-74-896 (early *Homo*) (**Table 3.3**). **Table 3.9** lists the cuboid facet angle values for fossil hominins alongside the values recorded for humans in the current study, as well as previously published values for apes and humans (Prang, 2015). **Figure 3.19** shows where these fossil hominins fall on a regression line of the calcaneal inclination angle and cuboid facet angle for the X-ray sample. Given that OH-8 has the highest cuboid facet angle of the three hominins (108°), this specimen is predicted to have had the highest calcaneal inclination angle, *i.e*., longitudinal arch. Omo 33-74-896 and MH2 have cuboid facet angles of 99° and 98°, respectively, and are predicted to have had a lower calcaneal inclination angle, *i.e*., a lower arch. **Figure 3.20** plots the cuboid facet angles of the hominins alongside box-plots of the median and interquartile range of the cuboid facet angle for individuals with "low", "low to average", "average", and "average" to high arches. Here, it is clear that the cuboid facet values of Omo 33-74-896 and MH2 fall below the range of cuboid facet values for individuals with "average" and "average to high" arches, and are within the range of individuals described as having "low" or "low to average" arches. The cuboid facet value of OH-8 (108°) is close to the mean value for this radiographic sample (Mean = 109.2°).

DISCUSSION

Cuboid Facet Angle and Calcaneal Inclination (Longitudinal Arch Height)

This study is the first to directly test the relationship between aspects of calcaneal morphology and longitudinal arch height in a sample of humans known to exhibit variation in arch height. The results of this study show that variation in the cuboid facet angle of the

calcaneus is positively correlated with two measures of longitudinal arch height in the X-ray sample, including the calcaneal inclination angle and talar height index. The positive correlation between the cuboid facet angle and the calcaneal inclination angle is consistent with predictions based on geometric principles. In other words, if the cuboid facet is aligned with a vertical plane within the foot, then any increase in the calcaneal inclination must be accompanied by an increase in the cuboid facet angle, or vice versa. This study found that the cuboid facet is aligned with, or very near, a vertical plane within the foot, though there is some variation in its alignment between individuals. It is possible that variation in the cuboid facet alignment explains some of the variation in the relationship between the cuboid facet angle and calcaneal inclination. The cuboid facet angle was also positively correlated with the talar height index in the radiographic sample, though only a small proportion of the variation in the talar height index was explained by the cuboid facet angle.

In the MRI sample, the cuboid facet angle was not correlated with any of the three measures of longitudinal arch height. There are a number of possible explanations for this finding. First, the MRI sample was much smaller than the radiographic sample, and may not have included individuals from the entire arch height continuum. Second, two of the three measures of arch height (the navicular height index and cuboid height index) may not accurately represent an individual's arch height because the MRIs were taken with the individual in a supine, non-weight-bearing position. Therefore, these indices are not synonymous with indices derived from the radiographic sample, given that the x-rays were collecting with the subject in a standing, weight-bearing position. And finally, taking measurements from MRIs is subject to a greater risk of user-introduced error given that the images are freely rotated by the user. Therefore, it is possible that the calcaneus was not in a consistent position for each individual, though an attempt was made to reduce this error.

On the other hand, the patients at the podiatrist office stand in a standard position for X-rays, which minimizes the difference in calcaneal position between individuals.

When considering all of the measures of longitudinal arch height used in this study, it is most informative that the cuboid facet angle was strongly correlated with the calcaneal inclination angle in the X-ray sample. This finding indicates that an aspect of calcaneal morphology (*i.e.*, the cuboid facet angle) is related to the position of the calcaneus within the foot. Importantly, it may be possible to estimate the elevation angle of the calcaneus of fossil hominins by aligning the cuboid facet with the vertical plane.

Ontogenetic and Adult Human Variation in the Cuboid Facet Angle

This study used the skeletonized remains of two archaeological populations to quantify population and age-related variation in the shape of the cuboid facet angle of the calcaneus. Longitudinal arch height was unknown for the individuals in the archaeological sample, so it was not possible to directly test the relationship between the cuboid facet angle and arch height. However, studies of contemporary populations show that the longitudinal arch develops in early childhood from a flat foot posture, usually by age 6 (Bertsch *et al*., 2004; Onodera *et al*., 2008; Müller et al., 2012). Therefore, finding that the cuboid facet angle increases throughout this developmental period could serve as additional evidence that the cuboid facet angle is directly related to longitudinal arch height.

The results of this study show that the mean cuboid facet angle of the calcaneus increases with age and does not statistically differ between populations. Given that the sample sizes were very small for the youngest individuals in the sample, only general trends are discussed. The cuboid facet of the calcaneus appears convex distally in infancy and toddlerhood, and begins to flatten between 4-6 years of age. Calcanei belonging to

individuals estimated to be between 1-2 years old and 2-4 years old exhibit a cuboid facet with a mean curvature index of 0.245 and 0.235, respectively. This index dropped to 0.133 in those aged 4-6 years, indicating that there is a shift in the morphology of the distal calcaneus around this age as the convex articular facet becomes flattened. This conclusion is supported by the observation that all calcanei estimated to belong to individuals aged 6-12 years displayed a flattened cuboid facet. Again, however, sample sizes for individuals under age 6 were very small, and future studies should measure the cuboid facet curvature on other subadult calcanei to improve our understanding of how the distal calcaneus changes during development.

The results of this study suggest that the cuboid facet angle increases gradually with age throughout the period of longitudinal arch development and foot growth. The longitudinal arch completes its development around age 6 (Bertsch *et al*., 2004; Onodera *et al*., 2008; Müller *et al*., 2012), and it was therefore predicted that the cuboid facet angle would increase over the first 6 years of life, but then remain stable. The youngest individual in the sample, estimated to be between 1-2 years of age, had a cuboid facet angle of 87.4°, and this angle increased to a mean of 92.8° in those aged 2-4 years, and 93.73° in those aged 4-6 years. The mean cuboid facet angle of those aged 6-12 years was 98.24°, however, showing that the angle continues to increase beyond the age of 6. There was no significant difference in the cuboid facet angle among individuals older than age 12, however, suggesting that the distal calcaneus achieves its adult morphology in early adolescence when foot growth is complete (which is around age 12-13 in females and 15 in males; Scheuer & Black, 2004).

The cuboid facet angle did not differ between males and females within each population, nor did it differ between the two populations as a whole. The archaeological populations exhibit a mean cuboid facet angle (Mis Island = 99.88°; Norris Farms =

101.76°) that is similar, but slightly lower, than what was reported for the MRI sample (103.58°), and even lower than what was presented for the X-ray sample (109.2°). Given that the cuboid facet angle is positively correlated with longitudinal arch height, these data suggest that individuals in the archaeological populations would have had lower longitudinal arches than those in the contemporary populations. The status of footwear use for the archaeological populations is unknown, but it is presumed that any shoes worn by these individuals would have been softer-soled and less constrictive than those worn by individuals in the contemporary X-ray and MRI samples. If so, then these data suggest that the un-shod, or more minimally-shod, populations have a lower longitudinal arch height than the habitually shod populations, a finding consistent with recent reports of arch height and footwear use in contemporary shod and habitually unshod Indians (D'Août *et al*., 2009). Future studies should directly compare variation in the cuboid facet angle between osteological samples representing presumably unshod populations and more contemporary populations who were known to have habitually worn footwear (such as the forensic collections at The University of Tennessee or Texas State University) to further investigate the effects of footwear use on calcaneal morphology and longitudinal arch height.

Cuboid Facet Angle and Longitudinal Arch Height in Fossil Hominins

This study identified a direct relationship between the cuboid facet angle of the calcaneus and longitudinal arch height, suggesting that the cuboid facet angle may be used to estimate arch height, not simply that an arch was present.

Omo 33-74-896 – early *Homo* (*ca.* 2.36 Ma)

Omo 33-74-896 is an isolated calcaneus from Omo (Shungura Formation, Tuff F) attributed to early *Homo* and dating to approximately *ca.* 2.36 Ma (Feibel *et al*., 1989; Gebo and Schwartz, 2006). The fossil was first described by Deloison (1986) as possessing a number of human-like morphologies, including a low longitudinal arch. A more recent review of the Omo 33-74-896 morphology by Gebo and Schwartz (2006) noted that the origin for the long plantar ligament is positioned more posteriorly in this specimen than it is in apes. Because the long plantar ligament is an important anatomical structure that supports the longitudinal arch, the presence of a more human-like insertion point for this structure is suggestive of a longitudinal arch in the Omo 33-74-896 hominin (Gebo and Schwartz, 2006). In contrast, Prang (2015) has recently argued that the Omo 33-74-896 fossil hominin did not have a human-like longitudinal arch based on the angular morphology of the talonavicular joint angle and other articular surfaces of the talus and calcaneus.

The recent study by Prang reported that the cuboid facet angle of Omo 33-74-896 is 99º. This value is greater than the mean cuboid facet angle reported for chimpanzees, orangutans, and gibbons, but close to the mean value of gorillas (Prang, 2015; **Table 3.9**). This value is also similar to the mean value of the Mis Island (Mean = 99.88°) and Norris Farms (Mean = 101.76°) adult individuals from the current study, but lower than the contemporary human samples from this study and the study by Prang (2015) (**Table 3.9**). The cuboid facet angle for the Omo specimen is also similar to the value reported for *Australopithecus sediba* (Prang, 2015; **Table 3.9**).

The results of the current study suggest that the Omo 33-74-896 hominin could have had a low longitudinal arch. It is important to note that the current study is considering just one metric, however, while the Prang study assigned the Omo specimen as ape-like following a discriminant function analysis of multiple variables. Nevertheless, the cuboid facet angle used here has now been shown to have a positive association with longitudinal arch height, and is directly suggestive of calcaneal elevation within the foot. Humans in the X-ray sample with a cuboid facet angle at or near 99º have a low calcaneal inclination angle and are described as having a "low" longitudinal arch from observation of the external surface of the foot. The Omo 33-74-896 specimen displays a number of ape-like morphologies, including a large peroneal tubercle and posterior extension of the posterior talocalcaneal facet, the latter of which is associated with increased mobility at the subtalar joint (Gebo and Schwartz, 2006). However, the Omo 33-74-896 calcaneus also exhibits a number of human-like features, such as the presence of a lateral plantar process and a large calcaneal body, and is similar in morphology to the AL 333-8 calcaneus (Gebo and Schwartz, 2006). This combination of features suggests that the Omo 33-74-896 hominin may have had low longitudinal arch, but exhibited exaggerated pronation, similar to what is observed in modern flat footed and/or low-arched individuals (Franco, 1987).

OH-8 – early *Homo* (*ca.* 1.8 Ma)

Olduvai Hominin 8 (OH-8) is a partial foot skeleton attributed to *Homo habilis* and dating to approximately *ca.* 1.8 Ma (Wood, 1992). The specimen includes a fragmentary calcaneus, talus, navicular, three cuneiform bones, cuboid, and all five metatarsals (though

the distal aspects are absent). The fact that there is debate surrounding whether OH-8 had a longitudinal arch is surprising, given the completeness of the specimen. Day and Napier (1964) asserted that OH-8 had a longitudinal arch in their initial description of the fossil, and this conclusion was supported by Day and Wood (1968) based on their analysis of the talar neck angle. Others, however, have argued that the OH-8 talus (as well as other hind-foot elements) is intermediate between humans and apes with regards to many aspects of its morphology (Lisowski *et al*., 1974, 1976; Oxnard, 1972; Oxnard & Lisowski, 1980; Kidd *et al*., 1996), suggesting that an arch was not present in this hominin. DeSilva and colleagues (2012) found that the torsion of the OH-8 metatarsal II was also intermediate between humans and apes, though their conclusion was that this feature was suggestive of the presence of a longitudinal arch.

The cuboid facet angle of OH-8 has been discussed by both Berillon (2003) and Prang (2015), each of whom has drawn a different conclusion about whether OH-8 had a longitudinally-arched foot. Berillon (2003) argued that OH-8 likely had an arch given that the cuboid facet angle is higher than the 90° value associated with flat-footed apes. Prang (2015) reports a human-like cuboid facet angle of 108° for OH-8, yet concluded that OH-8 did not have a longitudinal arch based on the results of a discriminant function analysis that sorted the OH-8 talus and calcaneus with apes based on the angular relationships of their joint surfaces. However, given the fragmentary nature of the OH-8 calcaneus, it is unclear whether 108° is an accurate measure of the cuboid facet angle for this specimen. The OH-8 calcaneus is missing much of its proximal end, which means that the plantar surface is not completely defined in order to facilitate the measurement of the cuboid facet angle. Therefore, the cuboid facet angle for OH-8 should be treated as an estimate.

According to data from the current study, the estimated cuboid facet angle of OH-8 (108°) is near the human mean for the X-ray sample (Mean = 109.2°) and the mean

reported by Prang (2015; Mean = 106°), but higher than the mean for the archaeological samples (Mis Island Mean = 99.88°; Norris Farms Mean = 101.76°). According to the regression equation generated from the X-ray sample, a human with a cuboid facet angle of 108º, the value for OH-8, is predicted to have a calcaneus that is elevated approximately 20º from the substrate, creating a longitudinal arch along the lateral column of the foot (**Figure 3.19**). Therefore, the data presented here suggests that the distal calcaneus of OH-8 was most likely elevated within the foot, consistent with the presence of a longitudinal arch.

MH2 (U.W. 88-99) – *Ausltralopithecus sediba* (*ca.* 1.98-1.78 Ma)

Malapa Hominin 2 (MH2) is a female partial skeleton attributed to *Australopithecus sediba* and dating to approximately *ca.* 1.98-1.78 Ma (Dirks *et al*., 2010). MH2 preserves an articulated distal tibia, talus, and calcaneus, described previously by Zipfel and colleagues (Zipfel *et al*., 2011). Zipfel and colleagues describe the cuboid facet as being "angled plantarly, similar to the condition in modern humans and suggestive of an arched foot", but do not report a value for the cuboid facet angle (Zipfel *et al*., 2011:1418). More recently, however, Prang (2015) has reported that the cuboid facet angle of the U.W. 88-99 specimen is 98º, a value greater than the maximum reported value for chimpanzees, orangutans, and gibbons, but close the mean reported for *Gorilla gorilla* (Prang, 2015; **Table 3.9**). As with the Omo specimen, which exhibits a similar cuboid facet angle, this value is similar to that reported for the archaeological human populations in this study, but below the mean values for the contemporary populations (**Table 3.9**). Contrary to Zipfel and colleagues (2011), Prang (2015) concluded that *Au. sediba* did not have a human-like longitudinal arch based on the morphology of cuboid facet and talonavicular angles, as

well as the insertion site of the Achilles' tendon. The results from the current study suggest that if *Au. sediba* had a longitudinal arch, it was likely low in height. Humans in the X-ray sample who have a cuboid facet angle at or near 98º have a low calcaneal inclination angle, and are described as having a "low" longitudinal arch from observation of the external surface of the foot (**Figure 3.19**; **Figure 3.20**). Some individuals in the X-ray sample with a cuboid facet angle of 98° were described as having arches as "low to average" height, and an individual with "average" arches had a facet angle of 97.29°, however, which illustrates that it is possible to have a relatively low cuboid facet angle yet still have a well-developed longitudinal arch.

CONCLUSIONS

- The cuboid facet angle is significantly positively correlated with two radiographic measures of longitudinal arch height: the calcaneal inclination angle and the talar height index.
- The cuboid facet is rounded in toddlerhood and early childhood, and appears to flatten around age 6, the age at which the longitudinal arch may be fully developed. The facet then becomes more plantarly-inclined at a gradual rate until approximately age 12, around the age when foot growth is complete.
- The cuboid facet angle was found to be lower in the two archaeological populations when compared to the contemporary populations, suggesting that longitudinal arch height was also lower in these past populations who presumably wore more flexible, less constrictive footwear.
- The fossil hominins represented by the Omo 33-74-896 (early *Homo*) and MH2 (*Au. sediba*) calcanei are estimated to have had low longitudinal arches, while

OH-8 is estimated to have had a well-developed arch similar to the mean arch height of modern humans.

- The sustentaculum tali angle was not correlated with longitudinal arch height in a small sample of humans, though future studies should continue to investigate the relationship between this angle and arch height to confirm that the current results are not due to sampling error.

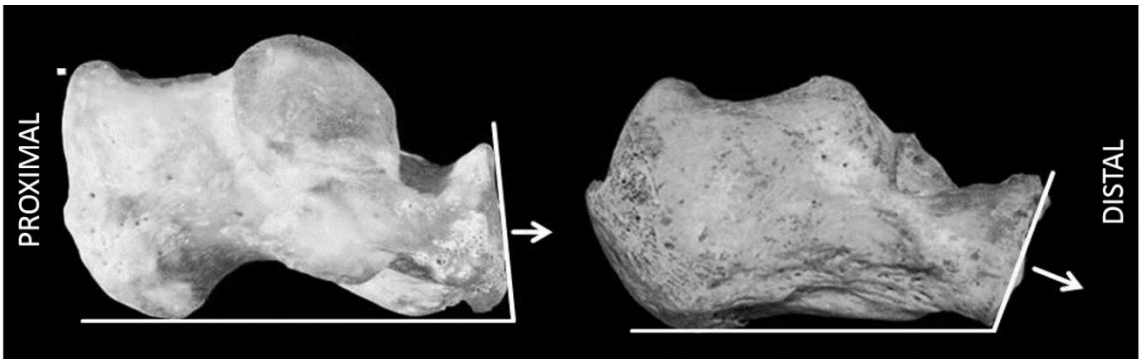

Figure 3.1: Comparison of the calcaneus of great apes and humans in lateral view. In great apes, as exhibited by *Pan* (left), the angle between the cuboid facet and the calcaneal body is near or below 90°. In humans (right), this angle is greater than 90°. Note: calcanei are not to scale; *Homo* is larger than *Pan*.

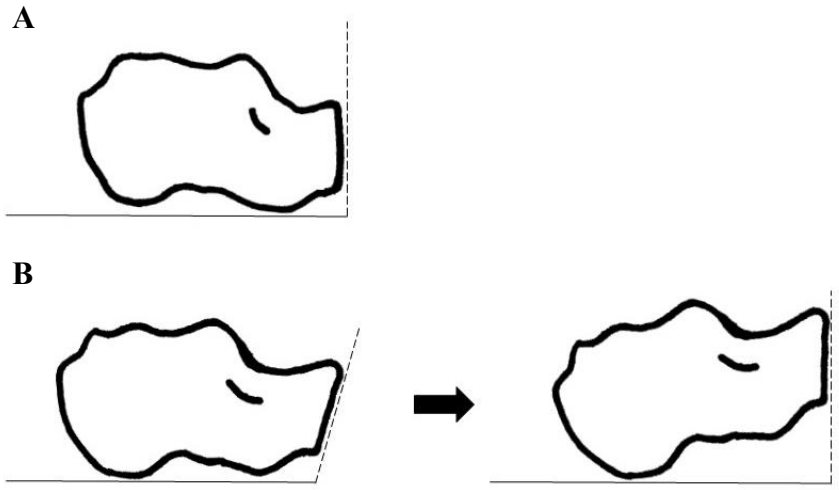

Figure 3.2A: Illustration of the proposed relationship between cuboid facet angle and longitudinal arch height in humans. A) When the cuboid facet is aligned approximately 90º relative to the calcaneal body (as is common among apes), the calcaneus will be positioned horizontally within the foot, aligning the cuboid facet with the vertical plane. B) As the cuboid facet becomes more plantarly-inclined (i.e., cuboid facet angle increases), the distal calcaneaus must assume a more elevated position within the foot in order to align the cuboid facet with the vertical plane. The greater the plantar inclination of the cuboid facet, the higher the distal calcaneus must be elevated to maintain alignment between the cuboid facet and the vertical plane, and thus the higher the longitudinal arch.

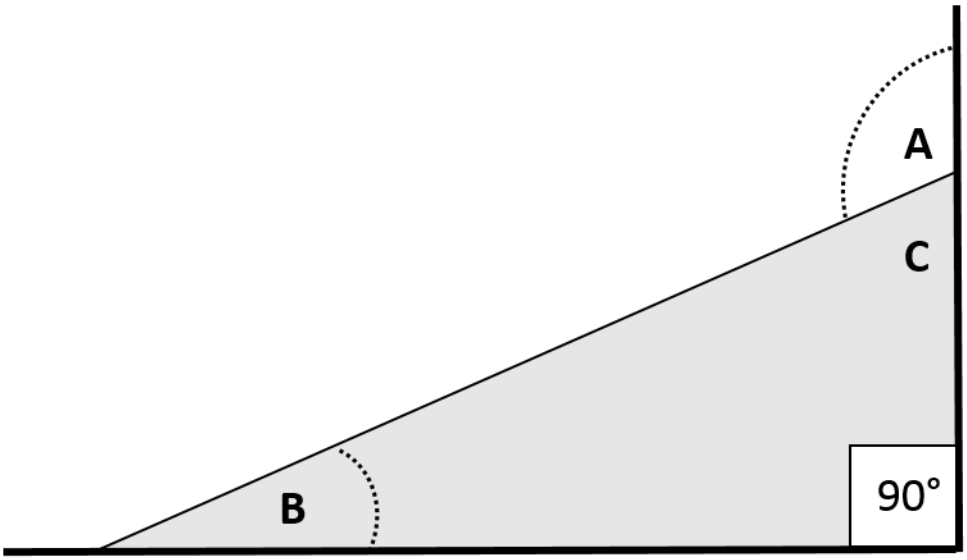

Figure 3.2B: Modeling the relationship between the cuboid facet angle of the calcaneus and calcaneal elevation as exterior (A) and remote (B) angles of a right triangle. Given that the included angles of the triangle must sum to 180°, the elevation of the calcaneus (B) is equal to 90° - C, where C is equal to 180° - A, the cuboid facet angle.

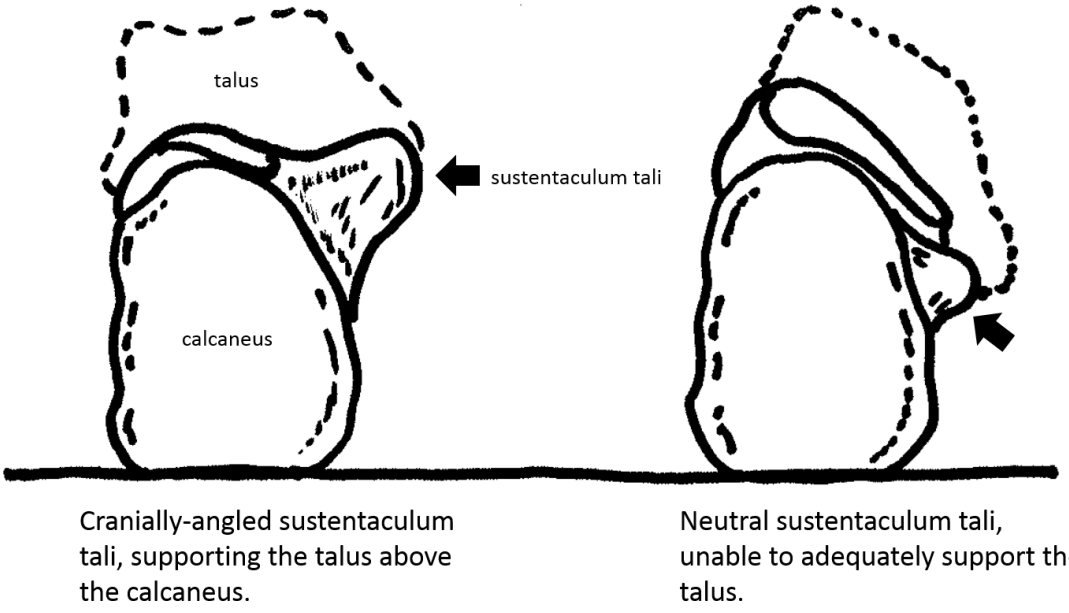

Figure 3.3: Illustration of variation in the sustentaculum tali angle.

	Age Categories (years)						
	1-2	**2-4**	**4-6**	**6-12**	**12-20**	**>20**	**TOTAL**
Mis Island	0	1	7	11	8	160	189
Norris Farms	1	6	0	5	11	29	52
TOTAL	1	7	7	16	19	981	241

Table 3.1: Summary of the number of calcanei included in the study.

Specimen	Species	CFA (°)	Source
Omo 33-74-896	early *Homo* (possibly *Paranthropus*)	99	Prang, 2015
OH-8	early *Homo*	108	Prang, 2015
MH-2	*Au. sediba*	98	Prang, 2015

Table 3.2: Summary of cuboid facet angle (CFA) values reported for fossil hominin tibiae in the published literature.

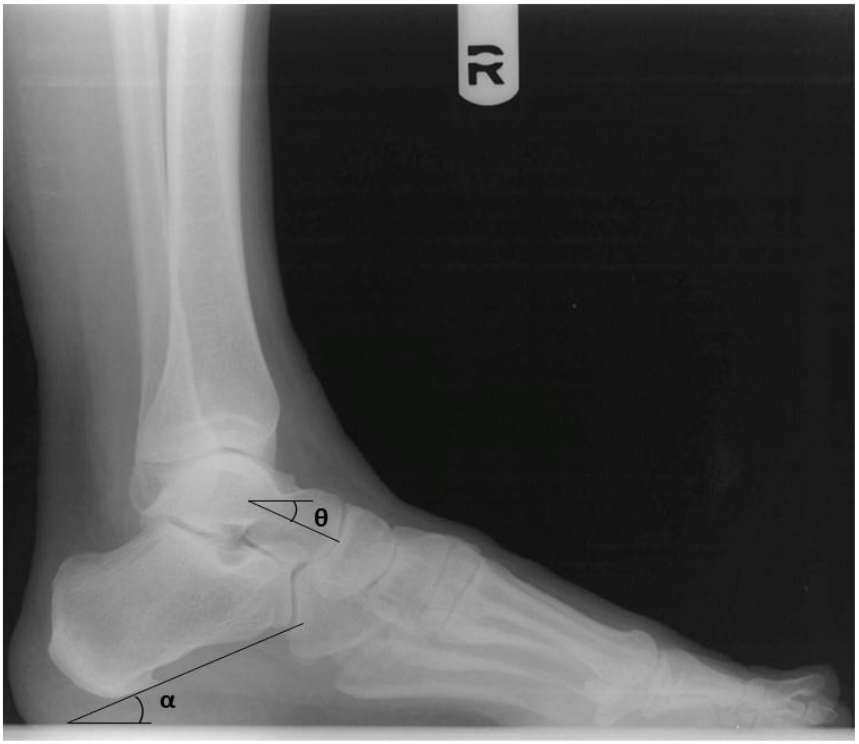

Figure 3.4A: Radiometric angular measures of medial longitudinal arch height. α = calcaneal inclination angle; β = 1st metatarsal angle; θ = talar declination angle.

Figure 3.4B: Radiometric linear measures of medial longitudinal arch height. ω = navicular height; ε = talar head height; λ = bony foot length. The navicular height index (NHI) = ω/λ. The talar height index (THI) = ε/λ.

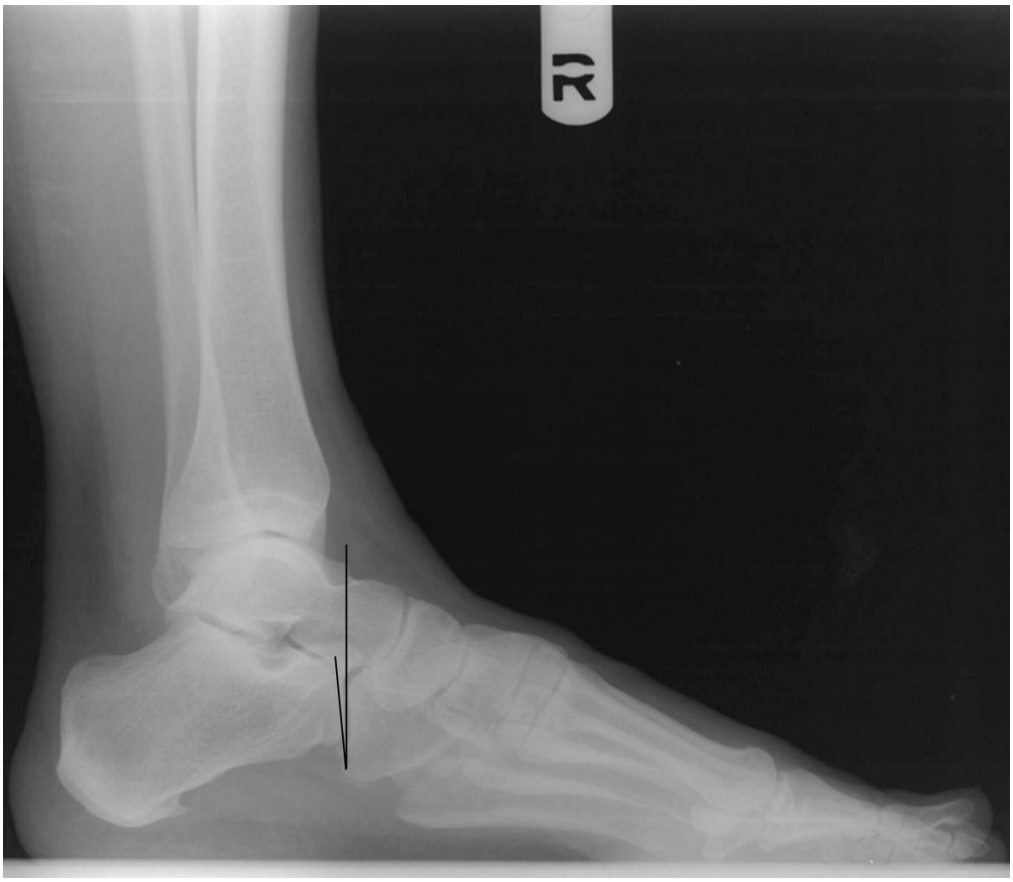

Figure 3.5: Measurement of the deviation of the cuboid facet from the vertical plane. Angles deviated proximally to the vertical plane (i.e., to the left in this image) are negative, while those deviated distally (i.e., to the right in this image) are positive.

Figure 3.6: Measurement of the cuboid facet angle of the calcaneus on x-rays using ImageJ NIH software (modified from Berillon, 2003). Arrow indicates the curved dorsal margin present in some individuals; this bony prominence was not used to measure the cuboid facet angle. Instead, the cuboid facet was measured along the flattest margin of the joint.

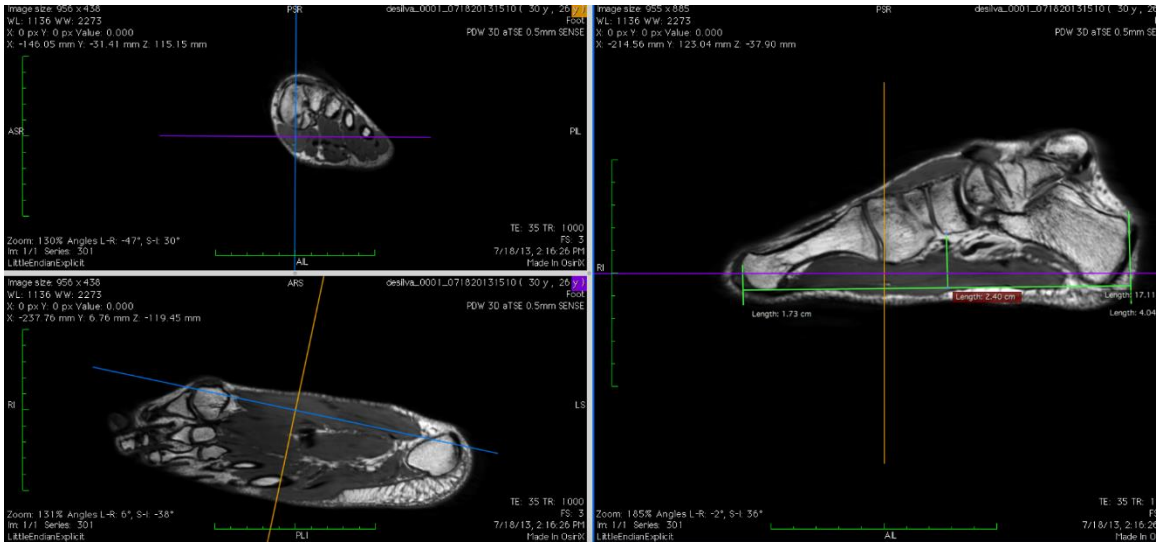

Figure 3.7: Example of OsiriX viewer showing foot in three orthogonal planes. Top left: coronal plane; bottom left: transverse plane; right: sagittal plane.

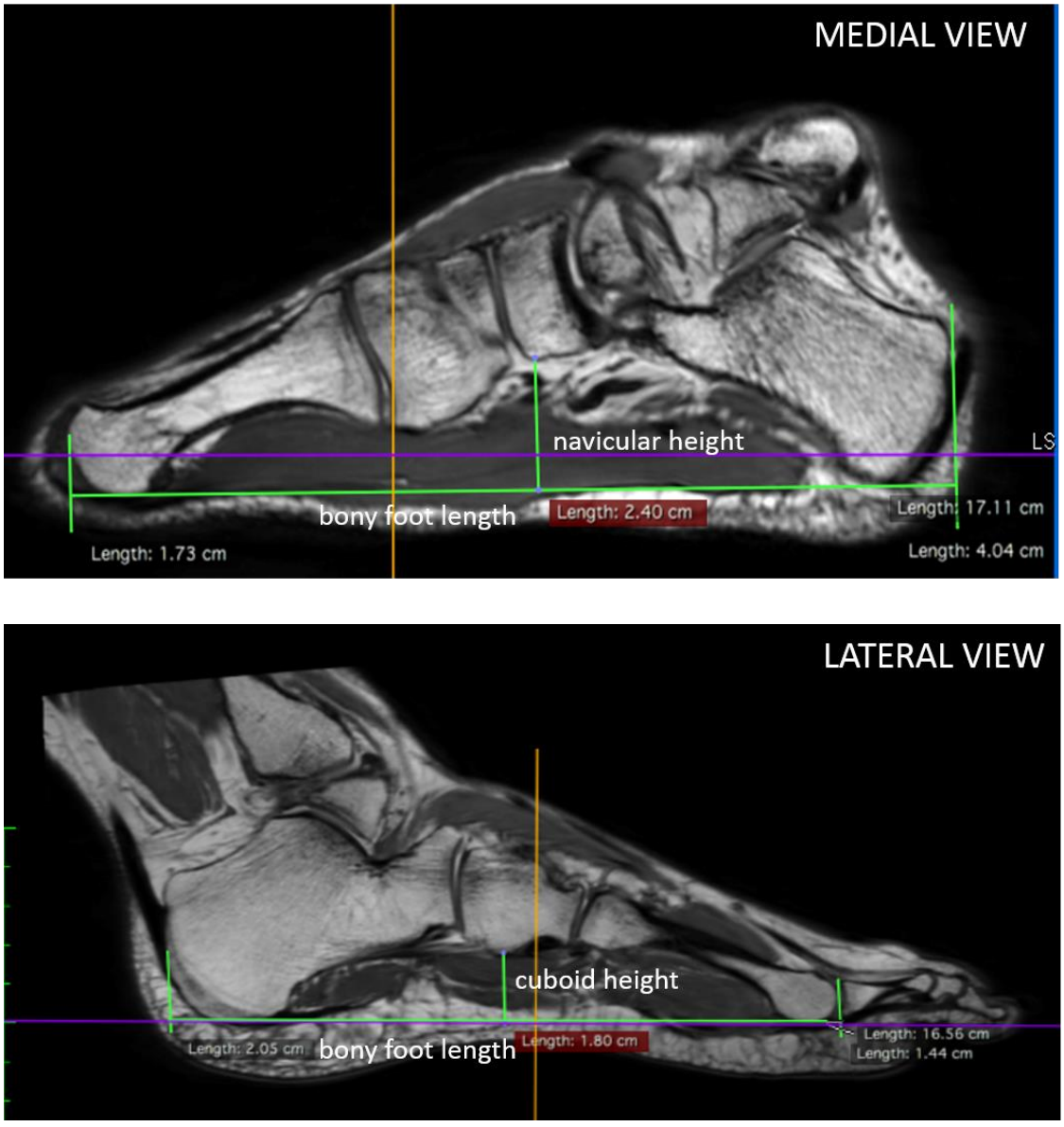

Figure 3.8: Bony measures of longitudinal arch height taken from MRI. Top row: Navicular Height Index (NHI) = navicular height / medial bony foot length; Bottom: Cuboid Height Index (CHI) = cuboid height / lateral bony foot length. Bony foot length is measured as the distance between the proximal aspect of the calcaneus and the distal aspect of the first and fifth metatarsals, respectively. Green lines represent the metrics; orange and purple lines mark the location of the coronal and transverse view frames, respectively.

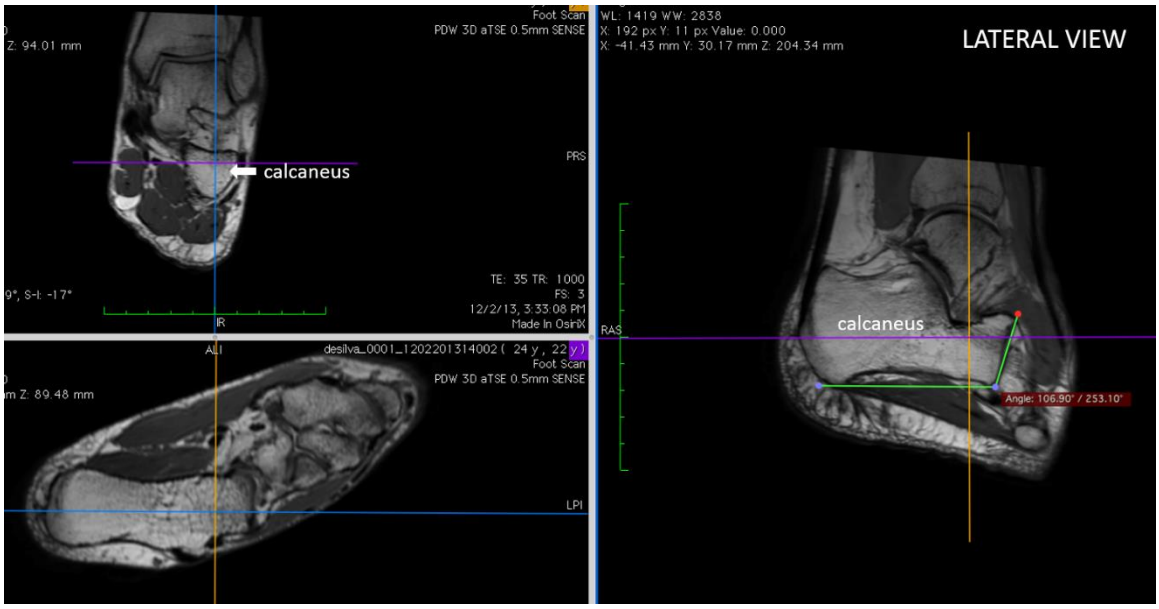

Figure 3.9: Measurement of the cuboid facet angle on an MRI. The green lines in the sagittal plane viewer to the right represent the measurement of the cuboid facet angle. The coronal (top left) and transverse (bottom left) viewers are included to show how the calcaneus was positioned for measurement. The purple, orange, and blue lines mark the location of the transverse, coronal, and sagittal view frames, respectively.

Figure 3.10A: Measurement of the sustentaculum tali angle of the calcaneus on MRI scans using OsiriX DICOM software. This image shows all three view frames to show how the calcaneus was positioned for measurement. Top left: coronal plane; bottom left: transverse plane; right: sagittal plane.

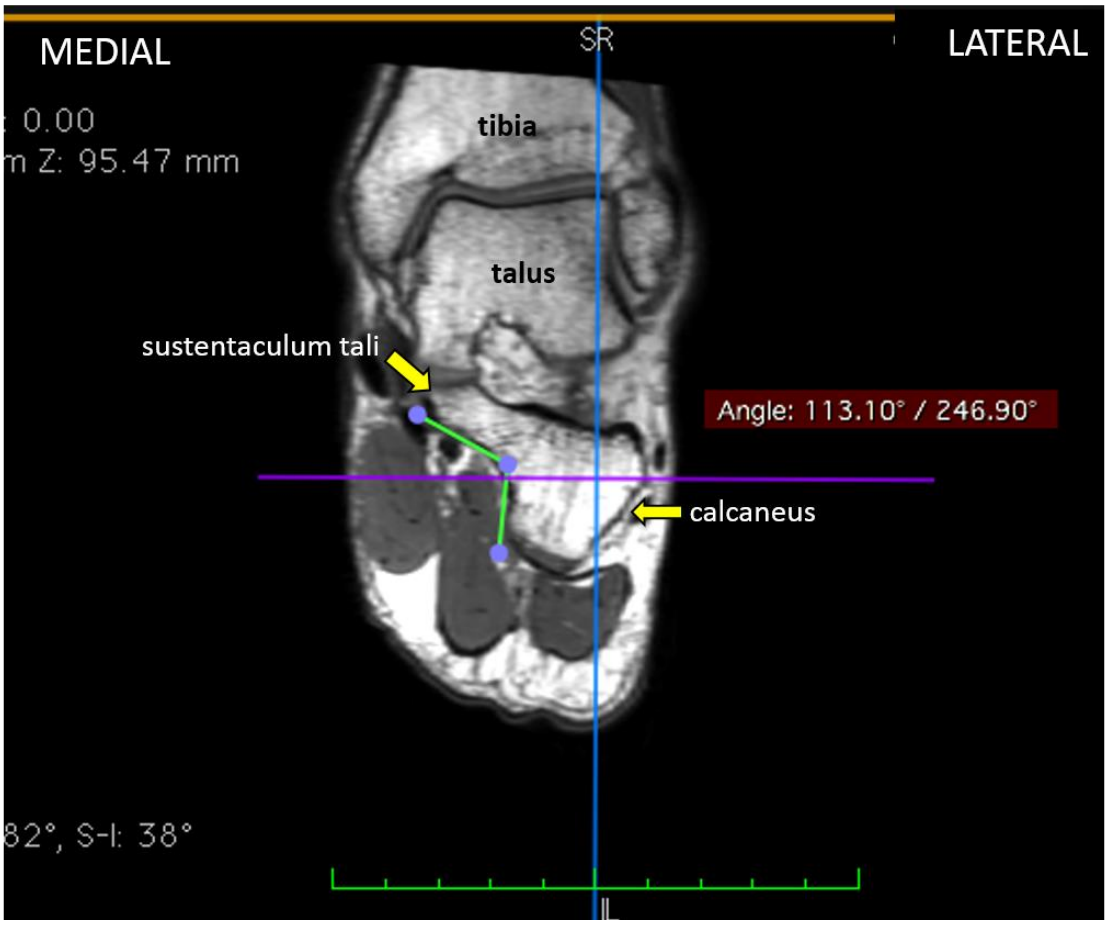

Figure 3.10B: Measurement of the sustentaculum tali angle of the calcaneus on MRI scans, zoomed-in view. This image shows a closer look at the coronal view frame. The sustentaculum tali angle was measured as the angle enclosed between a line along the plantar surface of the sustentaculum tali and a line along the medial aspect of the calcaneal body (shown in green). The purple and blue lines mark the location of the transverse and sagittal view frames, respectively.

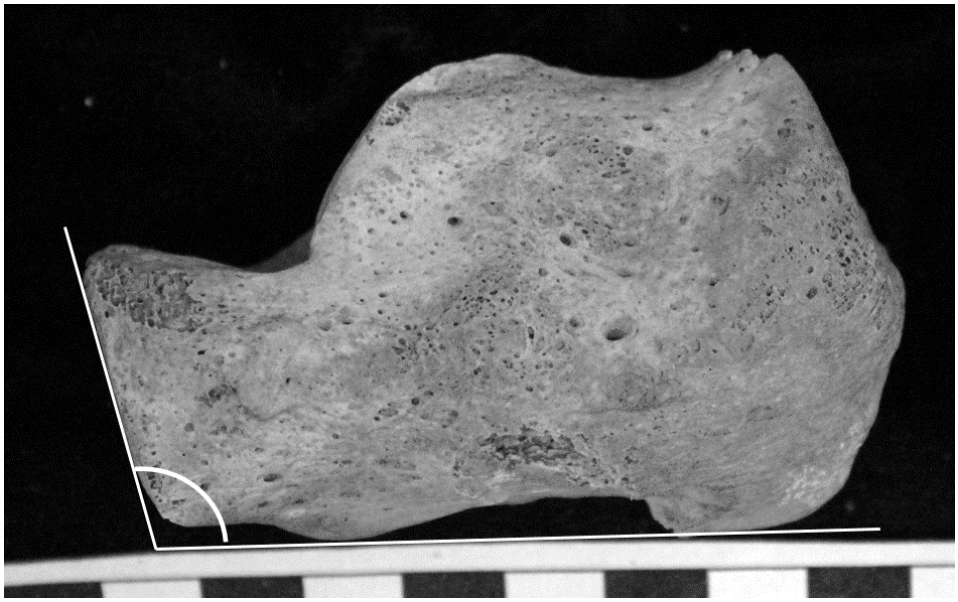

Figure 3.11A: Measurement of the cuboid facet angle of the calcaneus on an adult osteological specimen. The cuboid facet angle is the angle enclosed between the plantar surface of the calcaneus and the flattest margin of the cuboid articular facet.

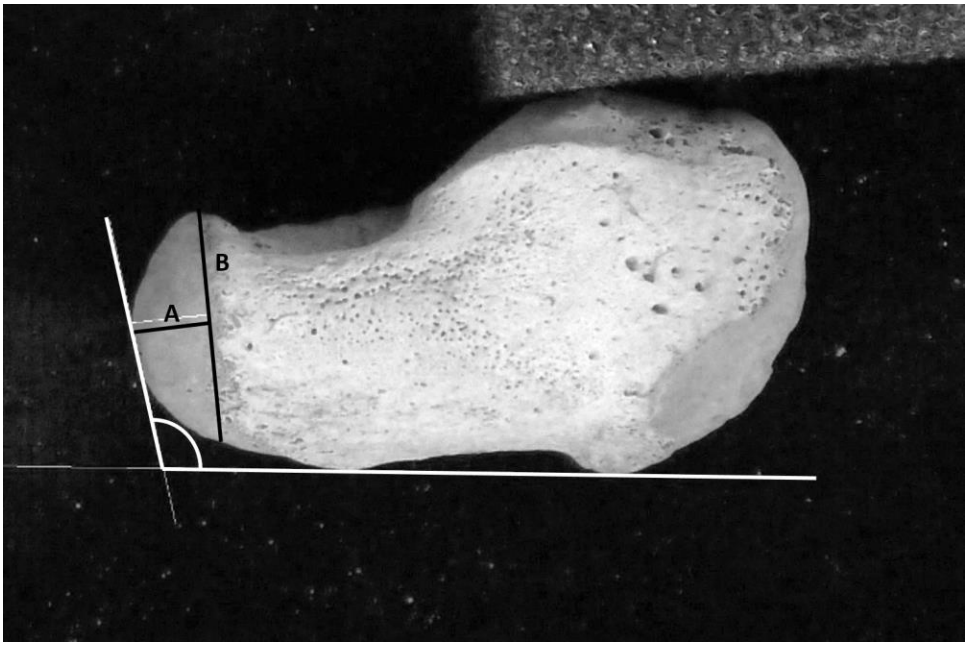

Figure 3.11B: Measurement of the cuboid facet curvature index and cuboid facet angle on a juvenile specimen. The cuboid facet curvature index was calculated as the length of line "A" divided by the length of line "B". The cuboid facet angle is the angle enclosed between the plantar surface of the calcaneus and the flattest margin of the cuboid articular facet.

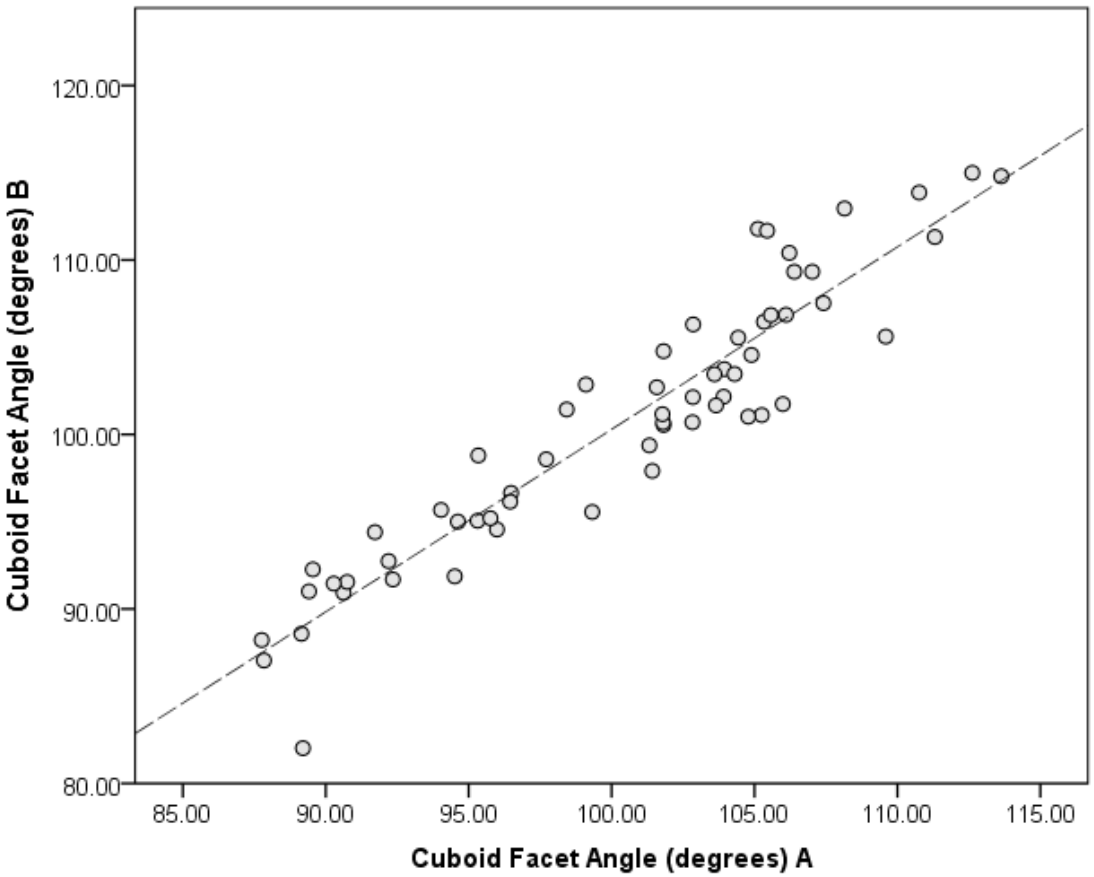

Figure 3.12: Scatter-plot of CFA measurements taken by author during data collection for full study (A) and during data collection for a pilot study (B) on a subset of calcanei from the Mis Island sample (N = 60).

	N	MEAN	SD	MIN	MAX
Radiograph Variables					
vertical deviation of facet	119	-0.10	5.01	-15.52	14.74
cuboid facet angle	119	109.20	6.44	94.80	127.84
Radiographic Measures of Longitudinal Arch Height					
calcaneal inclination angle	119	19.68	5.17	4.58	37.07
talar declination angle	118	25.89	6.01	13.30	43.56
navicular height index	103	0.16	0.03	0.10	0.23
talar height index	113	0.24	0.03	0.17	0.34
MRI Variables					
cuboid facet angle	18	103.58	4.60	96.12	110.93
sustentaculum tali angle	17	122.52	11.47	100.14	141.48
MRI Measures of Longitudinal Arch Height					
Chippaux-Smirak Index	18	0.167	0.04	0.09	0.27
Navicular Height Index	17	0.184	0.05	0.11	0.35
Cuboid Height Index	17	0.102	0.05	0.06	0.22

Table 3.3: Descriptive statistics for the cuboid facet angle, sustentaculum tali angle, and radiographic and MRI measures of longitudinal arch height.

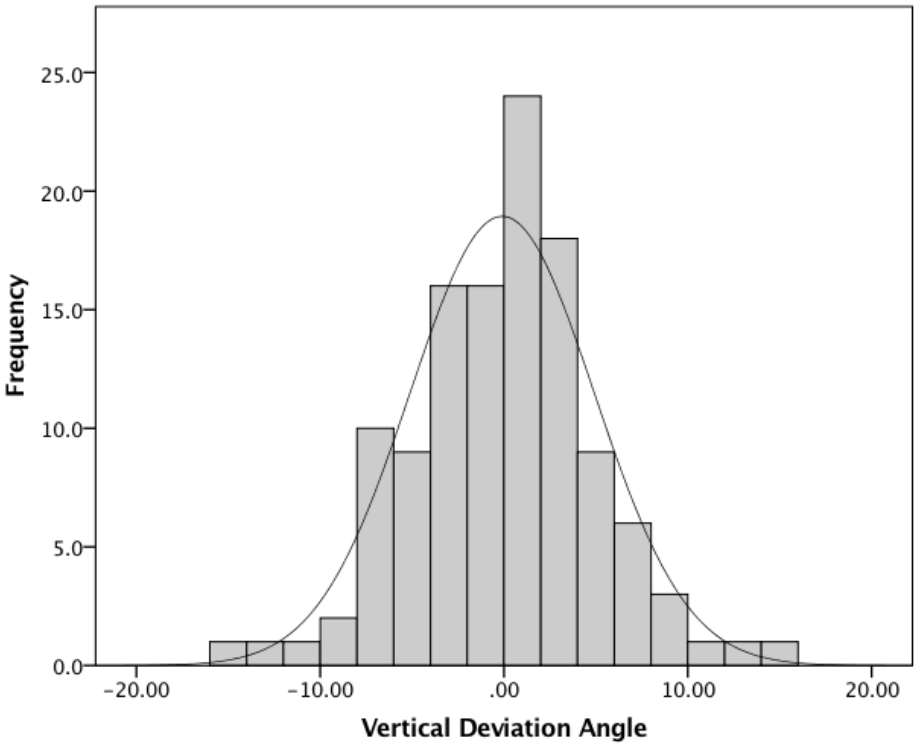

Figure 3.13: Histogram of the deviation of the flattest margin of the cuboid facet from a vertical plane measured on 119 lateral foot and ankle radiographs.

Cuboid Facet Angle (CFA)	N	Mean	SD	Min	Max
complete radiographic sample	122	109.01	6.51	94.8	127.8
“low”	6	104.92	6.62	96.13	109.9
“low to average”	79	109.01	6.54	94.8	122.7
“average”	19	110.01	5.24	97.29	120.8
“average to high”	2	108.66	2.74	106.7	110.6

Table 3.4: Descriptive statistics for the cuboid facet angle (CFA) for the complete radiographic sample and within each of the four arch height categories.

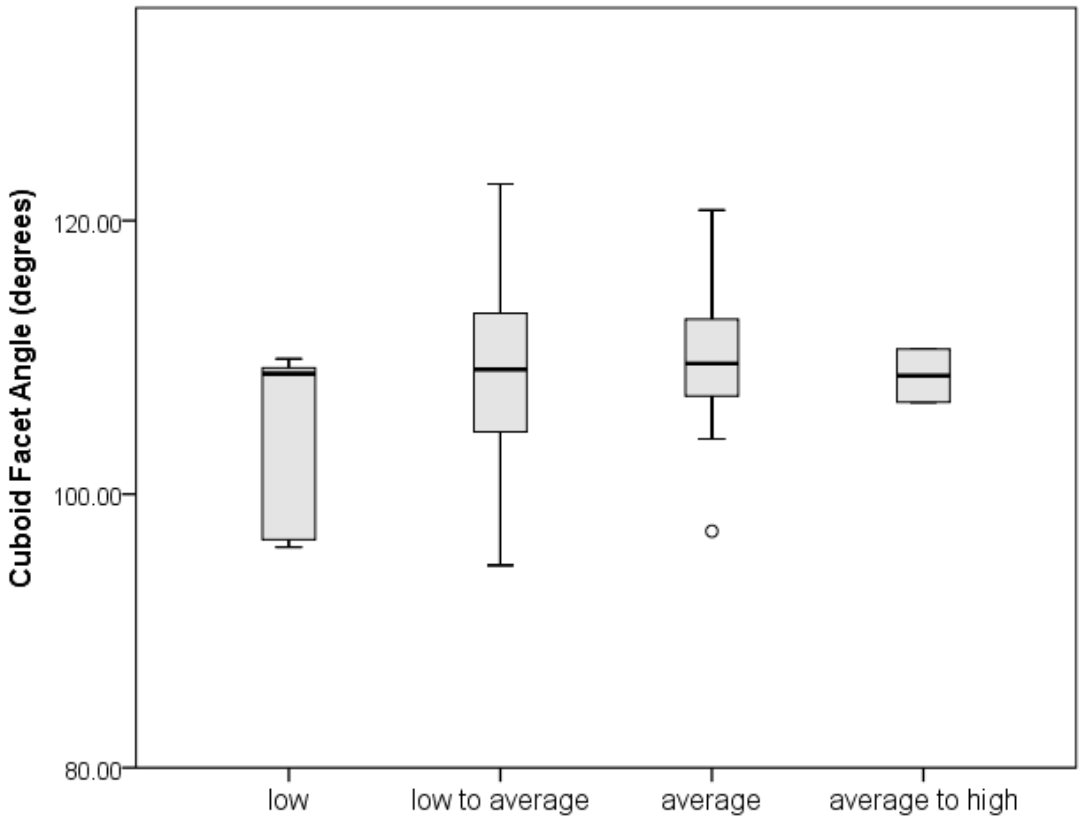

Figure 3.14: Box-plot of median and interquartile range of the cuboid facet angle (CFA) for the radiographic sample across four arch height categories.

	Pearson's r	p -value
Radiograph Data		
calcaneal inclination angle	0.621	0.001*
talar declination angle	-0.063	0.500
navicular height index	-0.106	0.285
talar height index	0.238	0.011*
MRI data		
Chippaux-Smirak Index	0.330	0.181
Navicular Height Index	0.444	0.199
Cuboid Height Index	0.347	0.139

Table 3.5: Correlation coefficients of cuboid facet angle and measures of longitudinal arch height. *significant correlations

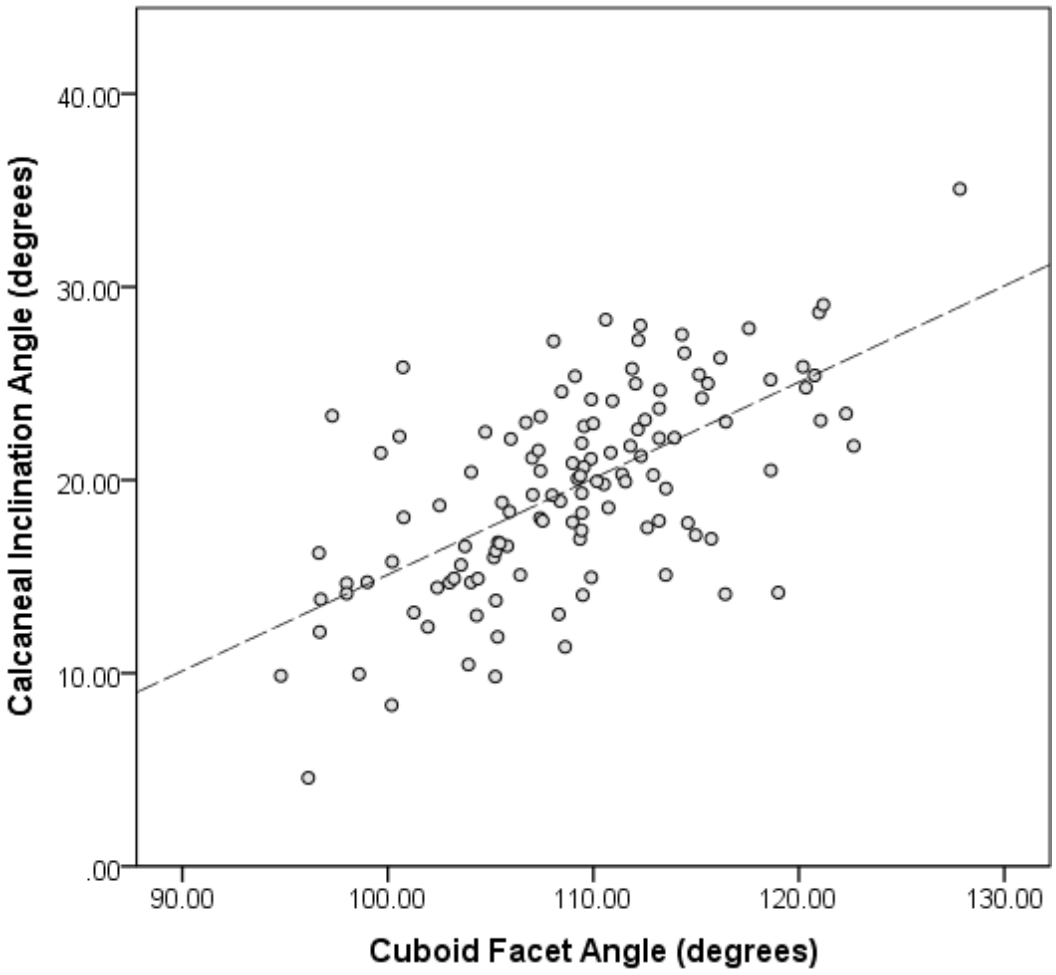

Figure 3.15A: Scatter-plot of cuboid facet angle (degrees) and calcaneal inclination angle (degrees) for the radiographic sample.

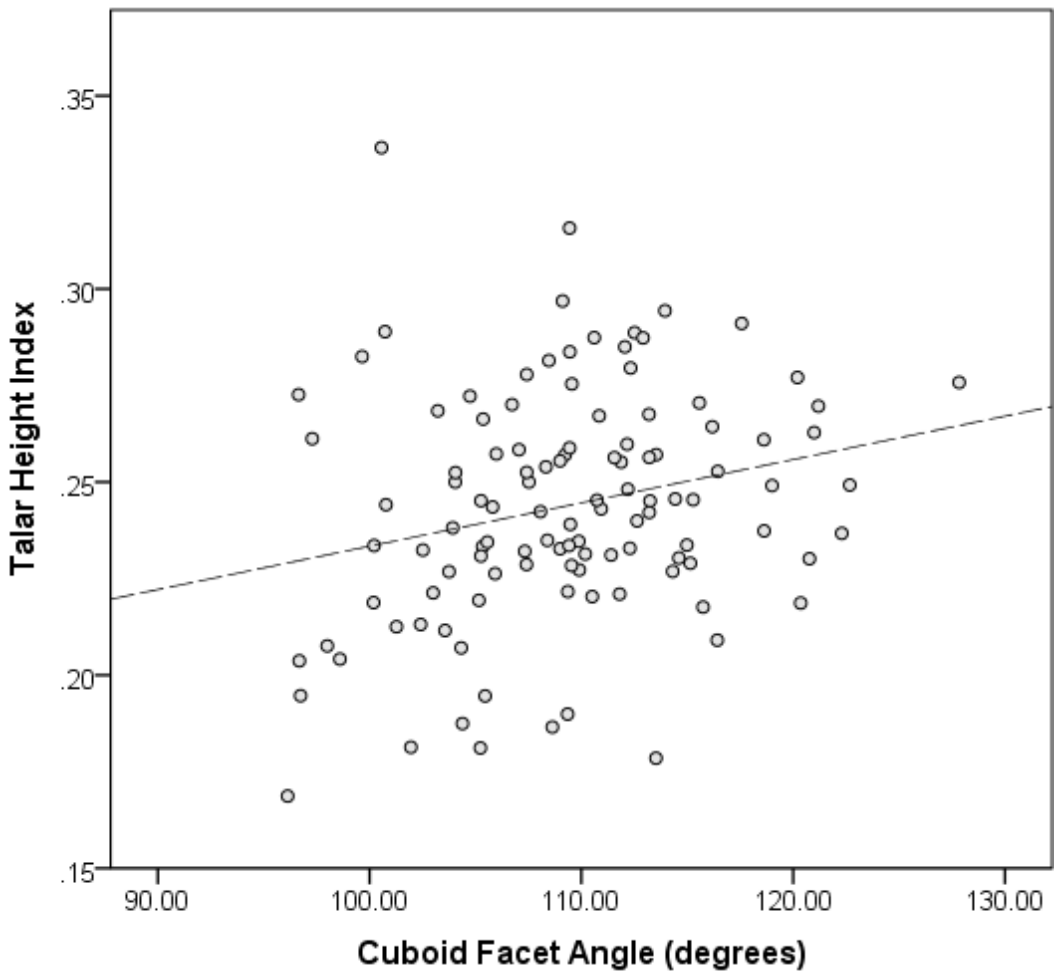

Figure 3.15B: Scatter-plot of cuboid facet angle (degrees) and talar height index for the radiographic sample.

***Sustentaculum Tali Angle* vs.**	**Pearson's r**	**p-value**
Chippaux-Smirak Index	-0.012	0.963
Navicular Height Index	0.178	0.493
Cuboid Height Index	0.201	0.578

Table 3.6: Correlation coefficients of sustentaculum tali angle and measures of longitudinal arch height.

AGE (years)	SAMPLE	N	MEAN	STD	MIN	MAX
1-2	MI	0	----	----	----	----
	NF	1	87.4	----	87.4	87.4
2-4	MI	1	92.18	----	92.18	92.18
	NF	6	93.42	5.05	84.61	97.83
4-6	MI	7	93.73	7.32	80.87	103.94
	NF	0	----	----	----	----
6-12	MI	11	93.53	6.96	79.58	105.33
	NF	5	102.95	8.58	90.61	110.55
12-20	MI	8	100.59	7.38	90.28	111.60
	NF	11	99.76	5.56	89.16	110.08
>20	MI	160	99.88	6.71	81.82	114.78
	NF	29	101.76	4.42	94.12	114.88
TOTAL PER SAMPLE	MI	189	99.34	7.01	79.58	114.78
	NF	52	100.21	5.99	84.61	114.88
TOTAL OVERALL	combined samples	241	99.53	6.80	79.58	114.88

Table 3.7: Descriptive statistics for the cuboid facet angle in the archaeological samples. MI = Mis Island, NF = Norris Farms.

AGE CATEGORY	N	MEAN	STD	MIN	MAX
1-2	3	0.245	0.094	0.17	0.35
2-4	6	0.235	0.055	0.17	0.33
4-6	2	0.133	0.004	0.13	0.14
TOTAL	11	0.204	0.075	0.13	0.35

Table 3.8: Descriptive statistics for the cuboid facet curvature index for juveniles in the combined archaeological samples.

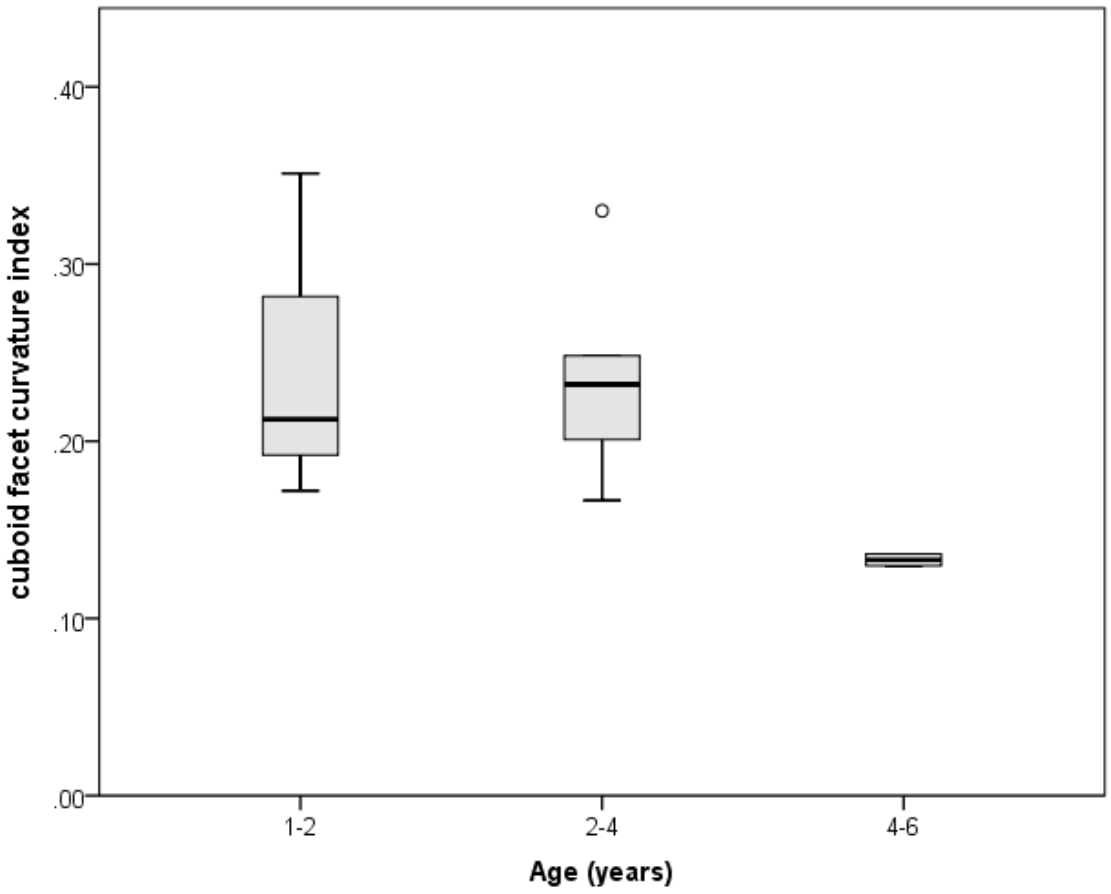

Figure 3.16: Box-plot of the median and interquartile range of the cuboid facet curvature index across three age categories.

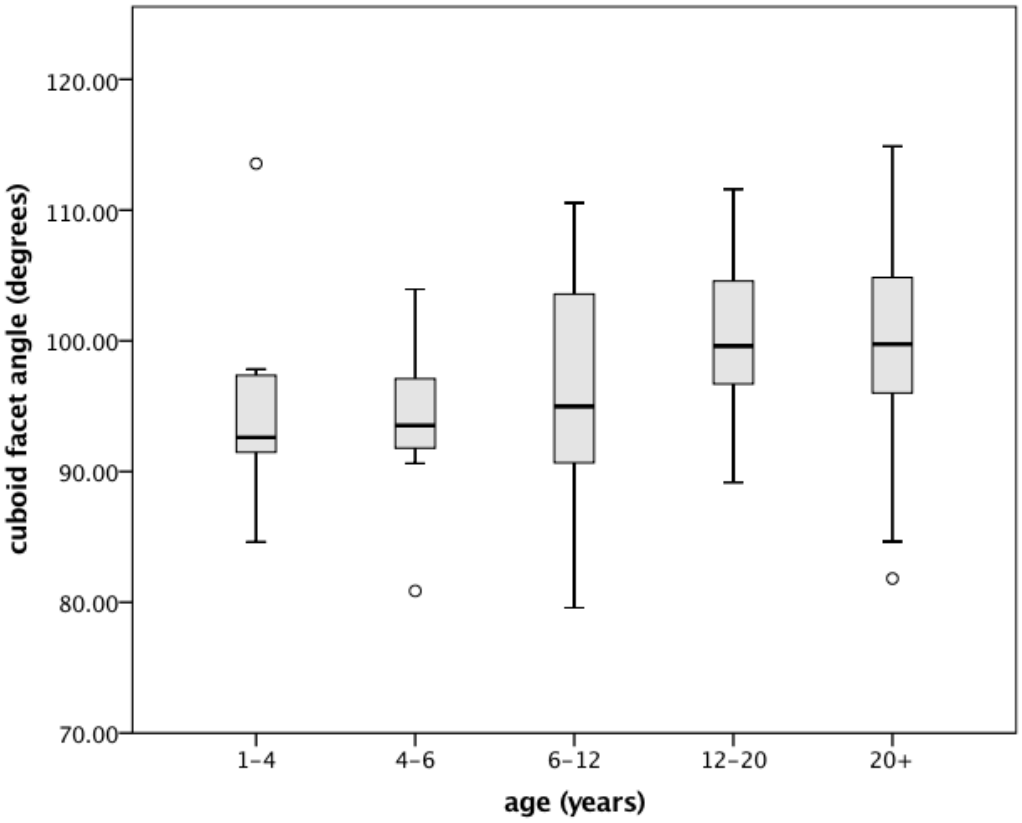

Figure 3.17: Box-plot of the median and interquartile range of the cuboid facet angle across five age ranges.

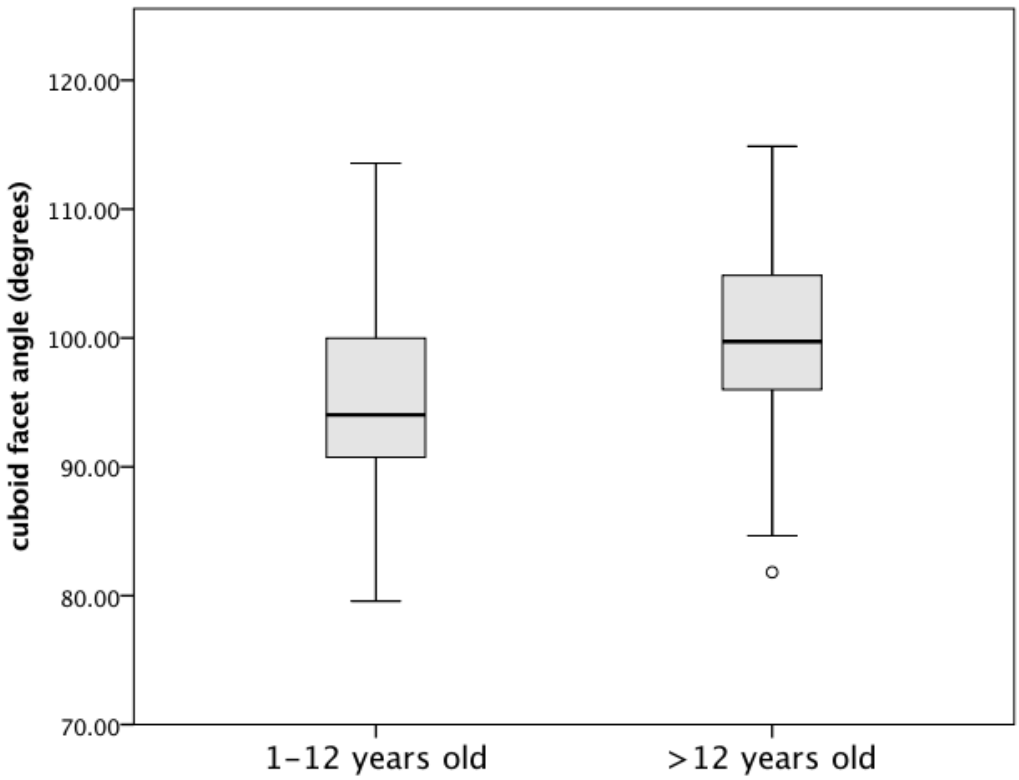

Figure 3.18: Box-plot of the median and interquartile range of the cuboid facet angle across two age ranges.

Taxon	N	Mean ± SD	Min	Max	Source
Homo sapiens	119	109.2 ± 6.4	94.8	127.8	x-rays, current study
	18	103.6 ± 4.6	96.1	110.9	MRI, current study
	160	99.88 ± 6.7	81.82	114.78	Mis Island, current study
	29	101.76 ± 4.4	94.12	114.88	Norris Farms, current study
	30	106 ± 4	97	114	Prang, 2015
Pan troglodytes	33	91 ± 4	84	100	Prang, 2015
Gorilla gorilla	25	100 ± 5	92	110	Prang, 2015
Pongo pygmaeus	15	83 ± 4	75	92	Prang, 2015
Hylobates	21	88 ± 6	77	99	Prang, 2015
MH2 *Au. sediba*	1	98			Prang, 2015
OH-8 early *Homo*	1	108			Prang, 2015
Omo 33-74-896 early *Homo*	1	99			Prang, 2015

Table 3.9: Summary of measures of the cuboid facet angle for humans, extant apes, and hominins. To maintain consistency with other studies, values for the Mis Island and Norris Farms archaeological samples are for adults only.

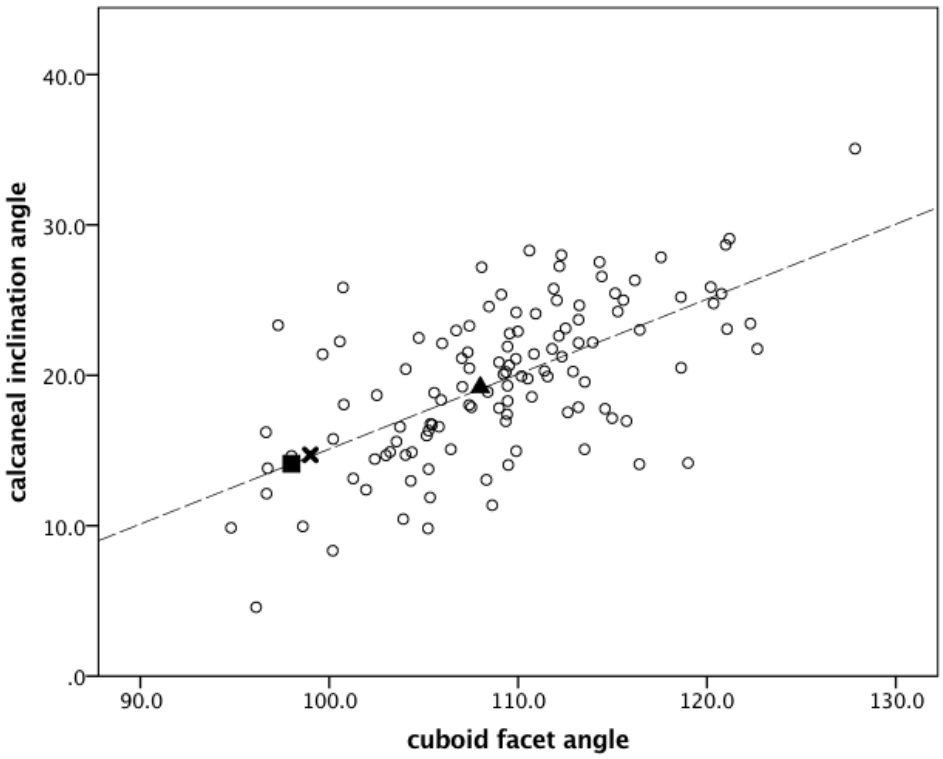

Figure 3.19: Regression of calcaneal inclination angle on cuboid facet angle for the radiographic sample. Hominins are included: square = MH2, X = Omo 33-74-896; triangle = OH-8.

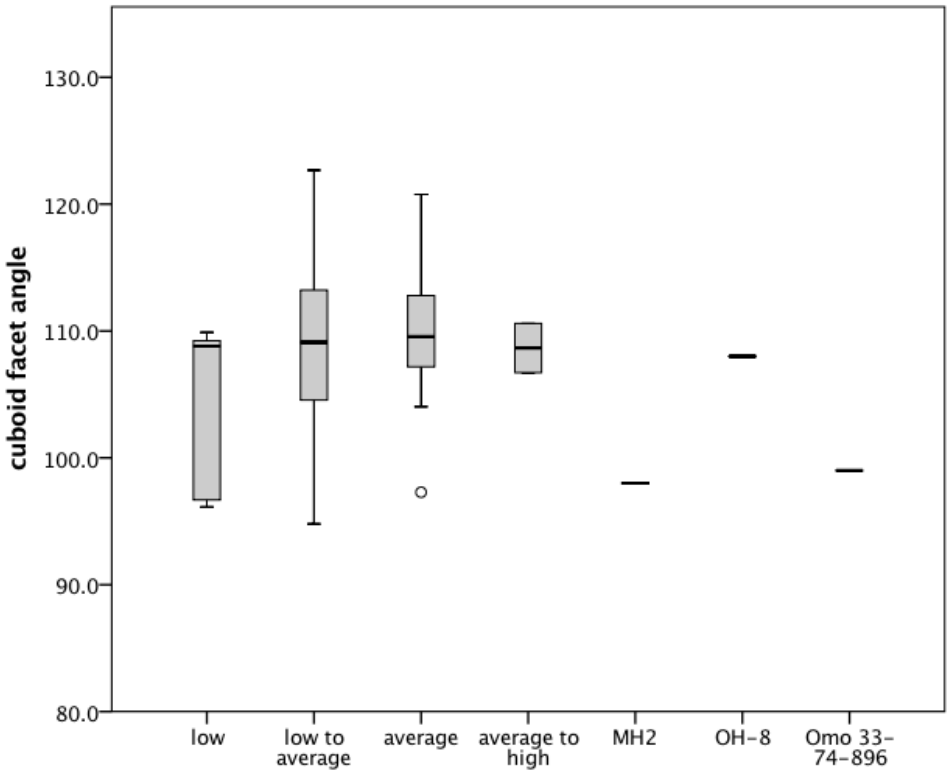

Figure 3.20: Box-plot of the median and interquartile range of cuboid facet angle for subjects from the radiographic sample described as having low, low to average, average, and average to high arches. Hominins MH2, OH-8, and Omo 33-74-896 are included for comparison.

Chapter 4: Ontogenetic and Adult Variation in Human Metatarsal Morphology and its Relation to Longitudinal Arch Height

INTRODUCTION

Metatarsal bone morphology varies among primates in ways that reflect differences in locomotor mode and foot function (Duncan *et al*., 1994; Berillon, 2003; Marchi, 2010; Mitchell *et al*., 2012; Drapeau & Harmon, 2013). In humans, the metatarsal bones act as the anterior pillar of the plantar longitudinal arch and play a key functional role in transferring weight from the hind foot to the forefoot during bipedal locomotion (Morton, 1924). In recent years, it has been suggested that some aspects of human metatarsal morphology may reflect the presence of the longitudinal arch and could therefore be used to assess whether an arch was present in fossil hominins (Berillon, 2003; Pontzer *et al*., 2010; Ward *et al*., 2011; Kuo *et al*., 2016). For example, the proximal base of metatarsal IV (MT IV) is angled plantarly relative to the metatarsal diaphysis in humans, and this morphology has been argued to reflect the elevated position of the proximal metatarsal within a longitudinally-arched foot (Berillon, 2003; Ward *et al.*, 2011). Human metatarsals also exhibit varying degrees of torsion along the shaft, and while this trait contributes to the formation of the plantar transverse arch, some authors have argued that the pattern of human metatarsal torsion may also be related to the presence of the longitudinal arch (*e.g.*, Pontzer *et al*., 2010; Ward *et al*., 2011). Others, however, have challenged the idea that information about whether an arch was present in fossil hominins can be gleaned from metatarsal morphology based on the fact that humans, gorillas, and cercopithecoids overlap in various aspects of their metatarsal morphology, yet only humans have a longitudinal arch (*e.g.*, Mitchell *et al*., 2012). Moreover, humans exhibit variation in longitudinal arch

height, included flat footedness (Hoffmann, 1905; Staheli *et al.,* 1987; Cavanagh *et al*., 1997; Morag & Cavanagh, 1999; Wunderlich & Cavanagh, 2001; D'Août *et al*., 2009), which means uniquely-human morphologies may not necessarily be associated with the presence of a longitudinal arch. Therefore, we require a clearer understanding of whether purported arch-related morphologies actually reflect longitudinal arch presence in humans if we are to use these traits to assess foot form in fossil hominins.

Berillon (2003) was the first to proposed that the base-diaphysis angle of MT IV should reflect longitudinal arch presence in humans. In humans, the metatarsal heads are in contact with the substrate and the proximal base of each element is elevated to a varying degree to articulate with the three cuneiform bones and cuboid of the midfoot. The articulation of the metatarsal bases with these midfoot tarsal elements occurs at an elevated position above the substrate as a result of the presence of both the transverse and longitudinal arches. In order to maintain congruency of the articular surfaces at the tarso-metatarsal joint, the base of the fourth metatarsal is angled plantarly relative to its shaft (>90°) (**Figure 4.1**; Berillon, 2003; Ward *et al*., 2011). In contrast, the metatarsal base of apes has a neutral angle (roughly 90°) relative to its shaft, consistent with a flat foot (Berillon, 2003; Ward *et al*., 2011). Ward and colleagues (2011) note that the base-diaphysis angle of the A.L. 333-160 fourth metatarsal is human-like, and cite this as evidence that a longitudinal arch was present in *Au. afarensis*. However, a subsequent study by Mitchell and colleagues (2012) found that the base-diaphysis angle of A.L. 333-160 falls within the range of variation of *Gorilla gorilla beringei* males, in addition to modern humans. Given that a longitudinal arch is not present in *G. g. beringei*, the results of Mitchell and colleagues' study demonstrate that there is overlap in metatarsal morphology between species who lack a longitudinal arch, such as gorillas, and humans, who have one.

The second aspect of metatarsal morphology that has been argued to indirectly indicate that a longitudinal arch was present is torsion of the metatarsal shaft (Pontzer *et al*., 2010; Ward *et al*., 2011). Torsion of the metatarsal shafts creates the transverse arch of the foot, which is a feature shared by all primates, although the relative degree of torsion of the different metatarsal elements differs between primate groups (Weidenreich, 1923; Morton, 1935; Elftman and Manter, 1935a; Mitchell *et al.,* 2012; Drapeau and Harmon, 2013). In recent years, metatarsal torsion has been used to evaluate whether a hominin's foot had a transverse plantar arch, with the assumption that this would also indicate that a longitudinal arch was present (*e.g*., Pontzer *et al*., 2010; Ward *et al*., 2011). Pontzer and colleagues (2010) measured metatarsal torsion in the Dmanisi hominins and found that torsion of the Dmanisi hominin third and fourth metatarsals was within the range of modern humans and outside that of chimpanzees, suggesting that the Dmanisi hominins had a modern human-like transverse arch. Similarly, Ward and colleagues (2011) argued that the torsion value of the A.L. 333-160 MT IVspecimen attributed to *Au. afarensis* was consistent with the presence of a human-like transverse arch, and that this therefore implied the presence of a longitudinal arch. In both of these studies, metatarsal torsion was used to draw conclusions about the nature of the longitudinal arch, in spite of the fact that no previous study has directly tested the relationship between metatarsal torsion and longitudinal arch height.

Humans are not unique in having a transverse arch, as Drapeau and Harmon (2013) and many others have pointed out, so it is not appropriate to assume that torsion associated with the transverse arch would also indicate that a longitudinal arch was present. Comparative studies by Mitchell and colleagues (2012) and Drapeau and Harmon (2013) have been important in highlighting the fact that humans and cercopithecines overlap substantially in torsion of MT I, MT IV, and M TV, even though cercopithecines do not

have longitudinally-arched feet. Humans are unique, however, in lacking torsion of their second metatarsal and also having a high degree of torsion (eversion) of their third metatarsal (Drapeau and Harmon, 2013; **Figure 4.2**). This finding prompted Drapeau and Harmon to propose that the marked eversion of the third metatarsal in humans could be an indicator of the longitudinal arch, though this relationship has not yet been tested. Drapeau and Harmon (2013) have also noted that modern humans exhibit a large range of variation in metatarsal torsion, and cite population variation in footwear use as a potential cause of this variation. In their study, a sample of Native Americans, who presumably wore soft-sole shoes, was found to exhibit torsion values of MT II and MT IV that were significantly different from a sample of Eurocanadians, who wore hard-sole shoes (Drapeau & Harmon, 2013). Torsion values for the Native American population were closer to the ape range than were the values for the Eurocanadians, indicating that fossil hominins – who presumably did not use footwear – may also have had torsion values more similar to apes.

This study has two primary goals. First, this study directly tests the relationship between the base-diaphysis angle, metatarsal torsion, and longitudinal arch height for a sample of humans using data derived from magnetic resonance images (MRIs) to determine whether these aspects of metatarsal morphology can be used to assess whether a longitudinal arch was present in fossil hominins. Second, this study quantifies metatarsal torsion in two spatially and temporally-distinct archaeological populations of human skeletal remains, both of which are presumed to have worn soft-soled footwear. Torsion values are compared between the populations and across age categories to investigate whether torsion changes throughout ontogeny and how it varies among adults.

MATERIALS AND METHODS

Sample

Magnetic Resonance Images (MRI)

The sample includes 19 Magnetic Resonance Images (MRIs) of the feet of healthy adults previously described in Chapter 3.

Human Osteological Remains

The human osteological sample includes the metatarsals of skeletonized individuals from two archaeological populations (Mis Island and Norris Farms) previously described in Chapters 2 and 3. **Table 4.1** summarizes the number of metatarsals included in the study grouped according to the estimated age of the individual. The sample includes metatarsals II, III, and IV. Metatarsals I and V were excluded from the study given that torsion of these elements is not unique among humans in a way that could be related to arch height (Drapeau & Harmon, 2013).

Fossil Hominins

Metatarsal base-diaphysis and torsion angle values for fossil hominins were collected from Drapeau and Harmon, 2013.

Data Collection

Magnetic Resonance Images

Longitudinal Arch Height

Longitudinal arch height was quantified following the methods described in Chapter 3 for the MRI sample. To summarize, the Chippaux-Smirak index (CSI) was used to quantify longitudinal arch height from participant footprints (DeSilva *et al*., 2015), which is measured as the ratio between the minimum width of the mid-foot and the maximum width across the metatarsal heads. Longitudinal arch height was also quantified as a navicular height index and cuboid height index using metrics taken from the MRI image slices (see Chapter 3).

Metatarsal Base-Diaphysis Angle

The base-diaphysis angle was measured on metatarsals II, III, and IV of the MRI sample using OsiriX DICOM image viewer software. The pan and rotation tools were used to position the metatarsal of interest such that the diaphysis was bisected along both the sagittal and transverse planes (**Figure 4.3A**). A line (A) was then drawn along the metatarsal base, connecting it's dorsal- and plantar-most margins (**Figure 4.3B**). A second line (B) was drawn connecting the dorsal- and plantar-most margins of the metatarsal head. The midpoint of each of these two lines was identified, and then a third line (C) was drawn to connect these two midpoints. Finally, the angle tool was used to measure the dorsal angle enclosed between lines A and C (**Figure 4.3B**; following Ward *et al*., 2011).

Metatarsal Torsion

Metatarsal torsion was measured on metatarsals II, III, and IV of the MRI sample using OsiriX DICOM image viewer software. First, the pan and rotational tools were used to position the MRI so that the cross-hairs of the coronal view screen bisected the distal end (head) of the metatarsal of interest into approximately equal medial and lateral, and dorsal and plantar, halves (**Figure 4.4A**, panel A). Next, the metatarsal was aligned in the

sagittal and transverse viewers so that the metatarsal shaft was bisected along the median sagittal and mid-transverse planes. (**Figure 4.4A**, panel A). These rotations served to align the metatarsal head along a dorso-plantar vertical axis and position the proximal metatarsal base directly behind the distal metatarsal head. In other words, the metatarsal was positioned so that the person viewing the screen was looking directly at the distal head of the metatarsal, down through its shaft. While maintaining the metatarsal in this position, the image layers in the coronal plane viewer were scrolled through from distal to proximal, through the metatarsal shaft, until the proximal end was reached (location confirmed in both the sagittal and transverse viewers) (**Figure 4.4A**, panel B). Torsion was measured as the angle enclosed between a vertical line (representing the dorso-plantar median axis of the metatarsal head) and a line bisecting the dorsal and plantar midpoints of the metatarsal base (**Figure 4.4B**).

Human Osteological Remains

Metatarsal Torsion

Metatarsals were first sorted and assigned to a pedal ray based on the morphology of their proximal base and inter-metatarsal articular facet shapes. Sorting metatarsals is challenging for juvenile skeletal remains, but there are some morphological differences that made this task possible. The first metatarsal is larger than the lateral four and is easily distinguished from the others, even in the neonate skeleton (**Figure 4.5**). By approximately age two, the proximal bases of the lateral four metatarsals begin to acquire the shape differences that characterize adult metatarsals. Specifically, the base of metatarsal IV, which is more square in shape (when viewed from the proximal end), can be distinguished from the more triangular bases of metatarsals II and III. Metatarsals II and III are difficult

to distinguish from one another until they acquire their characteristic inter-metatarsal (*i.e.*, medial and lateral) articular facets around ages 6-8. Once these facets are present, the metatarsals can be articulated to confirm their designation as MT II or MT III. All complete metatarsals that could be confidently assigned as MT II, MT III, or MT IV were included in this study. Although torsion of MT II is not thought to be related to arch height (Drapeau & Harmon, 2013), this element was included in the study to test whether it exhibits the same degree of torsion (*i.e.*, minimal torsion) throughout development.

Metatarsal torsion was measured following the methods of Drapeau and Harmon (2013). A MicroScribe G2X digitizer with 5 degrees of freedom (Revware Products, Raleigh, NC) was used to collect coordinate data for four landmarks on each metatarsal. These landmarks include the dorsal and plantar midpoints of the proximal metatarsal base and the distal metatarsal head (**Figure 4.6**). For juvenile specimens where the distal epiphysis (*i.e.*, metatarsal head) had not yet fused to the diaphysis, the landmarks were placed at the dorsal and plantar midpoints of the distal-most aspect of the metaphyseal margin. Before digitizing the landmarks, each bone was secured to the tabletop with clay. Then, 3D landmarks were collected by positioning the MicroScribe's stylus on the landmark of interest and depressing a foot pedal attached to the MicroScribe. Depression of the foot pedal then sent x, y, z coordinates of the landmark's location to a Microsoft Excel © spreadsheet. Using **Figure 4.6** as a reference, torsion was calculated using a custom R script as the angle enclosed between a line connecting the dorso-plantar midpoints of the metatarsal base (points 1 and 2) and a line connecting the dorsoplantar midpoints of the metatarsal head (points 3 and 4) in the coronal plane.

Data Analysis

Relationship between Metatarsal Morphology and Longitudinal Arch Height

This study investigates whether two aspects of metatarsal morphology, the base-diaphysis angle and torsion, are related to longitudinal arch height. Correlation statistics were used to examine the relationship between the base-diaphysis angle and torsion of metatarsals II, III, and IV and the three measures of longitudinal arch height associated with each MRI.

Ontogenetic and Adult Variation in Metatarsal Torsion

Descriptive statistics were calculated for metatarsal torsion in the archaeological samples. These statistics were calculated separately for each archaeological sample and for each age category within each of the two archaeological samples. The six age categories are as follows: 1-2 years (early bipedal walkers that lack a longitudinal arch); 2-4 years (bipedal walkers beginning to develop a longitudinal arch); 4-6 years (bipedal walkers with a developing longitudinal arch); 6-12 years (bipedal walkers with a developed longitudinal arch and a growing foot); 12-20 years (bipedal walkers with a developed longitudinal arch and adult-sized foot, but continue to grow in stature); and 20+ (bipedal walkers with an adult foot size and stature). Age-related variation in metatarsal torsion was investigated using a one-way analysis of variance (ANOVA), where appropriate. Adult variation in metatarsal torsion was investigated between the sexes and between populations using an independent samples t-test.

All statistical analyses were carried out using SPSS version 23.0 (IMB).

RESULTS

Relationship between Metatarsal Morphology and Longitudinal Arch Height

Base Diaphysis Angle

The base-diaphysis angle was measured on metatarsals II, III, and IV from the MRIs of 17 individuals. **Table 4.2** summarizes the descriptive statistics for the base-diaphysis angle. The results of a Pearson's product moment correlation test show no significant relationship between the base-diaphysis angle of metatarsals II, III, and IV and any of the three measures of longitudinal arch height (**Table 4.3**).

Torsion

Torsion was measured on metatarsals II, III, and IV from the MRIs of 17 individuals. Consistent with previous studies (Drapeau & Harmon, 2013), the second metatarsal exhibited only slight torsion, while metatarsals three and four exhibited eversion of the proximal metatarsal base relative to the distal metatarsal head (**Table 4.2**). The results of a Pearson's product moment correlation test are summarized in **Table 4.4**. Torsion of MT II and MT III was not significantly positively correlated with any of the three measures of longitudinal arch height. Torsion of MT IV was not significantly positively correlated with Chippaux-Smirak Index or Navicular Height Index, but was significantly correlated with the Cuboid Height Index ($r = 0.566$, $p = 0.014$; **Table 4.4**; **Figure 4.7**). However, the statistical significance of this relationship appears to be driven by what could be an outlier data point. When this individual is removed from the sample, the correlation is no longer significant ($r = 0.247$, $p = 0.340$; **Figure 4.8**). Until a future study with a larger sample size can determine whether this individual is, in fact, an outlier,

the results of this study indicate that there is no correlation between torsion of the fourth metatarsal and longitudinal arch height.

Ontogenetic and Adult Variation in Metatarsal Torsion

Table 4.5 summarizes the descriptive statistics for metatarsal torsion for the archaeological samples, all ages considered. Torsion was measured on 595 metatarsals belonging to 270 individuals. For juvenile individuals, seven metatarsals could be excluded as being MT I, MT IV or MT V, but it was unclear if they belonged to MT II or MT III. These elements were therefore assigned as "MT II or III". Thirty metatarsals could be excluded as belonging to MT I or MT V, but could not be identified as either MT II, MT III, or MT IV. These elements were therefore assigned as "MT II, III, or IV."

Results of an independent t-test found no difference in mean torsion of MT II [$t(121) = -0.717$, $p = 0.475$] or MT III [$t(127) = 0.829$, $p = 0.409$] between elements estimated to have belonged to males and those estimated to have belonged to females for the Mis Island sample. Torsion of MT IV was significantly higher in females (Mean = 26.69, SD = 9.67) than males (Mean = 23.04, SD = 8.34) in this sample, however (**Figure 4.9**). In the Norris Farms sample, there was no significant difference in the torsion of MT II [$t(23) = 1.254$, $p = 0.222$], MT III [$t(6) = 0.439$, $p = 0.676$], or MT IV [$t(22) = 0.796$, $p = 0.434$] between males and females.

Table 4.6 summarizes the descriptive statistics of metatarsal torsion for the adult specimens in both samples. Results of an independent t-test show that adult individuals from the Norris Farms sample have significantly greater torsion of MT II [$t(150) = -2.924$, $p = 0.007$], and those from Mis Island have significantly greater torsion of MT III [t(140)

= 2.267, p = 0.025] (**Figure 4.10**). Torsion of MT IV did not differ statistically between the two populations.

Table 4.7 summarizes the descriptive statistics of metatarsal torsion for the juvenile specimens in both samples. Results of an independent t-test found no difference in torsion of MT II between the two samples [t(30) = 0.719, p = 0.478]. Juvenile individuals from the Mis Island sample exhibit significantly greater torsion of MT III [t(29) = 2.857, p = 0.008] and MT IV [t(40) = 2.717, p = 0.01], however, than juveniles from the Norris Farms sample (**Figure 4.11)**. There was no significant difference in the torsion of elements that could not be distinguished as belonging to digits II, III, or IV [t(28) = -0.916, p = 0.367].

Given that the two archaeological populations exhibit significant differences in their degree of metatarsal torsion, age-related differences in torsion were investigated separately for each population. **Table 4.8** and **Table 4.9** summarize the descriptive statistics for metatarsal torsion between age categories in the Mis Island and Norris Farms samples, respectively. Given the small sample sizes in the youngest age categories (see **Table 4.1**), it was necessary to collapse the youngest three age categories into a single 1-6 years old age category to permit statistical analysis of the effect of age on metatarsal torsion.

In the Mis Island sample, age did not exhibit a significant effect on torsion of MT II [F(2, 133) = 1.97, p=0.143], MT III [F(2, 139) = 0.482, p=0.618], or MT IV [F(3, 146) = 0.223, p = 0.881]. Also, there was no effect of age on torsion of MT II [F(2,45) = 3.076, p = 0.056], MT III [F(2, 28) = 0.710, p =0.500], or MT IV [F(2, 48) = 1.810, p = 0.175] for the Norris Farms sample. **Figures 4.12 A-C** show side-by-side box-plots of the median and interquartile range of torsion of MT II, MT III, and MT IV across the four age categories. These results indicate that metatarsal torsion does not increase with age. This non-significant result could be influenced by the small sample sizes in the youngest age

categories, however, especially in combination with the large standard deviations (**Tables 4.8** and **4.9**).

Finally, a correlation test was performed to investigate whether torsion of a given metatarsal element was correlated with torsion of the other elements. **Table 4.10** lists the correlation coefficients of the relationship between torsion of MT II and MT III, MT II and MT IV, and MT III and MT IV for adult individuals within each sample. Within the Mis Island sample, there was a significant positive correlation between the torsion of MT III and MT IV ($r = 0.213$, $p < 0.05$), indicating that individuals with a higher torsion of MT III also have higher torsion of MT IV. Within the Norris Farms sample, there was a significant positive correlation between torsion of MT II and MT III ($r = 0.737$, $p < 0.01$), MT II and MT IV ($r = 0.366$, $p < 0.05$), and MT III and MT IV ($r = 0.455$, $p < 0.05$) (**Figures 4.13 A-C**). These data indicate that individuals with a high degree of torsion of MT II also have high torsion of MT III and MT IV, and those with high torsion of MT III also have high torsion of MT IV. However, **Figure 4.13A** shows that the correlation between MT II and MT III may be driven by an outlier individual who has a very high degree of torsion of both elements. When this individual is removed from the sample, the relationship remains statistically significant, though in the opposite direction ($r = -0.167$, $p = 0.041$). Therefore, it is more conservative to conclude that torsion of MT II is not correlated with torsion of MT III in these samples.

Metatarsal Torsion in Fossil Hominins

Metatarsal torsion values have been published for hominins by Drapeau and Harmon (2013) for complete metatarsals, as well as estimates for incomplete fossils. **Table 4.11** lists the metatarsal torsion values for hominins alongside the values recorded for

humans in the current study, as well as previously published values for humans (Pontzer *et al*., 2010; Mitchell *et al*., 2012; Drapeau & Harmon, 2013). The MT II fossil elements belonging to StW 89 and StW 377 exhibit torsion values outside of the range for humans, irrespective of sample (**Table 4.11**). These specimens are intermediate to humans and apes, who exhibit highly inverted MT IIs (*i.e*., negative torsion value; *e.g*., Pan mean = -27.3; Drapeau & Harmon, 2013). Therefore, the torsion exhibited by the two MT II elements from Sterkfontein is unlike the torsion that has been observed among extant apes or modern humans.

Torsion values for the MT III fossil elements were estimated by Drapeau and Harmon (2013), as these three fossils are incomplete. The torsion of StW 388 (14.7°) is close to the mean of the Norris Farms population (13.42°), but is lower than that reported for other humans. The torsion of StW 477 (28.8°) is higher than the mean reported for modern humans, but is within one standard deviation of the MRI sample from the current study and the humans measured in the study by Pontzer and colleagues (2010). The torsion of StW 496 (18.7°) is close to the human mean reported for a number of samples, including that measured in the study by Drapeau and Harmon (2013; human mean = 18.19°), and the Mis Island (19.78°) sample from the current study. Therefore, if the estimates of torsion for these elements is accurate, then the three fossil MT III elements from Sterkfontein exhibit torsion values that are within the range of modern humans.

Torsion of the A.L. 333-160 MT IV fossil was first published by Ward and colleagues (2011) and is 17.8°. This value is below the human mean for all of the known samples for which MT IV torsion has been measured (**Table 4.11**). This value is within one standard deviation below the mean MT IV torsion reported for the Mis Island and Norris Farms archaeological populations, however, as well as the samples from the studies by Pontzer *et al*. (2010), Drapeau and Harmon (2013), and human males from the Mitchell

et al. (2012) study. Therefore, the A.L. 333-160 specimen exhibits torsion that is within the measured range for humans.

DISCUSSION

Metatarsal Morphology and Longitudinal Arch Height in Humans

This study is the first to directly test the relationship between aspects of metatarsal morphology and longitudinal arch height in a sample of humans known to exhibit variation in arch height. Using data derived from a sample of MRIs, this study did not find a statistically significant relationship between longitudinal arch height and either the base-diaphysis angle or torsion of metatarsals II, III, or IV. Therefore, it does not appear that either of these aspects of metatarsal morphology should be used to infer whether a hominin's foot had a longitudinal arch. This finding is considered preliminary, however, given that the sample of MRIs was small and may not have fully sampled individuals from across the full arch height continuum. Future studies should further investigate this relationship using a larger sample size of MRIs and/or human cadaver feet.

Implications for Fossil Hominins

The results presented here suggest that the base-diaphysis angle and/or torsion of fossil hominin metatarsals cannot be used to infer whether the hominin had a foot with a longitudinal arch. Rather, fossil hominins that exhibit metatarsal morphology consistent with that of modern humans could have been flat footed or have exhibited a longitudinal arch of varying heights. For example, the A.L. 333-160 hominin exhibits a base-diaphysis angle that is within the human range (Ward *et al.*, 2011) and torsion that is below the human mean, but within the low-end of the range for modern humans (Ward *et al*., 2011; Mitchell

et al., 2012; Drapeau & Harmon, 2013; **Table 4.11**). Therefore, we can infer that the lateral column of the A.L. 333-160 hominin's foot was human-like, and most likely had a transverse arch that was similar to modern humans. However, given that a transverse arch is a shared trait among primates (Weidenreich, 1923; Morton, 1935; Elftman and Manter, 1935a), and the overlap with gorillas and cercopithecines in both the base-diaphysis angle and torsion of the A.L. 333-160 element (Mitchell *et al*., 2012; Drapeau & Harmon, 2013), it would be misguided to conclude that a human-like transverse arch implicates that a longitudinal arch was also present. Whether there is a relationship between transverse arch height and longitudinal arch height among humans is unknown, and should be investigated.

Ontogenetic and Adult Human Variation in Metatarsal Torsion

Torsion of MT II, III, and IV was investigated in two spatially and temporally-distinct archaeological populations to further examine population-level variation in torsion and test whether torsion varies throughout ontogeny. Mean metatarsal torsion was found to exhibit no change throughout ontogeny, but was found to differ between populations, consistent with a previous study (Drapeau & Harmon, 2013). **Table 4.11** lists the metatarsal torsion values for this study along-side values previously published for other human populations (Pontzer *et al*., 2010; Mitchell *et al*., 2012; Drapeau & Harmon, 2013). Comparison of the adult torsion values for MT II, MT III, and MT IV with those published by Pontzer and colleagues (2010), Mitchell and colleagues (2012), and Drapeau and Harmon (2013) reveals both similarities and differences in torsion values between human populations. In the present study mean torsion of MT II was 8.72° for the Mis Island sample and 16.82° for the Norris Farms sample, values that are higher than the mean of 5.6° reported by Pontzer *et al*. (2010), and the mean of -2.37° reported by Drapeau and Harmon

(2013)[5] (**Table 4.11**). Torsion values for MT III and MT IV were more similar between the studies, however. Mean torsion of MT III was 19.78° for adults in the Mis Island sample, which is similar to published means of 20.4° (Pontzer *et al*., 2010) and 18.19° (Drapeau & Harmon, 2013), but significantly higher than the value of 13.42° measured for adults in the Norris Farms sample. Similarly, mean torsion of MT IV was 24.82° for adults in the Mis Island sample, which was higher (although not statistically significant) than the value of 22.09° for Norris Farms adults, and the value of 20.25° reported by Drapeau and Harmon (2013). Pontzer and colleagues (2010) report a mean torsion value of 23.7° for MT IV, similar to the value of 23.99° reported by Mitchell and colleagues (2012). Together, these data suggest that mean metatarsal torsion is variable between human populations, and this appears particularly true for MT II.

The current available data on population differences in metatarsal torsion suggest that torsion of MTII is more variable than torsion of MTIII and MTIV. This finding may indicate that there this is less variation in elements of the lateral column of the foot than the medial column. The lateral column of the longitudinal arch is functionally important during bipedalism, as weight is shifted to the lateral side of the foot before it is transferred to the metatarsal heads (Ledoux & Hillstrom, 2002). Therefore, any variation in foot bone shape that disrupts the lateral column's ability to participate in weight transfer could negatively impact gait mechanics. The results of this study raise questions about the morphological integration between structures of the medial column of the human foot compared to the lateral. Morphological integration refers to the tendency of morphological features to covary because they share an underlying developmental pathway (Hallgrimsson *et al*., 2002). While most studies of morphological integration have investigated patterns

[5] A negative torsion value indicates that the metatarsal head is inverted relative to the base, whereas a positive value indicates that it is everted relative to the base.

between anatomical regions on a larger scale, such as between the fore- and hind limbs or the hands and feet (*e.g.*, Hallgrimsson *et al*., 2002; Lawler, 2008; Rolian, 2009; Schmidt & Fischer, 2009; Williams, 2010), we know less about how characters could be integrated within an anatomical region, such as the foot. An inter-specific study of the degree of integration of foot morphology between the two columns of the foot could be informative.

The results of this study add to the body of data that shows human populations exhibit variation in metatarsal torsion. If metatarsal torsion reflects transverse arch height, as opposed to longitudinal arch height, then these data reflect population-level differences in the height of the transverse arch. Drapeau and Harmon (2013) noted a difference in torsion of MT II and MTIV between populations who were presumably unshod compared to those who were shod. The archaeological populations included the present study were also presumably unshod, yet they also differ in ways from the unshod data presented by Drapeau and Harmon (2013). A future study should broaden the comparative human sample to include contemporary populations who are known to have worn constrictive footwear (such as forensic collections at The University of Tennessee and/or Texas State University) and additional unshod populations to further investigate the effects of footwear use on metatarsal torsion.

CONCLUSIONS

- Neither the base-diaphysis angle or torsion of MT II, MT III, or MT IV were found to correlate with measures of longitudinal arch height.
- Metatarsal torsion does not change throughout ontogeny.

- Metatarsal torsion was lower in the Norris Farms population compared to the Mis Island population, offering further evidence that torsion varies between human populations.

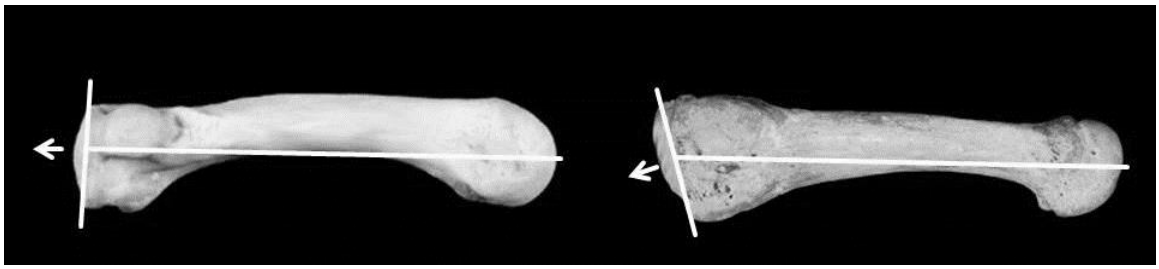

Figure 4.1: Comparison of metatarsal IV of apes and humans in medial view. In apes, as exhibited by *Pan* (left), the dorsal angle between the proximal metatarsal base and the metatarsal diaphysis is near or below 90°. In humans (right), the dorsal angle is greater than 90°.

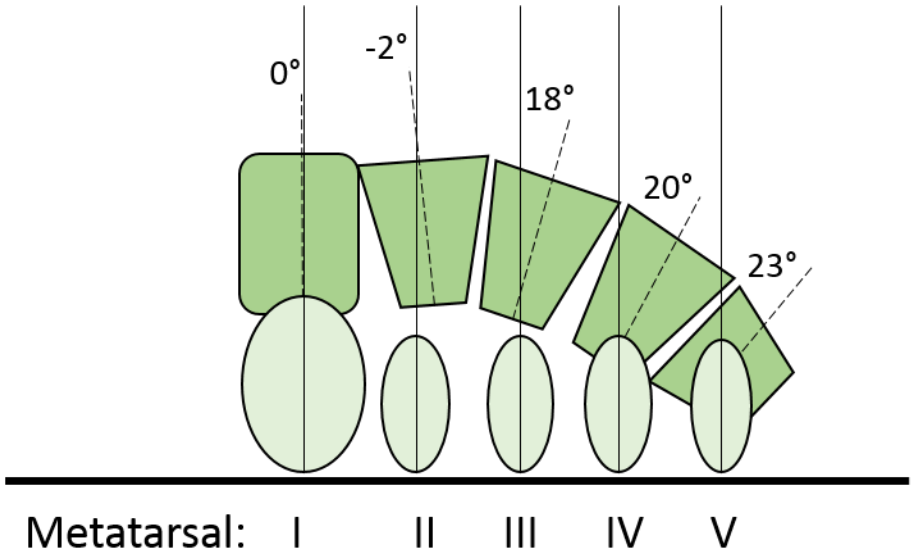

Figure 4.2: Example illustration of human metatarsal torsion. View is of distal metatarsal heads (ovals) looking proximally; rhomboids represent the metatarsal base. Torsion is measured as the angle enclosed between a line connecting the dorso-plantar midpoints of the metatarsal head (solid lines) and a line connecting the dorsoplantar midpoints of the metatarsal base (dotted lines). (Image modified after Drapeau and Harmon, 2013).

	MT II	MT III	MT IV	MT II or III	MT II, III, or IV	TOTAL
Mis Island						
1-2	0	0	1	0	7	8
2-4	0	0	1	0	7	8
4-6	0	0	2	4	0	6
6-12	3	3	6	3	0	15
12-20	8	8	8	0	0	24
20+	125	131	132	0	0	264
Norris Farms						
1-2	0	0	2	0	3	5
2-4	1	2	2	0	11	16
4-6	1	1	3	0	2	7
6-12	10	9	9	0	0	28
12-20	9	8	8	0	0	25
20+	27	11	27	0	0	65
TOTAL	184	173	201	7	30	595

Table 4.1: Summary of the number of metatarsals included in the study from the human osteological samples.

Figure 4.3A: Example of OsiriX viewer showing foot in three orthogonal planes aligned to measures the base-diaphysis angle. Top left: coronal plane; bottom left: transverse plane; right: sagittal plane.

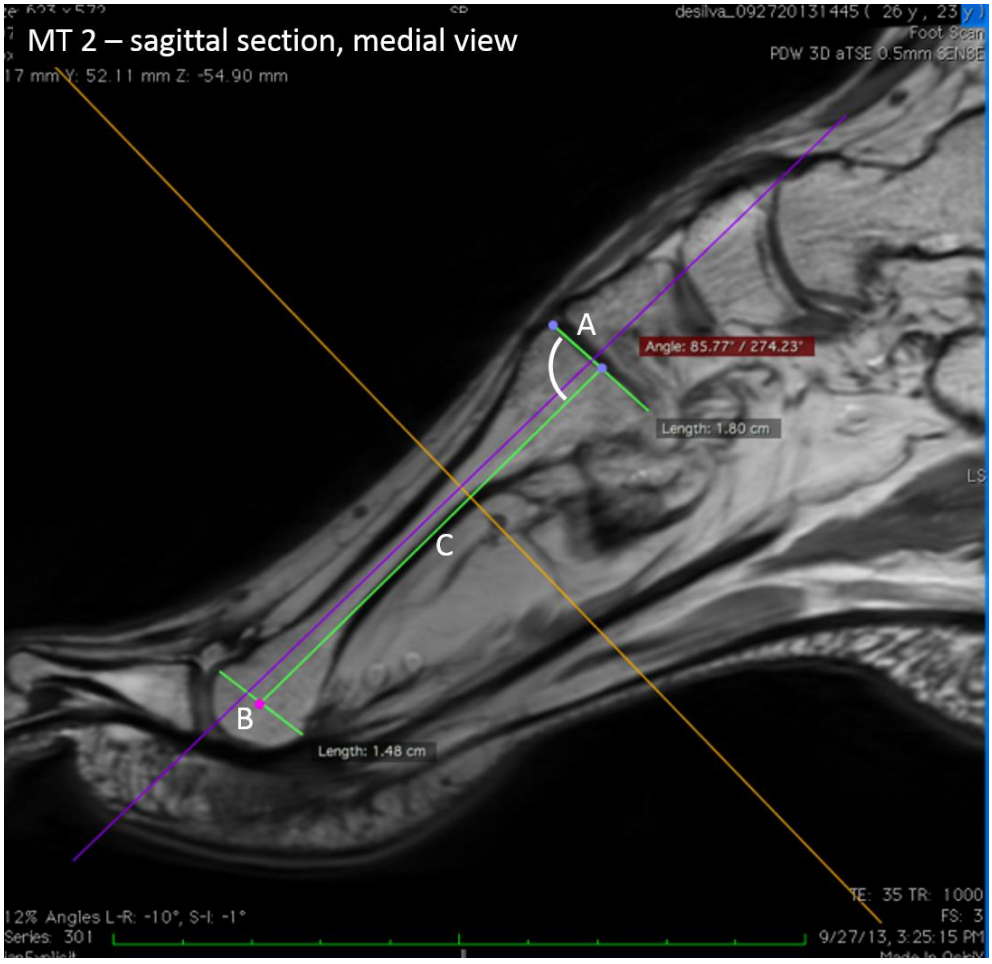

Figure 4.3B: Measurement of the base-diaphysis angle on an MRI. The base-diaphysis angle is measured as the angle enclosed between the green lines A and C. The purple and orange lines mark the location of the transverse and coronal view frames, respectively.

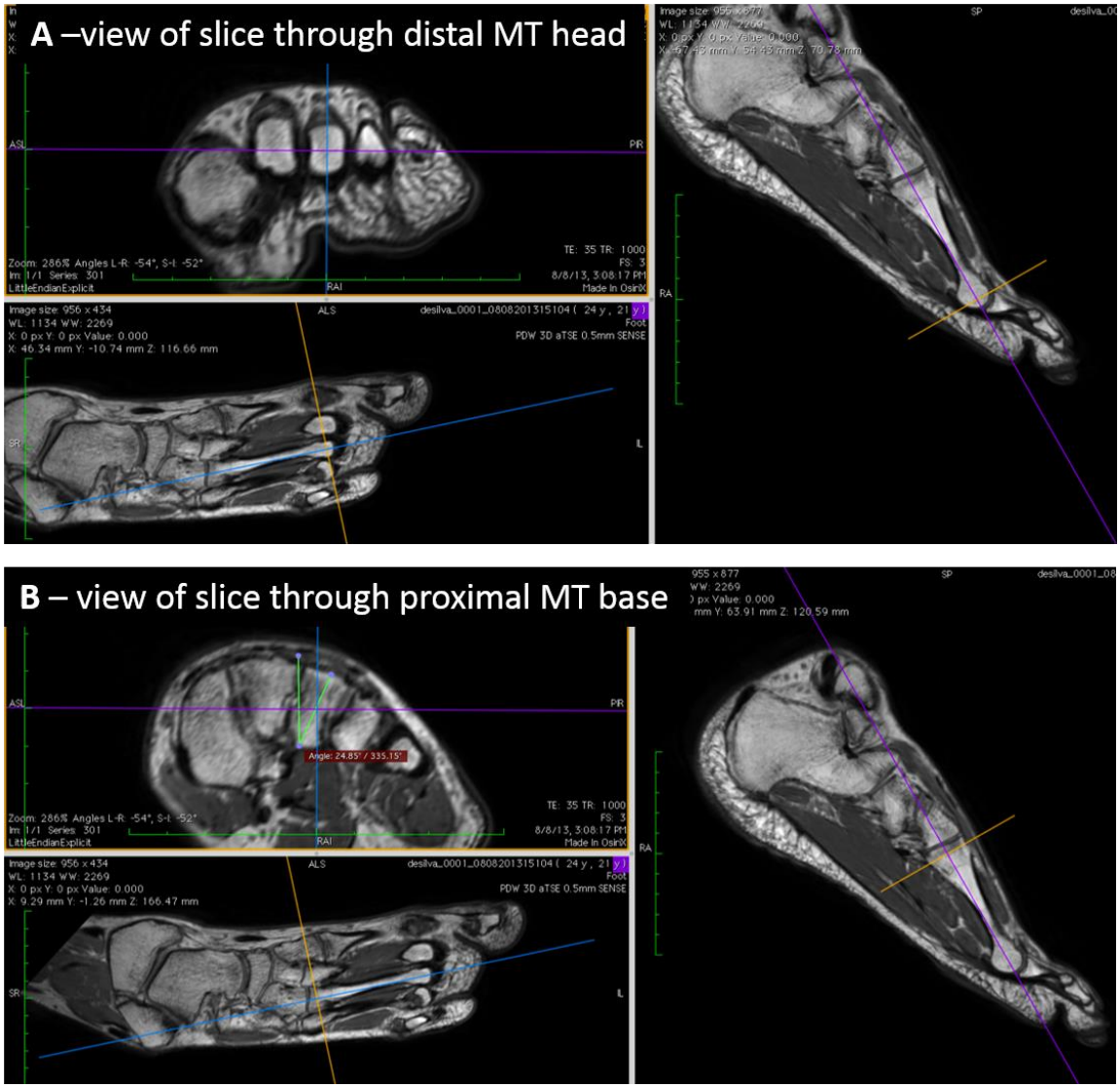

Figure 4.4A: Measurement of metatarsal torsion on MRI scans using OsiriX DICOM software. A) Metatarsal of interest was aligned such that that the cross-hairs (blue and purple lines in top left coronal view frame of panel A) bisected the distal end (head) into approximately equal medial and lateral, and dorsal and plantar, halves. Next, the metatarsal was aligned in the transverse (bottom left of panel A) and sagittal (right of panel A) viewers so that the metatarsal shaft was bisected along the median sagittal and mid-transverse planes. B) While maintaining the metatarsal in the same position (see transverse and sagittal view frames of panels A and B), the image layers in the coronal plane viewer (top left of panel B) were scrolled through from distal to proximal until the proximal end of the metatarsal was reached.

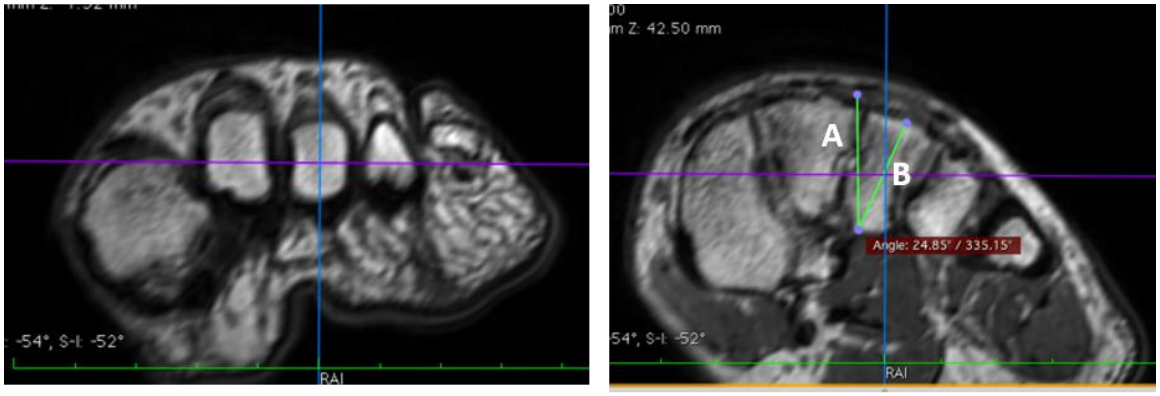

Figure 4.4B: Metatarsal torsion was measured as the angle enclosed between a vertical line (A), representing the dorso-plantar median sagittal axis of the metatarsal head (also represented by the blue line in the image on the left), and a line (B) bisecting the dorsal and plantar midpoints of the metatarsal base. Eversion of the base relative to the head is represented as a positive value, while inversion of the base relative to the head is represented as a negative value.

Figure 4.5: Medial view of metatarsals I - IV of four juvenile individuals from the Norris Farms 36 Cemetery collection. In each series, the proximal base of the metatarsal is towards the left and the distal head towards the right. The order of the metatarsals is MT I – MT IV, from bottom to top. MT V is not pictured.

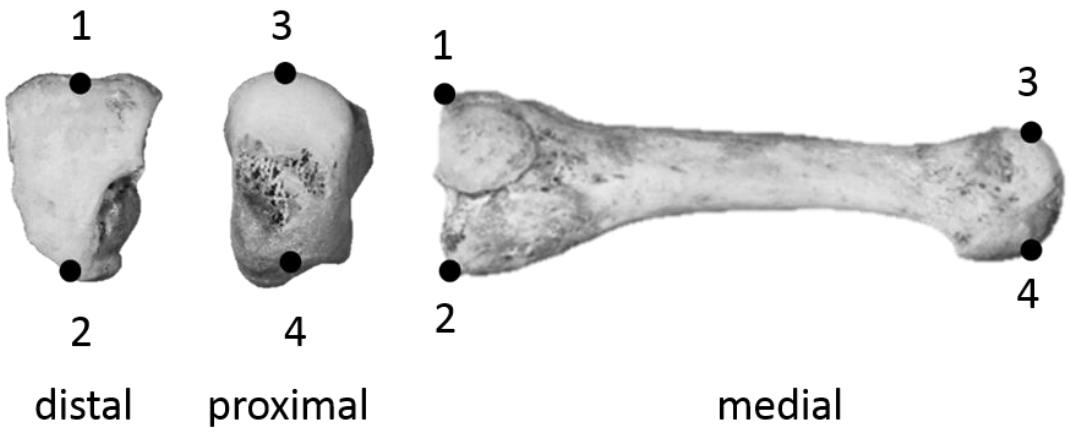

Figure 4.6: Location of four landmarks of the metatarsal used to calculate metatarsal torsion. Images from eSkeletons.org.

	N	MEAN	STD	MIN	MAX
MRI Variables					
MT II base-diaphysis angle	17	90.61	4.80	83.17	101.68
MT III base-diaphysis angle	16	88.64	4.24	83.06	96.55
MT IV base-diaphysis angle	17	96.95	5.71	87.07	105.77
MT II torsion	17	2.00	5.81	-6.70	12.84
MT III torsion	17	24.28	4.84	16.83	32.26
MT IV torsion	17	26.86	7.16	13.28	42.80
MRI Measures of Longitudinal Arch Height					
Chippaux-Smirak Index	18	0.167	0.04	0.09	0.27
Navicular Height Index	17	0.184	0.05	0.11	0.35
Cuboid Height Index	17	0.102	0.05	0.06	0.22

Table 4.2: Descriptive statistics for the base-diaphysis angle, metatarsal torsion, and radiographic and MRI measures of longitudinal arch height.

	Pearson's r	p-value
MT II		
Chippaux-Smirak Index	-0.108	0.680
Navicular Height Index	-0.160	0.541
Cuboid Height Index	-0.132	0.715
MT III		
Chippaux-Smirak Index	-0.010	0.971
Navicular Height Index	-0.135	0.618
Cuboid Height Index	-0.335	0.344
MT IV		
Chippaux-Smirak Index	-0.088	0.738
Navicular Height Index	0.046	0.861
Cuboid Height Index	-0.073	0.841

Table 4.3: Results of Pearson's product-moment correlation of the base-diaphysis angle and measures of longitudinal arch height for the MRI sample.

	Pearson's r	p-value
MT II		
Chippaux-Smirak Index	0.090	0.73
Navicular Height Index	-0.028	0.92
Cuboid Height Index	0.335	0.34
MT III		
Chippaux-Smirak Index	0.325	0.20
Navicular Height Index	0.279	0.28
Cuboid Height Index	0.405	0.08
MT IV		
Chippaux-Smirak Index	0.469	0.06
Navicular Height Index	0.467	0.06
Cuboid Height Index	0.566	0.014**

Table 4.4: Results of Pearson's product-moment correlation of metatarsal torsion and measures of longitudinal arch height for the MRI sample. *significant correlation

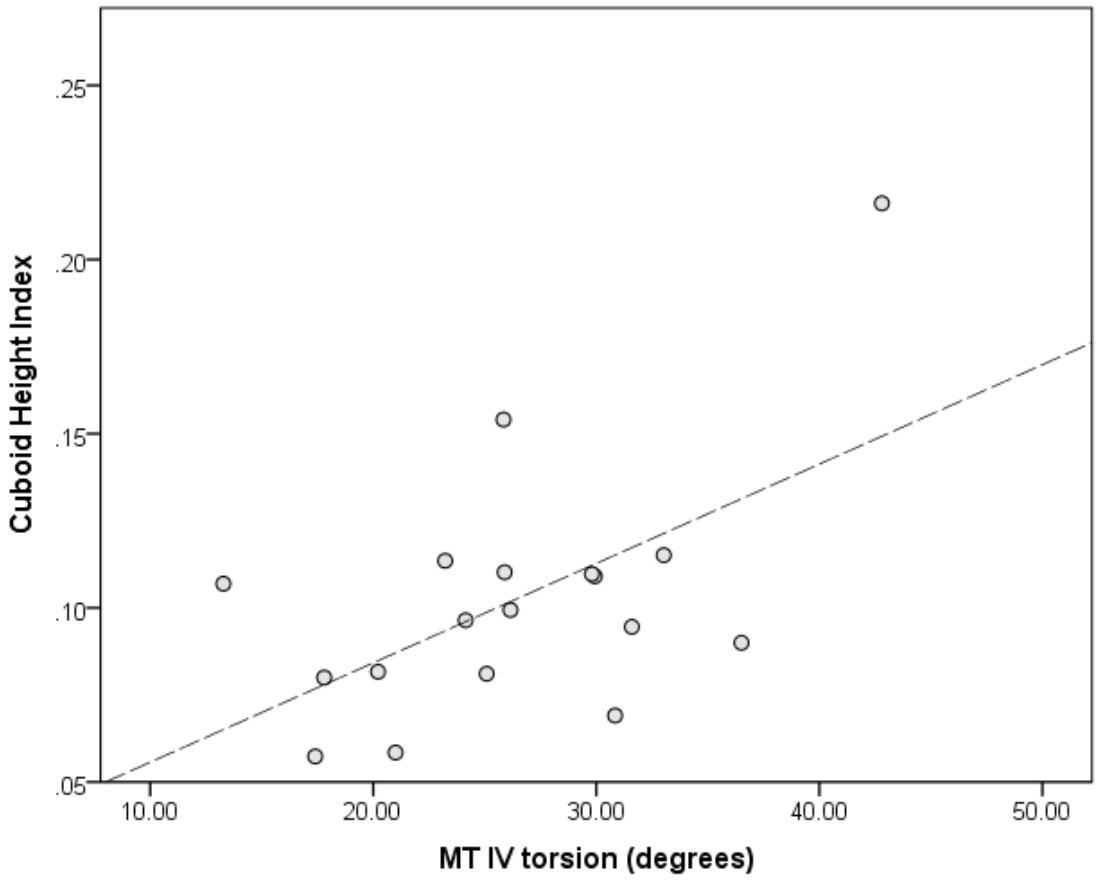

Figure 4.7: Scatter-plot of the cuboid height index and torsion of metatarsal IV for the MRI sample ($r = 0.566$, $p = 0.014$).

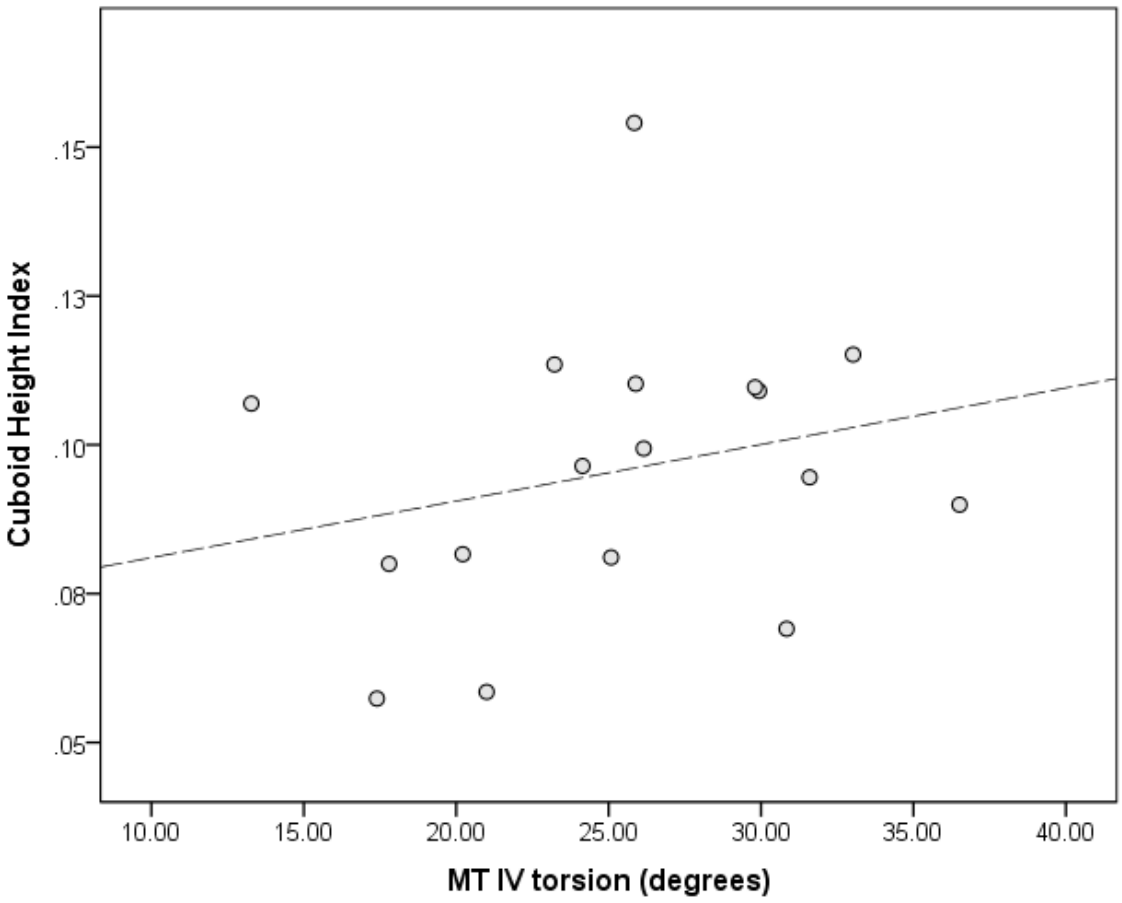

Figure 4.8: Scatter-plot of the cuboid height index and torsion of metatarsal IV for the MRI sample, outlier data point removed ($r = 0.247$, $p = 0.340$).

	N	Mean	SD	Minimum	Maximum
MT II					
Mis Island	136	8.89	7.17	0.15	36.11
Norris Farms	48	13.26	12.13	0.05	49.52
TOTAL	184	10.03	8.91	0.05	49.52
MT III					
Mis Island	142	19.57	8.52	0.82	45.57
Norris Farms	31	11.57	8.43	0.60	38.19
TOTAL	173	18.14	9.02	0.60	45.57
MT IV					
Mis Island	150	24.69	8.87	0.06	45.96
Norris Farms	51	19.89	9.72	5.95	48.12
TOTAL	201	23.47	9.31	0.06	48.12
MT II or III					
Mis Island	7	9.54	10.05	0.65	30.57
Norris Farms	0	----	----	----	----
TOTAL	7	9.54	10.05	0.65	30.57
MT II, III, or IV					
Mis Island	14	7.36	6.98	0.11	20.85
Norris Farms	16	9.55	6.14	0.31	21.07
TOTAL	30	8.52	6.53	0.11	21.07

Table 4.5: Descriptive statistics of metatarsal torsion for the combined archaeological samples, all ages considered.

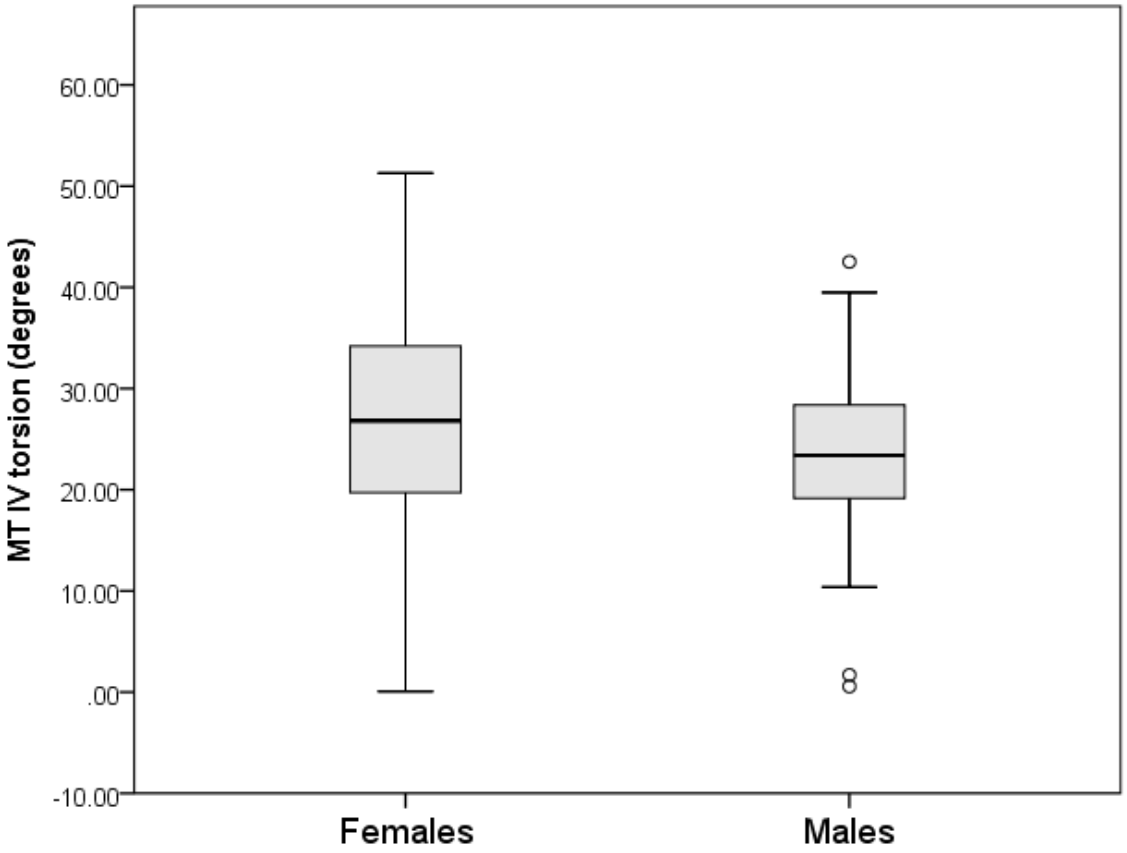

Figure 4.9: Box-plots of the median and interquartile range of MT IV torsion (degrees) between females and males of the Mis Island sample.

	N	Mean	SD	Minimum	Maximum
MT II					
Mis Island	125	8.72	6.95	0.15	36.11
Norris Farms	27	16.82	14.02	1.02	49.52
TOTAL	152	10.16	9.12	0.15	49.52
MT III					
Mis Island	131	19.78	6.95	0.82	45.57
Norris Farms	11	13.42	11.94	0.60	38.19
TOTAL	142	19.28	9.05	0.60	45.57
MT IV					
Mis Island	132	24.82	9.10	0.06	45.96
Norris Farms	27	22.09	10.96	6.11	48.12
TOTAL	159	24.36	9.46	0.06	48.12

Table 4.6: Descriptive statistics of metatarsal torsion for the combined archaeological samples, adults only.

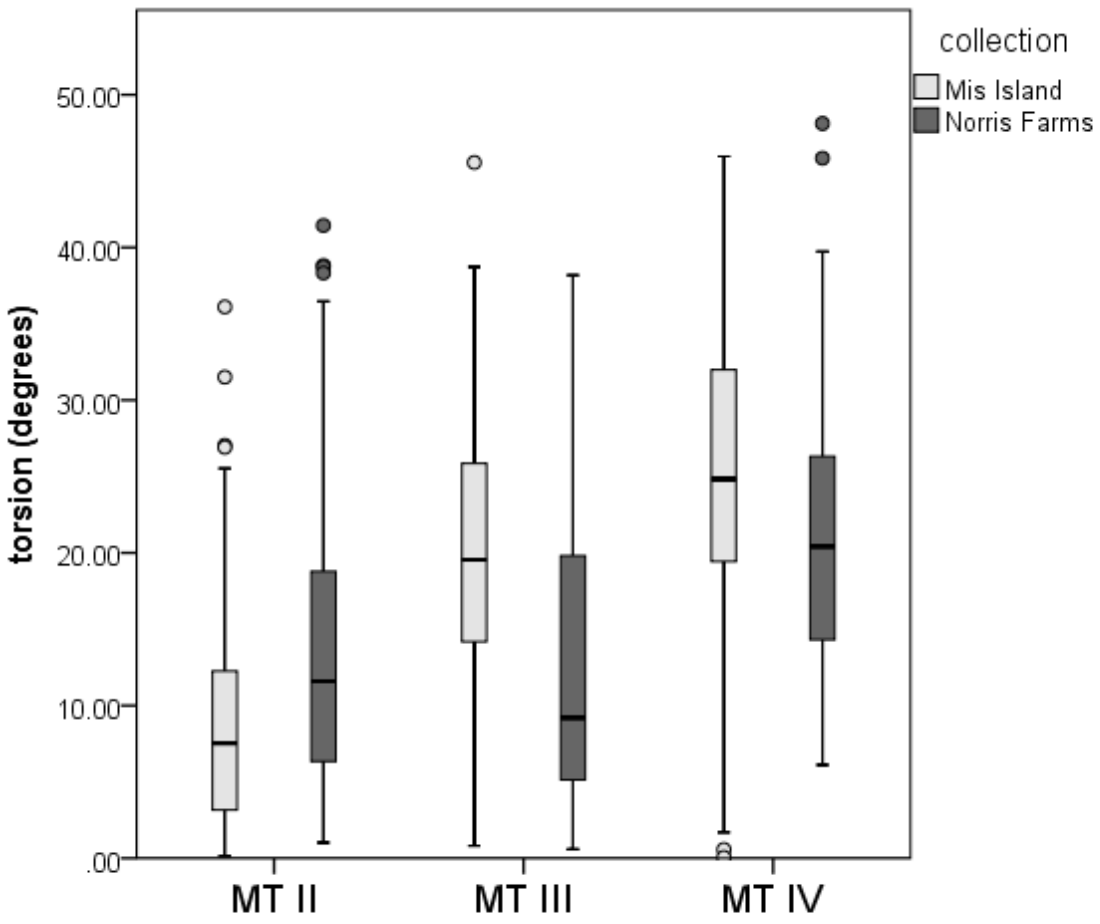

Figure 4.10: Side-by-side box-plots of the median and interquartile range of torsion of MT II, MT III, and MT IV compared between the two archaeological samples, adults only.

	N	Mean	SD	Minimum	Maximum
MT II					
Mis Island	11	10.81	9.49	2.03	30.64
Norris Farms	21	8.68	7.11	0.05	24.13
TOTAL	32	9.41	7.92	0.05	30.64
MT III					
Mis Island	11	17.15	6.72	7.31	26.89
Norris Farms	20	10.55	5.84	0.92	21.50
TOTAL	31	12.89	6.85	0.92	26.89
MT IV					
Mis Island	18	23.66	7.08	10.18	34.43
Norris Farms	24	17.41	7.58	5.95	31.49
TOTAL	42	20.09	7.92	5.95	34.43
MT II or III					
Mis Island	7	9.54	10.05	0.65	30.57
Norris Farms	0	----	----	----	----
TOTAL	7	9.54	10.05	0.65	30.57
MT II, III, or IV					
Mis Island	14	7.36	6.98	0.11	20.85
Norris Farms	16	9.55	6.14	0.31	21.07
TOTAL	30	8.52	6.53	0.11	21.07

Table 4.7: Descriptive statistics of metatarsal torsion for the combined archaeological samples, juveniles only.

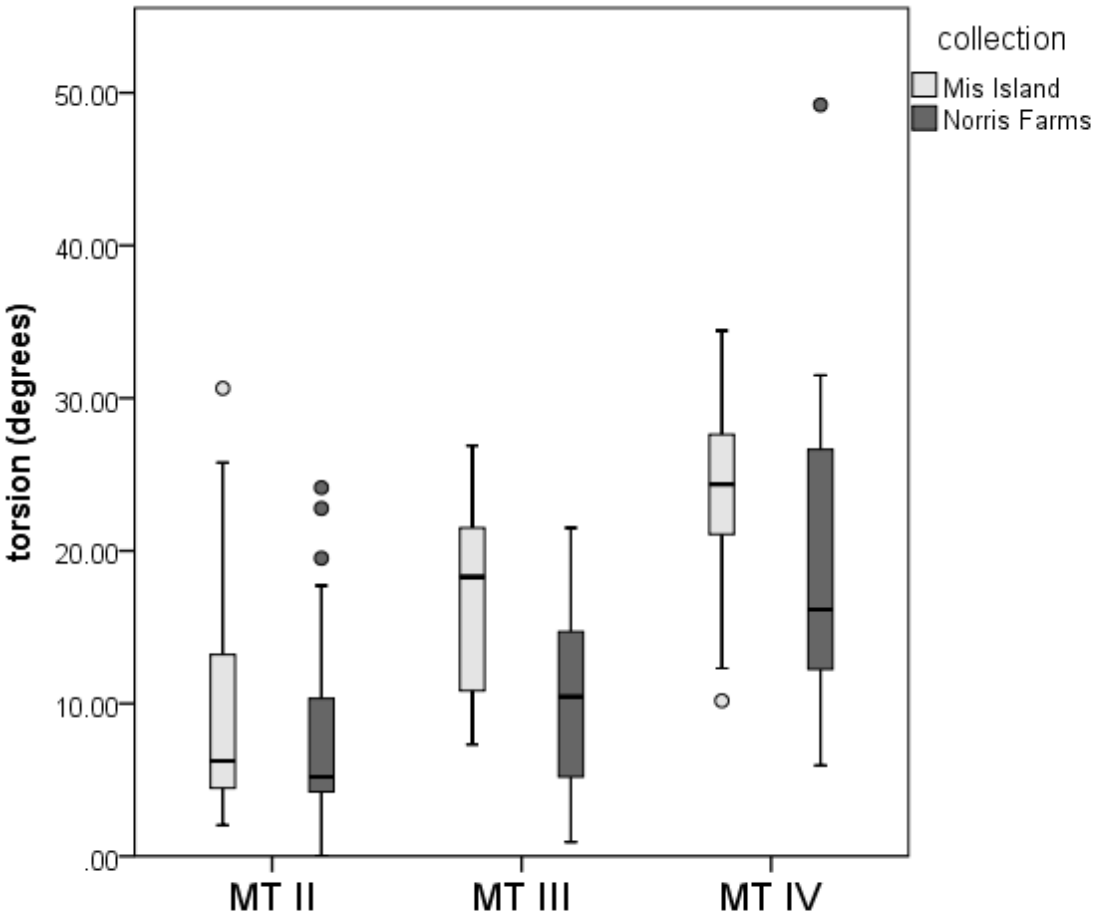

Figure 4.11: Side-by-side box-plots of the median and interquartile range of torsion of MT II, MT III, and MT IV compared between the two archaeological samples, juveniles only.

Age Range (yrs)	N	Mean	SD	Minimum	Maximum
MT II					
1-6	0	----	----	----	----
6-12	3	4.68	1.71	2.72	5.86
12-20	8	13.11	10.27	2.03	30.64
20+	125	8.72	6.95	0.15	36.11
MT III					
1-6	0	----	----	----	----
6-12	3	16.70	8.81	7.31	24.79
12-20	8	17.32	6.50	8.85	26.89
20+	131	19.78	8.65	0.82	45.57
MT IV					
1-6	4	26.14	4.57	21.32	31.79
6-12	6	22.75	9.83	10.18	34.43
12-20	8	23.10	6.25	12.31	31.92
20+	132	24.82	9.10	0.06	45.96
MT II or III					
1-6	4	7.13	4.96	0.65	12.71
6-12	3	12.75	15.45	3.15	30.57
12-20	0	----	----	----	----
20+	0	----	----	----	----
MT II, III, or IV					
1-6	4	7.36	6.98	0.11	20.85
6-12	0	----	----	----	----
12-20	0	----	----	----	----
20+	0	----	----	----	----

Table 4.8: Descriptive statistics of metatarsal torsion for individuals in the Mis Island sample.

Age Range (yrs)	N	Mean	SD	Minimum	Maximum
MT II					
1-6	2	13.31	13.38	3.86	22.78
6-12	10	7.07	5.31	0.05	19.52
12-20	9	9.42	7.95	1.43	24.13
20+	27	16.82	14.02	1.02	49.52
MT III					
1-6	3	7.01	6.79	1.21	14.48
6-12	9	12.32	7.19	0.92	21.50
12-20	8	9.89	3.23	4.92	14.56
20+	11	13.42	11.94	0.60	38.12
MT IV					
1-6	7	19.73	8.71	9.33	30.55
6-12	9	15.22	7.90	5.95	29.14
12-20	8	17.86	6.38	11.77	31.49
20+	27	22.09	10.96	6.11	48.12
MT II or III					
1-6	0	----	----	----	----
6-12	0	----	----	----	----
12-20	0	----	----	----	----
20+	0	----	----	----	----
MT II, III, or IV					
1-6	3	9.55	6.14	0.31	21.07
6-12	0	----	----	----	----
12-20	0	----	----	----	----
20+	0	----	----	----	----

Table 4.9: Descriptive statistics of metatarsal torsion for individuals in the Norris Farms sample.

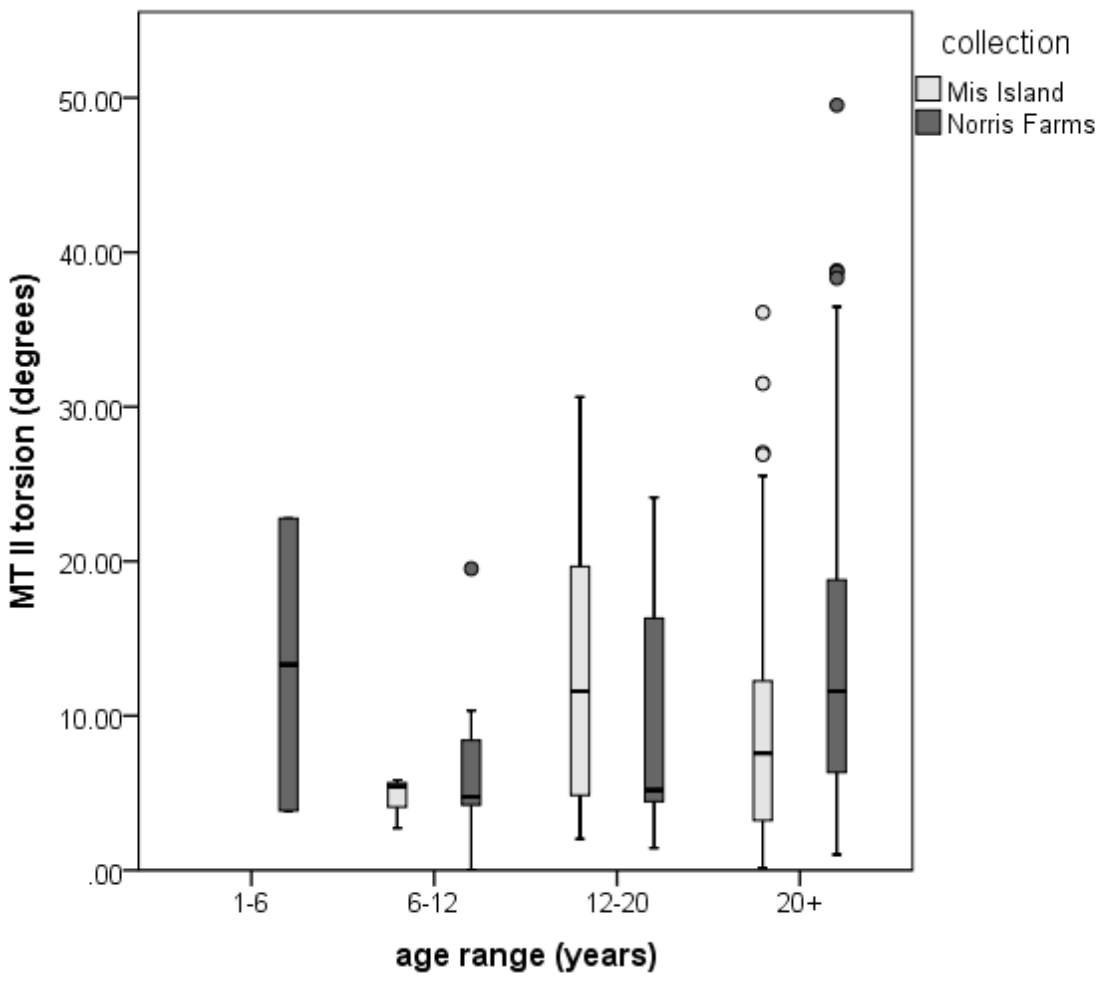

Figure 4.12A: Side-by-side box-plots of the median and interquartile range of torsion of MT II for the Mis Island and Norris Farms samples.

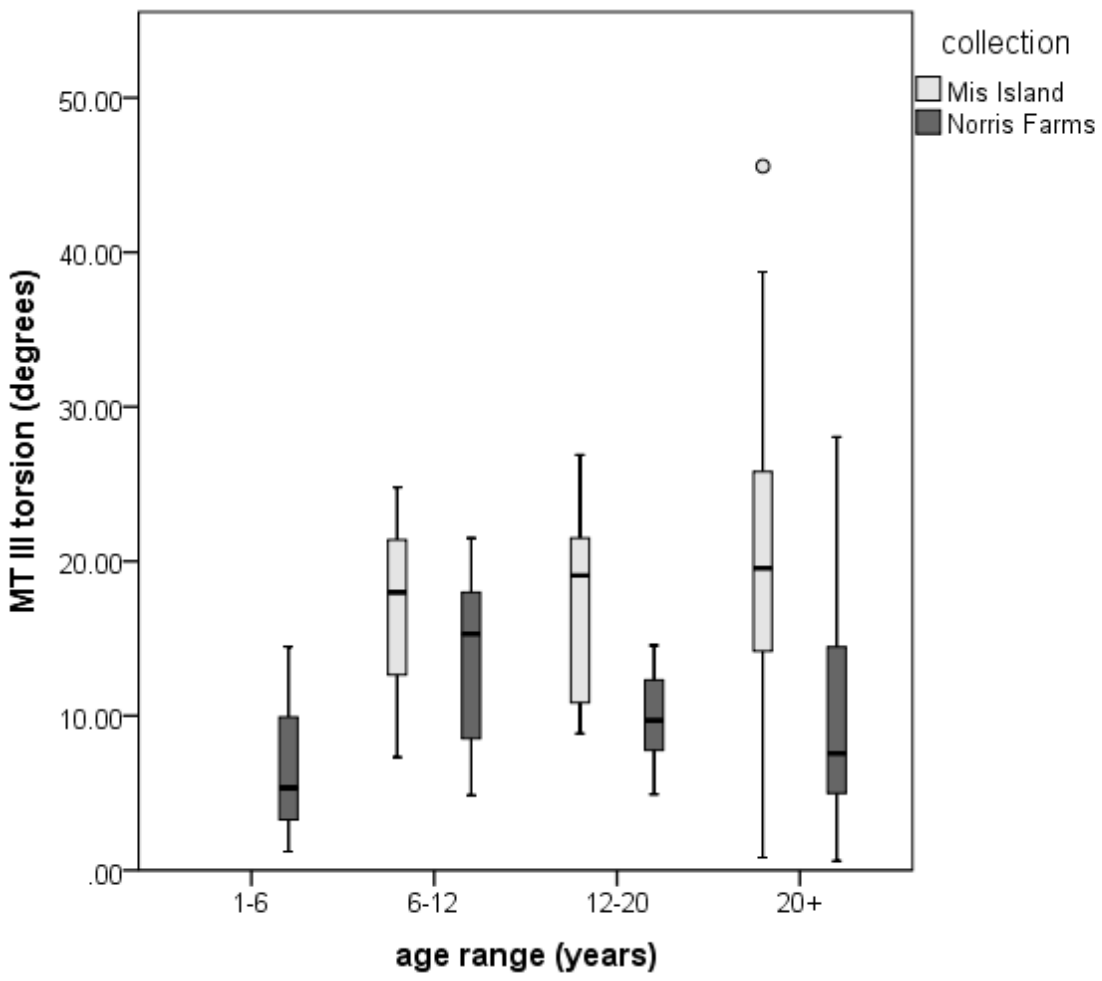

Figure 4.12B: Side-by-side box-plots of the median and interquartile range of torsion of MT III for the Mis Island and Norris Farms samples.

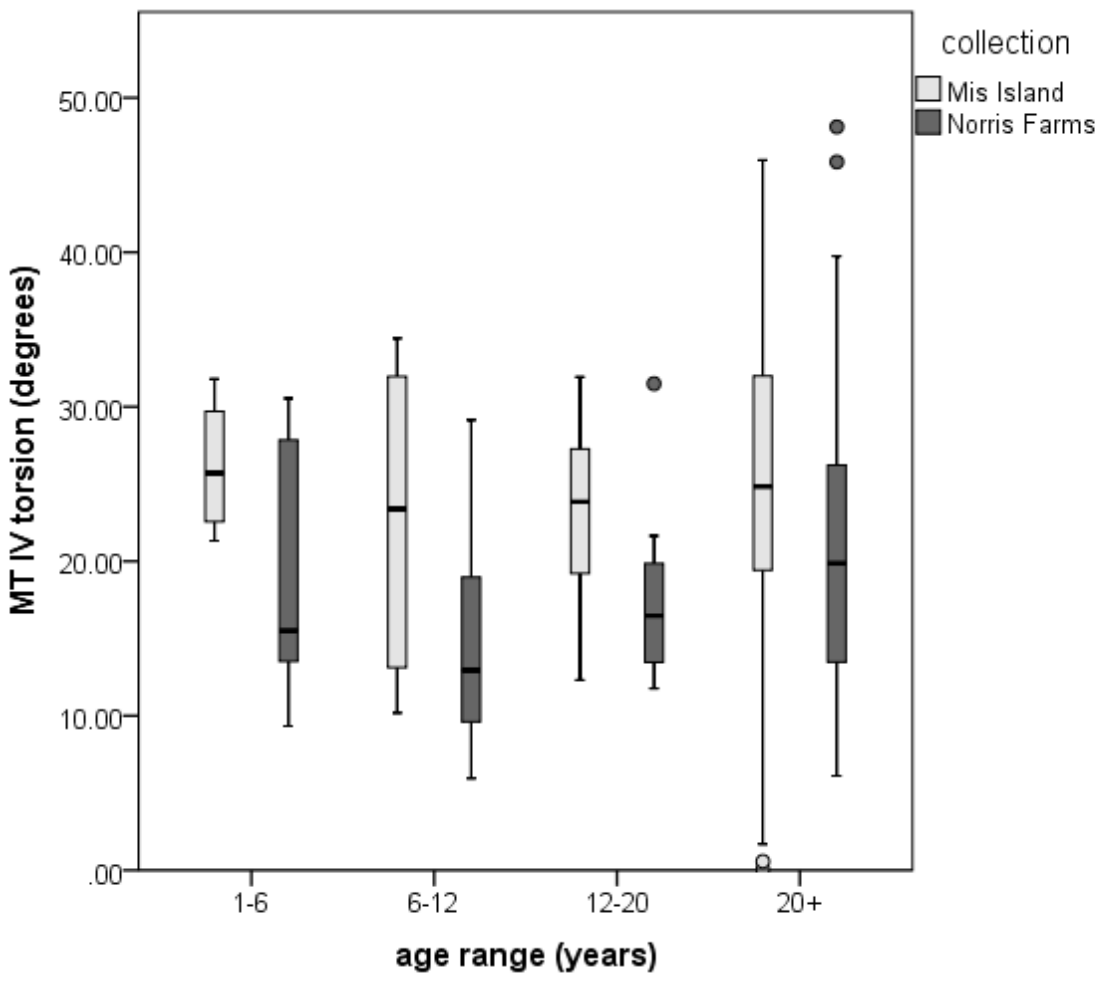

Figure 4.12C: Side-by-side box-plots of the median and interquartile range of torsion of MT IV for the Mis Island and Norris Farms samples.

Sample		MT III	MT IV
Mis Island	**MT II**	-0.119	-0.044
	MT III	----	0.213*
Norris Farms	**MT II**	0.737**	0.366*
	MT III	----	0.455*

Table 4.10: Results of Pearson's product moment correlation of metatarsal torsion within and between adults of the two archaeological samples. *Correlation significant at the $\alpha = 0.05$ level; **Correlation significant at the $\alpha = 0.01$ level.

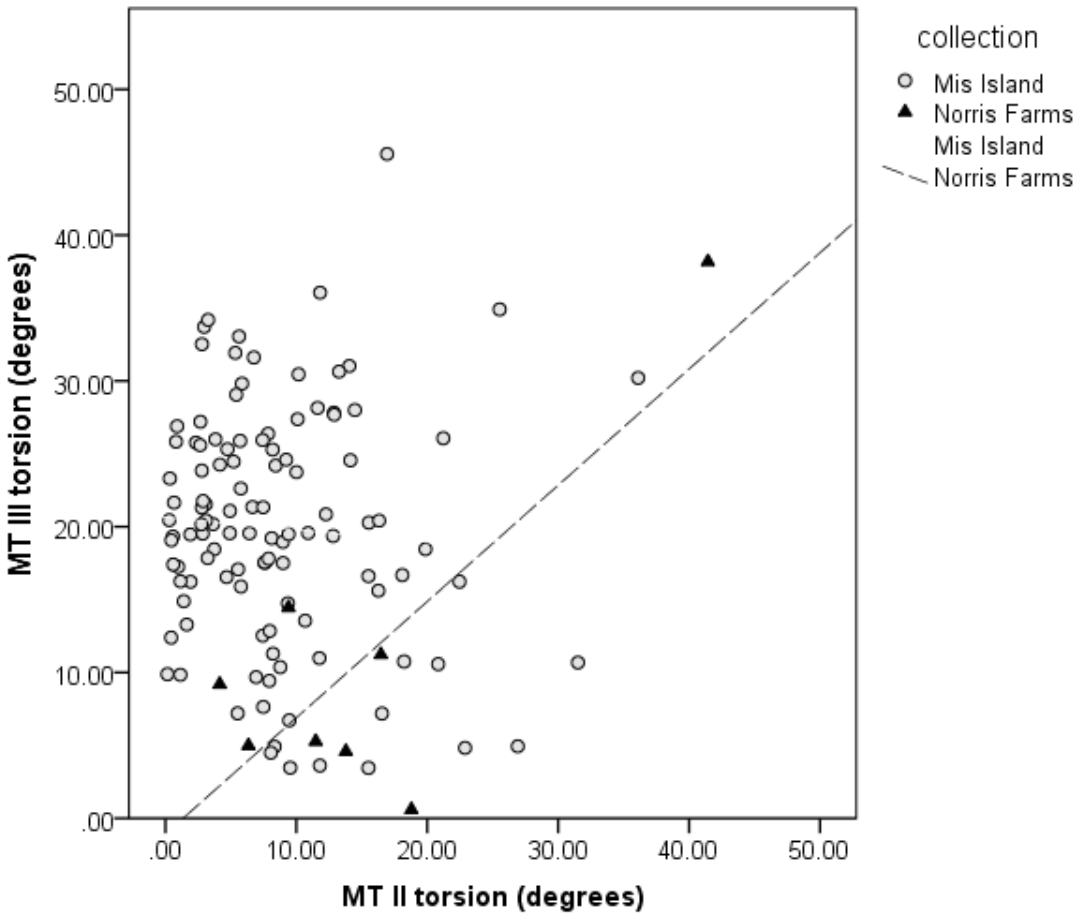

Figure 4.13A: Correlation between MT II torsion and MT III torsion for the Mis Island (circles) and Norris Farms (triangles) samples. The relationship is significant for Norris Farms.

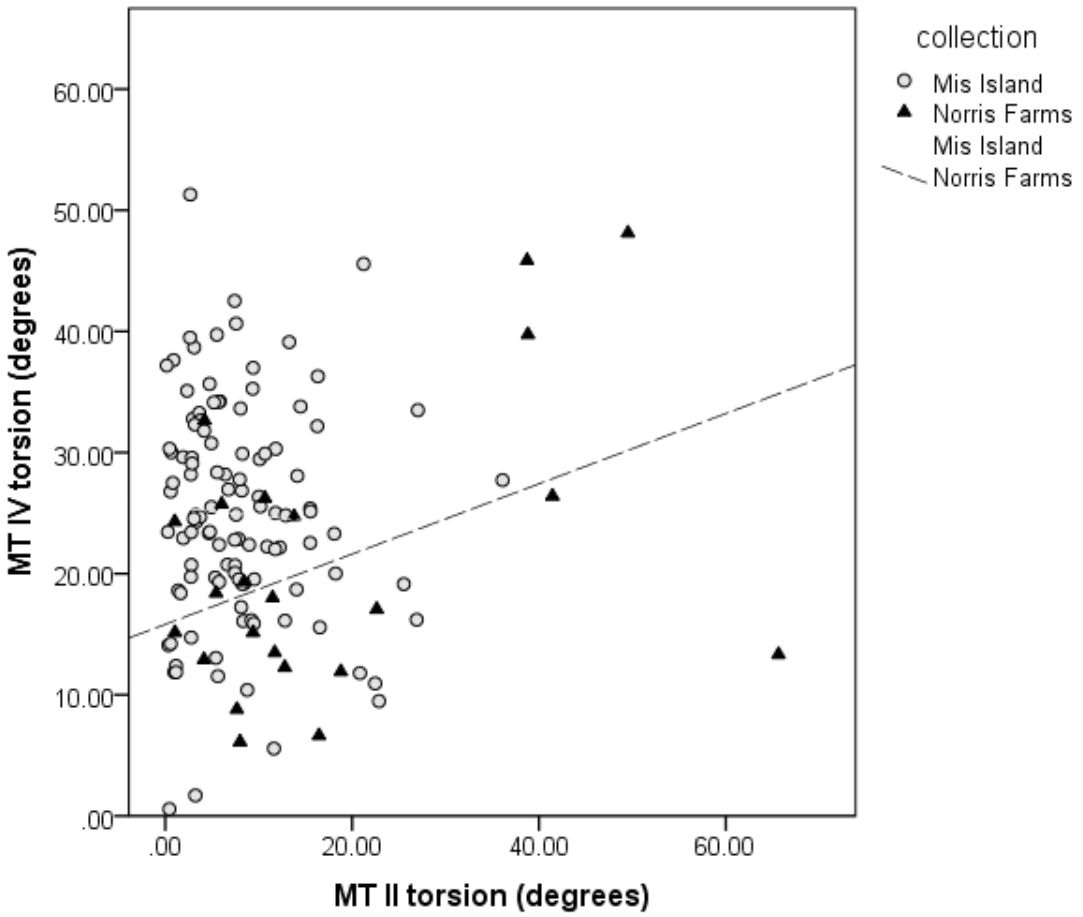

Figure 4.13B: Correlation between MT II torsion and MT IV torsion for the Mis Island (circles) and Norris Farms (triangles) samples. The relationship is significant for Norris Farms.

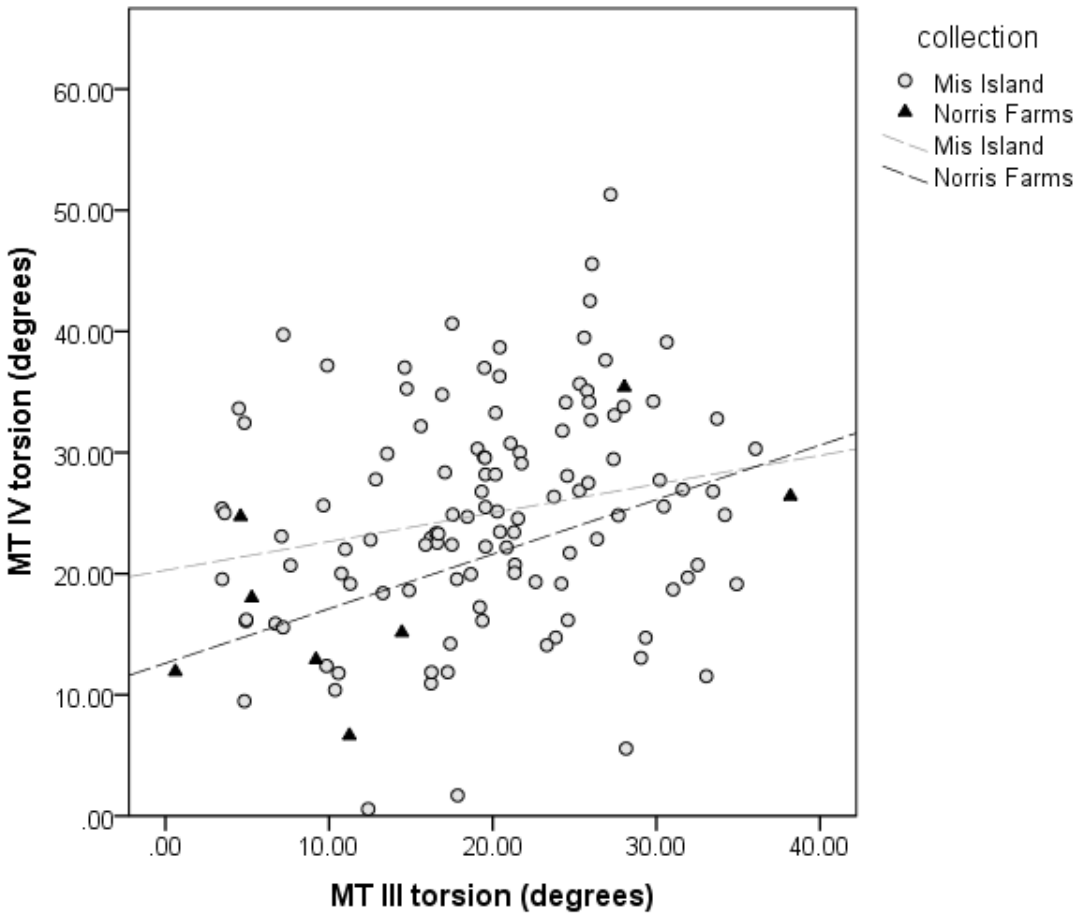

Figure 4.13C: Correlation between MT III torsion and MT IV torsion for the Mis Island (circles) and Norris Farms (triangles) samples.

	N	Mean	SD	Range	Min	Max
MT II						
MRI sample	17	2.00	5.81	19.54	-6.70	12.84
Mis Island	125	8.72	6.95	35.96	0.15	36.11
Norris Farms	27	16.82	14.02	48.32	1.02	49.52
Pontzer et al., 2010	10	5.6	8.2	----	----	----
Drapeau & Harmon, 2013	42	-2.37	5.51	----	----	----
MT III						
MRI sample	17	24.28	4.84	15.43	16.83	32.26
Mis Island	131	19.78	6.95	44.75	0.82	45.57
Norris Farms	11	13.42	11.94	37.59	0.60	38.19
Pontzer et al., 2010	10	20.4	9.6	----	----	----
Drapeau & Harmon, 2013	45	18.19	7.17	----	----	----
MT IV						
MRI sample	17	26.86	7.16	29.52	13.28	42.80
Mis Island	132	24.82	9.10	45.9	0.06	45.96
Norris Farms	27	22.09	10.96	42.01	6.11	48.12
Pontzer et al., 2010	10	23.6	7.1	----	----	----
Drapeau & Harmon, 2013	48	20.25	8.40	----	----	----
Mitchell et al., 2012 (males)	91	23.99	8.16	----	----	----
Mitchell et al., 2012 (females)	64	28.00	8.39	----	----	----

Table 4.11: Summary of measures of metatarsal for humans. To maintain consistency with other studies, values for the Mis Island and Norris Farms archaeological samples are for adults only.

Chapter 5: Effects of Longitudinal Arch Height, Foot Shape, and Speed on Midfoot and Total Foot Loading in an Ontogenetic and Adult Sample of Humans

INTRODUCTION

The longitudinal arch has historically been cited as the key anatomical adaptation that allows the human foot to function as a stiff, propulsive lever, distinguishing it from the highly mobile midfoot of non-human primates, particularly apes (Elftman & Manter, 1935a,b). This dichotomy of stiff-footed humans and mobile-footed (non-human) primates has persisted in the literature for decades; however, recent studies have challenged this paradigm in demonstrating that, despite having a longitudinal arch, a small percentage of humans exhibit midfoot mobility similar to non-human primates (Crompton *et al*., 2012; Bates *et al*., 2013; DeSilva & Gill, 2013; DeSilva *et al*., 2015). In addition, studies are increasingly reporting that humans exhibit a large range of variation in arch height, including flat footedness (e.g., D'Août *et al*., 2009; Stolwijk *et al*., 2013). Therefore, it is no longer appropriate to generalize all humans as having a longitudinal arch or a stiff foot. Instead, we must recognize that human are variable in longitudinal arch height and midfoot mobility, and this fact has important implications for how we infer foot function from fossil foot bones.

The dichotomy of stiff-footed humans and mobile-footed non-human primates was first outlined by Elftman and Manter (1935a). In an early description of the distribution of stress experienced by the feet of humans and chimpanzees during walking, Elftman and Manter (1935a) noted that the human midfoot had a longitudinal arch and therefore did not contact the substrate during walking, particularly along the medial side. Chimpanzees, however, were observed to dorsiflex at, and experience stress beneath, the midfoot region,

presumably at the transverse tarsal joint. Subsequent studies have reported similar observations of midfoot dorsiflexion in chimpanzees (Meldrum & Wunderlich, 1998) and other non-human primates, such as gibbons (Vereecke *et al*., 2005), macaques (Hirasaki *et al.,* 2010), olive baboons (Berillon *et al*., 2010), and other cercopithecines (Meldrum, 1991). Midfoot dorsiflexion came to be known as the "midtarsal break" (Bojsen-Møller, 1979; Elftman & Manter, 1935a; Meldrum, 1991; Susman, 1983), and recent studies have identified more specific information about the exact locations where joint motion occurs. A cineradiographic analysis of chimpanzee walking has demonstrated that midfoot dorsiflexion occurs at both the talonavicular and calcaneocuboid (*i.e*., "midtarsal") joints in this species (Thompson *et al*., 2014). Work by DeSilva (2010) has shown, however, that lateral midfoot dorsiflexion occurs at the cubometatarsal joint and less so at the calcaneocuboid joint, and he has proposed that it is therefore more appropriate to refer to motion in the primate midfoot region as the "midfoot break", as opposed to the "midtarsal break." A recent cadaveric study by Greiner and Ball (2014) has also shown that lateral midfoot motion occurs at the cubometatarsal joints in a sample of macaques, baboons, chimpanzees, and humans, while motion at the calcaneocuboid joint was found to be minimal in these species. In humans, the extent of dorsiflexion at the cubometatarsal joint was slightly less than that observed in chimpanzees, but more than what was observed in *Papio*, demonstrating that humans are capable of a similar range of lateral midfoot motion to what has historically only been observed, and expected, in non-human primates (Greiner & Ball, 2014). A recent kinematic study of chimpanzee and human feet during walking has shown that humans use a large range of midfoot motion during stance, especially in the sagittal plane (Holowka *et al*., 2017). Moreover, studies of plantar pressure in non-pathological humans have found evidence of lateral midfoot motion in a small percentage of humans who exhibit midfoot dorsiflexion during walking (Bates *et al*., 2013; Crompton

et al., 2011; DeSilva & Gill, 2013; DeSilva *et al*., 2015), presumably at the cubometatarsal joint (DeSilva *et al*., 2015).

Humans who exhibit a "midfoot break" experience greater pressure beneath the lateral midfoot region, ostensibly in response to the increased motion at the lateral cubometatarsal joint (DeSilva and Gill, 2013; DeSilva *et al*., 2015). DeSilva and colleagues (2015) found that individuals who exhibit a "midfoot break" and elevated lateral midfoot plantar pressure (>200 kPa) have a more rounded base of the fourth metatarsal, indicating that midfoot mobility and subsequent loading is driven, in part, by differences in foot bone morphology between individuals. Variation in midfoot loading among humans may also be affected by aspects of an individual's anthropometry, as well as both structural and functional aspects of the foot and gait kinematics. Peak pressure of the midfoot region has been reported to have a positive relationship with body mass and foot pronation, and a negative relationship with longitudinal arch height and speed (Rosenbaum *et al*., 1994; Morag & Cavanagh, 1999; DeSilva and Gill, 2013). In a comprehensive study of the effects of both structural and functional variables on plantar pressure, Morag and Cavanagh (1999) concluded that structural variables had a greater effect on midfoot loading than functional variables, while functional variables were more strongly associated with loading of other foot regions. Using multiple regression analysis, these authors demonstrated that variation in the calcaneal inclination angle and arch index (*i.e*., two measures of longitudinal arch height), age, and foot eversion explained approximately 50% of the variance in midfoot pressure, with factors that measured arch height being the best predictors of midfoot loading (Morag & Cavanagh, 1999). Together, the findings of these studies demonstrate that human feet are variable in form and function, highlight that the relationship between foot bone morphology, foot mobility, longitudinal arch height, and foot loading in humans is only beginning to be understood.

The goal of this study was to investigate the relationship between body size, foot shape, longitudinal arch height, and speed on loading of the medial and lateral midfoot region and over the total foot in children and adults. The study by Morag and Cavanagh (1999) that identified arch height as a strong predictor of midfoot loading considered its effect in the context of a large number of structural and functional variables, including aspects of foot bone alignment, soft tissue thickness, and joint range of motion. The study did not distinguish the relative effects of these variables on medial versus lateral midfoot loading, however, a distinction that will be made in the present study given the recent reports of elevated lateral midfoot loading in humans (Crompton *et al*., 2011; Bates *et al*., 2013; DeSilva & Gill, 2013; DeSilva *et al*., 2015). Also, the Morag and Cavanagh (1999) study included only adults, and more recent work has shown that longitudinal arch height is negatively correlated with midfoot pressure in children as well (Bertsch *et al*., 2004; Bosch *et al*., 2010). To my knowledge, a comprehensive analysis of the relationship between longitudinal arch height and other aspects of foot shape or anthropometry on plantar pressure has not been conducted for children, yet could be informative for understanding the relationship between arch height and foot loading in hominins given that the earliest hominin species were of a small stature and body mass (Jungers, 1982; McHenry, 1992; Grabowski *et al*., 2015).

Here, the relationship between participant variables (longitudinal arch height, body mass, foot shape, speed) and 1) relative maximum force (as a percent of body mass), and 2) peak pressure of the medial midfoot, lateral midfoot, and total foot was investigated for three groups of participants. Group A consisted of young children for whom the longitudinal arch was undergoing development. Group B consisted of older children from whom the longitudinal arch was developed, but foot growth was ongoing. And Group C consisted of individuals who had a mature longitudinal arch and adult-sized foot. Between

the three groups, child participants in Group A were predicted to have a lower longitudinal arch and a relatively wider foot (for its length) than individuals in Group B and Group C (Bertsch *et al*., 2004). As a result, child participants in Group A were also predicted to experience greater loading of the medial midfoot region, measured as relative maximum force and peak pressure, than participants in Groups B and C. Participants in Group A were also predicted to experience lower relative maximum force and peak pressure in the lateral midfoot region due to their small body size and in spite of the fact that they should have a lower arch than participants in Groups B and C. Finally, participants in Group A were predicted to experience lower total foot loading than Groups B and C, again in response to their small body size. Within each group, loading of the medial and lateral midfoot regions, as well as over the total foot, was predicted to be higher among individuals with a low longitudinal arch, a higher body mass, and a relatively wider foot, irrespective of age (Morag & Cavanagh, 1999; DeSilva & Gill, 2013; DeSilva *et al*., 2015). Finally, participants were also predicted to experience reduced loading (*i.e.*, lower relative maximum force and peak pressure) in the medial and lateral midfoot regions as walking and running speed increased (Rosenbaum *et al*., 1994).

MATERIALS & METHODS

Sample

Participants were recruited from The University of Texas at Austin main campus and local day-care facilities. The study was advertised using recruitment flyers and was listed on the UT Events online calendar and appeared in daily emails sent to university faculty and students generated from this calendar. Participants were excluded from the study if had a history of foot-related injury or pathology. A total of 78 participants between

the ages of 1 and 57 were recruited to participate in the study (**Table 5.1**). Six of the youngest participants returned to the lab for a second visit 3-4 months following their first visit, bringing the total number of participant records to 84.

Participant Protection

The study protocol received University of Texas at Austin IRB approval for human subjects research (IRB Protocol #2014-04-0020). Parents of minor participants (aged 1-15 years) gave written consent to allow their child to participate in the study. Children aged 7-15 years were asked to read through a description of the study, and additionally gave verbal consent to participate in the study. Adult participants (aged 18-60 years) gave written consent to participate in the study. Participants were compensated for their time in the amount of $20.00 per study session.

Data Collection

Schedule of Data Collection

Collection of foot shape and plantar pressure data occurred between May 6 and September 1, 2015. Minor participants aged 1-6 years were asked to attend additional study sessions in order to track intra-individual changes in foot growth and plantar pressure over the period of longitudinal arch development. Of the 19 children in this age range, 8 returned for a second study session scheduled 3-4 months following their first session. Adult participants attended a single study session that lasted approximately 20-30 minutes.

Anthropometric Data Collection

Anthropometric measurements were recorded on all subjects, including body mass, stature, hip height, and knee height. Body mass was measured using a digital scale. Height measurements were collected using wooden meter sticks attached to the wall (stature) and tailor's measuring tape (hip and knee height).

Foot Shape Data Collection

Longitudinal Arch Height

Longitudinal arch height was measured on each participant as the linear distance between the floor and the navicular tuberosity. Because differences in body size and/or foot size likely affect navicular height, this linear metric was divided by the individual's total foot length in order to create a relative measure of arch height, the navicular height index (NHI). The NHI has been found to correlate strongly with radiographic (*i.e.*, bony, structural) indices of medial longitudinal arch height (Saltzman *et al*., 1995). In addition, longitudinal arch height was calculated from the pressure data as the Arch Index (AI), quantified as the ratio of the midfoot contact area to the total foot contact area (Cavanagh & Rodgers, 1987). This calculation was performed using the mean midfoot and mean total foot contact areas from each individual's walking trials.

3D Landmarks and Measurements

A MicroScribe G2X (Revware, Inc., Raleigh, NC) was used to collect a series of 6 landmarks on the external surface of the foot in order to quantify each participant's foot shape. **Figure 5.1** summarizes the locations of these landmarks. Landmarks were digitized on the right foot by a single observer as the participant stood with feet positioned shoulder-width apart. Because collection of landmark data requires that the participant stands

absolutely still, it was not possible to collect these data on the toddlers and young children who participated in the study.

A series of 5 linear distances were calculated from the landmark coordinates in Excel using the Euclidean distance formula, $d(P_1, P_2) = \sqrt{[(x_2 - x_1)^2 + (y_2 - y_1)^2 + (z_2 - z_1)^2]}$, where P_1 = the location of point 1, and P_2 = the location of point 2. With **Figure 5.1** as a reference for the landmark points, the calculated distances include foot length (2, 5), metatarsal breadth (4, 6), bi-malleolar breadth (1, 3), instep length (2, 4), and lateral foot length (2, 6). These metrics were previously used by Wunderlich and Cavanagh (2001) to quantify differences in foot and ankle shape.

Linear Measurements

In order to quantify foot shape metrics for all participants in the study, a second method was employed that did not require the participant to stand motionless for more than a brief amount of time. Each participant was asked to stand relaxed, shoulder-width apart with their right foot on a piece of paper. Then, a tracing was made of the foot from which linear distances were then taken with a metric ruler. The metrics taken from these tracings include foot length, and foot breadth at 25%, 50%, and 75% of foot length (**Figure 5.2**). A correlation test was performed between the foot length measure derived from the foot tracings and the foot length values calculated from the 3D landmark data in order to test the fit between the two methods used to quantify foot shape. The two measures of foot length are significantly positively correlated ($r = 0.996$, $p < 0.001$), indicating that the two methods are comparable and data from both methods are therefore used in this study to quantify foot shape (**Figure 5.3**).

Plantar Pressure Data Collection

Plantar pressure data were collected at a spatial resolution of 0.5cm^2 and a temporal resolution of 50Hz as participants moved barefoot across an EMED-ST plantar pressure mat (Novel, Inc., St. Paul, MN). In order to sample data at a range of speeds, child participants were asked to move across the pressure mat at a self-selected walking gait 5 times, and at a self-selected faster walking or running gait (if possible) an additional 5 times. Adult participants were asked to move across the pressure mat at a self-selected walking gait 5 times; a self-selected jogging gait 5 times; and a self-selected running gait 5 times.

In order to calculate the speed of participant movement, participants wore a reflective marker on their right hip and were filmed with a Basler 602f monochrome camera (Basler Vision Technologies, Ahrensburg, Germany) at a temporal resolution of 100Hz as they moved across the pressure mat. In an effort to maintain participant anonymity, the lens of the camera was positioned such that it filmed the participants from the shoulders down. Two-dimensional coordinates of the right hip marker were generated using Peak Motus (v. 9.2) software (Vicon Motion Systems, Oxford, UK) and were used to calculate each participant's speed. To account for the fact that anthropometric differences in size (e.g., limb length) affect speed, Froude number, a dimensionless measure of speed, was calculated for each participant and used for statistical analyses (Hof, 1996).

For analysis, the foot was divided into 10 anatomical regions using Novel Database software (**Figure 5.4**). These regions are automatically defined by the software according to the participant's foot print morphology, and include the medial hindfoot, lateral hindfoot, medial midfoot, lateral midfoot, 1st metatarsal, 2nd metatarsal, 3rd through 5th metatarsals, 1st toe (hallux), 2nd toe, and 3rd through 5th toes. Pressure data were extracted for each of the 10 anatomical regions, including maximum force (N) and peak pressure (kPa). In order

to account for differences in participant body size, maximum force as a percent of body mass [Maximum Force / (Body Mass*9.80665)] was calculated and used in place of absolute maximum force in statistical analyses.

Data Analysis

The first step was to establish the three different groups within which the relative effects of arch height and other variables on midfoot loading were to be investigated. In other words, while it was a goal of this study to investigate these effects in both children and adults, using age as the primary factor to separate these groups is not necessarily appropriate given that arch maturation and foot growth are complete prior to the age at which one is considered an adult (Forriol and Pascual, 1990; Bertsch *et al*., 2004; Scheuer & Black, 2004; Onodera *et al.,* 2008; Müller *et al*., 2012; Waseda *et al*., 2014). While a number of studies report that the arch is developed around age 6 (Bertsch *et al.,* 2004; Müller *et al*., 2012; Onodera *et al*., 2008), others contend that the arch continues to develop until the early teenage years (Forriol and Pascual, 1990; Waseda *et al*., 2014). Therefore, it was necessary to determine the age of arch maturation specific to the present sample. This age range was determined by first investigating the relationship between arch height and age for the sample to determine whether there was a natural point (*i.e*., age) at which arch height stabilized. A LOESS curve was fit to the data points plotted for both the morphological (navicular height index) and pressure (arch index) longitudinal arch measures against age in order to estimate the age at which arch height stabilized (see below). Participants younger than this age were placed into Group A: juveniles, arch developing. Participants older than this age were placed into Groups B and C. Membership into Groups B and C was determined by investigating the relationship between foot length

and age to determine whether there was a natural point (*i.e.*, age) at which foot length was complete. A LOESS curve was fit to the data points plotted for the foot length measures against age in order to estimate the age of adult foot length (see below). Participants younger than this age were placed into Group B: juveniles, arch developed; those older than this age were placed into Group C: adults.

Descriptive statistics were used to describe sample variation in longitudinal arch height, static anthropometric and foot shape variables, speed (Froude number), and foot loading variables, including relative maximum force and peak pressure of the medial midfoot, lateral midfoot, and total foot. Differences in variable means between the groups were tested using a one-way ANOVA or Kruskal-Wallis test, where appropriate. Relationships between variables within each group were tested using correlation statistics. Finally, a stepwise multiple regression analysis was used to determine which of the static participant variables were significant predictors of relative maximum force and peak pressure beneath the medial and lateral midfoot regions for each of the three age groups. First, Pearson product-moment correlation coefficients were computed to test for relationships between each of the static participant variables (*i.e.*, arch height, anthropometric and foot shape metrics). Variables that were found to have a statistically significant correlation with one another were removed from the potential list of explanatory variables included in the multiple regression. Also, because speed is a factor known to influence foot loading (Rosenbaum *et al.*, 1994), a Pearson product-moment correlation test was performed to determine whether it was necessary to control for speed as a covariate for the multiple regression analysis. Finally, static participant variables that were determined to have a significant correlation with plantar loading were entered into a stepwise multiple linear regression to determine their relative importance in explaining variation in loading of the medial and lateral midfoot regions. Speed was included as a

covariate, where appropriate. These regression analyses were performed for each group (A, B, C) for two different gait types (walk, Froude < 0.50; and run, Froude ≥ 0.50).

Longitudinal Arch Height Assessment – Creating Group A

Longitudinal arch height was measured from each participant's foot as the Navicular Height Index (NHI) and from their pressure data as the Arch Index (AI). It was not possible to measure the navicular height on a number of the youngest participants in the study because they were not able to stand still long enough to take the measurement. Therefore, a NHI was not calculated for all study participants. However, because AI is calculated from the dynamic pressure data, an AI value is available for all participants. NHI and AI are significantly negatively correlated with one another (Pearson's $r = -0.381$, $p = 0.001$), though this relationship is weak and NHI only explains approximately 14.5% of the variance in AI (**Figure 5.5**). The correlation between these two measures of arch height is weaker than predicted, and may be influenced by inter-individual differences in plantar tissue thickness. A decision was made to include both measures of arch height given that NHI is known to correlate strongly with radiographic measures of arch height (Saltzman *et al*., 1995), and AI is available for the entire study sample.

First, a Student's t-test was performed to determine whether arch height was similar between males and females in each group, as previous studies have reported gender differences in this trait in both children and adults (*e.g*., Ashizawa *et al*., 1997; Barker & Scheuer, 1998; Wunderlich & Cavanagh, 2001; Echarri & Forriol, 2003; Stavlas *et al*., 2005; Pfeiffer *et al*., 2006; Mickle *et al*., 2008; Chen *et al*., 2009; Bosch *et al*., 2010; Chang *et al*., 2010; but see El *et al*., 2006). In this sample, however, a gender difference in longitudinal arch height was not detected when measured as the AI [$t(78) = 0.135$, $p =$

0.893] or NHI [t(68) = -0.036, p = 0.971]. Therefore, males and females were pooled for subsequent analyses.

The relationship between NHI and AI with age was investigated to determine the age of arch maturation in the study sample. **Figure 5.6A** shows a scatter plot with LOESS curve of NHI and age for all study participants, and **Figure 5.6B** shows the same relationship for only participants less than 20 years of age. Note that a small NHI indicates a low longitudinal arch, and NHI increases directly with arch height. **Figure 5.7A** shows a scatter plot with LOESS curve of AI and age for all study participants, and **Figure 5.7B** shows the same relationship for only participants less than 20 years of age. Note that a small AI indicates a high longitudinal arch, and AI decreases as arch height increases. After visual inspection of **Figures 5.6 A-B** and **Figures 5.7 A-B**, it was decided that arch height appears mature in this sample around age 6 as AI clearly stabilizes beyond this age (**Figure 5.7B**). While this trend is not as clear for NHI (**Figure 5.6B**), there are fewer data points for NHI at young ages due to difficulties in measuring NH, and the absence of these data is likely affecting the trend captured in the LOESS curve. Therefore, all individuals age 6 and under were grouped together as Group A: Juveniles, Arch Developing. The age of 6 for arch maturation is consistent with previous studies of foot development (*e.g.*, Bertsch *et al.*, 2004).

Foot Length Assessment – Creating Groups B and C

The relationship between foot length and age was investigated to determine when foot length was mature for the study sample. Foot Length values taken from the foot tracings were used in this comparison since it was possible to measure foot length in this manner on more study participants, and given that this measure correlated so highly with

measurements calculated with the 3D landmark data ($r = 0.996$, $p < 0.001$; **Figure 5.3**). **Figure 5.8A** shows a scatter plot with LOESS curve of foot length against age for all study participants, and **Figure 5.8B** shows the same relationship for only participants less than 25 years of age. After visual inspection of **Figures 5.8 A-B**, it was decided that foot length appears mature in this group around age 15 as foot length clearly stabilizes beyond this age (**Figure 5.8B**). Also, there is a gap in the sample with respect to age, as there are no participants aged 16 and 17 years (**Table 5.1**). Therefore, Group B includes participants between the ages of 6 and 15, and Group C includes participants older than age 15. Group B represents juveniles with a developed longitudinal arch, and Group C represents individuals with an adult-like foot.

RESULTS

Difference in Variables Between Groups A, B, and C

Static Participant Variables

Table 5.2 summarizes the mean and standard deviation for the static variables of participant anthropometry and foot shape for Groups A, B, and C. Group membership had a significant effect on all absolute measurements at the $p = 0.05$ level. Body mass, height, hip height, knee height, foot length, foot breadth, heel breadth, and bi-malleolar (ankle) breadth are all lowest for Group A, are higher in Group B, and are highest in Group C. These differences reflect that aspects of an individual's size increase with age throughout ontogeny.

Because absolute measurements of foot shape do not account for differences in individual size, three relative measures of foot breadth were calculated, including relative foot breadth at 25%, 50%, and 75% of foot length. This ratio was calculated as foot breadth

divided by foot length. **Table 5.2** also summarizes the mean and standard deviation of these ratios for the three groups. Relative foot breadth was significantly different between the three groups at the $p < 0.001$ level. Post-hoc analyses reveal that relative foot breadth at 25%, 50%, and 75% of foot length (*i.e.*, hindfoot) was significantly larger in Group A compared to Groups B and C, but Groups B and C did not differ from one another (**Figure 5.9 A-C**). This finding indicates that child participants in Group A, for whom the longitudinal arch was developing, have a relatively wider hindfoot, midfoot, and forefoot for their foot length than individuals for whom the longitudinal arch was developed. This difference also likely reflects the fact that participants in Group A presumably retain the pediatric fat pat, at least the youngest individuals.

On a related note, contact area of the medial midfoot was predicted to be greater in Group A compared to Groups B and C, though no difference was observed in absolute medial midfoot contact area between the groups [$F(2,78) = 1.232$, $p = 0.297$] (**Table 5.2**). However, when contact area of the medial midfoot as a percentage of total foot contact area was compared across the groups, participants in Group A were found to have a statistically significant higher relative medial midfoot contact area than Groups B and C [$F(2,78) = 11.911$, $p < 0.001$] (**Table 5.2**; **Figure 5.10**). This finding reflects the fact that individuals in Group A have a pediatric fat pad and presumably a lower longitudinal arch (see below) than those in Groups B and C. Total foot contact area was also found to differ between all three groups, with those in Group A have the smallest total foot contact area and Group C having the largest [$F(2,78) = 101.011$, $p < 0.001$) (**Table 5.2**; **Figure 5.11**). This finding reflects differences in foot size between the three groups.

Longitudinal arch height was measured as the navicular height index (NHI) and arch index (AI). NHI was significantly lower in Group A than Group C ($p = .005$), and in Group B than Group C ($p = .015$), but Groups A and B did not differ in NHI ($p = .911$)

(**Table 5.2**; **Figure 5.12A**). AI was not lower in Group A compared to Groups B and C, as was predicted, however [$F(2,77) = 0.413$, $p = 0.663$] (**Table 5.2**). The finding that mean AI was not statistically significantly higher in Group A compared to Groups B and C was unexpected, especially given that AI was a factor used to separate Group A from Groups B and C. **Figure 5.12B** shows the median and interquartile range of AI for each group, and it is clear that AI is more variable for participants in Group A than in Groups B and C. It is likely that the non-significant difference in AI between the groups is driven by a few participants in Group A who have a high longitudinal arch (*i.e.*, low AI).

Dynamic Pressure Variables

Table 5.3 summarizes the mean and standard deviation for relative maximum force (as a percent of body mass) and plantar pressure for the medial midfoot, lateral midfoot, and total midfoot for Groups A, B, and C during walking trials (Froude < 0.5) and running trials (Froude ≥ 0.50).

For walking trials, group membership had a significant effect on all variables at the $p = 0.05$ level, with the exception of relative maximum force experienced in the lateral midfoot region (**Table 5.4**). Consistent with predictions, post-hoc pairwise comparisons show that relative maximum force in the medial midfoot region is significantly higher in Group A compared to Group B, and in Group A compared to Group C, but Groups B and C were not significantly different from one another (**Figure 5.13**). This result reflects the fact that participants in Group A have a relatively larger medial midfoot contact area that can receive loads. Relative maximum force over the total foot is significantly lower in Group A compared to Group C, but Groups B and C do not differ from one another (**Figure**

5.14). This finding likely results from the much lower body mass of participants in Group A.

Peak pressure of the medial midfoot is significantly lower in Group A compared to Group C during walking, and in Group B than Group C, though Groups A and B do not differ from one another (**Figure 5.15**). Participants in Group A likely experience a lower peak pressure over the medial midfoot given that they have absolutely lower body mass (*i.e.*, force) that is distributed over a relatively larger medial midfoot contact area. Peak pressure of the lateral midfoot in Group A is significantly lower than Group C, but Groups A and B, and B and C, do not differ from one another (**Figure 5.16**). Again, this result likely reflects the lower body mass of participants in Group A. Finally, peak pressure over the total foot is significantly different between all three groups, with Group A experiencing the lowest pressure and Group C experiencing the highest pressure (**Figure 5.17**).

For running trials, group membership had a significant effect on all variables at the $p = 0.05$ level, with the exception of relative maximum force (as a percentage of body weight) experienced in the lateral midfoot region and over the total foot (**Table 5.5**). Post-hoc pairwise comparisons show that relative maximum force in the medial midfoot is significantly higher in Group A than Group C (**Figure 5.18**), and peak pressure is significantly lower in Group A than Group C (**Figure 5.19**), but these variables do not differ between Groups A and B, and B and C. This finding reflects that participants in Group A experience higher force for their body mass in the medial midfoot region given that more of their medial midfoot is in contact with the ground. However, given their smaller body mass and the larger contact area, peak pressure experienced in this region is lower for Group A compared to Group C. Peak pressure in the lateral midfoot region is also significantly lower in Group A than Group C, but does not differ between Groups A and B, or B and C (**Figure 5.20**). Here, the lower peak pressure experienced by Group A

is a result of their lower body mass. Finally, peak pressure in the total foot is significantly different between all three groups, with Group A experiencing the lowest pressure and Group C experiencing the highest pressure (**Figure 5.21**).

Correlation of Body Mass, Foot Shape, and Arch Height with Dynamic Pressure Variables Within Groups A, B, and C during Walking Trials

Group A

Table 5.6 summarizes the correlation coefficients between static participant variables and the dynamic pressure variables during walking trials for Group A. Here, only the three relative measures of foot breadth were used to quantify foot shape given that there was high correlation among the static participant variables within each group. In Group A, relative maximum force experienced in the medial midfoot region was significantly negatively correlated with body mass, such that individuals of a higher mass experienced lower force for their body mass beneath the medial midfoot. This trend is likely due to the fact that the larger individuals are also older in age and thus have a higher longitudinal arch, as indicated by the statistically significant positive relationship between relative maximum force of the medial midfoot and the arch index. In other words, participants with a low arch (*i.e.*, high arch index) experience greater relative maximum force beneath their medial midfoot than those with a high arch. Individuals with a low arch also experience greater relative maximum force in the lateral midfoot region, a finding consistent with previous reports of lateral midfoot loading in adults (DeSilva *et al*., 2015).

Relative foot breadth was significantly positively correlated with relative maximum force and peak pressure in the medial and lateral midfoot regions. This finding indicates that individuals with relatively wider feet experience greater force for their body mass and

pressure across the entire midfoot, though not across the total foot. Total foot peak pressure was significantly positively correlated with body mass and negatively correlated with hindfoot breadth. In other words, individuals of a larger body mass and narrower hindfoot (*i.e.*, smaller area) experience greater pressure.

Group B

Table 5.7 summarizes the correlation coefficients between static participant variables and the dynamic pressure variables during walking trials for Group B. In Group B, relative foot breadth was significantly positively correlated with relative maximum force in the medial midfoot region, where individuals with relatively wider feet experienced higher force for their body mass. Individuals with a lower navicular height index (*i.e.*, longitudinal arch) also experienced relatively higher maximum force in the medial midfoot region, as well as higher peak pressure. Peak pressure of the medial midfoot was also higher among individuals with a relatively wider hindfoot region. In the lateral midfoot, individuals with a high arch index (*i.e.*, low longitudinal arch) experienced greater relative maximum force than those with a low arch index. Peak pressure of the lateral midfoot was significantly positively correlated with body mass, consistent with the findings of DeSilva and colleagues (2015) for a sample of adults. Peak pressure experienced over the total foot was also significantly positively correlated with body mass, and was significantly negatively correlated with relative midfoot breadth. The latter of these findings indicates that individuals with a relatively narrow midfoot region experience higher pressure over the total foot, presumably resulting from a smaller contact area over which their body mass (*i.e.*, force) can be distributed.

Group C

Table 5.8 summarizes the correlation coefficients between static participant variables and the dynamic pressure variables during walking trials for Group C. In Group C, individuals with a relatively wider hindfoot, forefoot, and higher arch index (*i.e.*, lower longitudinal arch) experienced greater relative maximum force and peak pressure beneath their medial midfoot than individuals with narrow feet and higher arches. Greater relative maximum force in the lateral midfoot region was also experienced by participants who had relatively wider feet and lower longitudinal arches. Lateral midfoot peak pressure was higher among those of larger body mass, relatively wider hindfoot, and a lower longitudinal arch, a finding that is consistent with a previous study (DeSilva *et al*., 2015). Relative maximum force and peak pressure experienced over the total foot was not correlated with body size, foot shape, or arch height.

Relationship Between Speed and Midfoot and Total Foot Loading

Table 5.9 summarizes the correlation coefficients between Froude number, a dimensionless measure of speed, and relative maximum force (as a percent of body mass) and peak pressure experienced in the medial midfoot, lateral midfoot, and total foot. Froude number had a statistically significant positive correlation with all six dynamic variables for the complete sample and within Groups B and C. In Group A, Froude number had a significant positive correlation with five of the six dynamic variables, the exception being relative maximum force experienced in the medial midfoot region. Therefore, an increase in speed is associated with an increase in relative maximum force and peak pressure beneath the medial midfoot, lateral midfoot, and total foot for all participants who have a mature longitudinal arch. Young child participants for whom the arch is developing did not experience an increase in relative maximum force beneath their medial midfoot as speed

increased, however. And although Froude number was found to have a statistically significant positive correlation with midfoot and total foot loading, the strength of the relationship differs between these regions of the foot. Froude number was most strongly correlated with relative maximum force experienced over the total foot for the complete sample and in Groups B and C. In Group A, Froude number was most strongly correlated with peak pressure of the lateral midfoot and total foot. It is unclear whether the different pattern observed for Group A is related to immature gait kinematics and/or the absence of a longitudinal arch.

DISCUSSION

Longitudinal Arch Height and Foot Loading

This study investigated differences in dynamic pressure variables of the midfoot and total foot between three groups that were defined, in part, according to the development of the longitudinal arch—children aged 1-6 years, for whom the longitudinal arch was still developing (Group A); children aged 6-15 years, for whom the longitudinal arch was developed (Group B); and adults over 18 years of age, who had a fully developed longitudinal arch and foot (Group C). Group A consisted of young children for whom the longitudinal arch was is a state of development. In this sample, the longitudinal arch appeared to have reached maturity in children approximately age six and older, a finding that is consistent with previous studies (Bertsch *et al.,* 2004; Müller *et al.,* 2012; Onodera *et al*., 2008). The age of six is also significant with respect to bipedal gait maturity, as studies have shown that the kinematics of the developing child's gait also reach maturity around this age (Sutherland, 1997; Samson *et al.,* 2011). Group B consisted of children for whom the longitudinal arch was developed, yet were still experiencing foot growth. In this

sample, foot length was assessed to have reached maturation around age 15, a finding that is consistent with other publications on foot growth (Scheuer & Black, 2004).

Consistent with expectations, longitudinal arch height was lowest in Group A, higher in Group B, and highest in Group C, when measured as the navicular height index, a static measure of arch height. Arch index, however, was not significantly different between the groups, indicating that inter-individual variation in morphological arch height may be lost when arch height is measured dynamically. As is evident in **Figure 5.5**, individuals with a given navicular height index can exhibit dramatically different arch indices. These differences may result from inter-individual variation in plantar tissue thickness. In other words, two individuals may have a similar navicular height to foot length ratio; yet, if one individual has thicker plantar tissue beneath the medial midfoot than the other, the one with the thicker tissue may have a higher arch index because the contact area of the midfoot region will be greater relative to the total foot contact area than it would be for the individual with more minimal plantar tissue thickness. For this reason, assessing longitudinal arch height in multiple ways could enhance our understanding of the relative contributions of soft tissue and bony structural anatomy on foot loading patterns.

Longitudinal arch height was not found to consistently affect loading of the medial and/or lateral midfoot, or total foot among the three groups. However, whenever a statistically significant relationship was observed, the trend was consistent: a lower longitudinal arch was associated with higher relative maximum force or peak pressure in that region. This finding is consistent with previous studies such as Morag and Cavanagh (1999), who found that variation in arch height was the primary structural factor that explained midfoot loading. While the Morag and Cavanagh (1999) study investigated the effects of arch height on midfoot loading as a whole, the present study divided the midfoot into medial and lateral components to investigate the effects of arch height on both regions,

as well as the total foot. In addition, this study investigated whether arch height explained variation in midfoot loading in children, as well as adults. In the present study, arch index was significantly positively correlated with relative maximum force (as a percent of body mass) in the medial and lateral midfoot regions for Groups A and C, and with relative maximum force of the lateral midfoot for Group C (**Tables 5.6 – 5.8**). However, arch index was not correlated with relative maximum force over the total foot in any group, indicating that the effects of arch height on relative maximum force are more localized (*i.e.*, to the midfoot versus the total foot), irrespective of age. However, arch index was significantly positively correlated with peak pressure of the medial and lateral midfoot in the adult sample only (**Table 5.8**). This finding is likely due to the fact that the feet of adult individuals must support an absolutely greater load per unit area than children.

The relationship between navicular height index and the dynamic pressure variables was different than what was observed for the arch index. In other words, navicular height index and arch height did not share the same significant relationships with the dynamic pressure variables (**Tables 5.6 – 5.8**). When statistically significant correlations were found, however, navicular height index was found to exhibit a negative relationship with the dynamic pressure variables, showing again that a low arch is associated with higher relative maximum force and/or peak pressure in the given region. One methodological item to note, however, is that the navicular height index could not be calculated for a number of the participants in Group A, and some in Group B. Therefore, it is possible that non-significant correlations in Group A is an artifact of low sample size. However, it may also be the case that some dynamic pressure variables (*e.g.*, relative maximum force and peak pressure in the medial midfoot for Group B; **Table 5.7**) were significantly positively correlated with navicular height index, but not arch index, because these indices are measuring slightly different aspects of arch-related anatomy (*i.e.*, NHI = bony anatomy,

while AI = bony + soft tissue anatomy). Therefore, the arch index may be a more appropriate measure of arch height in clinical contexts because it more accurately quantifies how much of the foot is contacting the substrate, while the navicular height index may be more appropriate when thinking about foot function in fossil hominins because it is very difficult to discern soft tissue anatomy from bony fossils alone.

Relationship Between Static Participant Variables and Midfoot and Total Foot Loading

In this study, child participants for whom the longitudinal arch was developing (Group A) experienced a higher force for their body weight in the medial midfoot region during both walking and running strides than did individuals who had a mature longitudinal arch (Groups B and C), yet experienced lower pressure in this region (**Table 5.3**). This finding is likely related to the fact that participants in Group A have a lower longitudinal arch and therefore a greater midfoot contact area than both child and adult participants with a mature longitudinal arch. Also, the absolute force experienced in this region is lower for Group A, which would contribute to a lower peak pressure. The finding that children in the sample for whom the arch is developing experience greater force for their body weight beneath the medial midfoot region is consistent with previous studies documenting age-related changes in foot loading patterns (*e.g.*, Hennig & Rosenbaum, 1991; Bertsch *et al.*, 2004).

Variation in the relative maximum force experienced in the medial midfoot region was correlated with similar participant variables for each group. Among the child participants for whom the arch was developing (Group A), individuals who were of a smaller body mass and had relatively wider feet with a low longitudinal arch experienced greater force for their body mass in the medial midfoot region while walking. Among the

child participants with a developed arch (Group B), a similar trend was observed, where those participants who had relatively wider feet and a low longitudinal arch experienced higher force for their body mass in the medial midfoot region during walking. Body mass was not correlated with relative maximum force of the medial midfoot in this group, however, or among adult participants. For adult participants (Group C), those with a low longitudinal arch height and a relatively wide hindfoot and/or forefoot experienced greater relative maximum force for their body mass beneath the medial midfoot. Therefore, it seems that individuals with a relatively wider foot and a lower longitudinal arch experience greater relative maximum force beneath the medial midfoot region, regardless of body size and age. A similar trend was observed for peak pressure experienced in the medial midfoot region, where participants from all three groups who had relatively wider feet and a lower longitudinal arch experienced higher pressure beneath the medial midfoot. Within each group, body size was not significantly correlated with peak pressure in this region, which may indicate that aspects of an individual's foot shape and arch height are more important in determining pressure experienced beneath the medial midfoot than body size. The peak pressure experienced in the medial midfoot was similar among child participants irrespective of arch maturation (*i.e.*, Groups A and B), and was significantly higher for adult participants (Group C). Given that pressure is the quotient of force over area, this finding indicates that while although children in Group A experienced greater relative maximum force in the medial midfoot region, their lower absolute force compared to adults results in a lower peak pressure. Other studies have reported a similar finding that peak pressures beneath children's feet are lower in all anatomical regions than adults (Hennig & Rosenbaum, 1991). Given that peak pressure in the medial midfoot was not significantly different between Groups A and B in this study, it appears that children experience lower peak pressure in the medial midfoot than adults, regardless of arch maturation.

A number of recent studies have reported that a small percentage of non-pathological humans exhibit elevated lateral midfoot loading only previously thought to characterize non-human primates (*e.g.*, Crompton *et al.* 2012; Bates *et al*., 2013; DeSilva & Gill, 2013; DeSilva *et al*., 2015). Individuals of a higher body mass and with a lower longitudinal arch have been reported to experience higher peak pressure in the lateral midfoot region among adults during walking trials (DeSilva *et al*., 2015), but it was unclear if these same relationships occur in children. In the current study, all groups experienced a similar maximum force relative to their body mass in the lateral midfoot region (**Table 5.4**). However, peak pressure in this region was lower for child participants compared to adults, regardless of arch maturation. Again, this difference is likely because the children experience absolutely lower force than adults. Among participants in all three groups, those who had a lower longitudinal arch (*i.e.*, higher arch index) experienced greater relative maximum force for their body mass in the lateral midfoot while walking (**Tables 5.6-5.8**). In Groups A and C, participants with a relatively wider foot also experienced higher maximum force for their body mass in this region, though this trend was not observed among members of Group B. Peak pressure experienced in the lateral midfoot region was higher among participants in Group A who had a relatively wider hindfoot and midfoot, but was not higher among participants who had a lower arch or a larger body size. In Group B, body size was found to have a significant positive correlation with lateral midfoot peak pressure, consistent with a relationship previously observed among adults (DeSilva *et al*., 2015). Here, adult participants who were of a larger body size and lower longitudinal arch (*i.e.*, higher arch index) were also observed to experience higher peak pressure beneath the lateral midfoot, similar to what has been reported in previous studies (DeSilva *et al*., 2015). Therefore, the results of this study demonstrate foot shape (*i.e.*, relative breadth) is more important in determining lateral midfoot loading among young children for whom the

longitudinal arch is developing than is arch height or body size. Among participants for whom the arch is mature (Groups B and C), those who are of a larger body size experience greater loading of the lateral midfoot region. Relative foot breadth and arch height also affect lateral midfoot loading among adult participants, where those who have a relatively wider foot and lower arch experience greater loads.

The relative maximum force as a percentage of body mass experienced over the total foot was lowest in child participants for whom the arch was developing (Group A), and was significantly lower than that experienced by adult participants during walking trials (**Table 5.4**; **Figure 5.14**). During running, however, children in this young age group experience similar force over the total foot given their body weight as that experienced by older children and adults for whom the longitudinal arch is fully developed (**Table 5.3**). Previous studies have reported that the foot experiences forces approximately 2.5 times greater during running (Robbins & Hanna, 1987), and the results of this study are consistent with that estimate for all three groups (**Table 5.3**). Interestingly, relative maximum force experienced over the total foot was not significantly correlated with body mass, foot shape, or longitudinal arch height among participants in any group. Peak pressure over the total foot was significantly different between the three groups, showing yet again that children experience lower peak pressure than adults, irrespective of arch maturation (**Table 5.4**). Among child participants in Groups A and B, peak pressure experienced over the total foot was higher among those who were of a larger body mass, and was also higher among those with a narrow hindfoot and midfoot in Group A and B, respectively (**Tables 5.6** and **5.7**). In general, total foot relative maximum force and peak pressure was correlated with the fewest number of static participant variables when compared to other dynamic pressure variables. This finding is possibly due to the fact that kinematic aspects of an individual's gait may explain a greater portion of the variance in total foot loading than static

anthropometric variables alone (Morag & Cavanagh, 1999). While a previous study by Morag and Cavanagh (1999) have found this to be true for adults, the results of the current study show that this may also be true for children.

Effects of Speed on Midfoot and Total Foot Loading

Speed (measured as Froude number) had a significant positive relationship with midfoot and total foot loading, where an increase in speed was associated with an increase in relative maximum force and peak pressure (**Table 5.9**). A previous study by Rosenbaum and colleagues (2004) noted that when adult individuals increased their walking speed, they experienced a significant increase in peak pressure beneath the heel and medial forefoot, and a significant decrease in pressure under the midfoot and lateral forefoot. Therefore, the results of the present study are not consistent with this previous study. Here, an increase in speed (which included both walking and running gaits) was associated with an increase in midfoot and total foot loading, and the relationship was particularly strong for the total foot in all three groups (**Table 5.9**).

Speed and Midfoot Motion

While midfoot motion was not measured in the present study, a number of participants were observed to exhibit midfoot motion on the videos used to measure speed (**Figure 5.22**). In a recent study by DeSilva and colleagues (2015), a lateral midfoot peak pressure $\geq$ 200 kPa was associated with midfoot dosiflexion, and was observed in approximately 8% of participants, all of whom were walking. In the present study, 60 out of 191 trials (31%) were recorded where lateral midfoot peak pressure was greater than or equal to 200 kPa. Of these trials, 6 (10%) occurred during walking and 54 (90%) occurred

during running. Therefore, midfoot mobility may be affected by locomotor speed in humans. To demonstrate this, **Figure 5.23** shows the pressure maps of two individuals moving at three increasing speeds. Here, it is evident that the pressure experienced in the lateral midfoot region – at the cubometatarsal joint – increases with speed. Therefore, studies of human foot mobility should consider the effects of speed on midfoot motion.

Implications for Inferring Foot Loading in Fossil Hominins

The results of this study are consistent with previous reports that there is a negative relationship between longitudinal arch height and foot loading of the midfoot region (*e.g.*, Morag & Cavanagh, 1999; DeSilva *et al*., 2015). The results of this study add to our understanding of this relationship between arch height and midfoot loading by demonstrating that this trend is present within children as well as adults. While previous reports of foot loading in developing children have shown that midfoot loading decreases as arch height increases (Bertsch *et al*., 2004), the relationship was not well explored in children for whom the arch was already mature. Given that early hominins were of a smaller body size than contemporary adults who comprise the samples of most plantar pressure studies (McHenry, 1992; Grabowski *et al*., 2015), finding this same negative relationship in children means that a similar pattern could have been present in small-bodied hominins. In addition, this study found that young, small-bodied participants and adults who have relatively wider feet also experience greater loading of the midfoot region. Given that early hominins have been estimated to have had relatively broad feet for their foot length and stature, similar to habitually unshod populations (Tuttle *et al*., 1990; Meldrum, 2004; Hatala *et al.*, 2016), the results of this study also suggest that early

hominins may have experienced greater midfoot loading than modern humans as a result of their foot shape.

If a low longitudinal arch is associated with greater loading of the medial and lateral midfoot, then it follows that foot bone morphologies linked with arch height may be suggestive of midfoot loading in fossil hominins. Unfortunately, directly testing the link between foot bone morphology, arch height, and midfoot loading was outside the scope of this chapter. One observation can be made, however, given data that were reported in earlier chapters of this dissertation. Morag and Cavanagh (1999) found that the calcaneal inclination angle, a radiographic measure of longitudinal arch height, explained a significant amount of the variance in midfoot loading. In Chapter 3 of this dissertation, the cuboid facet angle of the calcaneus was found to be significantly positively correlated with the calcaneal inclination angle. Therefore, it is hypothesized that individuals who exhibit a low cuboid facet angle, and therefore a low calcaneal inclination angle (arch height), would also exhibit elevated midfoot loading. Future studies should combine data on foot bone shape (via x-ray and/or MRI), longitudinal arch height, and foot loading to address this and related hypotheses.

CONCLUSIONS

- In general, relative maximum force (as a percentage of body weight) is higher in the medial and lateral midfoot regions among those who exhibit a lower longitudinal arch and a relatively wider foot, irrespective of whether the arch is undergoing development or if its development is mature.

- Peak pressure of the medial and lateral midfoot regions is higher in adults who have a lower longitudinal arch, but arch height does not affect peak pressure in the midfoot in children.
- Relative maximum force (as a percent of body weight) experienced over the total foot is not related to participant differences in body size, foot shape, or longitudinal arch height, indicating that the effects of arch height on foot loading are more localized.
- Relative maximum force and peak pressure of the medial midfoot, lateral midfoot, and total foot increases with locomotor speed, though the effects are greater for the total foot than the midfoot.
- Lateral midfoot peak pressures in excess of 200 kPa were observed in this sample, primarily during running trials. Therefore, locomotor speed may affect midfoot mobility, with greater motion occurring at faster speeds.

Age (years)	N
1-2	7
2-3	7
3-4	2
4-5	10
5-6	1
6-7	3
7-8	2
8-9	2
9-10	1
10-11	2
11-12	1
12-13	2
13-14	1
14-15	2
15-16	2
18-20	3
21-25	13
25-30	7
30-35	6
35-40	4
40-45	2
45-50	2
50+	1
TOTAL	84

Table 5.1: Summary of the number of sample participants by age.

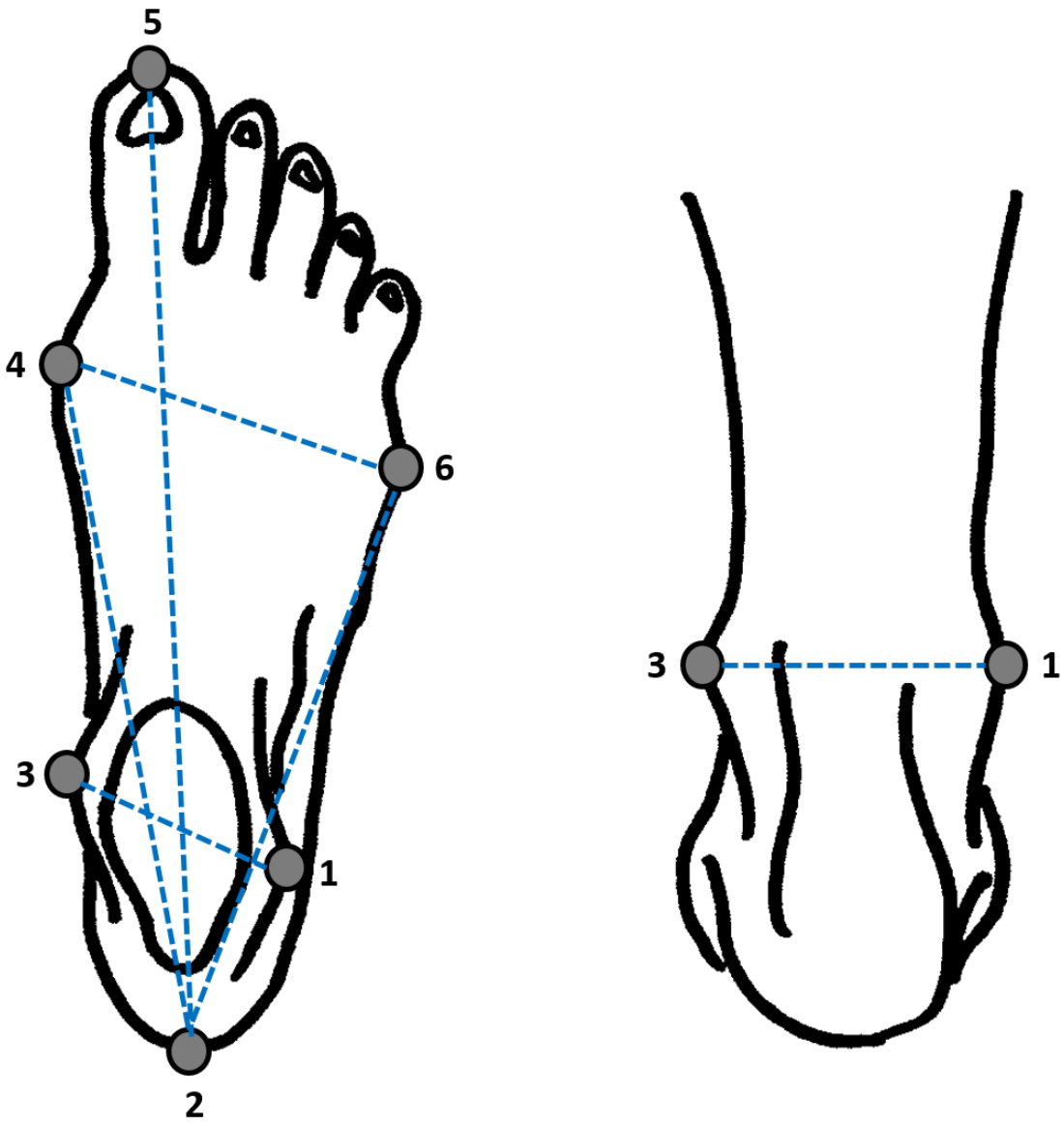

Figure 5.1: Landmarks and metrics of the external surface of the foot and ankle. 1 = lateral malleolus; 2 = posterior-most aspect of heel; 3 = medial malleolus; 4 = medial-most point of 1st metatarsal head; 5 = distal-most point of 1st digit; 6 = lateral-most point of 5th metatarsal head.

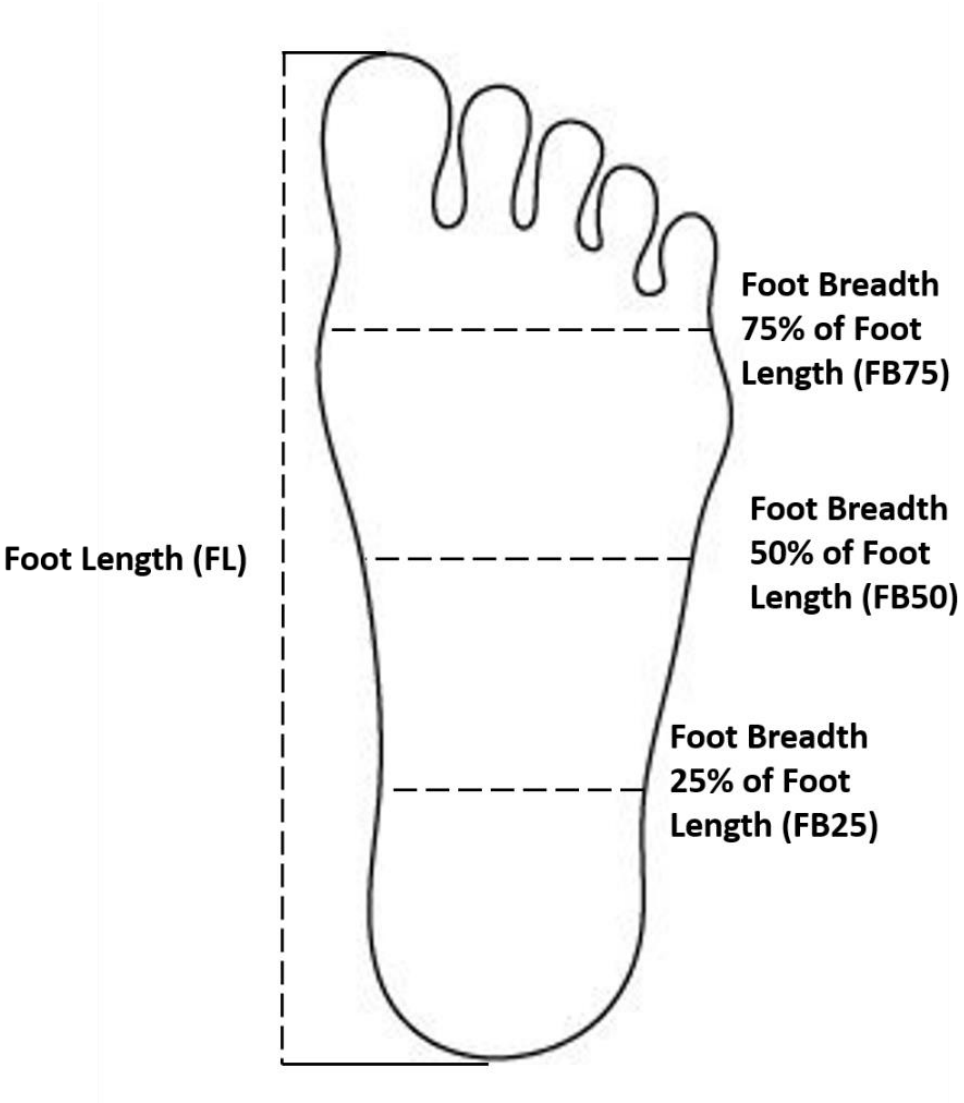

Figure 5.2: Linear metrics collected from tracings of each participant's right foot.

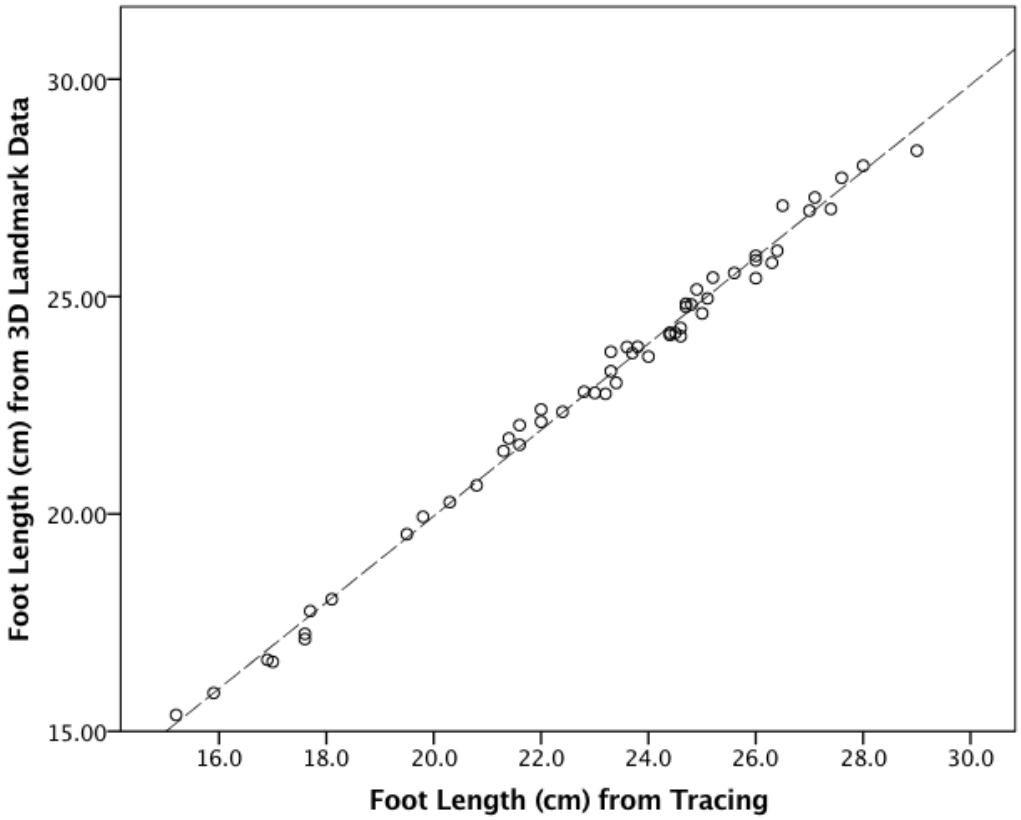

Figure 5.3: Scatter-plot of two independent measures of foot length ($r = 0.996$, $p < 0.001$).

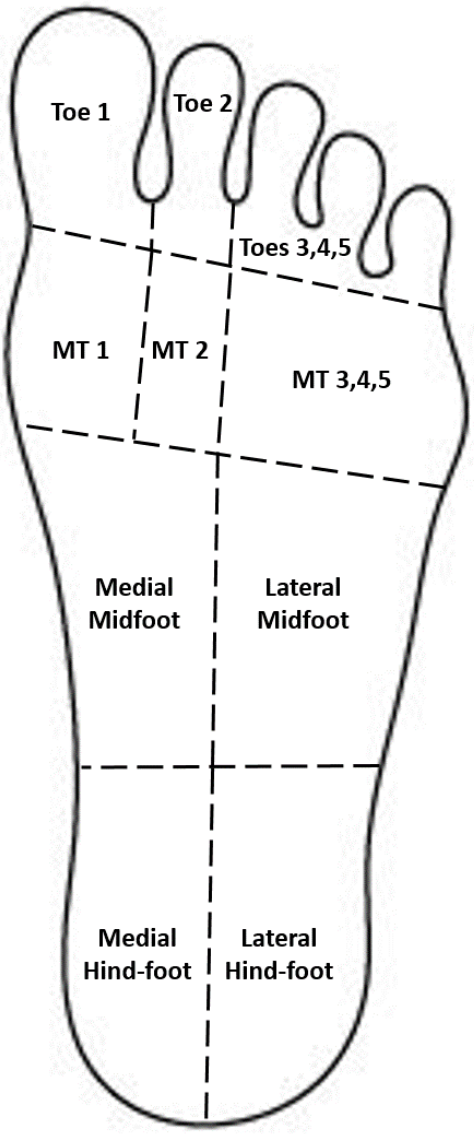

Figure 5.4: Anatomical regions of the foot.

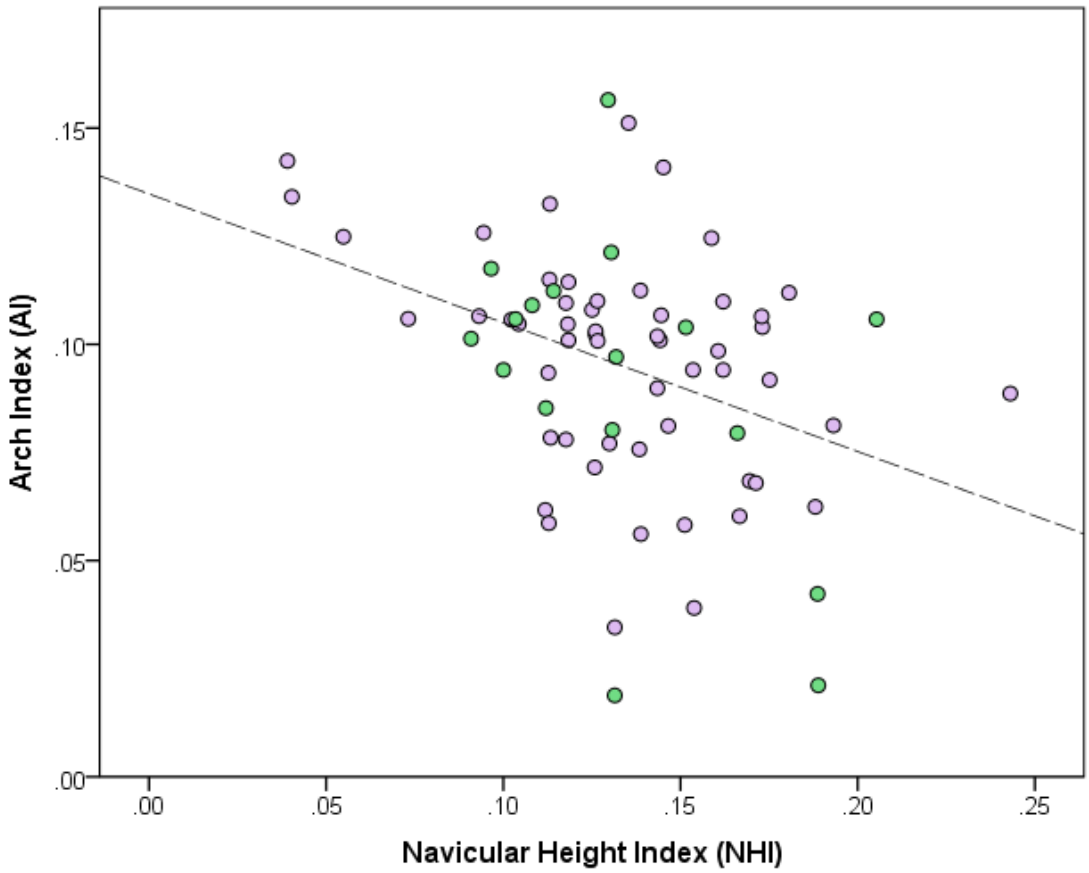

Figure 5.5: Scatter-plot of Arch Index (AI) and Navicular Height Index (NHI) for the participant sample. Males = green circles, Females = lavender circles.

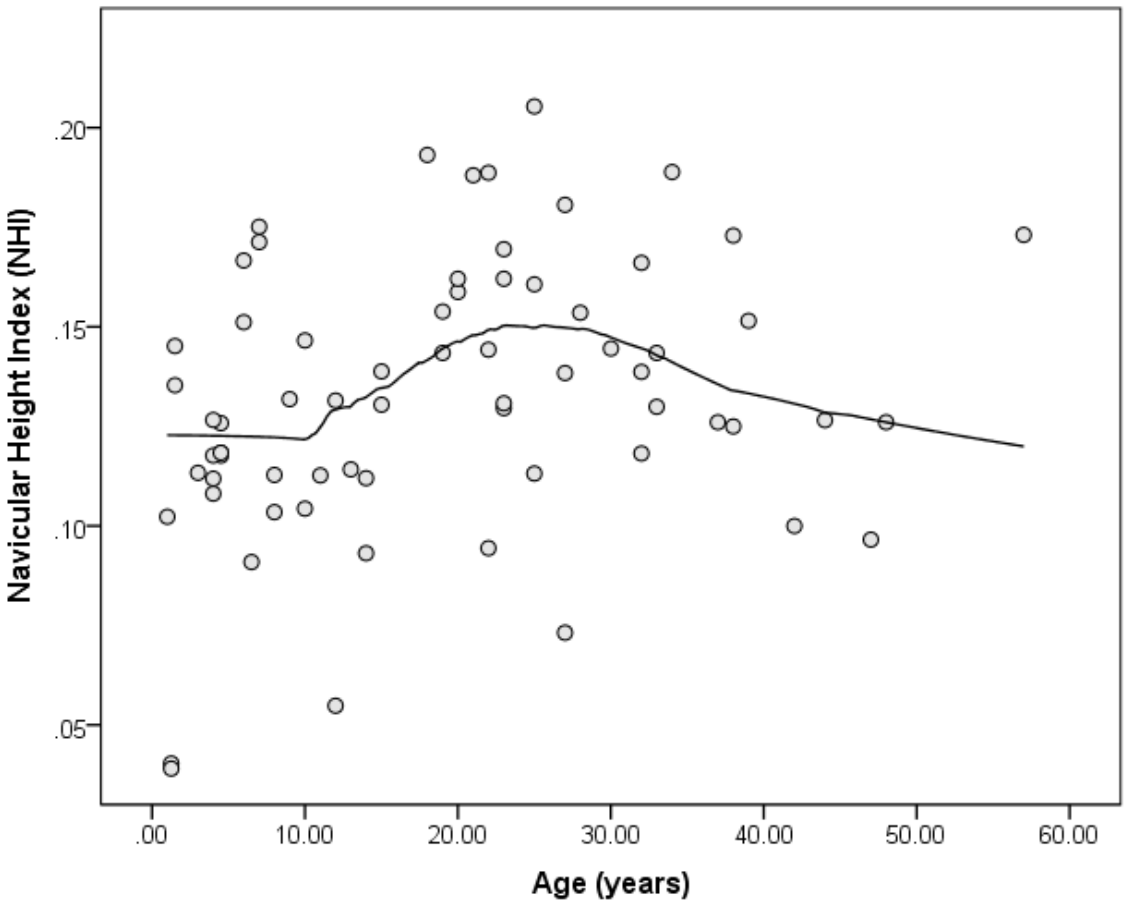

Figure 5.6A: Scatter-plot with LOESS curve of Navicular Height Index and Age for all study participants.

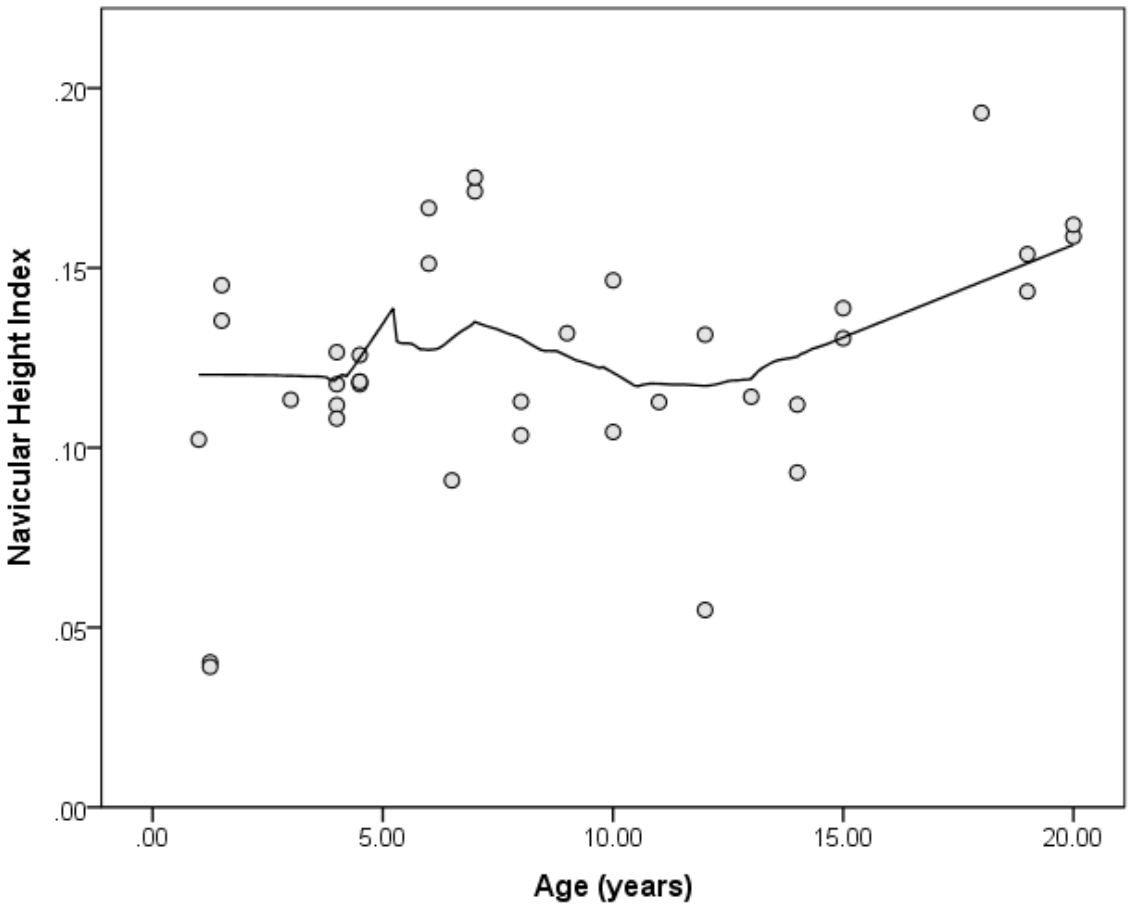

Figure 5.6B: Scatter-plot with LOESS curve of Navicular Height Index and Age for study participants under 20 years of age.

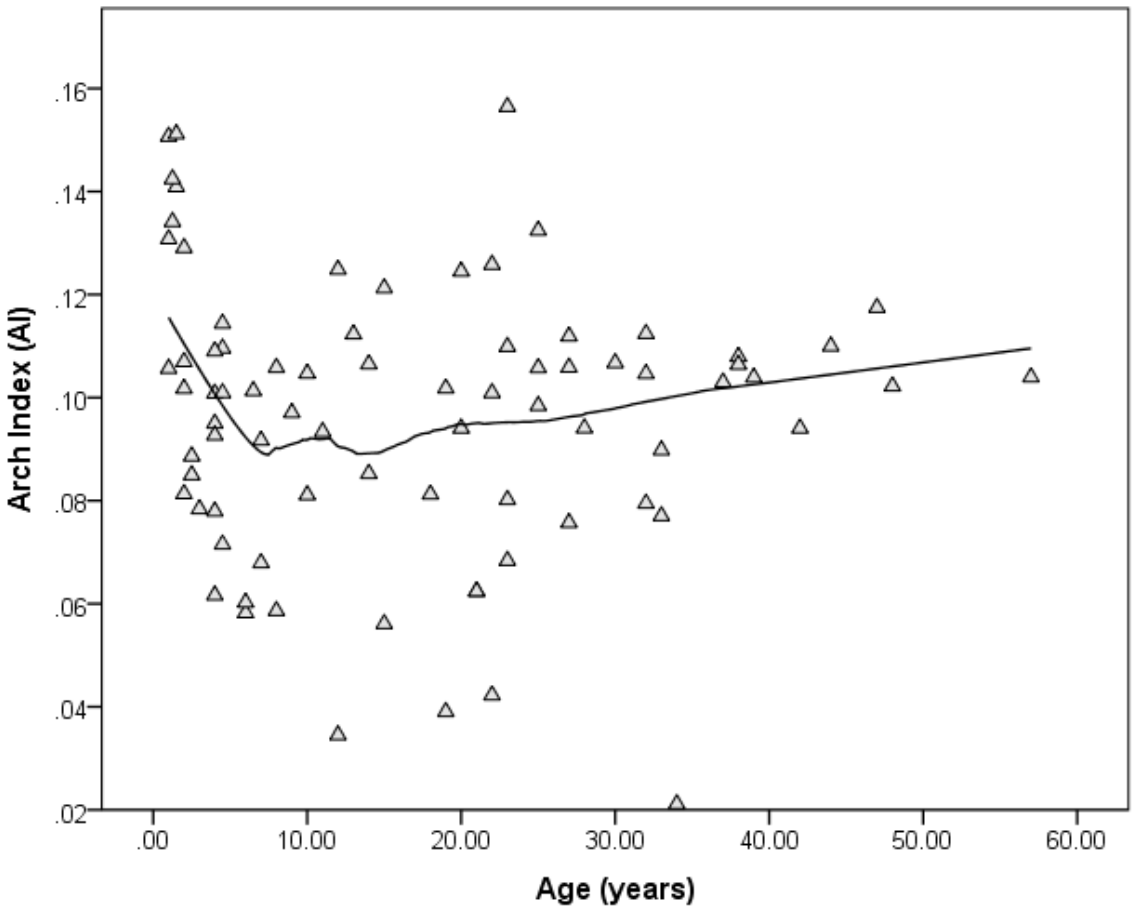

Figure 5.7A: Scatter-plot with LOESS curve of Arch Index and Age for all study participants.

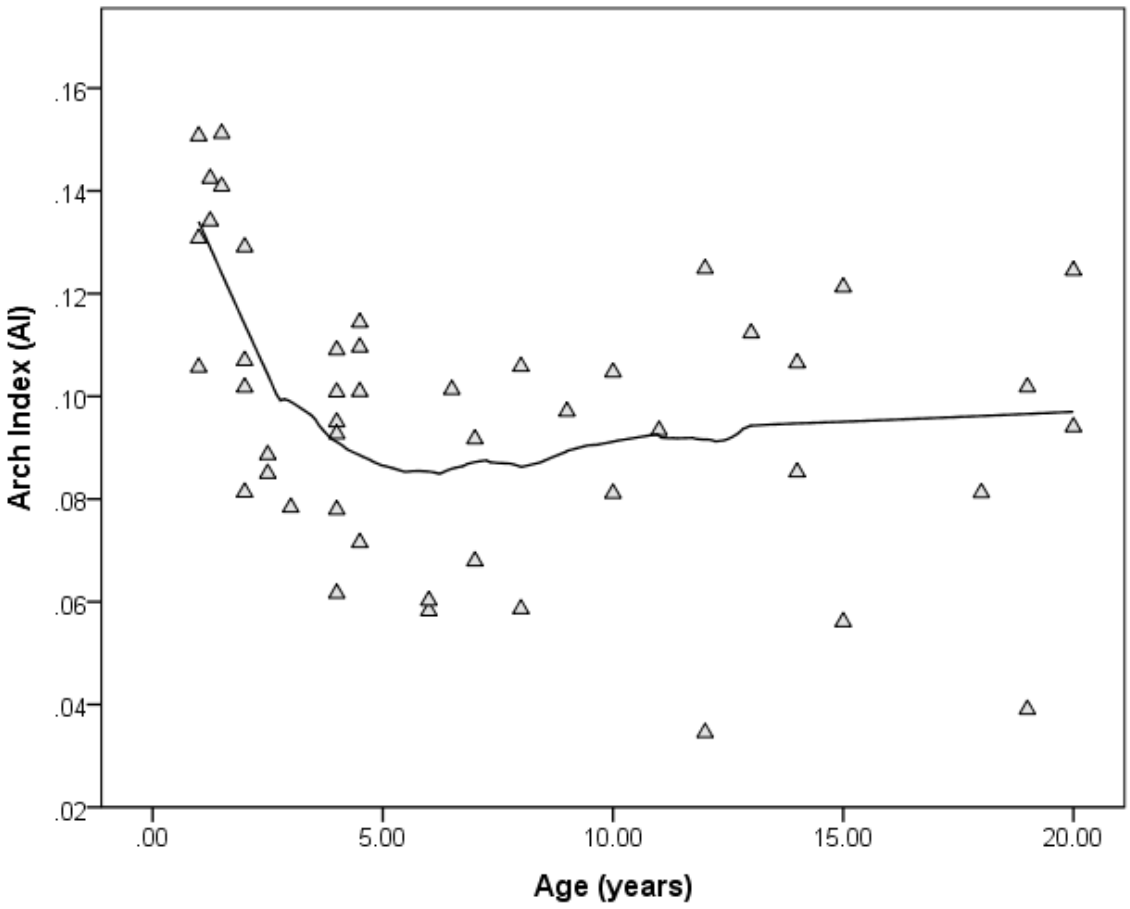

Figure 5.7B: Scatter-plot with LOESS curve of Arch Index and Age for study participants under 20 years of age.

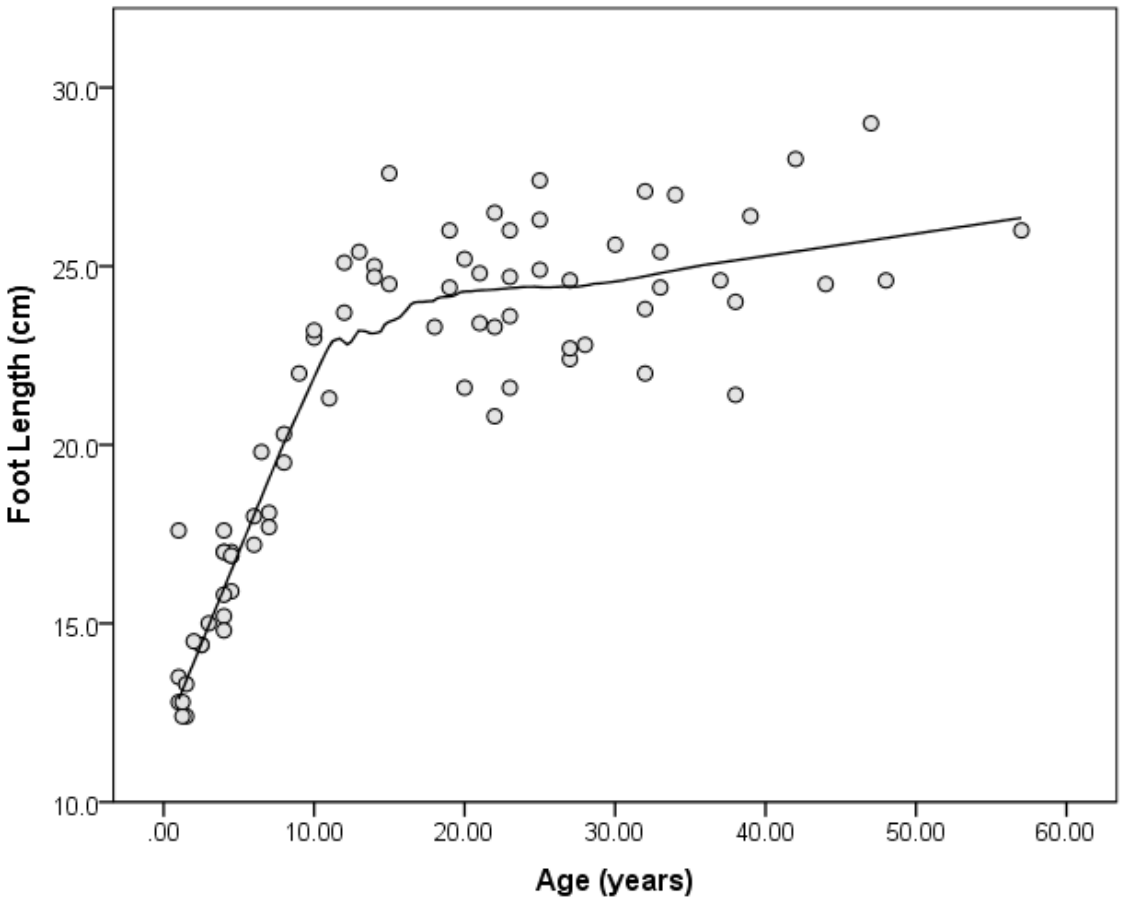

Figure 5.8A: Scatter-plot with LOESS curve of foot length and age for all study participants.

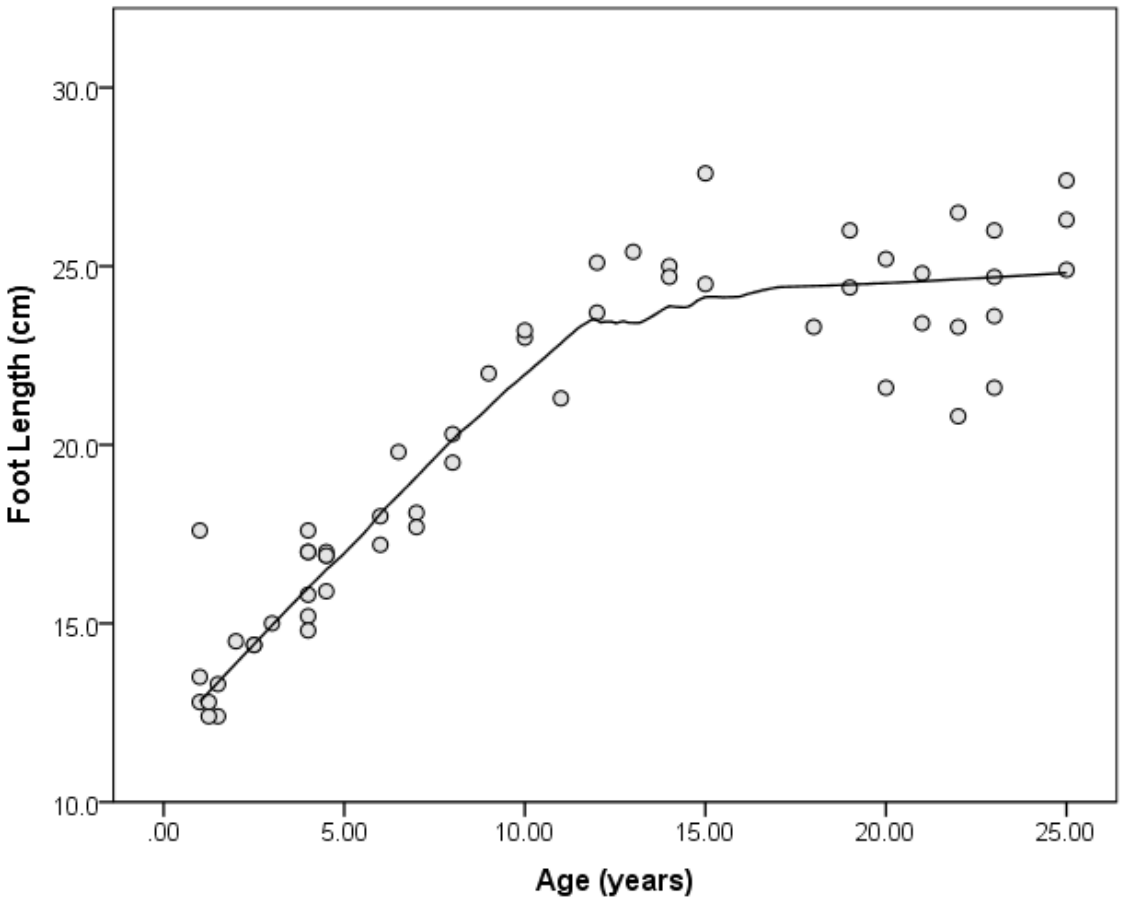

Figure 5.8B: Scatter-plot with LOESS curve of foot length and age for study participants under 25 years of age.

	Group A (N=27)	**Group B** (N=17)	**Group C** (N=37)
Static Participant Variables – Absolute Measurements			
Body Mass (kg)	14.63 ± 3.57	36.25 ± 12.83	66.84 ± 14.74
Height (cm)	97.28 ± 16.73	145.19 ± 17.92	165.91 ± 10.06
Hip Height (cm)	44.59 ± 7.67	75.82 ± 12.65	89.74 ± 5.66
Knee Height (cm)	24.60 ± 3.96	40.32 ± 6.38	46.98 ± 3.43
Foot Length (cm)	15.35 ± 1.87	22.22 ± 3.10	24.60 ± 1.95
Foot Breadth 25% length (cm)	4.42 ± 0.32	5.49 ± 0.83	6.38 ± 0.67
Foot Breadth 50% length (cm)	5.37 ± 0.34	6.95 ± 0.93	7.99 ± 0.76
Foot Breadth 75% length (cm)	6.37 ± 0.48	8.36 ± 0.97	9.18 ± 0.66
Metatarsal breadth (cm)	7.16 ± 1.04	8.42 ± 1.13	9.66 ± 0.73
Heel Breadth (cm)	3.99 ± 0.91	4.39 ± 0.54	5.04 ± 0.61
Bi-Malleolar Breadth (cm)	5.21 ± 0.48	6.15 ± 0.65	6.76 ± 0.57
Instep Length (cm)	7.33 ± 0.97	8.97 ± 1.23	10.42 ± 1.17
Lateral Foot Length (cm)	14.98 ± 2.59	18.19 ± 2.61	20.50 ± 1.60
Ratios of Foot Size			
Relative Breadth 25%	.29 ± 0.037	.25 ± 0.021	.26 ± 0.022
Relative Breadth 50%	.35 ± 0.037	.31 ± 0.017	.32 ± 0.021
Relative Breadth 75%	.42 ± 0.028	.38 ± 0.021	.37 ± 0.018
Contact Area			
Medial Midfoot Contact Area (cm^2)	3.17 ± 1.59	2.73 ± 1.86	4.08 ± 4.12
Total Foot Contact Area (cm^2)	53.37 ± 14.30	92.80 ± 23.73	118.93 ± 17.95
Medial Midfoot Contact Area / Total Foot Contact Area	0.0662 ± 0.039	0.0295 ± 0.018	0.0324 ± 0.026
Longitudinal Arch Height			
Navicular Height Index	0.116 ± 0.034	0.120 ± 0.029	0.145 ± 0.031
Arch Index	0.099 ± 0.032	0.092 ± 0.025	0.095 ± 0.026

Table 5.2: Mean and standard deviation for static participant variables in Groups A (Age 1≤6 years), B (Age 6≤15 years), and C (Age >15 years).

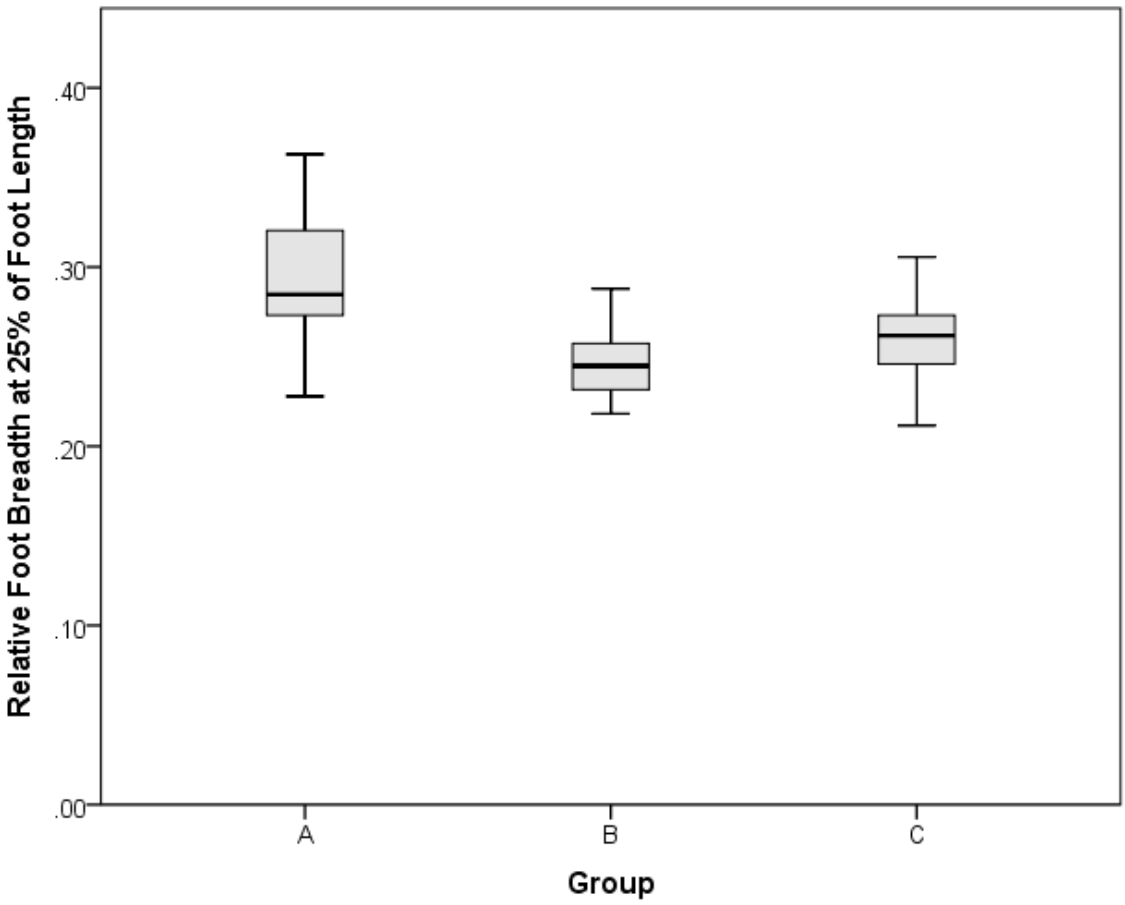

Figure 5.9A: Box-plots of median and interquartile range of relative foot breadth at 25% of foot length for Groups A, B, and C. Group A has a significantly wider hindfoot than Groups B and C [$F(2,74) = 15.237$, $p < 0.001$].

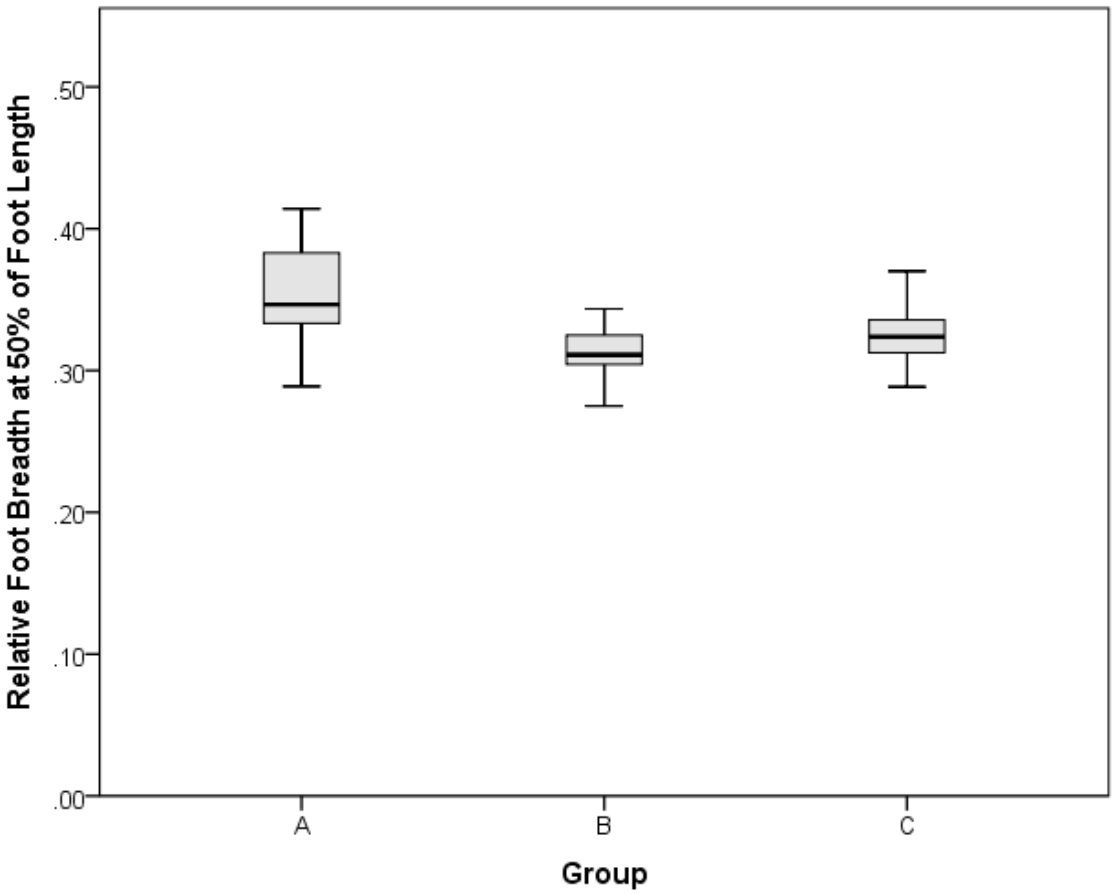

Figure 5.9B: Box-plots of median and interquartile range of relative foot breadth at 50% of foot length for Groups A, B, and C. Group A has a significantly wider midfoot than Groups B and C [$F(2,74) = 13.297$, $p < 0.001$].

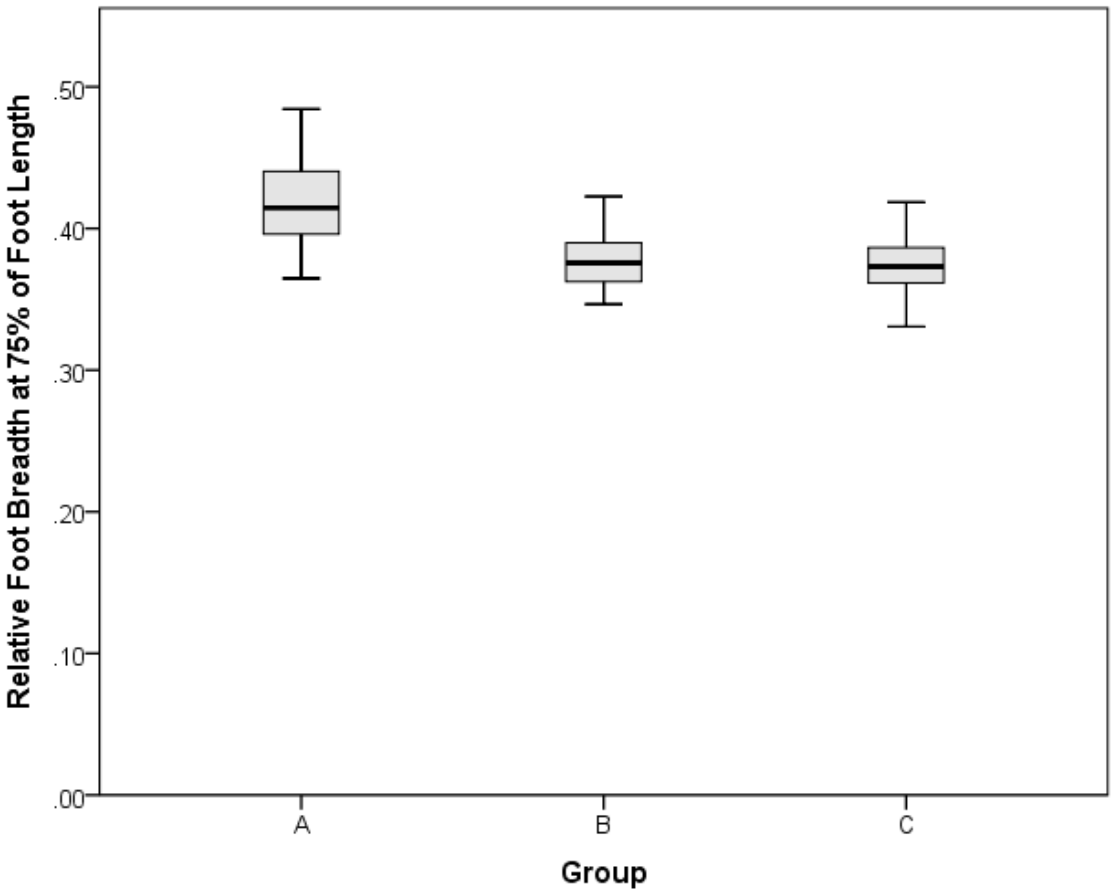

Figure 5.9C: Box-plots of median and interquartile range of relative foot breadth at 75% of foot length for Groups A, B, and C. Group A has a significantly wider forefoot than Groups B and C [$F(2,74) = 30.445$, $p < 0.001$].

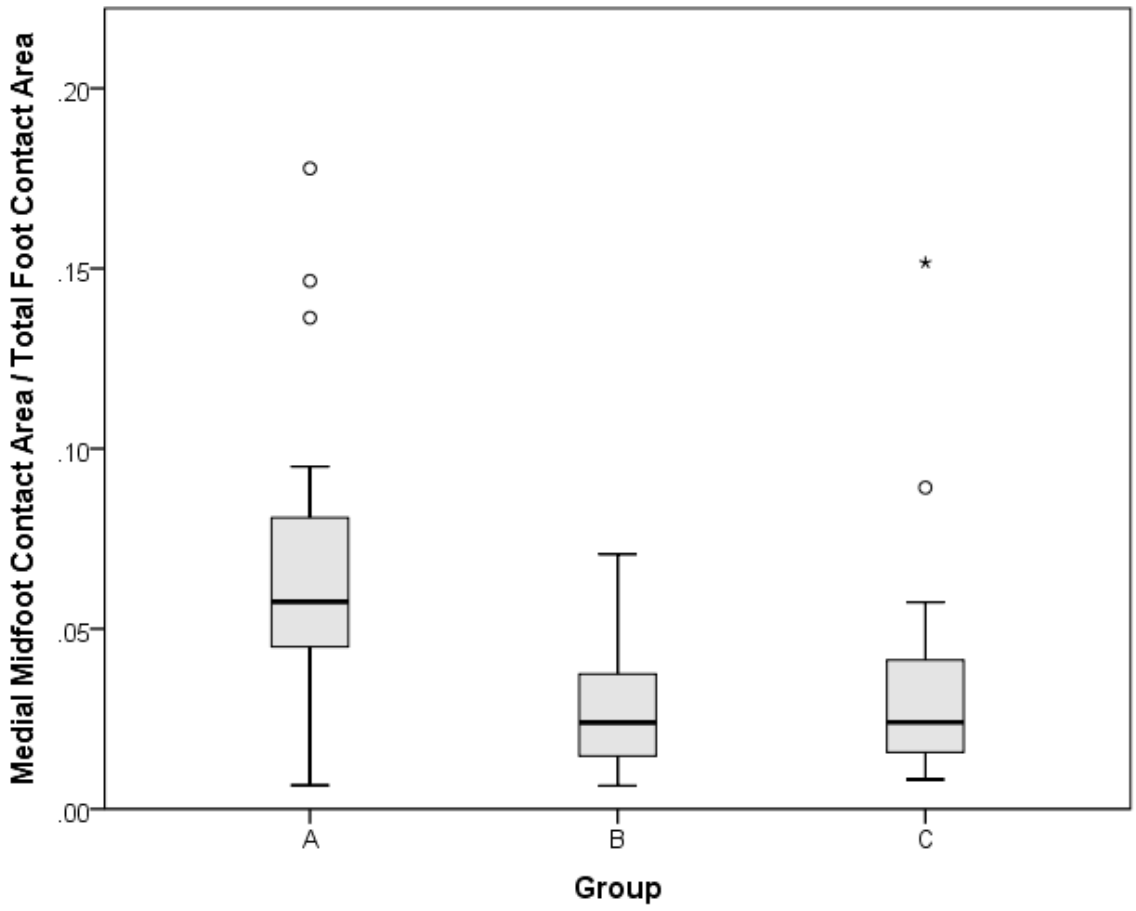

Figure 5.10: Box-plots of median and interquartile range of relative medial midfoot contact area for Groups A, B, and C. Group A has a significantly greater relative midfoot contact area than Groups B and C ($p < 0.001$).

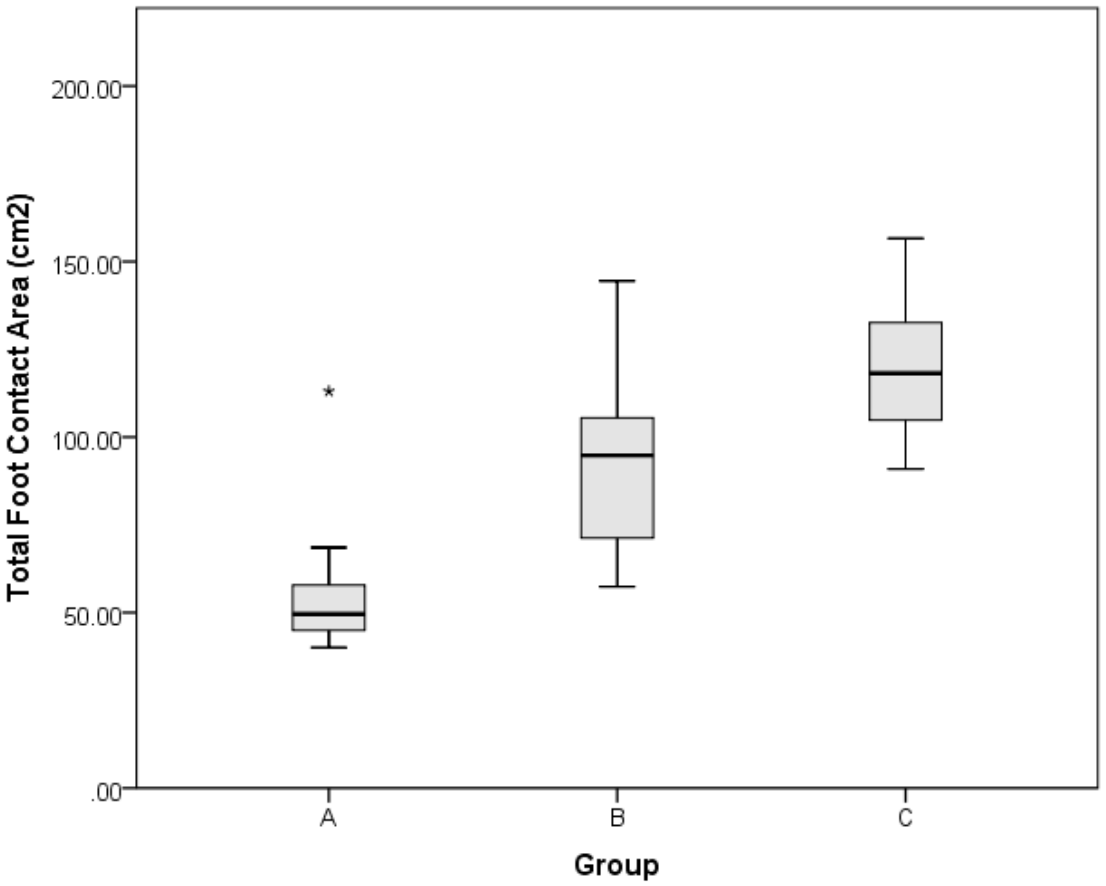

Figure 5.11: Box plots of median and inter-quartile range of total foot contact area (cm^2) for Groups A, B, and C. There is a statistically significant difference in total foot contact area between the three groups ($p < 0.001$).

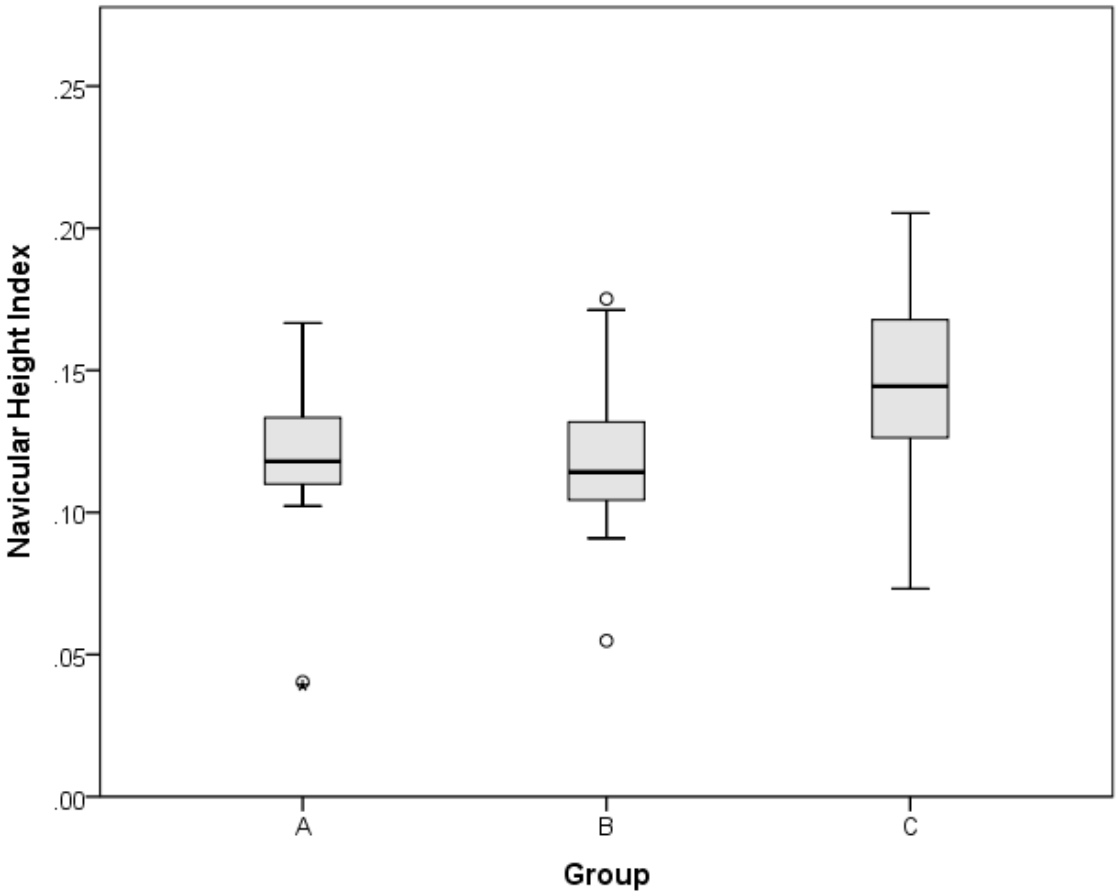

Figure 5.12A: Box-plots of median and interquartile range of navicular height index for Groups A, B, and C. Groups A and B have significantly lower arches than Group C [$F(2,66) = 7.292$, $p < 0.001$].

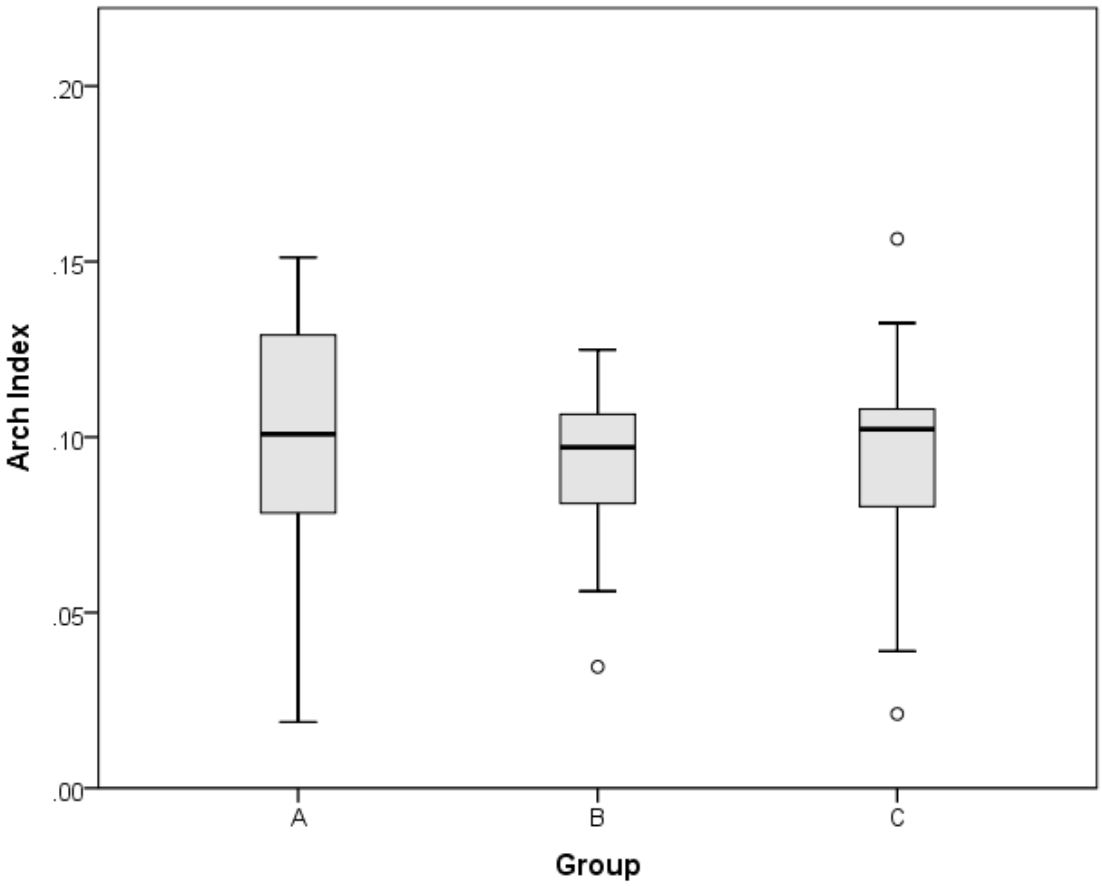

Figure 5.12B: Box-plots of median and interquartile range of Arch Index (AI) for Groups A, B, and C. AI does not statistically differ between the three groups.

	Group A		Group B		Group C	
	walk N = 10	**run N = 26**	**walk N = 14**	**run N = 21**	**walk N = 31**	**run N = 77**
Medial Midfoot						
relative maximum force	.11 ± .09	.19 ± .16	.04 ± .03	.12 ± .1	.04 ± .04	.08 ± .1
peak pressure	78.4 ± 26.8	120.2 ± 36.1	81.1 ± 24.6	129.1 ± 4	121.4 ± 53.1	149.0 ± 58.2
Lateral Midfoot						
relative maximum force	.21 ± .11	.33 ± .23	.21 ± .1	.44 ± .3	.16 ± .1	.41 ± .2
peak pressure	79.03 ± 26.65	116.6 ± 28.0	103.0 ± 33.4	192.3 ± 126.4	131.8 ± 42.9	245.3 ± 128.5
Total Foot						
relative maximum force	1.4 ± .28	2.7 ± 2.0	1.3 ± .10	2.5 ± .6	1.2 ± .06	2.42 ± .4
peak pressure	273.7 ± 62.46	479.9 ± 246.1	515.2 ± 207.6	717 ± 168.8	852.3 ± 221.7	1021.6 ± 221.8

Table 5.3: Mean and standard deviation for dynamic pressure variables in Groups A (Age 1≤6 years), B (Age 6≤15 years), and C (Age >15 years). Maximum force represents the maximum force experienced in the region as a percentage of body mass; peak pressure is in kPa.

	df	F	p <
Medial Midfoot			
relative maximum force	2, 52	8.993	**.001****
peak pressure	2, 52	5.979	**.005****
Lateral Midfoot			
relative maximum force	2, 52	2.130	.129
peak pressure	2, 52	8.134	**.001****
Total Foot			
relative maximum force	2, 52	8.088	**.001****
peak pressure	2, 52	36.834	**.001****

Table 5.4: Results of one-way ANOVA of the effect of group membership on six dynamic pressure variables when Froude < 0.5.

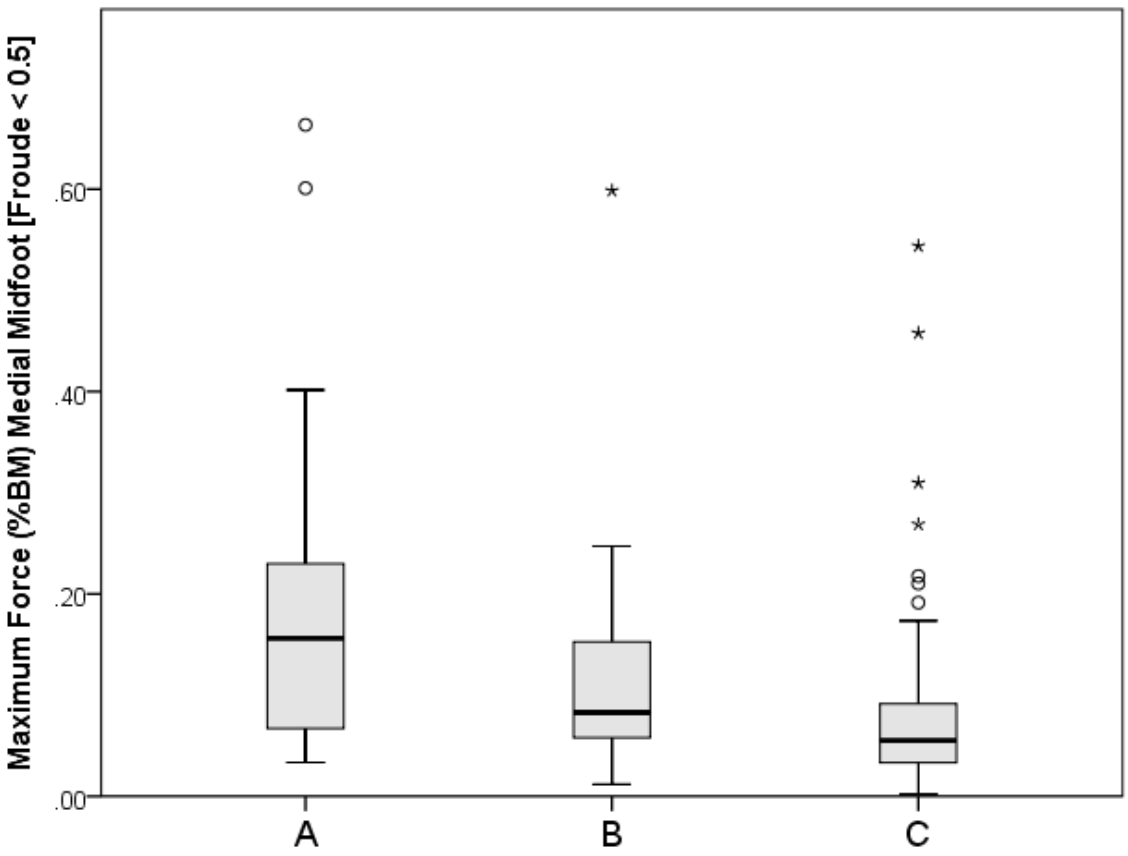

Figure 5.13: Box-plots of median and interquartile range of maximum force (as a percent of body mass) of the medial midfoot during walking trials (Froude < 0.5) for Groups A, B, and C.

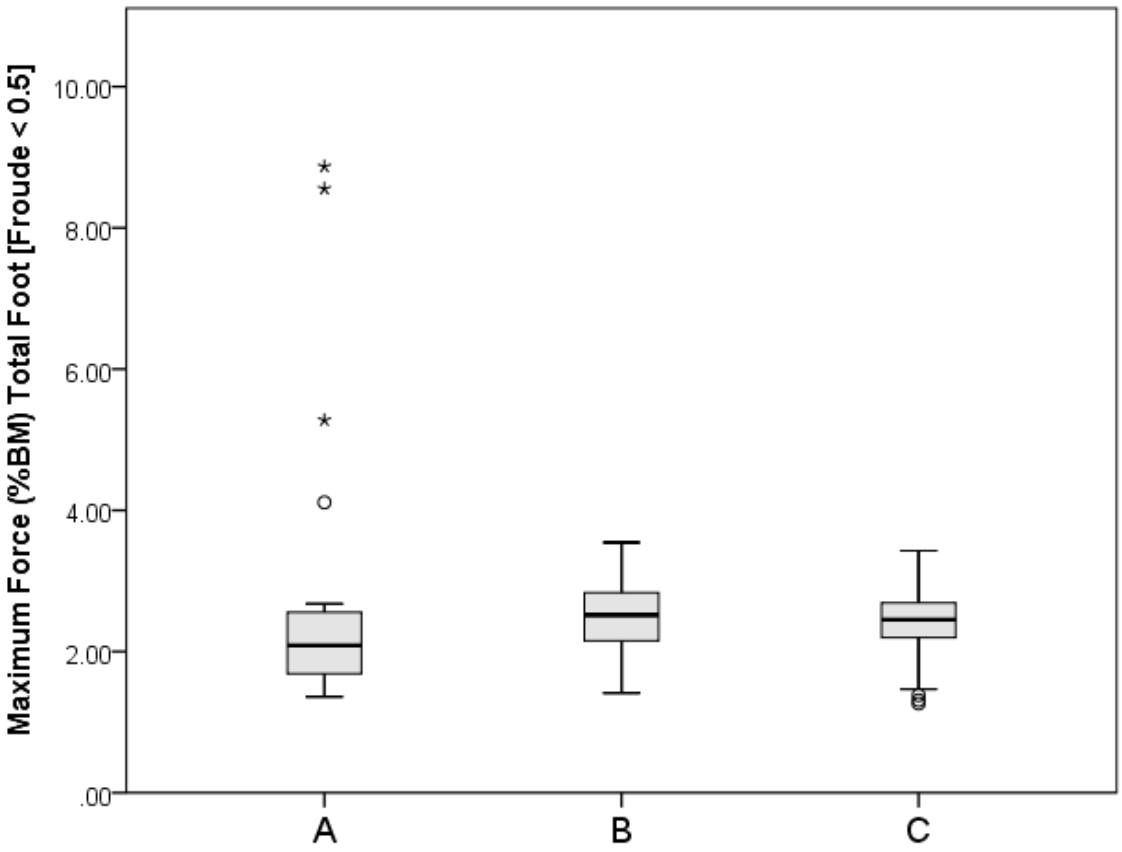

Figure 5.14: Box-plots of median and interquartile range of maximum force (as a percent of body mass) of the total foot during walking trials (Froude < 0.5) for Groups A, B, and C.

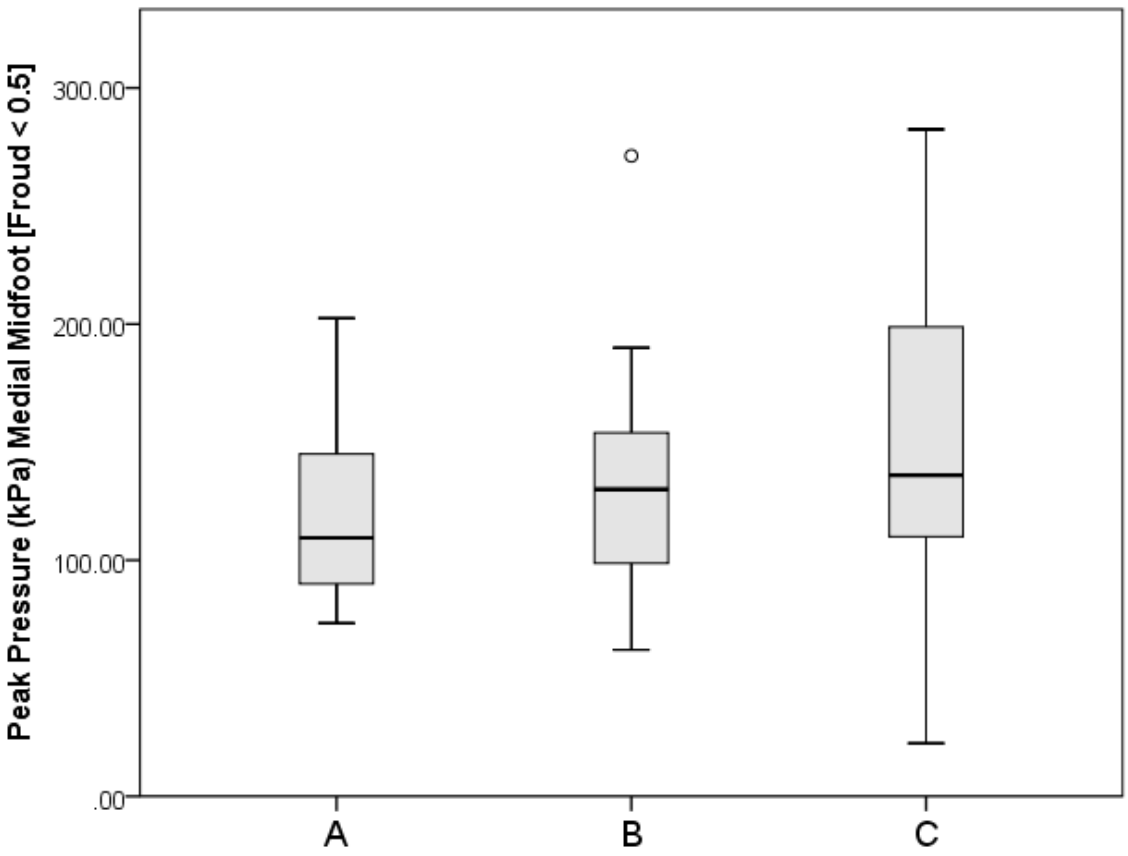

Figure 5.15: Box-plots of median and interquartile range of peak pressure (kPa) of the medial midfoot during walking trials (Froude < 0.5) for Groups A, B, and C.

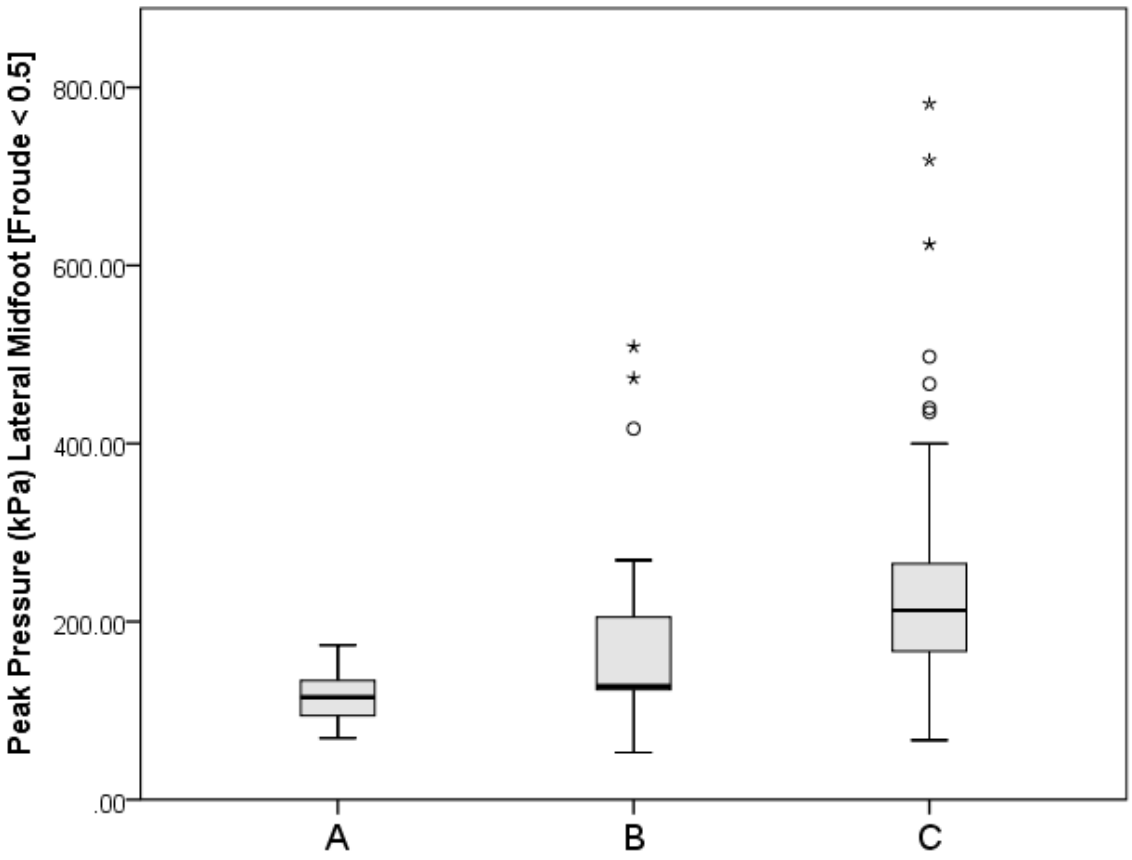

Figure 5.16: Box-plots of median and interquartile range of peak pressure (kPa) of the lateral midfoot during walking trials (Froude < 0.5) for Groups A, B, and C.

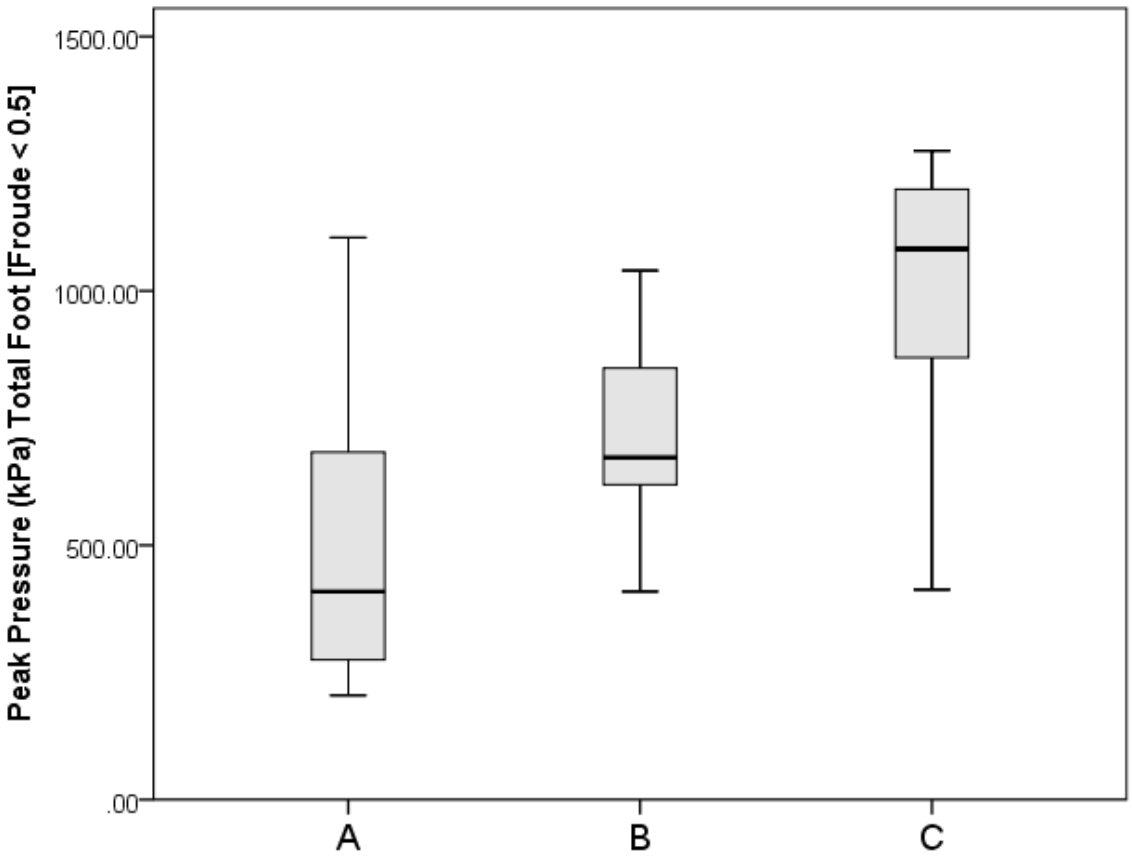

Figure 5.17: Box-plots of median and interquartile range of peak pressure (kPa) of the total foot during walking trials (Froude < 0.5) for Groups A, B, and C.

	df	F	p <
Medial Midfoot			
relative maximum force	2, 121	8.659	**.001****
peak pressure	2, 121	3.400	**.037****
Lateral Midfoot			
relative maximum force	2, 121	1.958	.146
peak pressure	2, 121	12.507	**.001****
Total Foot			
relative maximum force	2, 121	.795	.454
peak pressure	2, 121	64.290	**.001****

Table 5.5: Results of one-way ANOVA of the effect of Group membership on six dynamic pressure variables when Froude ≥ 0.5.

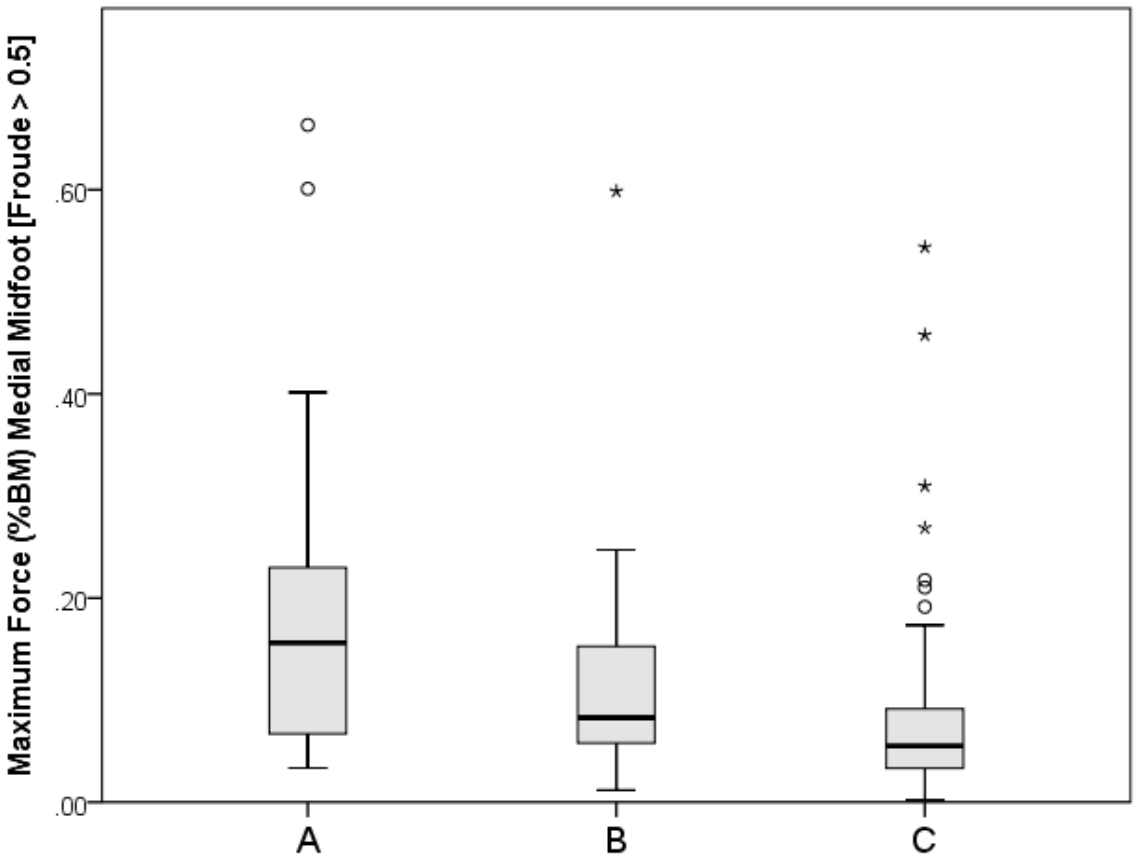

Figure 5.18: Box-plots of median and interquartile range of maximum force (as a percent of body mass) of the medial midfoot during running trials (Froude ≥ 0.5) for Groups A, B, and C.

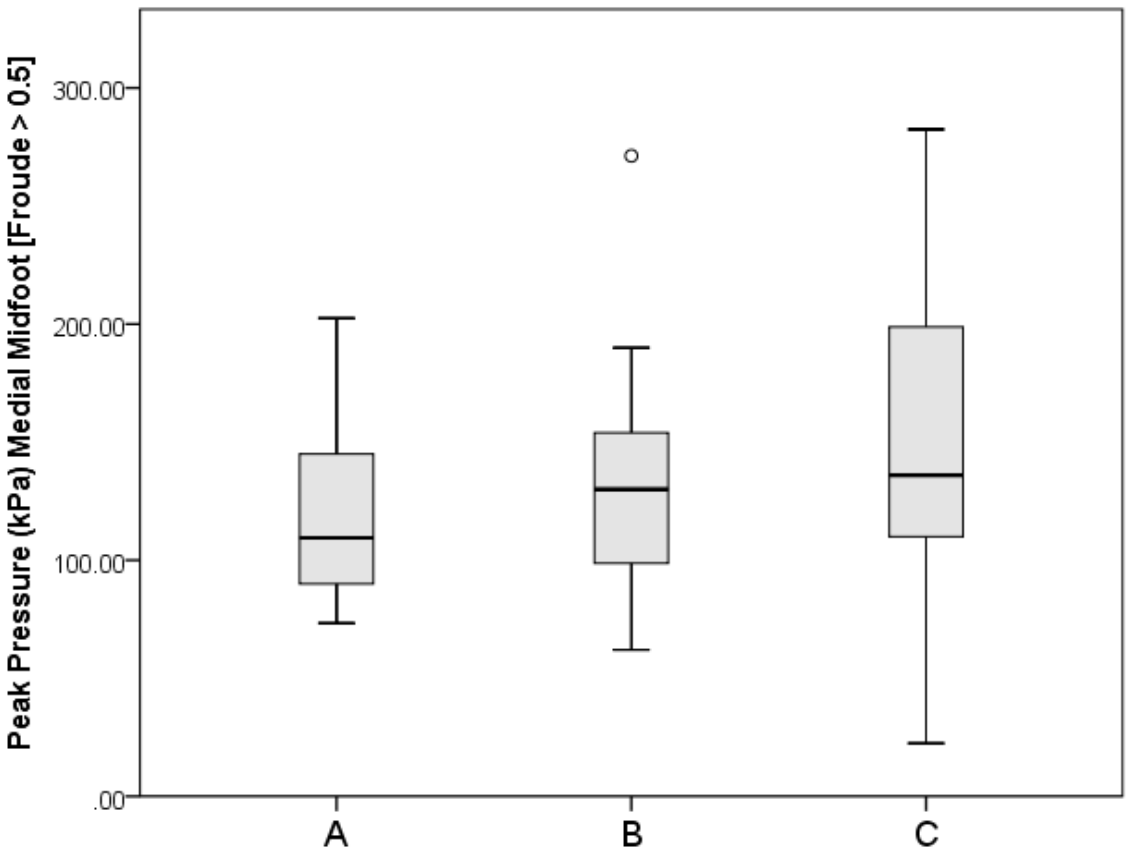

Figure 5.19: Box-plots of median and interquartile range of peak pressure (kPa) of the medial midfoot during running trials (Froude ≥ 0.5) for Groups A, B, and C.

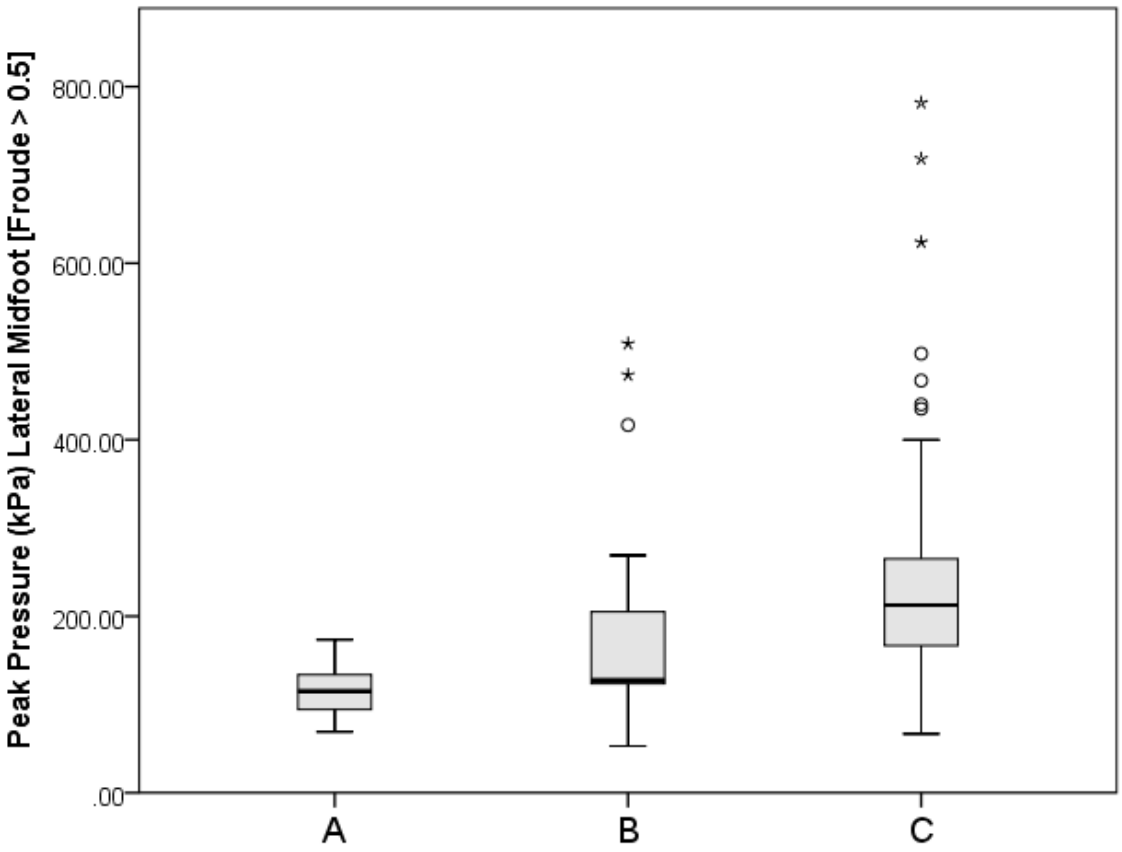

Figure 5.20: Box-plots of median and interquartile range of peak pressure (kPa) of the lateral midfoot during running trials (Froude ≥ 0.5) for Groups A, B, and C.

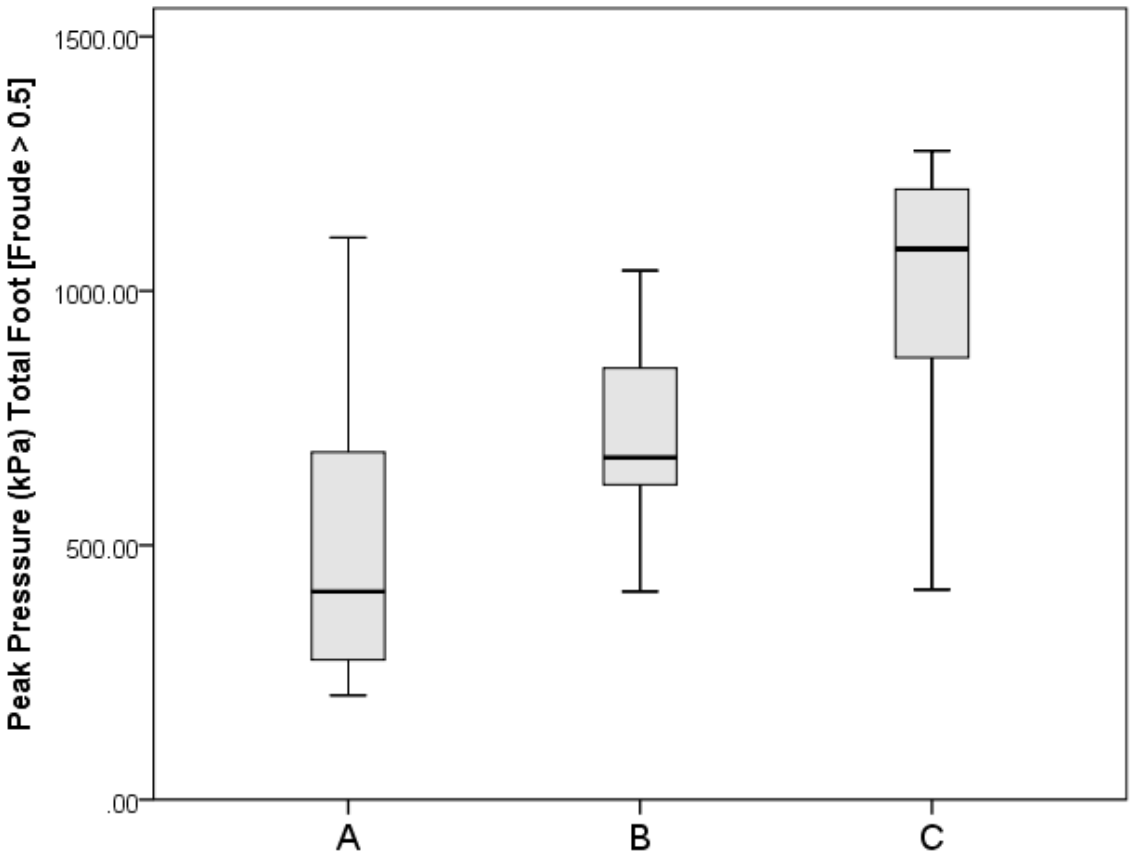

Figure 5.21: Box-plots of median and interquartile range of peak pressure (kPa) of the total during running trials (Froude ≥ 0.5) for Groups A, B, and C.

GROUP A	Medial Midfoot		Lateral Midfoot		Total Foot	
	MF %BM	**PP**	**MF %BM**	**PP**	**MF %BM**	**PP**
Body Mass (kg)	**-.887****	-.298	-.560	-.260	-.611	**.653***
Relative Foot Breadth 25% length (cm)	**.694****	**.457***	**.755****	**.516***	.035	**-.462***
Relative Foot Breadth 50% length (cm)	**.735****	**.447***	**.804****	**.514***	.110	-.362
Relative Foot Breadth 75% length (cm)	**.467***	**.436***	**.682****	.401	.249	-.210
Navicular Height Index	.658	-.195	-.186	-.284	.007	-.408
Arch Index	**.678***	.490	**.869****	.572	.542	-.508

Table 5.6: Correlation coefficients between static participant variables and dynamic pressure variables for the medial and lateral midfoot regions and over the total foot for Group A. *Significant at the $p < 0.05$ level; **Significance at the $p < 0.01$ level.

GROUP B	Medial Midfoot		Lateral Midfoot		Total Foot	
	MF %BM	**PP**	**MF %BM**	**PP**	**MF %BM**	**PP**
Body Mass (kg)	-.324	.230	.458	**.755****	-.256	**.565***
Relative Foot Breadth 25% length (cm)	**.650****	**.554***	.272	.275	.315	-.219
Relative Foot Breadth 50% length (cm)	**.702****	.313	.481	.340	.150	**-.503***
Relative Foot Breadth 75% length (cm)	**.518****	.066	-.040	-.134	.187	-.370
Navicular Height Index	**-.589***	**-.544***	-.329	-.128	.000	-.163
Arch Index	.405	-.189	**.833****	.292	-.246	-.388

Table 5.7: Correlation coefficients between static participant variables and dynamic pressure variables for the medial and lateral midfoot regions and over the total foot for Group B. *Significant at the $p < 0.05$ level; **Significance at the $p < 0.01$ level.

GROUP C	Medial Midfoot		Lateral Midfoot		Total Foot	
	MF %BM	**PP**	**MF %BM**	**PP**	**MF %BM**	**PP**
Body Mass (kg)	.119	.419	.055	**.432***	.323	.070
Relative Foot Breadth 25% length (cm)	**.534****	**.473****	**.441****	**.403***	.131	.026
Relative Foot Breadth 50% length (cm)	.316	.173	**.603****	.248	.259	.045
Relative Foot Breadth 75% length (cm)	**.402***	**.337***	**.332***	.303	.266	.108
Navicular Height Index	-.256	-.110	**-.468****	-.257	-.152	-.213
Arch Index	**.714****	**.386***	**.851****	**.450***	.308	.163

Table 5.8: Correlation coefficients between static participant variables and dynamic pressure variables for the medial and lateral midfoot regions and over the total foot for Group C. *Significant at the $p < 0.05$ level; **Significance at the $p < 0.01$ level.

Froude	Medial Midfoot		Lateral Midfoot		Total Foot	
	MF %BM	**Peak Pr**	**MF %BM**	**Peak Pr**	**MF %BM**	**Peak Pr**
complete sample	**.219****	**.239****	**.532****	**.458****	**.608****	**.315****
Group A	.202	**.444****	**.347***	**.593****	**.460****	**.593****
Group B	**.432****	**.478****	**.524****	**.413***	**.894****	**.371***
Group C	**.239***	**.222***	**.591****	**.517****	**.846****	**.352****

Table 5.9: Correlation coefficients between Froude number (dimensionless speed) and six dynamic pressure variables for the total sample and within Groups A, B, and C. "MF %BM" = relative maximum force as a percent of body mass; "Peak Pr" = peak pressure (kPa). *Significant at the $p < 0.05$ level; **Significance at the $p < 0.01$ level.

Figure 5.22: Example of a participant who exhibited lateral midfoot dorsiflexion at the cubometatarsal joint (white arrow).

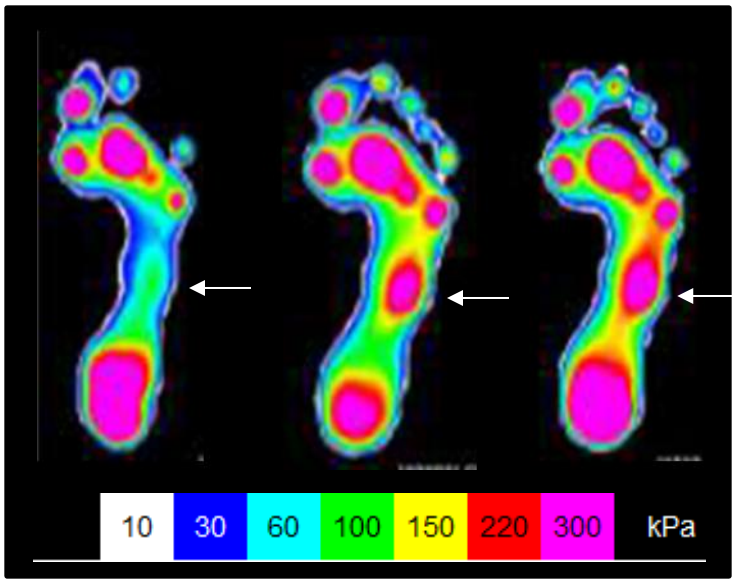

Figure 5.23: Pressure maps recorded from the participant pictured in Figure 5.22 showing elevated pressure beneath the lateral midfoot (cubometatarsal joint; white arrow) with increasing speed of locomotion. Speed increases in figures from left to right.

Chapter 6: Summary and Future Directions

The primary goal of this dissertation was to enhance our understanding of the relationship between foot bone shape and longitudinal arch height. For too long, studies have used the human versus ape comparative framework as a means of identifying aspects of foot bone morphology that could be structurally-related to longitudinal arch presence (*e.g.*, Lamy, 1986; Berillon, 2003; Ward *et al*., 2011; Prang, 2015; but see DeSilva & Throckmorton, 2010). This approach has overlooked the fact that the longitudinal arch varies continuously among humans, many of whom are flat footed (Hoffmann, 1905; Staheli *et al*., 1987; Cavanagh *et al*., 1997; Morag & Cavanagh, 1999; Wunderlich & Cavanagh, 2001; D'Août *et al*., 2009; Stolwijk *et al*., 2013). Therefore, the approach of this dissertation was to investigate the relationship between bony morphology and longitudinal arch height *within* humans, utilizing the fact that humans exhibit variation in arch height to identify these links. In addition to exploring these relationships among adults who vary in arch height, this dissertation also investigated whether aspects of bony morphology thought to be linked to arch presence change in morphology over the period of longitudinal arch development, as the child's foot transforms from a having a flat plantar surface to having an arch. And finally, this dissertation investigated the effects of longitudinal arch height on dynamic plantar loading of the midfoot region and total foot to improve our understanding of how variation in foot form affects foot function.

CHAPTER SUMMARIES

Chapter 2 of this dissertation included a study that addressed whether variation in the sagittal angle of the distal tibia was positively related to variation in longitudinal arch height in adult humans, and also investigated whether this angle acquired its adult

morphology during the period of longitudinal arch development. Following the work of DeSilva and Throckmorton (2010), this study tested the relationship between the distal tibia sagittal angle and radiographic measures of longitudinal arch height using a sample of lateral foot and ankle radiographs. The results of this study were inconsistent with those of DeSilva and Throckmorton (2010), however, as a significant positive relationship between the distal tibia sagittal angle and the measured of longitudinal arch height was not independently detected in this sample. Two archaeological samples of skeletonized human remains were used to look for age-related changes in the sagittal angle of the distal tibia. The results of this aspect of the study show that the angle does undergo changes throughout ontogeny, achieving its adult morphology around age 12, the age around which adult foot size is typically achieved (Scheuer & Black, 2004). Whether ontogenetic changes in the distal tibia sagittal angle are driven by forces experienced at the ankle joint is unclear. The changes do not appear to be related to the development of the longitudinal arch, however, as proposed by DeSilva and Throckmorton (2010). Therefore, the results of this study caution against using the distal tibia sagittal angle to infer whether a fossil hominin had a longitudinal arch.

Chapter 3 of this dissertation included a study of the relationship between two aspects of calcaneal morphology and longitudinal arch height using a sample of lateral foot and ankle radiographs and magnetic resonance images (MRI). The cuboid facet angle of the calcaneus was found to have a significant positive correlation with two radiographic measures of longitudinal arch height, while the sustentaculum tali angle was not correlated with measures of arch height obtained from the MRIs. The morphology of the cuboid facet angle was further investigated using the archaeological sample of skeletonized human remains to assess whether the facet angle changed (increased) throughout the period of longitudinal arch development. The cuboid facet was found to be rounded in toddlers and

young children under the age of 6, though sample sizes were very small for these ages. The cuboid facet appears to flatten around age 6, however, which is consistent with the age at which the longitudinal arch and bipedal gait kinematics mature (Sutherland, 1997; Bertsch *et al*., 2004; Onodera *et al*., 2008; Samson *et al*., 2011; Müller *et al*., 2012). The cuboid facet was found to become more plantarly-inclined until approximately age 12, which is near the age that foot growth is complete (Scheuer & Black, 2004), and also the age at which some authors have argued that arch development is complete (Forriol and Pascual, 1990; Waseda *et al*., 2014). The general finding from this study is that the cuboid facet angle of the calcaneus can reveal information about calcaneal position (*i.e*., inclination) within the foot, and could therefore be informative for reconstructing the hind foot and arch morphology of fossil hominins. Using data from this study, the longitudinal arch height of the Omo 33-74-896 (early *Homo*) specimen, the MH2 (*Au. sediba*) specimen, and OH-8 (early *Homo*) was predicted. The fossil hominins represented by the Omo 33-74-896 (early *Homo*) and MH2 (*Au. sediba*) calcanei were estimated to have had low longitudinal arches, consistent with the results of a recent study of joint angles (Prang, 2015). The OH-8 hominin was estimated to have had a well-developed arch similar to the mean arch height of modern humans, however, a finding that is inconsistent with some reconstructions of arch height in this specimen (*e.g*., Lisowski *et al*., 1974, 1976; Oxnard, 1972; Oxnard & Lisowski, 1980; Kidd et al., 1996; Prang, 2015), though consistent with others (*e.g*., Day & Napier, 1964; Day & Wood, 1968; Berillon, 2003; DeSilva *et al*., 2012).

Chapter 4 of this dissertation included a study of the relationship between two aspects of metatarsal morphology and longitudinal arch height using a sample of MRIs. The base diaphysis angle and torsion of MT II, MT III, and MT IV were not found to exhibit a significant relationship with arch height, calling into question the use of these metrics for assessing arch presence in fossil hominins. This study also investigated

ontogenetic changes in metatarsal torsion in the archaeological samples to determine whether torsion changed throughout the period of longitudinal arch development. Torsion did not change over this period, but was found to differ between the two archaeological populations. Metatarsal torsion was found to be highly variable within and between populations, especially torsion of MT II.

Finally, Chapter 5 of this dissertation included a study of the relationship between body mass, longitudinal arch height, foot shape, speed, and dynamic pressure variables of the midfoot region and over the total foot. Consistent with previous studies, individuals who have a low longitudinal arch and large body mass (adults) experience greater loading (measured as relative maximum force for their body weight) of the medial and lateral midfoot region, but not the total foot, irrespective of age and status of arch maturation. In other words, children for whom the arch was developing, children for whom the arch was developed, and adults who have a low arch experience greater force for their body weight in both the medial and lateral midfoot region than participants with higher arches. In addition, individuals with relatively wider feet also experience higher loads, and loading increases with locomotor speed. Given that an increase in speed was associated with elevated pressure in the lateral midfoot region, and pressure may reflect mobility, the effects of speed on midfoot mobility in humans should be considered in future studies.

FUTURE DIRECTIONS

Improve Study of Foot Bone Shape in Relation to Longitudinal Arch Height

This dissertation was the first to test the relationship between foot bone shape and longitudinal arch height. However, there are a number of aspects of the study design that are worth improving and expanding upon to more thoroughly test these relationships. First,

this study utilized an existing sample of lateral foot and ankle radiographs that was taken from a podiatrist office, and thus a pathological population. While an attempt was made to minimize any instances of severe pathology, it is unclear whether the relationship between foot bone shape and arch height in this population is representative of the relationship in non-pathological humans. Therefore, actually recruiting subjects on which imaging could be performed would be a good first step towards improving the study design. The MRI sample used in this study was recruited in such a fashion, though the sample was small and not necessarily recruited with the intent of sampling a large range of variation in arch height. As the cost of medical imaging becomes more reduced, it would be ideal to perform MRIs to capture information about foot shape (as opposed to x-rays), given that more information about foot bone geometry can be extracted from three dimensional rendering of foot bones.

Second, this study investigated the relationship between arch height and aspects of foot bone shape that had previously been identified as purported markers of longitudinal arch presence. Therefore, it is very likely that other aspects of foot bone morphology not included in this study could reveal information about arch height. For example, recent work by Holowka and colleagues (2017) has demonstrated significant motion between the cuboid and 5th metatarsal in humans, and it is possible that the morphology of these reciprocal surfaces may reflect range of motion. DeSilva and colleagues (2014) have already shown that humans who exhibit lateral midfoot dorsiflexion tend to have a more dorsally convex 4th metatarsal base, but curvature of the 5th metatarsal base and/or distal cuboid has not been quantified. Similarly, Berillon (2003) proposed that the morphology of the navicular bone may serve as a marker of arch presence given that humans and apes exhibit different morphology of the distal navicular articular surfaces. To date, no study

has addressed whether humans exhibit variation in navicular bone morphology, or whether this element could be related to differences in longitudinal arch height.

The ontogenetic components of this dissertation were really a first-look into how foot bone and ankle morphology changes throughout growth. Most studies that quantify ontogenetic changes have focused on long bone and/or cranio-dental development, often within the context of improving forensic techniques for age and stature estimation (*e.g.*, Feldsman, 1992; Scheuer, 2002). With the exception of the ossification schedule, we know relatively little about how foot bone shape changes throughout ontogeny, and how these changes in shape may dictate changes in pedal loading. While recent work by Zeininger (2014) has examined how foot loading may lead to differences in trabecular architecture in young toddlers, we know surprisingly little about how gross foot bone morphology changes with age.

Human variation was a common theme throughout this dissertation, and in a number of instances variation was detected where it was not expected. For example, metatarsal torsion was found to differ between the two archaeological samples, and also between the archaeological samples and the contemporary MRI sample. Previous studies of metatarsal torsion have also noted the presence of human variation in this trait (Drapeau & Harmon, 2013), indicating that there is more variation among humans than has previously been recognized. When considering foot bone morphology, the presence of population-levels of variation ultimately leads to questions about the effects of footwear use and activity on pedal form. Given that footwear use is a relatively recent invention (Trinkaus, 2005), understanding how footwear may affect foot bone shape is crucial for setting up our expectations of foot form for fossil hominins. With the introduction of footwear, authors have noted the presence of secular change in the angle between the first and second ray (Funakoshi, 1988) and an increase in the presence of bony lesions on the

foot (Zipfel & Berger, 2007). Future studies should further examine variation in foot bone shape between unshod and shot populations, in addition to differences in gross foot morphology and function.

Finally, inferring foot function from fossil foot bones requires a stronger understanding of whether variation in foot bone shape can be linked to differences in foot loading. The recent work by DeSilva and colleagues (2015) serves as a useful example of how these links can be investigated. Given that this dissertation identified the cuboid facet angle of the calcaneus and metatarsal torsion as markers of longitudinal arch height, the next logical step is to test whether humans who exhibit variation in these characters exhibit any systematic differences in foot loading. Whether variation in foot bone shape is linked to variation in foot loading is worth knowing, as either answer—yes, or no—will be useful for informing what types of conclusions can be drawn about hominin bipedalism from fossilized foot bones.

References

Abdel Fattah, M. M., Hassanin, M. M., Felembane, F. A., & Nassaane, M. T. (2006). Flat foot among Saudi Arabian army recruits: prevalence and risk factors.

Alexander, R., Ker, R., Bennet, M., Bibby, S., & Kester, R. (1987). The spring in the arch of the human foot. *Nature*, *325*(6100), 147–149.

Ashizawa, K., Kumakura, C., Kusumoto, A., & Narasaki, S. (1997). Relative foot size and shape to general body size in Javanese, Filipinas and Japanese with special reference to habitual footwear types. *Annals of Human Biology*, *24*(2), 117–129.

Barker, S. L., & Scheuer, J. L. (1998). Predictive value of human footprints in a forensic context. *Medicine, Science and the Law*, *38*(4), 341–346.

Barnett, C. H. (1962). The normal orientation of the human hallux and the effect of footwear. *Journal of Anatomy*, *96* (Pt 4), 489–494.

Barnicot, N. A., & Hardy, R. H. (1955). The position of the hallux in West Africans. *Journal of Anatomy*, *89* (Pt 3), 355–361.

Basmajian, J. V., & Bentzon, J. W. (1954). An electromyographic study of certain muscles of the leg and foot in the standing position. *Surgery, Gynecology & Obstetrics*, *98*(6), 662–666.

Bates, K. T., Collins, D., Savage, R., McClymont, J., Webster, E., Pataky, T. C., … Crompton, R. H. (2013). The evolution of compliance in the human lateral mid-foot. *Proc. R. Soc. B*, *280*(1769), 20131818.

Bennett, M. R., Harris, J. W. K., Richmond, B. G., Braun, D. R., Mbua, E., Kiura, P., … Gonzalez, S. (2009). Early Hominin Foot Morphology Based on 1.5-Million-Year-Old Footprints from Ileret, Kenya. *Science*, *323*(5918), 1197–1201.

Berillon, G. (2003). Assessing the longitudinal structure of the early hominid foot: A two-dimensional architecture analysis. *Human Evolution*, *18*(3–4), 113–122.

Berillon, Gilles, Daver, G., D'Août, K., Nicolas, G., Villetanet, B. de la, Multon, F., … Dubreuil, G. (2010). Bipedal versus Quadrupedal Hind Limb and Foot Kinematics in a Captive Sample of *Papio anubis*: Setup and Preliminary Results. *International Journal of Primatology*, *31*(2), 159–180.

Bertsch, C., Unger, H., Winkelmann, W., & Rosenbaum, D. (2004). Evaluation of early walking patterns from plantar pressure distribution measurements. First year results of 42 children. *Gait & Posture*, *19*(3), 235–242.

Birkner, R. (1978). Normal radiographic patterns and variances of the human skeleton—an X-ray atlas of adults and children. *Baltimore (Munich): Urban and Schwarzenberg*.

Bojsen-Møller, F. (1979). Calcaneocuboid joint and stability of the longitudinal arch of the foot at high and low gear push off. *Journal of Anatomy*, *129*(Pt 1), 165–176.

Bosch, K., Gerß, J., & Rosenbaum, D. (2010). Development of healthy children's feet—Nine-year results of a longitudinal investigation of plantar loading patterns. *Gait & Posture*, *32*(4), 564–571.

Bramble, D. M., & Lieberman, D. E. (2004). Endurance running and the evolution of Homo. *Nature*, *432*(7015), 345–352.

Caravaggi, P., Pataky, T., Günther, M., Savage, R., & Crompton, R. (2010). Dynamics of longitudinal arch support in relation to walking speed: contribution of the plantar aponeurosis. *Journal of Anatomy*, *217*(3), 254–261.

Carrier, D. R., Kapoor, A. K., Kimura, T., Nickels, M. K., Scott, E. C., So, J. K., & Trinkaus, E. (1984). The Energetic Paradox of Human Running and Hominid Evolution [and Comments and Reply]. *Current Anthropology*, *25*(4), 483–495.

Cavanagh, P. R., & Rodgers, M. M. (1987) The arch index: A useful measure from footprints. *Journal of Biomechanics, 20* (5), 547-551.

Cavanagh, P. R., Morag, E., Boulton, A. J. M., Young, M. J., Deffner, K. T., & Pammer, S. E. (1997). The relationship of static foot structure to dynamic foot function. *Journal of Biomechanics*, *30*(3), 243–250.

Chang, J.-H., Wang, S.-H., Kuo, C.-L., Shen, H. C., Hong, Y.-W., & Lin, L.-C. (2010). Prevalence of flexible flatfoot in Taiwanese school-aged children in relation to obesity, gender, and age. *European Journal of Pediatrics*, *169*(4), 447–452.

Chen, J.-P., Chung, M.-J., & Wang, M.-J. (2009) Flatfoot prevalence and foot dimensions of 5 to 13-year-old children in Taiwan. *Foot & Ankle International 30* (4), 326-332.

Crompton, R. H., Pataky, T. C., Savage, R., D'Août, K., Bennett, M. R., Day, M. H., … Sellers, W. I. (2012). Human-like external function of the foot, and fully upright gait, confirmed in the 3.66 million year old Laetoli hominin footprints by topographic statistics, experimental footprint-formation and computer simulation. *Journal of The Royal Society Interface*, *9*(69), 707–719.

D'Août, K., Pataky, T. C., Clercq, D. D., & Aerts, P. (2009). The effects of habitual footwear use: foot shape and function in native barefoot walkers. *Footwear Science*, *1*(2), 81–94.

Davis, P. R. (1964). Hominid Fossils from Bed I, Olduvai Gorge, Tanganyika: A Tibia and Fibula. *Nature*, *201*(4923), 967–968.

Day, M. H., & Napier, J. R. (1964). Fossil Foot Bones. *Nature*, *201*, 969–970.

Day, M. H., & Wood, B. A. (1968). Functional Affinities of the Olduvai Hominid 8 Talus. *Man*, *3*(3), 440–455.

Deloison, Y. (1986). Description d'un calcanéum fossile de primate et sa comparaison avec des calcanéums de pongidés, d'australopithèques et d'Homo. *Comptes Rendus de l'Académie Des Sciences. Série 3, Sciences de La Vie*, *302*(7), 257–262.

DeSilva, J. M. (2009). Functional morphology of the ankle and the likelihood of climbing in early hominins. *Proceedings of the National Academy of Sciences*, *106*(16), 6567–6572.

DeSilva, J. M. (2010). Revisiting the "midtarsal break." *American Journal of Physical Anthropology*, *141*(2), 245–258.

DeSilva, J. M., Bonne-Annee, R., Swanson, Z., Gill, C. M., Sobel, M., Uy, J., & Gill, S. V. (2015). Midtarsal break variation in modern humans: Functional causes, skeletal correlates, and paleontological implications. *American Journal of Physical Anthropology*, *156*(4), 543–552.

DeSilva, J. M., & Gill, S. V. (2013). Brief communication: A midtarsal (midfoot) break in the human foot. *American Journal of Physical Anthropology*, *151*(3), 495–499.

DeSilva, J. M., Proctor, D. J., & Zipfel, B. (2012). A complete second metatarsal (StW 89) from Sterkfontein Member 4, South Africa. *Journal of Human Evolution*, *63*(3), 487–496.

DeSilva, J. M., & Throckmorton, Z. J. (2010). Lucy's Flat Feet: The Relationship between the Ankle and Rearfoot Arching in Early Hominins. *PLOS ONE*, *5*(12), e14432.

Dirks, P. H. G. M., Kibii, J. M., Kuhn, B. F., Steininger, C., Churchill, S. E., Kramers, J. D., … Berger, L. R. (2010). Geological Setting and Age of *Australopithecus sediba* from Southern Africa. *Science*, *328*(5975), 205–208.

Donatelli, R. (1985). Normal biomechanics of the foot and ankle. *Journal of Orthopaedic & Sports Physical Therapy*, *7*(3), 91–95.

Doran, D. M. (1992). The ontogeny of chimpanzee and pygmy chimpanzee locomotor behavior: a case study of paedomorphism and its behavioral correlates. *Journal of Human Evolution 23* (2), 139-157.

Doran, D. M. (1997). Ontogeny of locomotion in mountain gorillas and chimpanzees. *Journal of Human Evolution 32* (4), 323-344.

Duncan, A. S., Kappelman, J., & Shapiro, L. J. (1994). Metatarsophalangeal joint function and positional behavior in *Australopithecus afarensis*. *American Journal of Physical Anthropology, 93* (1), 67-81.

Echarri, J. J., & Forriol, F. (2003). The development in footprint morphology in 1851 Congolese children from urban and rural areas, and the relationship between this and wearing shoes. *Journal of Pediatric Orthopaedics B*, *12*(2), 141–146.

Edwards, M. R., Jack, C., & Singh, S. K. (2008). Tibialis posterior dysfunction. *Current Orthopaedics*, *22*(3), 185–192.

El, O., Akcali, O., Kosay, C., Kaner, B., Arslan, Y., Sagol, E., … Peker, O. (2006). Flexible flatfoot and related factors in primary school children: a report of a screening study. *Rheumatology International*, *26*(11), 1050–1053.

Elftman, H., & Manter, J. (1935a). Chimpanzee and human feet in bipedal walking. *American Journal of Physical Anthropology*, *20*(1), 69–79.

Elftman, H., & Manter, J. (1935b). The evolution of the human foot, with especial reference to the joints. *Journal of Anatomy*, *70* (Pt 1), 56.

Engle, E. T., & Morton, D. J. (1931). Notes on Foot Disorders Among Natives of the Belgian Congo. *J Bone Joint Surg Am*, *13*(2), 311–318.

Feibel, C. S., Brown, F. H., & McDougall, I. (1989). Stratigraphic context of fossil hominids from the Omo group deposits: Northern Turkana Basin, Kenya and Ethiopia. *American Journal of Physical Anthropology*, *78*(4), 595–622.

Feldesman, M. R. (1992). Femur/stature ratio and estimates of stature in children. *American Journal of Physical Anthropology, 87*(4), 447-459.

Fessler, D. M., Haley, K. J., & Lal, R. D. (2005). Sexual dimorphism in foot length proportionate to stature. *Annals of Human Biology*, *32*(1), 44–59.

Fiolkowski, P., Brunt, D., Bishop, M., Woo, R., & Horodyski, M. (2003). Intrinsic pedal musculature support of the medial longitudinal arch: an electromyography study. *The Journal of Foot and Ankle Surgery*, *42*(6), 327–333.

Forriol, F., & Pascual, J. (1990). Footprint Analysis Between Three and Seventeen Years of Age. *Foot & Ankle*, *11*(2), 101–104.

Franco, A. H. (1987). Pes cavus and pes planus. *Phys Ther*, *67*, 688–694.

Frost, H. M. (1997). Biomechanical control of knee alignment: some insights from a new paradigm. *Clinical Orthopaedics and Related Research*, (335), 335–342.

Frost, Harold M. (1999). Joint anatomy, design, and arthroses: Insights of the Utah paradigm. *The Anatomical Record*, *255*(2), 162–174.

Funakoshi, K. (1988). Secular changes in the angle of divergence of the first two metatarsals in the Japanese. *American Journal of Physical Anthropology*, *75*(3), 341–345.

García-Rodríguez, A., Martín-Jiménez, F., Carnero-Varo, M., Gómez-Gracia, E., Gómez-Aracena, J., & Fernández-Crehuet, J. (1999). Flexible Flat Feet in Children: A Real Problem? *Pediatrics*, *103*(6), e84–e84.

Gebo, D. L., & Schwartz, G. T. (2006). Foot bones from Omo: Implications for hominid evolution. *American Journal of Physical Anthropology*, *129*(4), 499–511.

Giles, E., & Vallandigham, P. H. (1991). Height estimation from foot and shoeprint length. *Journal of Forensic Science*, *36*(4), 1134–1151.

Goldmann, J.-P., Potthast, W., & Brüggemann, G.-P. (2013). Athletic training with minimal footwear strengthens toe flexor muscles. *Footwear Science*, *5*(1), 19–25.

Gould, N., Moreland, M., Alvarez, R., Trevino, S., & Fenwick, J. (1989). Development of the child's arch. *Foot & Ankle International*, *9*(5), 241–245.

Grabowski, M., Hatala, K. G., Jungers, W. L., & Richmond, B. G. (2015). Body mass estimates of hominin fossils and the evolution of human body size. *Journal of Human Evolution, 85*, 75-93.

Greiner, T. M., & Ball, K. A. (2014). Kinematics of primate midfoot flexibility. *American Journal of Physical Anthropology*, *155*(4), 610–620.

Griffin, N. L., Miller, C. E., Schmitt, D., & D'Août, K. (2015). Understanding the evolution of the windlass mechanism of the human foot from comparative

anatomy: Insights, obstacles, and future directions. *American Journal of Physical Anthropology*, *156*(1), 1–10.

Hallgrímsson, B., Willmore, K., & Hall, B. K. (2002). Canalization, developmental stability, and morphological integration in primate limbs. *American Journal of Physical Anthropology*, *119*(S35), 131–158.

Hamilton, W. G., Hamilton, L. H., Marshall, P., & Molnar, M. (1992). A profile of the musculoskeletal characteristics of elite professional ballet dancers. *The American Journal of Sports Medicine*, *20*(3), 267–273.

Hankey, K. (2009). Tibialis Posterior Dysfunction. *SportEX Dynamics*, (21).

Harcourt-Smith, W. (2002). *Form and function in the hominoid tarsal skeleton*. Doctoral Dissertation, University College London.

Harcourt-Smith, W. E. H., & Aiello, L. C. (2004). Fossils, feet and the evolution of human bipedal locomotion. *Journal of Anatomy*, *204*(5), 403–416.

Harris, E. J. (2010). The Natural History and Pathophysiology of Flexible Flatfoot. *Clinics in Podiatric Medicine and Surgery*, *27*(1), 1–23.

Hatala, K. G., Wunderlich, R. E., Dingwall, H. L., & Richmond, B. G. (2016) Interpreting locomotor biomechanics from the morphology of human footprints. *Journal of Human Evolution, 90*, 38-48.

Heard-Booth, A. N. (2013) Morphological and ontogenetic variation in three osteological correlates of the longitudinal arch. *American Journal of Physical Anthropology, 150* (Supplement 56), 146.

Hennig, E. M., & Rosenbaum, D. (1991). Pressure distribution patterns under the feet of children in comparison with adults. *Foot & Ankle International, 11* (5), 306-311.

Hicks, J. H. (1954). The mechanics of the foot. *Journal of Anatomy*, *88*(Pt 1), 25–30.1.

Hirasaki, E., Higurashi, Y., & Kumakura, H. (2010). Brief communication: Dynamic plantar pressure distribution during locomotion in Japanese macaques (Macaca fuscata). *American Journal of Physical Anthropology*, *142*(1), 149–156.

Hoerr, N. L. (1962). *Radiographic atlas of skeletal development of the foot and ankle: a standard of reference*. Thomas.

Hoffmann, P. (1905). Conclusions drawn from a comparative study of the feet of barefooted and shoe-wearing peoples. *Am J Orthop Surg*, *s2-3*(2), 105–136.

Holowka, N. B., O'Neill, M. C., Thompson, N. E., & Demes, B. (2017). Chimpanzee and human midfoot motion during bipedal walking and the evolution of the longitudinal arch of the foot. *Journal of Human Evolution*, *104*, 23–31.

Hurst, C. V. (2013). *Growing up in medieval Nubia: health, disease, and deathof a medieval juvenile sample from Mis Island*. Doctoral Dissertation, Michigan State University.

Jungers, W. L. (1982). Lucy's limbs: skeletal allometry and locomotion in Australopithecus afarensis. *Nature*, *297*(5868), 676–678.

Kaufman, K. R., Brodine, S. K., Shaffer, R. A., Johnson, C. W., & Cullison, T. R. (1999). The Effect of Foot Structure and Range of Motion on Musculoskeletal Overuse Injuries. *The American Journal of Sports Medicine*, *27*(5), 585–593.

Keith, A. (1929). The History of the Human Foot and Its Bearing on Orthopaedic Practice. *J Bone Joint Surg Am*, *11*(1), 10–32.

Kelly, L. A., Cresswell, A. G., Racinais, S., Whiteley, R., & Lichtwark, G. (2014). Intrinsic foot muscles have the capacity to control deformation of the longitudinal arch. *Journal of The Royal Society Interface*, *11*(93), 20131188.

Kidd, R. S., O'Higgins, P., & Oxnard, C. E. (1996). The OH8 foot: a reappraisal of the functional morphology of the hindfoot utilizing a multivariate analysis. *Journal of Human Evolution*, *31*(3), 269–291.

Korpelainen, R., Orava, S., Karpakka, J., Siira, P., & Hulkko, A. (2001). Risk Factors for Recurrent Stress Fractures in Athletes. *The American Journal of Sports Medicine*, *29*(3), 304–310.

Krauss, I., Grau, S., Mauch, M., Maiwald, C., & Horstmann, T. (2008). Sex-related differences in foot shape. *Ergonomics*, *51*(11), 1693–1709.

Kusumoto, A., Suzuki, T., Kumakura, C., & Ashizawa, K. (1996). A comparative study of foot morphology between Filipino and Japanese women, with reference to the significance of a deformity like hallux valgus as a normal variation. *Annals of Human Biology*, *23*(5), 373–385.

Lamy, P. (1986). The settlement of the longitudinal plantar arch of some African Plio-Pleistocene hominids: a morphological study. *Journal of Human Evolution*, *15*(1), 31–46.

Lawler, R. R. (2008). Morphological integration and natural selection in the postcranium of wild Verreaux's sifaka (Propithecus verreauxi verreauxi). *American Journal of Physical Anthropology*, *136*(2), 204–213.

Leakey, M. G., Feibel, C. S., McDougall, I., Ward, C., & Walker, A. (1998). New specimens and confirmation of an early age for *Australopithecus anamensis*. *Nature*, *393*(6680), 62–66.

Ledoux, W. R., & Hillstrom, H. J. (2002). The distributed plantar vertical force of neutrally aligned and pes planus feet. *Gait & Posture*, *15*(1), 1–9.

Lisowski, F. P., Albrecht, G. H., & Oxnard, C. E. (1974). The form of the talus in some higher primates: A multivariate study. *American Journal of Physical Anthropology*, *41*(2), 191–215.

Lisowski, F. P., Albrecht, G. H., & Oxnard, C. E. (1976). African fossil tali: Further multivariate morphometric studies. *American Journal of Physical Anthropology*, *45*(1), 5–18.

Marchi, D. (2010) Articular to diaphyseal proportions of human and great ape metatarsals. *American Journal of Physical Anthropology, 143* (2), 198-207.

McHenry, H. M. (1992). Body size and proportions in early hominids. *American Journal of Physical Anthropology*, *87*(4), 407–431.

Meldrum, D. J. (1991). Kinematics of the cercopithecine foot on arboreal and terrestrial substrates with implications for the interpretation of hominid terrestrial adaptations. *American Journal of Physical Anthropology*, *84*(3), 273–289.

Meldrum, D. J. (2004). Fossilized Hawaiian footprints compared with Laetoli hominid footprints. In: Meldrum, D. J., & Hilton, C. E. (eds), *From Biped to Strider*., Springer US, 63-83.

Meldrum, D. J., & Wunderlich, R. E. (1998). Midfoot flexibility in ape foot dynamics, early hominid footprints and bipedalism. *American Journal of Physical Anthropology, 26* (Supplement), 168.

Mente, P. L., Aronsson, D. D., Stokes, I. A., & Iatridis, J. C. (1999). Mechanical modulation of growth for the correction of vertebral wedge deformities. *Journal of Orthopaedic Research*, *17*(4), 518–524.

Mente, P. L., Spence, H., Aronsson, D. D., & others. (1997). Progression of vertebral wedging in an asymmetrically loaded rat tail model. *Spine*, *22*(12), 1292–1296.

Mickle, K. J., Steele, J. R., & Munro, B. J. (2008). Is the Foot Structure of Preschool Children Moderated by Gender?: *Journal of Pediatric Orthopaedics*, *28*(5), 593–596.

Miller, E. E., Whitcome, K. K., Lieberman, D. E., Norton, H. L., & Dyer, R. E. (2014). The effect of minimal shoes on arch structure and intrinsic foot muscle strength. *Journal of Sport and Health Science*, *3*(2), 74–85.

Milner, G. R., & Smith, V. G. (1990). Oneota human skeletal remains. *Archaeological Investigations at the Morton Village and Norris Farms*, *36* (11).

Mitchell, P. J., Sarmiento, E. E., & Meldrum, D. J. (2012). The AL 333-160 fourth metatarsal from Hadar compared to that of humans, great apes, baboons and proboscis monkeys: Non-conclusive evidence for pedal arches or obligate bipedality in Hadar hominins. *HOMO - Journal of Comparative Human Biology*, *63*(5), 336–367.

Morag, E., & Cavanagh, P. R. (1999). Structural and functional predictors of regional peak pressures under the foot during walking. *Journal of Biomechanics*, *32*(4), 359–370.

Morton, D. J. (1922). Evolution of the human foot. *American Journal of Physical Anthropology*, *5*(4), 305–336.

Morton, D. J. (1924). Evolution of the longitudinal arch of the human foot. *J Bone Joint Surg Am*, *6*(1), 56–90.

Mosca, V. S. (2001). *The cavus foot*. LWW.

Müller, S., Carlsohn, A., Müller, J., Baur, H., & Mayer, F. (2012). Static and dynamic foot characteristics in children aged 1–13 years: A cross-sectional study. *Gait & Posture*, *35*(3), 389–394.

Musiba, C. M., Tuttle, R. H., Hallgrimsson, B., & Webb, D. M. (1997). Swift and sure-footed on the savanna: a study of Hadzabe gaits and feet in Northern Tanzania. *American Journal of Human Biology*, *9*(3), 303–321.

Onodera, A. N., Sacco, I. C. N., Morioka, E. H., Souza, P. S., Sá, M. R. de, & Amadio, A. C. (2008). What is the best method for child longitudinal plantar arch assessment and when does arch maturation occur? *The Foot*, *18*(3), 142–149.

O'rahilly, R., Gardner, E., & Gray, D. J. (1960). The skeletal development of the foot. *Clinical Orthopaedics*, *16*, 7–14.

Oxnard, C. E. (1972). Some African fossil foot bones: A note on the interpolation of fossils into a matrix of extant species. *American Journal of Physical Anthropology*, *37*(1), 3–12.

Oxnard, C. E., & Lisowski, F. P. (1980). Functional articulation of some hominoid foot bones: Implications for the Olduvai (hominid 8) foot. *American Journal of Physical Anthropology*, *52*(1), 107–117.

Pataky, T. C., Caravaggi, P., Savage, R., Parker, D., Goulermas, J. Y., Sellers, W. I., & Crompton, R. H. (2008). New insights into the plantar pressure correlates of walking speed using pedobarographic statistical parametric mapping (pSPM). *Journal of Biomechanics*, *41*(9), 1987–1994.

Pfeiffer, M., Kotz, R., Ledl, T., Hauser, G., & Sluga, M. (2006). Prevalence of Flat Foot in Preschool-Aged Children. *Pediatrics*, *118*(2), 634–639.

Pontzer, H., Rolian, C., Rightmire, G. P., Jashashvili, T., Ponce de León, M. S., Lordkipanidze, D., & Zollikofer, C. P. E. (2010). Locomotor anatomy and biomechanics of the Dmanisi hominins. *Journal of Human Evolution*, *58*(6), 492–504.

Prang, T. C. (2015). Rearfoot posture of Australopithecus sediba and the evolution of the hominin longitudinal arch. *Scientific Reports*, *5*.

Rao, U. B., & Joseph, B. (1992). The influence of footwear on the prevalence of flat foot. A survey of 2300 children. *Bone & Joint Journal*, *74–B*(4), 525–527.

Reeser, L. A., Susman, R. L., & Stern, J. T. (1983). Electromyographic studies of the human foot: experimental approaches to hominid evolution. *Foot & Ankle International*, *3*(6), 391–407.

Reid, E. (1984). *Understanding Buildings: A Multidisciplinary Approach*. MIT Press.

Reilly, D. T., & Burstein, A. H. (1975). The elastic and ultimate properties of compact bone tissue. *Journal of Biomechanics*, *8*(6), 393–405.

RITTER, M. A., DEROSA, G. P., & BABCOCK, J. L. (1976). Tibial Torsion?. *Clinical Orthopaedics and Related Research*, *120*, 159–163.

Robbins, S. E., & Hanna, A. M. (1987). Running-related injury prevention through barefoot adaptations. *Med Sci Sports Exerc*, *19*(2), 148–156.

Rolian, C. (2009). Integration and evolvability in primate hands and feet. *Evolutionary Biology*, *36*(1), 100–117.

Rosenbaum, D., Hautmann, S., Gold, M., & Claes, L. (1994). Effects of walking speed on plantar pressure patterns and hindfoot angular motion. *Gait & Posture*, *2*(3), 191–197.

Ryan, T. M., & Sukhdeo, S. (2016). KSD-VP-1/1: Analysis of the Postcranial Skeleton Using High-Resolution Computed Tomography. In *The Postcranial Anatomy of Australopithecus afarensis* (pp. 39–62). Springer.

Sachithanandam, V., & Joseph, B. (1995). The influence of footwear on the prevalence of flat foot. A survey of 1846 skeletally mature persons. *Bone & Joint Journal*, *77*(2), 254–257.

Saltzman, C. L., Nawoczenski, D. A., & Talbot, K. D. (1995). Measurement of the medial longitudinal arch. *Archives of Physical Medicine and Rehabilitation*, *76*(1), 45–49.

Samson, W., Dohin, B., Desroches, G., Chaverot, J.-L., Dumas, R., & Cheze, L. (2011). Foot mechanics during the first six years of independent walking. *Journal of Biomechanics*, *44*(7), 1321–1327.

Sarmiento, E. E., & Marcus, L. F. (2000). The Os Navicular of Humans, Great Apes, OH 8, Hadar, and Oreopithecus: Function, Phylogeny, and Multivariate Analyses. *American Museum Novitates*, 1–38.

Saylor, B. Z., Alene, M., Deino, A., Gibert, L., Haile-Selassie, Y., Melillo, S. M., & Scott, G. (2016). The Geologic Context of Korsi Dora and the Partial Skeleton KSD-VP-1/1. In Y. Haile-Selassie & D. F. Su (Eds.), *The Postcranial Anatomy of Australopithecus afarensis* (pp. 13–23). Springer Netherlands.

Scheuer, L. (2002). Application of osteology to forensic medicine. *Clinical Anatomy 15* (4), 297-312.

Scheuer, L., & Black, S. (2004). *The juvenile skeleton*. Academic Press.

Schmidt, M., & Fischer, M. S. (2009). Morphological integration in mammalian limb proportions: dissociation between function and development. *Evolution*, *63*(3), 749–766.

Schuenke, M., Schulte, E., & Schumacher, U. (2014). *General Anatomy and Musculoskeletal System* (2 edition). New York, New York: Thieme.

Shibuya, N., Jupiter, D. C., Ciliberti, L. J., VanBuren, V., & La Fontaine, J. (2010). Characteristics of Adult Flatfoot in the United States. *The Journal of Foot and Ankle Surgery*, *49*(4), 363–368.

Sim-Fook, L., & Hodgson, A. R. (1958). A Comparison of Foot Forms Among the Non-Shoe and Shoe-Wearing Chinese Population. *The Journal of Bone & Joint Surgery*, *40*(5), 1058–1062.

Simkin, A., Leichter, I., Giladi, M., Stein, M., & Milgrom, C. (1989). Combined Effect of Foot Arch Structure and an Orthotic Device on Stress Fractures. *Foot & Ankle*, *10*(1), 25–29.

Soler, A. (2012). *Life and death in a medieval Nubian farming community: the experience at Mis Island*. Doctoral Dissertation, Michigan State University.

Staheli, LYNN T., Chew, D. E., Corbett, M., & others. (1987). The longitudinal arch. *J Bone Joint Surg Am*, *69*(3), 426–428.

Staheli, Lynn T., & Engel, G. M. (1972). Tibial torsion: a method of assessment and a survey of normal children. *Clinical Orthopaedics and Related Research*, *86*, 183–186.

Stavlas, P., Grivas, T. B., Michas, C., Vasiliadis, E., & Polyzois, V. (2005). The Evolution of Foot Morphology in Children Between 6 and 17 Years of Age: A Cross-Sectional Study Based on Footprints in a Mediterranean Population. *The Journal of Foot and Ankle Surgery*, *44*(6), 424–428.

Stearne, S. M., McDonald, K. A., Alderson, J. A., North, I., Oxnard, C. E., & Rubenson, J. (2016). The Foot's Arch and the Energetics of Human Locomotion. *Scientific Reports*, *6*.

Stern Jr, J. T., & Susman, R. L. (1983). The locomotor anatomy of Australopithecus afarensis. *American Journal of Physical Anthropology*, *60*(3), 279–317.

Stolwijk, N. M., Duysens, J., Louwerens, J. W. K., Ven, Y. H. van de, & Keijsers, N. L. (2013). Flat Feet, Happy Feet? Comparison of the Dynamic Plantar Pressure Distribution and Static Medial Foot Geometry between Malawian and Dutch Adults. *PLOS ONE*, *8*(2), e57209.

Subotnick, S. I. (1985). The Biomechanics of Running Implications for the Prevention of Foot Injuries. *Sports Medicine*, *2*(2), 144–153.

Susman, R. L. (1983). Evolution of the Human Foot: Evidence from Plio-Pleistocene Hominids. *Foot & Ankle*, *3*(6), 365–376.

Sutherland, D. (1997). The development of mature gait. *Gait & Posture*, *6*(2), 163–170.

Tan, P. L., & Teh, J. (2007). MRI of the diabetic foot: differentiation of infection from neuropathic change. *The British Journal of Radiology*, *80*(959), 939–948.

Thompson, N. E., Holowka, N. B., O'Neill, M. C., & Larson, S. G. (2014). Brief communication: Cineradiographic analysis of the chimpanzee (Pan troglodytes) talonavicular and calcaneocuboid joints. *American Journal of Physical Anthropology*, *154*(4), 604–608.

Trinkaus, E. (2005). Anatomical evidence for the antiquity of human footwear use. *Journal of Archaeological Science, 32* (10), 1515-1526.

Tripeny, P., & Ambrose, J. E. (2012). Front Cover. In *Building Structures* (p. I). New York, NY: John Wiley & Sons.

Turner, M. S., & Smillie, I. S. (1981). The effect of tibial torsion of the pathology of the knee. *Bone & Joint Journal*, *63*(3), 396–398.

Tuttle, R. H., Webb, D. M., & Baksh, M. (1991). Laetoli toes andAustralopithecus afarensis. *Human Evolution*, *6*(3), 193–200.

Tuttle, R., Webb, D., Weidl, E., & Baksh, M. (1990). Further progress on the Laetoli trails. *Journal of Archaeological Science*, *17*(3), 347–362.

Venkataraman, V. V., Draft, T. S., & Dominy, N. J. (2013). Tree climbing and human evolution. *Proceedings of the National Academy of Sciences, 100* (4), 1237-1242.

Vereecke, E., D'Août, K., Van Elsacker, L., De Clercq, D., & Aerts, P. (2005). Functional analysis of the gibbon foot during terrestrial bipedal walking: Plantar pressure distributions and three-dimensional ground reaction forces. *American Journal of Physical Anthropology*, *128*(3), 659–669.

Villemure, I., & Stokes, I. A. F. (2009). Growth plate mechanics and mechanobiology. A survey of present understanding. *Journal of Biomechanics*, *42*(12), 1793–1803.

Walter, R. C. (1994). Age of Lucy and the First Family: Single-crystal 40Ar/39Ar dating of the Denen Dora and lower Kada Hadar members of the Hadar Formation, Ethiopia. *Geology*, *22*(1), 6–10.

Ward, C. V., Leakey, M. G., & Walker, A. (2001). Morphology of Australopithecus anamensis from Kanapoi and Allia Bay, Kenya. *Journal of Human Evolution*, *41*(4), 255–368.

Ward, Carol V., Kimbel, W. H., & Johanson, D. C. (2011). Complete Fourth Metatarsal and Arches in the Foot of *Australopithecus afarensis*. *Science*, *331*(6018), 750–753.

Waseda, A., Suda, Y., Inokuchi, S., Nishiwaki, Y., & Toyama, Y. (2014). Standard growth of the foot arch in childhood and adolescence—Derived from the measurement results of 10,155 children. *Foot and Ankle Surgery*, *20*(3), 208–214.

Weidenreich, F. (1923). Evolution of the human foot. *American Journal of Physical Anthropology*, *6*(1), 1–10.

Williams III, D. S., McClay, I. S., & Hamill, J. (2001). Arch structure and injury patterns in runners. *Clinical Biomechanics*, *16*(4), 341–347.

Williams, S. A. (2010). Morphological integration and the evolution of knuckle-walking. *Journal of Human Evolution*, *58*(5), 432–440.

Wood, B. (1992). Origin and evolution of the genus Homo. *Nature*, *355*(6363), 783–790.

Wunderlich, R. E., & Cavanagh, P. R. (2001). Gender differences in adult foot shape: implications for shoe design. *Medicine and Science in Sports and Exercise, 33*(4), 605–611.

Zipfel, B., & Berger, L. R. (2007) Shod versus unshod: The emergence of forefoot pathology in modern humans? *The Foot 17* (4), 205-213.

Zipfel, B., DeSilva, J. M., Kidd, R. S., Carlson, K. J., Churchill, S. E., & Berger, L. R. (2011). The foot and ankle of *Australopithecus sediba*. *Science, 333*(6048), 1417–1420.

Zeininger, A. (2014). Ontogeny of bipedalism: Pedal mechanics and trabecular bone morphology. Doctoral Dissertation, University of Texas at Austin.